

For Reference


NOT TO BE TAKEN FROM THIS ROOM

For Reference

NOT TO BE TAKEN FROM THIS ROOM

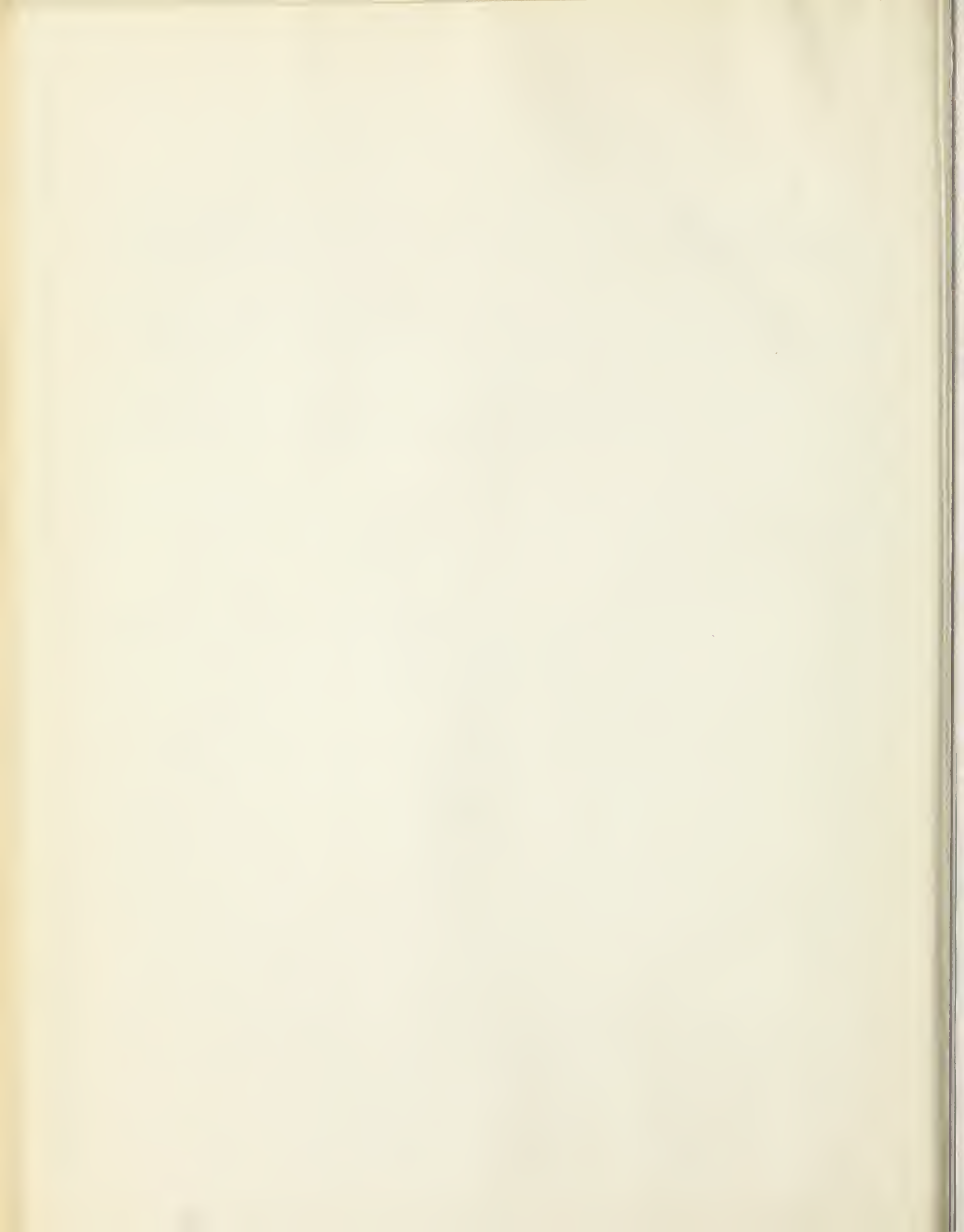
Ex LIBRIS
UNIVERSITATIS
ALBERTAENSIS





Digitized by the Internet Archive
in 2018 with funding from
University of Alberta Libraries

<https://archive.org/details/strongmotionseis00ghsj>



thesis
1963(F)
#10D

UNIVERSITY OF ALBERTA

STRONG MOTION SEISMIC EFFECTS OF THE SUFFIELD EXPLOSIONS

by

G. H. S. JONES

A THESIS

SUBMITTED TO THE FACULTY OF GRADUATE STUDIES

IN PARTIAL FULFILLMENT OF THE REQUIREMENTS FOR THE DEGREE

OF DOCTOR OF PHILOSOPHY

DEPARTMENT OF PHYSICS

EDMONTON, ALBERTA

10th OCTOBER, 1963



AERIAL VIEW OF SMOKE CLOUD AND HALO

ABSTRACT

Full details are given of the seismic measurements undertaken on the series of explosive charges detonated at Suffield Experimental Station in the period 1958-1963. Seismograms are included for charges ranging in size from 8 lb to 200,000 lb TNT, surface burst, and for a variety of buried charges.

The P wave is analysed only to the extent of identification and the derivation of an approximate layering system for the test site.

The surface waves are analysed in some detail in terms of their particle trajectories. In the radial-vertical phase the seismograms from surface-burst charges are divided into two distinct regions by the arrival of the airblast. Preceding the airblast a dispersed surface wave is evident, which, in general, is retrograde in habit at short distances and prograde at longer distances from the explosion. After the arrival of the airblast the seismograms consist of a series of large amplitude pulses, apparently coupled to the airblast, upon which is superimposed an air-coupled wave of Press-Ewing type.

The results from the surface-burst charges are compared with those from buried charges. It is shown that the buried charges generate a succession of phases which alternate in habit between the retrograde and prograde forms. A form of dispersion analysis similar to that of Satô is described, and applied to certain of the phases. It is shown that the experimental dispersion curves from the buried shots cross the sonic velocity, thus indicating that Press-Ewing coupling may occur to at least one phase.

Theoretical Rayleigh Wave dispersion curves are computed by the Anderson programme for models which approximate to the test site. It is shown that the major features of the seismograms can be interpreted in terms of dispersion curves of the type computed, but that a full analysis will require detailed analysis by similar methods of all the phases detectable in the records.

It is shown that in the transverse component there is repeatability in the wave form in a given azimuth when shots are repeated on the same ground zero, and that there is some form of coupling between the radial-vertical modes and the transverse modes.

The data given provide a clear picture of the general pattern to be expected in the seismograms from very large detonations in the region of the Western Plains. The research described has led to the publication of a wide range of reports and papers by the present writer and others, dealing with limited aspects of the problem, and these are listed or quoted at the relevant points. The research has developed to the stage where further interpretation requires a long period of routine analysis of the spectral content and the dispersion characteristics of the individual phases.

Extensions of the experimental programme to investigate special aspects of the problem are suggested.

In addition to the strong motion seismograms, some experimental data are given which allow the correlation of the ground shock and airblast right in to the crater area to be demonstrated.

ACKNOWLEDGEMENTS

The operations reported herein were large and complex, with some unique features, and could only have been carried out by successful teamwork among the scientists, engineers, administrators and others involved. Individual acknowledgement, even for considerable effort, is therefore not always possible. Where the writer has benefited by direct technical assistance, this assistance has for the most part been acknowledged by joint authorship of the many papers and reports listed in the bibliography. Nevertheless, the writer wishes to acknowledge the special assistance given by F. H. Winfield, in the field programme, by S. A. Cyganik in preparing data and producing the figures included in the dissertation, and by Mrs E. P. Torn, whose constant good humour and feeling for the subtleties of grammar aided considerably in the preparation of the text. The outstanding help given by O. Hastrup is acknowledged elsewhere.

The data used in this dissertation are published by permission of the Chairman, Defence Research Board of Canada. The freedom given to the writer in planning and executing the programme, together with the granting of academic leave with financial support, is gratefully acknowledged.

The writer wishes also to acknowledge the encouragement provided by many people not actively engaged in this research. The late Prof. R. M. Davies originally introduced the writer to the fascinating field of Stress Waves, and Prof. J. Tuzo Wilson re-awakened interest in geophysics and added to it by many stimulating lectures and conversations. Dr Milton Dobrin graciously guided the first fumbling approach to the air-coupled wave, and Dr Don L. Anderson assisted materially by providing the details of his dispersion calculations. Dr W. Fraser helped considerably by

processing the computations on the University of Toronto IBM 7090.

Finally, the encouragement provided by Dr Carl Kisslinger, of Saint Louis University, and by the staff of the University of Alberta in Edmonton over a period of several years, is sincerely recognized by the writer.

TABLE OF CONTENTS

	<u>Page</u>
1.00 <u>INTRODUCTION</u>	
1.10 General Background to the Study	1
1.20 The Nature of the Force Functions	8
1.30 Statement of the Problem and the Scope of the Dissertation	12
2.00 <u>EXPERIMENTAL WORK</u>	
2.10 Equipment and Methods	16
2.20 Description of Test Sites	18
2.30 The Primary Experiments	20
2.31 8 lb Series	
2.32 30 lb Series	
2.33 60 lb Series	
2.34 500 lb Series	
2.35 10,000 lb Series	
2.36 40,000 lb Series	
2.37 200,000 lb Series	
2.40 The Subsidiary Experiments	28
2.41 Contained and Venting Charges at SES	
2.42 40,000 lb Charges at the Nevada Test Site	
2.43 Records at Longer Distances from SES Charges	
3.00 <u>GENERAL ANALYSIS</u>	
3.10 Zero Time and the Arrival of the Airblast	35
3.20 The P Wave and Postulated S Wave	36
3.30 On Dispersion in Strong Motion Seismograms	38
3.40 The Surface Wave Preceding the Airblast	51

	<u>Page</u>
3.50 The Surface Waves from Contained and Venting Charges	59
3.60 The Waves Following the Airblast	66
3.70 The Transverse Motion	77
3.80 Remote Effects	82
4.00 <u>CONSOLIDATION OF THE OBSERVATIONS</u>	85
5.00 <u>THE SEISMOGRAMS</u>	

TABLES

BIBLIOGRAPHY

APPENDICES

- A Formal Mathematical Theory of Air-coupling
- B Seismic Survey of the Two Main Sites
- C Theoretical Rayleigh Wave Dispersion for Various Models
- D Edited Extracts from Semi-Annual Reports on Contract AF 19 (604)-7402
- E A Modified Satô Programme for Determining Phase Velocities
- F Spectral Analysis of Post Air Blast Phase of Two Seismograms

LIST OF FIGURES

1. Pressure-Distance Curve for 200,000 lb Surface Burst Charge
2. Typical Shock-bubble Photograph
3. 40,000 lb Charge Crater After 24 Hours
4. Standard Response Curve for Sprengnether Seismographs
5. Dynamic Magnification Nomogram
6. Topographical Map of Test Sites
7. Seismic Net for 200,000 lb Trial
8. Air-coupled Ground Roll 55,000 ft from 40,000 lb Charge
9. Travel-time Curves for Two Events
10. Illustrative diagram of Dispersion Curves
11. Vertical Dispersion -- 20 ton Charge
12. Vertical Dispersion -- 100 ton Charge
13. 5-ton Particle Trajectories, Drowning Ford Site (2500 ft -- 4500 ft)
14. 5-ton Particle Trajectories, Drowning Ford Site (5450 ft -- 7000 ft)
15. 5-ton Particle Trajectories, Watching Hill Site
16. 20-ton Particle Trajectories, Watching Hill Site
17. 100-ton Particle Trajectories, Watching Hill Site
18. 100-ton Particle Trajectories, Watching Hill Site (Cont'd)
19. 100-ton Particle Trajectories, Watching Hill Site (Cont'd)
20. 20-ton Particle Trajectories, Drowning Ford Site
21. Seismograms (Vertical Component) at 4000 ft from Buried and Surface 1000 lb Charges
22. Three Synthetic Seismograms
23. Particle Trajectory for Seismogram 97 J
24. Experimental Dispersion Curves for Prograde and Retrograde Phases of a 1000 lb Buried Charge
25. 100 Ton Particle Trajectory, Watching Hill Site, 12000 ft

26. 100 Ton Particle Trajectory, Watching Hill Site, 10,000 ft
27. 100 Ton Particle Trajectory, Watching Hill Site, 4,000 ft
28. 100 Ton Particle Trajectory, Watching Hill Site, 2,000 ft
29. Vertical Components from 20 Ton Seismograms Showing Effect of Airblast
30. 20 Ton Particle Trajectory, Watching Hill Site, 3000 ft
31. Times of Arrival of the Air and Ground Shock Fronts
32. Telluric Probe Records
33. Repeated Transverse Motion
34. Transverse Records at Various Azimuths, 10,000 lb Charge

APPENDIX FIGURES

- B 1 Location of Velocity and Refraction Survey
- B 2 Refraction and Velocity Profiles, Watching Hill Site
- B 3 Seismic Section - Watching Hill Site
- B 4 Time-Distance Plot, Watching Hill Site
- B 5 Vertical Velocity Survey, Watching Hill Site
- C 1 Chart for Layering Models
- C 2 Theoretical Dispersion Curves
- F 1 Computer Verification of Digitization - Vertical Components
- F 2 Post Airblast Orbit - 60W
- F 3 Post Airblast Orbit - 61W
- F 4 Post Airblast Orbit - 62W
- F 5 Fourier Integral Computation - 60W and 61W
- F 6 Spectral Amplitudes - Seismograms 60W and 61W
- F 7 Spectra 60W and 61W

LIST OF TABLES

1. Predicted Pressure-Distance Data for 200,000 lb TNT Surface Burst at the Watching Hill Site
2. Hopkinson's Law Scaling Factors for Various Charges
3. Classification of Soil Samples from Boring at GZ for 1961 100 Ton Test Shot
4. Acquisition Data for Seismograms
5. Airblast Travel-time from Seismograms
6. Data Relating to P Wave and Event A
7. Airblast and Ground Shock Arrival Times at Short Ranges

STRONG MOTION SEISMIC EFFECTS OF THE SUFFIELD TNT EXPLOSIONS

by

G. H. S. Jones

1.00 INTRODUCTION

1.10 General Background to the Study

1.11 Many of the complexities of the half-space problem are due to the generation of surface waves at the boundary, directly and by the conversion of P and S waves. Lord Rayleigh (1885 and 1900) predicted the existence of a free surface wave, but Lamb (1904 and 1916a, b) was one of the first to study in detail the propagation of pulses in the half-space.

The general literature has been well surveyed by Davies (1953), Miklowitz (1960), McLean and Caless (1961) and by Ewing, Jardetzky and Press (1957). Miklowitz lists 135 references, and Ewing et al. give a voluminous bibliography and have reduced much of the work to textbook status. As is becoming common, the latter is abbreviated 'EJP' in this dissertation.

Useful surveys in abstract form have been given by Bartunek and Igel (1955) and by Nestler (n.d.). These surveys list some of the limited circulation reports which are fairly generally available. Attention is also drawn to the Vela Uniform Periodic Information Digest (Vesiac) and the Preliminary Bibliography of Soviet Seismology and Seismometry (A.I.D. 1961). Any fresh survey, so soon after the above, would merely be a transcription, and attention is therefore limited to noting some papers which are of

particular interest in the present research.

1.12 Following upon the pioneer work of Rayleigh and Lamb (l.c.) and of Stoneley(1924) on interface waves, Sneddon (1951) made a theoretical study by Transform methods of the seismic effect of a travelling source of pressure moving over the boundary. This was for the case of a pulse travelling at a velocity less than that of shear waves in the medium (sub-sonic case) and the treatment was extended by Cole and Huth (1958) to the transonic case (velocity between that of shear and compressional waves) and the supersonic case (velocity greater than that of compressional waves). The nomenclature is not free from ambiguity.

In these cases the load was assumed to have been moving for some time so that the steady state solution was the one of interest. In such models the displacement tends to infinity at the singular point of the Rayleigh velocity, and also contains arbitrary constants as time tends to infinity. These inherent ambiguities may, in theory, be removed by using an axially symmetric model, with peak overpressure and the velocity of the pulse both decaying with distance from the origin. This approach has been undertaken by Miles (1960), but it is necessary to introduce many simplifying assumptions before the problem becomes amenable to solution.

1.13 Bateman (1938) discussed the interaction between ground and air resulting in free vibrations having the characteristics of Rayleigh waves except that the velocity is slightly less than the velocity of sound in air, rather than less than that of the shear wave in the ground. Press et al. (1951) showed experimentally that, under certain circumstances, resonant coupling may exist, producing a wave superficially

similar to that of Bateman, and gave an explanation based on an extension of the Lamb approach for a travelling line source. This treatment allowed the main features to be predicted, and, in the few years subsequent to this, theoretical and experimental approaches were made by Press and Ewing (1951a, b, c), Dobrin, Simon and Lawrence (1951), Haskell (1951) and Jardetzky and Press (1952). These showed that the explanation was adequate, at least for the case where the pressure pulse in the air travelled at essentially constant velocity.

It appears to be generally agreed (see e.g. EJP, page 230 et seq.) that the necessary and sufficient condition for the production of 'Press-Ewing' type coupled waves is a layered medium, in which dispersive Rayleigh waves can exist and can propagate at some frequency whose phase velocity is equal to that of the velocity of the travelling pulse of pressure in the air.

Under these circumstances a train of constant frequency waves is generated at the surface, with Rayleigh-type orbits, starting roughly in coincidence with the arrival of the airblast and lasting until a time consistent with an arrival at the group velocity corresponding with the selected frequency.

1.14 The cited papers do not make explicit reference to the source strength or dimensions, and it would appear that the solutions offered imply a constant frequency train independent of charge size. The period is fixed by the particular member of the dispersed train which has a phase velocity equal to the constant pressure-pulse velocity. Dr Dobrin appears to agree with this interpretation of the air-

coupled wave discussed in his papers*. Experimentally, the theory has been verified using small, constant size charges, monitored at points sufficiently remote to allow the airblast velocity to decay to a constant value, as envisaged by the theory.

Miles, however, in his theory introduces a pulse of decaying velocity and also, implicitly, the size of the charge. However, he makes no reference to the air-coupled wave, presumably because he is dealing with a semi-infinite medium and assumes a non-dispersive Rayleigh wave. In this case a singularity arises only at the single instant in time when the blast wave velocity is equal to the Rayleigh velocity.

Dix (1955) suggests that long-period waves such as those seen in ground roll, can be generated by a form of energy retention at the source, through backward propagation of waves deriving from the interaction of the spreading wave front and the various boundaries. Eventually the energy is dissipated by transmission in all the available modes, including the Rayleigh wave. Dix, however, made no mention of air-coupling and his approach is not really applicable.

Kogan, Pasechnik and Sultanov (1959) discuss the differences in periods associated with explosions and earthquakes, and suggest that

* In private communication:

'It would be quite essential to show that the frequency of the air-coupled wave is the same as that predicted from the dispersion curve from a hole shot at the velocity of sound in air'...'I feel that such air-coupling requires a dispersion curve which crosses the velocity of sound in air, giving a predictable frequency for the air-coupled wave corresponding to the point of crossing.'

the short periods are due to the small size of the explosive source. This suggests that the dominant periods will change with charge size, but they do not make the point explicitly.

1.15 The Suffield test sites were chosen primarily as being suitable for studying the propagation of blast waves from large charges to low overpressures over flat uniform ground. However, the low seismic surface velocity and the horizontal layering make the site very suitable for study of surface waves, with particular attention to the occurrence of classical or 'Press-Ewing' coupling between the surface wave and the airblast. Early work showed that air-coupling certainly existed, but it appeared that there were departures from the classical form and an apparent variation in the period, depending upon the charge size. The seismic participation was therefore planned essentially in terms of these air-coupled waves, though without prejudice to the possibility of fruitful excursions from the main theme. To the best of the writer's knowledge, this is the only series to date in which routine measurements have been made on surface waves close to the source, with charges of increasing size all on virtually identical flat ground. It would appear that such a series is essential for the complete verification of many theories which have been propounded on the basis of limited evidence and limited verification. This requirement justifies the publication of the complete range of seismograms in a way suitable for further analysis by other workers with specialized interests. Some seismograms have been published separately, but for the sake of completeness, reduced copies of all the main series and many subsidiary seismograms are included in this dissertation as a separate section.

1.16 It is convenient at this point to introduce several concepts which are relevant but which are not treated extensively in the following sections. The term air-coupled wave should not be confused with the term coupled wave, introduced by Leet (e.g., 1939, 1950, 1960). The trajectory of the latter wave is a diagonal line in the sense push-left-up then pull-right-down, or the inverse. It is claimed to have been observed in the records from dynamite blasts and the first nuclear test. The advent of nuclear energy stimulated interest in the strong-motion region, and historically interesting papers are Taylor (1940), Penney and Reines (1945), Coon, Houghton and Nobles (1945) and Leet (1945a, b). The coupled wave, christened 'C' and described by Leet, may be treated as a combination of a P and S wave. There is some argument about the reality of the wave as a distinct entity, and the present writer considers it likely that there have been at least some cases of wrong identification. However, an apparent coupling between a transverse mode and a radial-vertical mode surface wave is invariably present in the records from the Suffield site, and was also obtained by the writer at the Nevada Test Site. A preliminary discussion of this effect has been given elsewhere (Jones, 1962c).

Leet (1944 and 1962), and others, also discuss a surface wave with prograde* orbital motion, but otherwise similar to Rayleigh waves. This Leet terms a Hydrodynamic wave, H, and observed experimentally at

* This spelling appears to be common usage among seismologists. Neither Webster nor the New Oxford list this word, though both list 'progrede' (to move forward). Webster indicates that 'progrede' is 'rare'. Prograde appears to be an adoptive English antonym to retrograde, rather than a derivative of progredi. The listed antonym to retrograde is 'progressive'.

the first nuclear shot. Such prograde waves are distinct features of the Suffield records, and are discussed in some detail herein, and have also been obtained elsewhere. They are usually interpreted, after Sezawa and Kanai (1939), as equivalent to the antisymmetric vibration of a plate. An elegant treatment by ray theory has been given by Tolstoy and Usdin (1953).

Leet (1960) is, incidentally, guilty of a common error in stating (on page 75) that the air pressure wave from an explosion is first supersonic "but within a distance of about 20 to 50 times the diameter of the solid explosive, has levelled off at the speed of sound in air". This is quite incorrect. The distances correspond to about 6.7 ft and 16.6 ft from a 1 lb charge, ground burst. At these distances the respective Mach numbers of the shock are 1.503 and 1.108. In the case of the 100 ton charge (roughly 20 ft diameter), the corresponding distances are 401 ft and 1018 ft. Even at a distance of 59,900 ft from this charge the Mach number was still 1.0009*.

It is possible to use records such as those included herein to determine the motion of the originating source, according to the methods of Satô (1955a, b, 1956 and 1959). This method depends upon the dispersion in the wave train, and has been applied by Kisslinger (1960) to small explosions at Saint Louis. However, due to the intervening effect of the airblast, the method is only applicable to the regions of the traces ahead of the airblast. A modification of this approach is discussed herein.

The discussions of Pekeris (1955a, b, 1959 and 1960) are relevant to the prediction of wave forms from explosions. Again, it is probable that only portions of the seismograms may be used to verify his theory, due to

* Data supplied by T. K. Groves, SES.

the masking effect of the airblast which is not included in the theory.

1.20 The Nature of the Force Functions

1.21 The seismic effects are created by forces deriving from the detonation of an explosive charge in close contact with the surface. The distribution of these forces cannot be given in a theoretically-derived form, though many aspects may be described by empirical laws, and some theoretical symmetry laws are applicable within limits. Initially, the forces derive directly from the expansion of two hemispheres, one the shock hemisphere expanding in the air and the other that expanding into, and disrupting, the material upon which the charge lies. It is clear that this lower hemisphere very rapidly attenuates into elastic stress waves of the type commonly discussed in the theory of seismology. At points on the surface remote from Ground Zero (GZ) there will be weak disturbances due to the reflected and refracted P and S waves, together with surface waves which will depend upon the detailed structure of the upper layers in the ground. Normally, these effects are recorded by instruments of high to very high gain, remote from GZ.

When we pass beyond the region of disruption of the ground (the crater and plastic zone), we must consider the force function deriving from the expansion of the shock wave in the air. In the case of a charge actually on the surface, this is an expanding hemisphere at all relevant times. If the charge is above the surface, the primary shock from the charge combines with the reflected shock from the 'image point' to form an almost vertical Mach Stem. At some distance from GZ we may treat this expansion as that of a vertical cylinder whose axis runs through GZ. At the surface the two cases are distinguishable only in terms of the strength of the shock front.

1.22 Immediately beyond the true crater the forces deriving from the expanding shock front will be such that the material is strained beyond the (effective) elastic limit and shows permanent set. The annular area at the surface which shows permanent set is loosely defined as the Plastic Zone, the definition being a loose one, since the zone of permanent set may not coincide precisely with the onset of elastic transmission of energy by seismic waves. In addition, though the air blast tends to create a downward permanent set, this is balanced in part by the upward forces in the ground, and the set at a given point may be up, down, or zero, even close to the crater. The precise balance could possibly be defined for an ideal medium, but such speculation is fruitless in the real case, as has been shown by Penney and Raines (1945), Jones and Krohn (1960a, b) and Jones, Krohn and Dewey (1962).

1.23 No theoretical law exists for the rate of decay of pressure with distance from GZ, for the complete range. It is common practice to fit the data empirically to a law of the type

$Z = A/r + B/r^2 + C/r^3$ where Z is the peak pressure and r is the distance from GZ, A , B and C being fitting constants to which we cannot attach physical meaning. However, this law is better for nuclear shots than HE shots and a form which fits HE data better is

$$Z = \frac{A}{(r + A_0)} + \frac{B}{(r + B_0)^2} + \frac{C}{(r + C_0)^3}$$

In practice, the pressure values are derived from the Rankine-Hugoniot relationship $Z = M'(M' + 2) \left(\frac{2\gamma}{\gamma + 1} \right)$ where $M' = (\text{Mach Number} - 1)$

This we get from the radius-time relationship

$$\frac{r}{c} = \{a_0 + t + a_2 \ln(t + b) + a_3 [\ln(t + b)]^{1/2} + \dots\}$$

$$\text{and thus } M' = \frac{a_2}{t + b} + 1/2 \frac{a_3}{(t + b) \ln(t + b)^{1/2}} + \dots$$

where $a_0, a_2, a_3, \dots, b, \dots$ are fitting constants and c is the speed of sound ahead of the shock*. This relationship is far more general than the first, and may be used to fit data from all types of explosions. For different size charges, the law of geometrical similarity, originally formulated for explosive charges by Hopkinson** is obeyed very closely by all explosives, provided the air mass entrained is more than ten times the explosive mass. A discussion of this scaling law, following the well-known methods of dimensional analysis (cf Hubbert, 1937) has been given by Jones (1958). Taking this scale law into effect we may re-write the law of pressure decay, for the simplest case as

$$Z = \frac{A}{r/w^{1/3}} + \frac{B}{(r/w^{1/3})^2} + \frac{C}{(r/w^{1/3})^3}$$

and similarly modify r and the fitting constants in the other equations. In most experiments several sets of data are acquired, and the constants vary slightly for the sets of differently acquired data. The data themselves are only distinguishable by this 'best fit' constants variation. Detailed discussion of the curves is apparently only available in classified literature, but results from the Suffield explosions are available (Groves 1963a, b, c).

Fig. 1 is typical of the type of prediction plot used, being that for a 200,000 lb charge based on data from a 40,000 lb charge

* T.K. Groves. Private Communication.

** circa 1914. Precise reference not located.

similarly detonated on the Suffield site. Data giving a wider range are shown in Table 1. Table 2 gives the Hopkinson's Law scaling factors for a variety of charges. Fig. 2 is a photograph of a large-scale trial, typical of the cine photos from which travel time data are obtained. The expanding hemispherical shock is clearly visible. Fig. 3 shows a typical crater produced by a large surface-burst charge.

1.24 The decay of pressure with time at a given point after the passage of the shock front must also be treated more or less empirically. It is usually expressed in the form of a (modified) Friedlander Equation (Friedlander 1946) as

$$P = P_s(1 - t/\tau)e^{-at/\tau}$$

where P is the instantaneous pressure, P_s is the peak pressure and τ is the positive duration, t being measured from the time of arrival of the shock. This form fits the region of positive pressure reasonably well, but ignores the low pressure region, the second shock, and the negative phase which is usually present in practice. The constant a is derived empirically from the experimental pressure-time curves. The applicability of this equation to wide ranges of shock strengths is in doubt, but the simple form given above is usually considered in the open literature, and is probably valid in the low pressure regions. Note that Hopkinson's Law is incorporated through the parameter τ , which itself scales according to this law.

Some of the techniques of measurement used in these trials have been given by Harvey (1957), Mitalas and Harvey (1958), Groves (1960) and Dewey (1961 and 1962). A detailed discussion of the propagation of blast waves may be found in Bethe et al. (1951). A

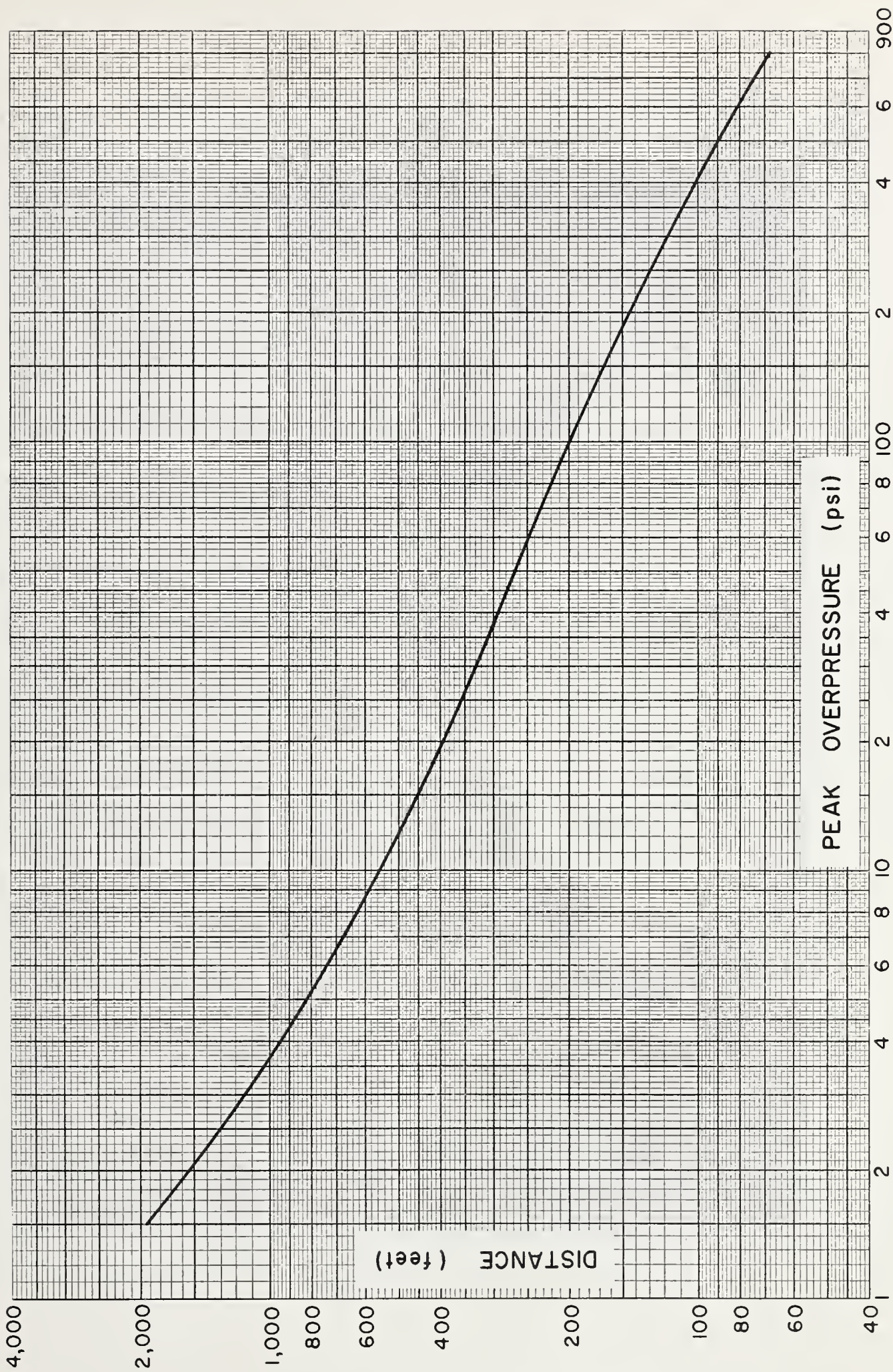


FIG.1
PREDICTED PRESSURE - DISTANCE CURVE
200,000 LB. T.N.T. SURFACE BURST



FIG. 2
TYPICAL SHOCK - BUBBLE PHOTOGRAPH



FIG. 3
40,000 LB. CRATER 24 HRS. AFTER DETONATION

simplified description of cylindrical and spherical blast waves has been given by Friedman (1960), while an approach to the problem of plane waves in granular materials has been made by Katz and Woeber (1960a, b). Parkin (1958) has discussed the dimensional scaling of some aspects of ground shock.

1.30 Statement of the Problem and the Scope of the Dissertation

Many of the mathematical approaches cited above are relevant to the interpretation of the strong motion records. In particular the formulation by Miles of the Blast Wave problem, Pekeris's formulation of the surface seismic pulse and the EJP discussion of Rayleigh and air-coupled waves in layered media and the papers by Sezawa and Kanai and by Tolstoy and Usdin have direct bearing. Even when we admit the gross simplifications inherent in all these theories, the problem is complex and not always amenable to explicit solution. The complete problem, allowing for the non-analytic form of the blast propagation, plastic deformation in an area comparable in diameter to the shot-detector distance, and the non-ideal medium, is mathematically over-complex. Nevertheless, the partial theories are approximately correct and allow satisfactory prediction of limited aspects of real seismograms. Generally speaking, in this dissertation the interpretation is based upon these theories.

A comprehensive body of data from the Suffield sites is included in such a way that additional interpretation may be undertaken by other workers. In addition, some data obtained in subsidiary experiments both on and off the main test site are included and discussed.

Theoretical dispersion curves for a variety of models, computed for the writer at the Computation Centre, University of Toronto, using the programme provided to the writer by Don L. Anderson*, are included and compared with the experimental data. The models chosen were selected by the writer to cover both the best estimate of the actual ground conditions and a number of comparatively standard systems likely to be of more general interest.

It is shown that the data produced at SES are internally consistent, and demonstrate a number of effects which have not been detected in a definitive way previously.

The modified air-coupled wave has not been reported previously, so far as the writer is aware, and no explicit theoretical treatment exists. However, the Press-Ewing theory implies that, on changing the assumption of constant velocity in the air pulse to a decaying velocity, the equivalent theory would indicate that a succession of frequencies would be excited as a modified form of air-coupled train. Two variants of the classical theory of air-coupling are presented in Appendix A.

For the data to be of value in further interpretation, it is essential to define the experimental conditions in some detail, and for this reason both the test site and the field operations are described. An appendix gives the main conclusions obtained from refraction and velocity log surveys carried out on the test site by the Century Geophysical Corporation of Canada in association with the writer.

* Seismology Lab., Pasadena. See Anderson (1962) and Harkrider and Anderson (1962).

Some interpretation of the transverse component of motion has been attempted, and is given in a separate section. It is shown that the surface wave transverse motion is repeatable in both amplitude and detailed profile in a given azimuth from repeated shots on the same ground zero, even though the crater has been excavated and refilled between shots. A note on this effect has been published (Jones, 1962b) and it is understood that a similar effect has been noted in charges detonated in water-filled craters on the Florissant Site by the Saint Louis Group.

The correlation between the Love and Rayleigh type events is discussed, and has also been discussed elsewhere by the writer (Jones, 1962c).

It is shown that a 'synthetic' seismogram, showing the characteristics of a multi-ton surface-burst charge seismogram may be produced by combining two seismograms from a pair of similar 1000 lb charges, one detonated on the surface and one detonated fully contained. A brief discussion of this problem has been given by Jones, Maureau and Cyganik (1963).

Several distinct phases of Rayleigh type may be detected in the seismograms from sub-surface charges. The phases alternate between the prograde and retrograde habit, the two dominant phases being a prograde phase preceding a retrograde phase. No reference has been located in the literature to this type of alternation, though both prograde and retrograde modes are known experimentally and predicted by theory.

Many aspects of the ground shock problem, dealing with cratering and plastic deformation as distinct from purely seismological

data, have been published separately by the writer and are referred to in the body of the dissertation.

Analysis of some of the seismograms by a method similar to that of Satô is included, and this analysis reveals several features of interest which have a bearing on the interpretation of the multi-ton seismograms and on the identification of explosion sources.

2.00 EXPERIMENTAL WORK

2.10 Equipment and Method

2.11 The experimental methods used in the present work have been described in previously published reports (Jones, 1960; Jones and Winfield, 1960; Jones, Kisslinger and Cyganik, 1961; and Vesso, Sanders and Winfield, 1963). The description herein is a general one of the developed system, and it should be realized that some of the early experiments used simpler systems.

2.12 The main instrumentation consisted of from one to eleven Sprengnether three-component portable seismographs. These instruments have a natural period of 0.75 sec. and are damped to 0.55 critical. There are two magnetically damped inverted pendula for the radial and transverse components and a magnetically damped spring supported beam for the vertical component. The instruments had no provision for recording zero-time or the time of arrival of the airblast, but modifications were introduced to provide these additional data. Details have been given by Vesso, Sanders and Winfield (1963). Basically, they consist of installing two neon lamps in each magazine, the light passing through small holes to record on the photographic paper at the correct position. There are two independent circuits: the zero time circuit which links all instruments and applies a triggering voltage to discharge a capacitor through the neon; secondly, individual circuits associated with each instrument, in which a microphone-operated relay triggers a similar capacitor system. These time marks are impressed with an accuracy of a few milliseconds, certainly better than the precision of reading events from the paper record.

2.13 The paper speed is not governed and varies slightly with the ambient conditions, the amount of paper in the magazines and the state of the batteries. Timing marks are impressed every 0.02 sec., with every 0.2 mark being thickened. These time marks appear to have a cumulative error of less than 0.01 sec. in ten seconds. A large number of consecutive tests on all instruments gave a true time of $0.2 \pm .0005$ sec. for the longer time interval*. This appeared to be independent of the state of the batteries provided they were reasonably well-charged, as was the case in all the trials, with a single known exception (seismogram 54W). The effect of large changes in ambient temperature has not been investigated since the majority of the trials were held in summer.

2.14 The majority of the instruments had static magnifications of about fifty, though some with magnifications of 7.5 and of about 150 were used in a few of the later trials. Details are given in Table 4, together with the other acquisition data. The instruments appear to satisfy the design criteria for portable seismographs given by Duval (1960), and have the standard response curve shown in Fig. 4. Mechanical seismographs of this type act as displacement meters for periods less than about half the natural period, and as accelerometers for periods greater than about twice the natural period. The dominant periods recorded in the present work were 0.16 to 0.34 for 500 lb charges, 0.35 to 0.60 for 10,000 lb charges, 0.40 to 0.65 for 40,000 lb charges and 0.40 to 0.90 for the 200,000 lb charge. This bracketing is unfortunate, but the effect is not serious as may be seen from Fig. 5, which is a nomogram after

* Determined by B. Sanders for the writer.
** Seconds.

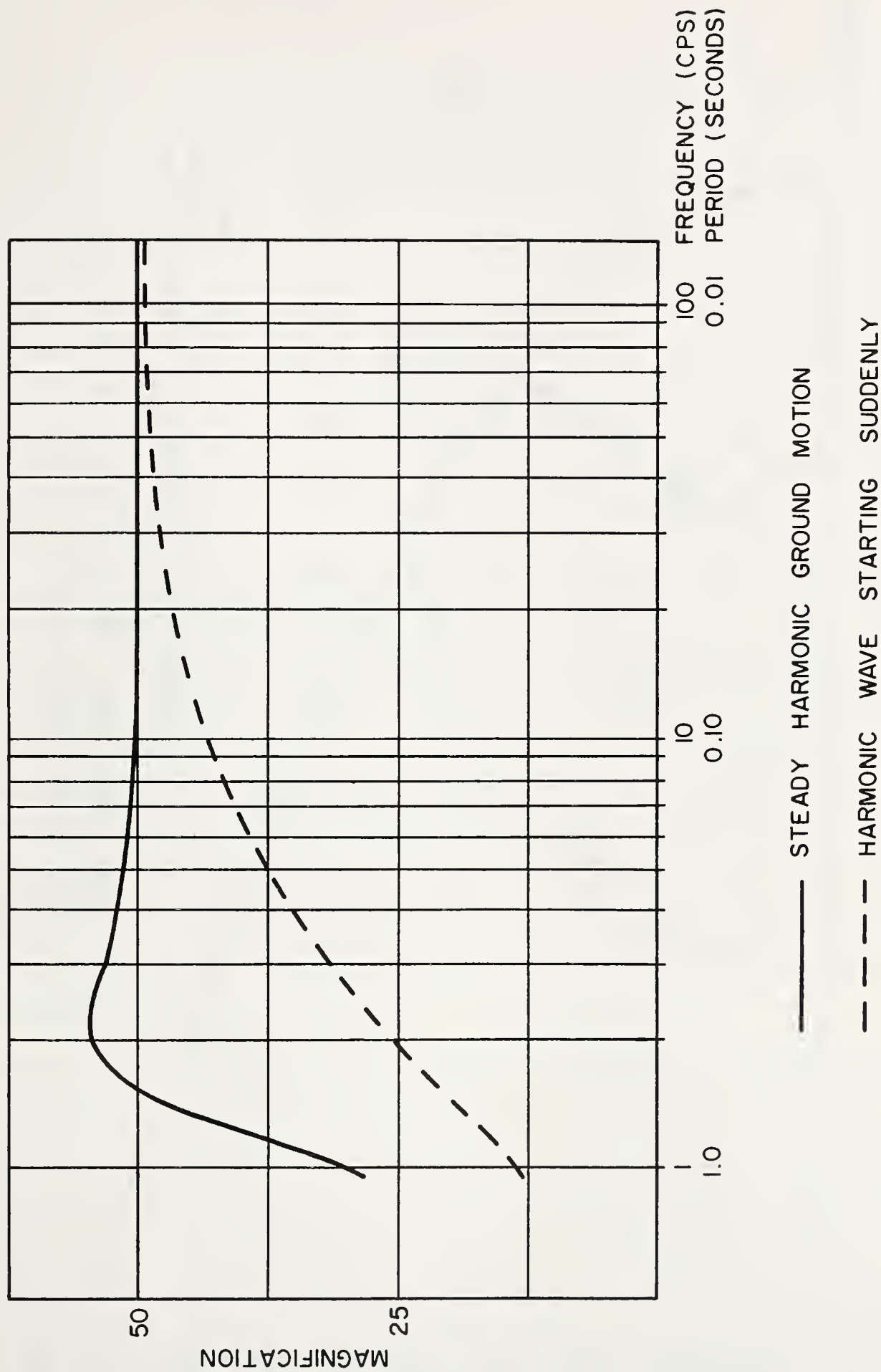


FIG. 4

STANDARD RESPONSE CURVE FOR
SPRENGNETHER PORTABLE SEISMOGRAPHS

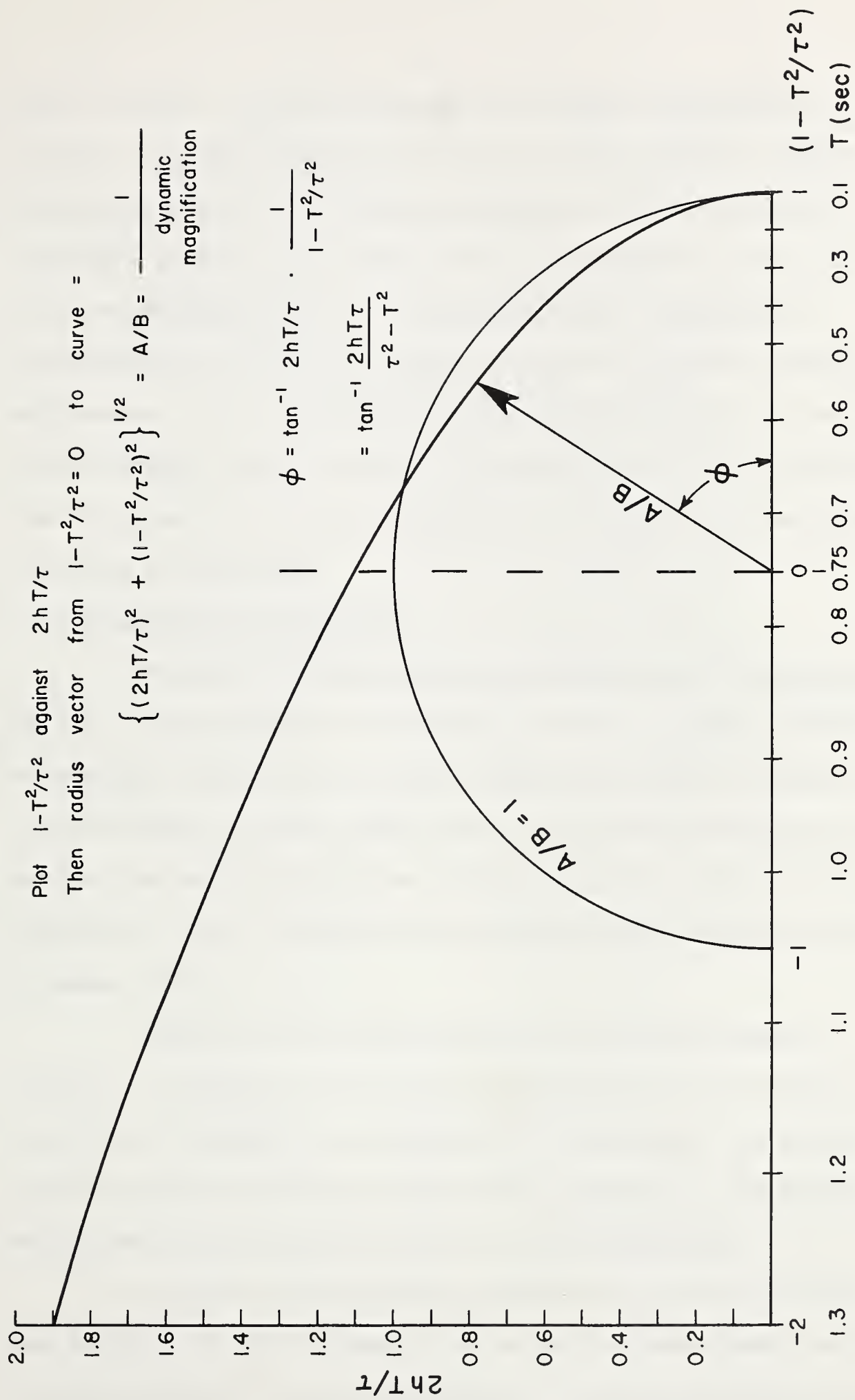


FIG. 5
 DYNAMIC MAGNIFICATION NOMOGRAM
 (AFTER RICHTER, 1958)

Richter (1958). It will be seen that the dynamic magnification is virtually constant, and the phase shift is about ± 10 deg. centred around 60 degrees. For any given charge size, the periods are virtually constant, and no great error is introduced by using the direct seismograph readings in deriving particle trajectories. Care should be taken when we attempt to compare the phase relationship between waves of different periods. If we disregard the records from the highest pressure levels, the records are not of the impulsive start type, and so the dynamic magnification curve for non-impulsive conditions is acceptable.

2.20 Description of Test Sites

Two test sites were used for the main series of experiments, the sites lying alongside one another, and known as Drowning Ford and Watching Hill respectively. Little detailed geological information is available about the area, though there are two Geological Survey Memoirs covering the Southern Plains area (Williams and Dyer, 1930; and Russell and Landes, 1940). The Pleistocene geology is also described briefly by Common (1962).

Towards the end of the present series of experiments, a velocity and refraction survey was prepared by the Century Geophysical Corporation of Canada, in association with the writer. The relevant details of this operation are discussed in Appendix B. The following description is based upon the writer's field observations.

The sites are towards the southern end of the Ross Depression (see Fig. 6) which appears to be an old drainage channel draining the large morainal area in the vicinity. It appears probable that the



FIG. 6
TOPOGRAPHICAL MAP OF TEST SITES

deposits to a depth of some 200 ft (on the Watching Hill site) are lacustrine, being formed at a time when the Ross Depression and an area to the South and West contained a rather large lake. What appears to be a late boundary of this lake is visible running from the river circling North to North-West around the Ross Depression. This boundary has the form of a distinct 'shoreline' of heavy boulder drift, the boundary showing a sharp transition between the almost stone-free lacustrine deposit and the heavy drift beyond. Juniper Flats and Dishpan Lake appear to be non-perennial vestiges of this lake.

The Drowning Ford site has been cut down to its present level by retreating meanders of the present South Saskatchewan river. Stalker (1961) indicates that the area is close to the confluence of the pre-Glacial Milk River and the pre-Glacial Oldman River. However, on p. 11 of the cited reference, it is stated that this particular branch of the buried valley has not been investigated.

The deposits, being typically lacustrine, consist mainly of uniform beds of clay and silt, with occasional sand lenses. These lenses appear to be of small lateral extent except for one at a depth of about 50 ft on the Watching Hill site. This particular bed is a thin stratum of sand-gravel and is waterfilled, though apparently it does not draw from any appreciable body of water as it may be drained easily. Comments on this point by Century Geophysical Corporation are given in Appendix B, together with some drillers' logs. There is a variation in detail, but a typical soil classification down to the waterbearing gravel is given in Table 3. This refers to an exploratory

log taken when exploring the ground to select the GZ of the 200,000 lb trial. The classification is based upon samples provided by the writer to the Waterways Experiment Station, Vicksburg. Details of the velocity layering are not given here, since they are included and discussed in para 3.20 and Appendix B.

Since some periods of nearly one second have been noted, at velocities around 1000 ft/sec., it would appear that depths somewhat greater than the Pleistocene deposits are of significance, though for the majority of the records, the Pleistocene geology will be dominant. The Pleistocene deposits are underlain by Upper Cretaceous beds of the Foremost formation, which, due to their horizontal attitude (dip in a few feet per mile) are effectively 'conformal', as far as the layering is concerned, with the Pleistocene deposits. These beds are mainly arenaceous, with soft 'Pale Beds' alternating with non-continuous indurated beds. Some shale and coal seams are typical of the system, but these are of small thickness and the dominant seismic members are probably the 'Pale Beds' since these are comparatively massive and continuous. At a depth which is greater than that significant for surface waves of the type under study, but effective in refracting P and S waves, the area is underlain by Mississippian limestone with a velocity of about 20,000 ft/sec.

2.30 The Primary Experiments

All the seismograms from the primary series of experiments are included in Section 5.00. Information on the coding, experimental conditions and so on are given in Table 4.

2.31 8 lb Charge Series. This series was carried out on the Drowning Ford site, using a single instrument at various distances from the charges. Each charge was on undisturbed prairie, and cratering effects have been reported by Jones, Spackman and Winfield (1959). The zero timer was under development so few zeros are recorded. There is no indication of the arrival of the airblast. The instrument was not really suitable for these charges, due to the small gain and low time resolution. Nevertheless, the seismograms have some value in association with other charges on this site and elsewhere. The three components of Seismogram 4D, at 75 feet from the charge, are included. The remaining seismograms at this scale are only shown as single, radial components. (At this charge size only, the vertical and transverse components are less consistent than the radial in profile).

2.32 30 lb Charge Series. These charges were better suited to the gain and paper speed. Zero marks are available on all records, but the time resolution is only about 0.01 sec. No time of arrival of the airblast is recorded. The charges were cast hemispheres initiated at the centre of the flat base, which was in contact with the prairie. Cratering data have been given by Jones et al. (1959). The seismograms are shown in sets representing one component of motion at a variety of distances.

2.33 60 lb Charge Series. These charges were centrally initiated cast spheres resting on the prairie. Zero time is available on all records, but not the air blast arrival time. Cratering data have been given by Jones et al. (1959). The seismograms are similar in form and distance to the 30 lb records, and are given in sets

showing one component at a time. The vertical component at all distances shows what is postulated to be a refracted P wave as a first arrival, a single crest showing at the shortest distance and a train of crests and troughs at the longest distance. At this distance, 800 feet, the train of refracted P waves has not separated completely from the strong motion. The phase also shows at much reduced amplitude in the radial component. Similar records have been obtained from identical charges detonated with their diametral planes at ground level. The records are basically similar to those from the surface bursts and are not discussed further in this dissertation.

2.34 500 lb Charge Series. These charges were transitional in type between the cast charges used for the smaller trials and the block-built charges used for the larger trials. This transition was, at the time, the main purpose of the series. Charges 30D and 31D were built from small blocks of TNT, charge 32D was a charge cast in 'slices' in a ring mould and charge 33D was a solid cast hemisphere. Details of the cratering have been given by Jones et al. (1959), and details of the methods of fabrication have been given by Pennie, Philips and Holdsworth (1960) and by Philips, Ditto and Holdsworth (1960). The experiments showed that the block method of construction was entirely adequate, and produced results indistinguishable from those of solid cast charges. Two distances were used for the seismic work, 500 ft and about 1000 ft. No zero marker was available. The records at 1000 ft are so similar that they are indistinguishable, thus verifying not only the uniformity of the charges and ground, but also that of the seismic recording system.

The seismogram for 500 ft (30D) and one of the 1000 ft seismograms (32D) are included in Section 3.00. The P wave shows up very clearly in the vertical and less distinctly in the radial trace. On the original record there is a faint displacement in the transverse trace also. At 1000 ft the P train has not quite separated from the strong motion.

In 1961 an additional 500 lb charge was detonated on the Watching Hill site, as an extension of the programme of additional experiments suggested by C. Kisslinger. The records are discussed later, in association with the buried charges of the same programme.

2.35 10,000 Charge Series. Many records are available at this charge size, since in addition to the direct series detonated for the SES programme, the Station acted as agent for Bell Telephone Laboratories in a further series. Advantage was taken of all these charges for seismic recording. The charges were divided fairly evenly between the Drowning Ford site and the Watching Hill site, and thus afford a means of comparing the two ranges. This is essential if we are to consider results from the two sites as a single series.

All the charges were block-built charges, initiated at the centre of the base. Cratering data for many of these charges have been given by Jones et al. (1959) and Jones and Krohn (1960a). Some of the seismograms, and preliminary discussion, are contained in a preliminary report (Jones, 1960).

The ten seismograms 34D-43D were the earliest ones obtained on the Drowning Ford site. All the records are closely similar in form with the exception of the closest, that at 2000 ft. This record shows a double pulse of large amplitude in the vertical and radial

traces at the start of the strong motion. This may be compared with a pulse of similar profile obtained at the Nevada Test Site (see para 2.40). Many of the records have both zero time and the airblast arrival recorded. Although a fresh GZ was chosen for each shot, the seismograms may be treated as a single series since all the measurements were taken along the same seismic line. In one shot, a rotation of two or three degrees was required in the instrument alignment. Seismograms 44W-46W were obtained on the Watching Hill site, in a similar way to the Drowning Ford records. Seismograms 47W to 58W were also obtained on the Watching Hill site but for this series re-consolidated GZ's were used, and the instruments were disposed in azimuth around GZ as a first attempt to study the symmetry of the wave propagation.

2.36 40,000 lb Charge Series. The first 40,000 lb charge was detonated on the Watching Hill site in August, 1960, as the focus of a large international trial involving agencies from Canada, the United States and Britain. Details of the experiments have been published (SES 1960, 1962). Data relating to cratering effects and permanent and transient displacements are contained in Jones and Krohn (1960b). Data on the power spectrum in the plastic zone have been given by Barton (1960).

Five seismographs were used on a single seismic line, from 3000 ft to 10,000 ft. Copies are included as 59W-63W herein. The seismic line coincided approximately with that of 44W, 45W and 46W at the 10,000 lb level. In addition to these main series seismograms, records were obtained from a 25 cps geophone spread

at 55,000 ft on an extension of the same line. The latter records are discussed in para 2.43.

The second 40,000 lb charge was detonated on the Drowning Ford site on 17 August, 1962. The charge was used primarily for test purposes by the Bell Telephone Laboratories, but some participation of a pure research nature was included by SES teams. The seismic participation consisted of a single line of instruments every 1000 ft from 3000 ft to 7000 ft from GZ. Excellent records were obtained which included zero time marks and time-of-arrival marks on all records. These records are included herein as 75D to 79D and provide a direct comparison between the Watching Hill site (records 59W-63W) and the Drowning Ford site at identical distances from two similar charges.

In addition to the on-site participation, seismic records were obtained by teams from the University of Alberta (U. of A.--SES MOHO project*) in the vicinity of High River. Some aspects of the records obtained are discussed elsewhere in this dissertation.**

2.37 200,000 lb Charge Experiment

This charge was detonated at 17:30:1, GMT on 3 August, 1961, as the focus of the largest international trial yet held at Suffield. It is believed that up to the present this is the largest non-nuclear

* A programme undertaken by the University of Alberta to investigate the true attitude of the MOHO and Conrad discontinuities under the western plains. The University was supported by grants from DRB and from A.R.P.A., and by Munitions and Field teams from SES.

** A third 40,000 lb charge was fired July, 1963. See 127D-131D Table 4.

detonation of this controlled type in history*. Field data, and a listing of projects have been published (SES 1962). Obviously it will be several years before all the data have been published. Papers** available to date include Jones, Krohn and Dewey (1962), Jones, Kisslinger and Cyganik (1961), Jones, Reiniger and Cyganik (1962), Jones (1961), Kisslinger (1961, 1962), Kempster (1962), Winfield (1962), Johnson (1962), Beare (1962), Dewey (1962) and Groves (1962). The high pressure level ground shock spectrum was recorded by Space Technology Laboratories and a preliminary report is available (Halsey and Barton, 1961). It is doubtful that this spectrum is directly relevant to the present analysis.

Excellent records were obtained by G. Frantti*** of the body waves and surface waves near the village of Hays, 100 Km from the test site. Instruments used were of the Benioff three-component type.

The strong motion seismic recording was undertaken jointly by the writer and Dr Kisslinger, Saint Louis University. By combining the instruments from the two establishments in a single network, exceptionally good coverage was obtained. Eleven instruments were used on three lines radiating from GZ as shown in Fig. 7. The main line was similar to that used on smaller trials, and included all the

* A similar charge of 1,000,000 lb TNT is scheduled for July, 1964 at SES.

** Classified papers not listed.

*** University of Michigan - personal communication.

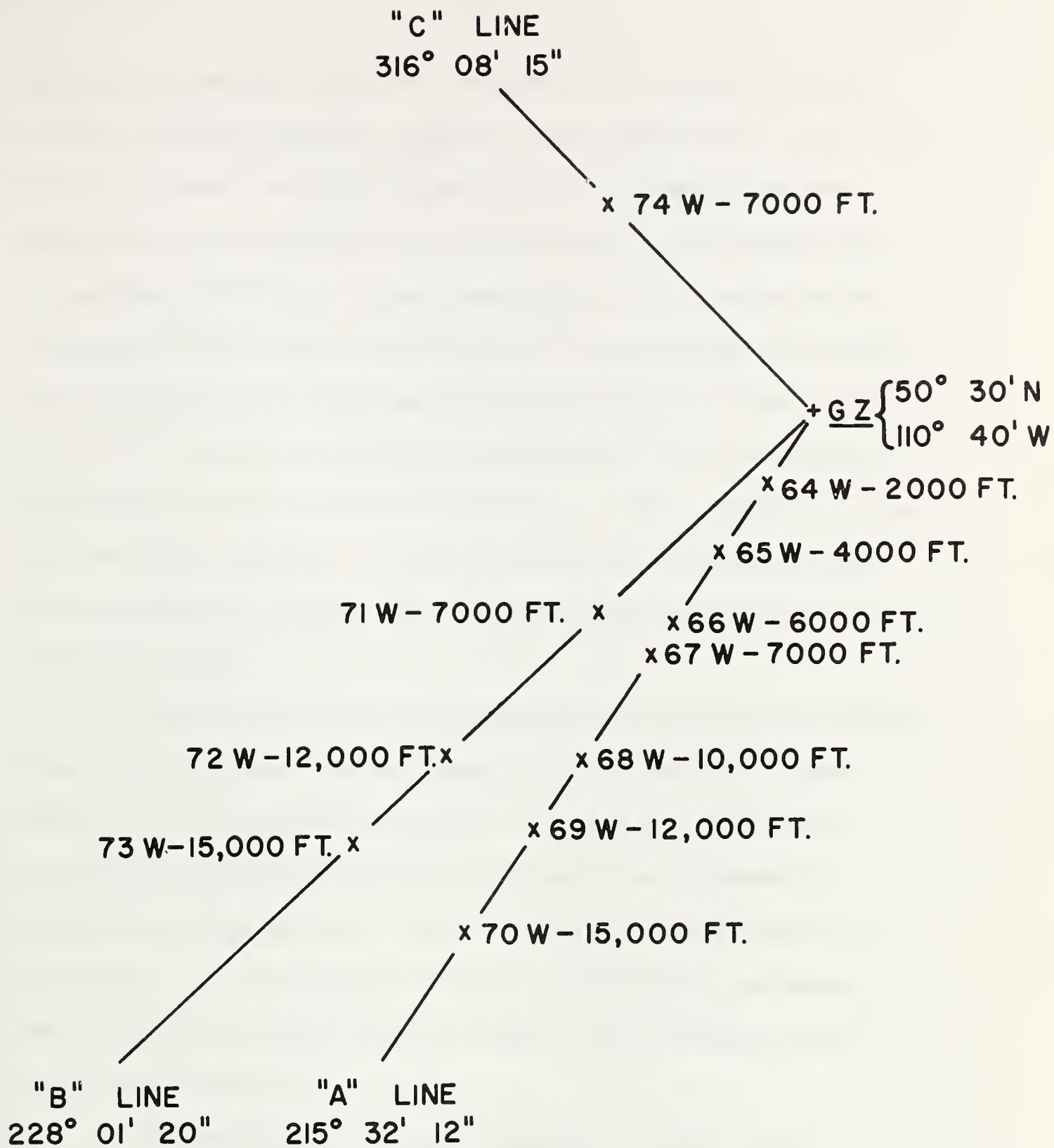


FIG. 7
SEISMIC NET
100 TON TRIAL - 1961

Suffield instruments. The other two lines were intended to detect azimuthal asymmetry, the main interest of the Saint Louis team. The 2000 ft instrument was of low magnification, 7.5 static, and was installed in a shallow pit, being firmly bonded to the ground. The pit was then covered with a heavy steel plate and the edges sealed to exclude at least part of the airblast. The remaining instruments were mounted in the standard way directly on lightly scraped prairie.

No zero time was recorded on the trial (i.e. directly on the seismic records), due to the failure of a surge suppressing diode after the dress rehearsal. However, zero can be obtained with adequate precision by a variety of indirect methods (see Jones, Kisslinger and Cyganik, 1961).

In spite of the very long records (in excess of 45 seconds) it was found that the trace positions at the end of the run were identical with the pre-shot positions. There was no detectable instrumental drift and obviously no instrument was subjected to accelerations large enough to cause bodily displacement relative to the ground. It is believed that the low magnification instrument at 2000 ft was in as high a pressure region as any previously used for recording of this type.

The seismograms obtained are given in reduced form in Section 5.00. It will be appreciated that, due to the length of these records, considerable reduction in size is necessary for printing purposes. Nevertheless, these prints are adequate for measurement purposes provided very minor events are not under study.

2.40 Subsidiary Experiments

2.41 Contained and Venting Charges at SES

In order to elucidate certain aspects of the multi-ton records, and with the auxiliary purpose of providing sources for the U. of A.-SES MOHO project, several charges of 1000 lb TNT were detonated in geometries different from that used for the main series of experiments. These are enumerated and the records presented without comment in this section. Discussion of the records is contained in Section 3.50.

Charge FE 549-4 was a 1000 lb cast sphere of TNT buried in a shaft dug approximately on the main seismic line of the 200,000 lb trial, in the region between Watching Hill and Juniper flats. The charge centre was at a depth of 23.5 ft, chosen to correspond with one of the scaled depths of the Stagecoach shots (see Section 2.42), and the shaft was stemmed with the excavated material to the original surface level. Seismographs were placed along a single line every 1000 ft from 1000 to 5000 ft. The charge produced a large cavity collapse crater with some venting, but the airblast pressure was very low, equivalent to that from less than half a pound of TNT at the surface zero*. The seismograms obtained are included herein as 94J-98J.

Charges FE 549-1 and -3 were similar charges consisting of cylinders of cast TNT, lightly cased in a case 6 ft long by 18 inches in diameter, weighing 1000 lb (TNT) and detonated at the bottom of fully tamped wells 53 ft deep on the flank of Watching Hill. On the first charge seismographs were used at every 2000 ft from 2000 ft to 10,000 ft. The recording at 2000 ft was not successful, but the remaining four

* T.K. Groves - unpublished data.

records are included herein as 100H-103H. For the second trial the seismographs were disposed in azimuth at a distance of 2000 ft from the surface zero. Seismograms are included as 104H-108H.

Charges FE 552-7 and -8 were similar in geometry and location to the last two trials, with the exception that water tamping was employed instead of soil tamping. On the first trial of this pair the seismographs were disposed in azimuth at 2000 ft, as for FE 549-3, while for the second trial only two seismographs, similarly disposed were employed for confirmation purposes. The records are included as 109H to 116H.

LT 285-1 consisted of a charge of 296 lb detonated at a depth of 3 lambda (20 ft) on the Drowning Ford test site. This charge vented, though previous experience on other test sites had indicated that the charge was at containment depth. This may have been partly due to the fact that the wooden cribbing was not removed from the shaft during the stemming process. Records were obtained at 500 ft and at every 1000 ft from 1000 to 5000. Records are included as 89D to 93D.

2.42 40,000 lb Charges at the Nevada Test Site

The writer was fortunate in being invited to lead a team from Canada to participate in Operation Stagecoach at the Nevada Test Site during March 1960. The operation was carried out in Area 10 of the test site, in close proximity to the craters of the Teapot S and Buster-Jangle Nuclear shots, and close to the later trial of 1,000,000 lb TNT called Operation Scooter. The shallow geology of the site is one of a thick deposit of desert alluvium, consisting mainly of lightly cemented sands

and gravels. The upper levels, to a depth of between 50 and 100 ft derive mainly from a limestone source, while the deeper levels to at least 500 ft derive mainly from Rhyolite and Tuff.

The three shots of Stagecoach were identical, with the exception of the depth of burial of the charges. In each case, a cylindrical shaft was sunk to the required depth, a spherical cavity excavated, and the charge built in this cavity as a nominally spherical charge of 40,000 lb TNT. Initiation was by a single electric detonator in a spherical booster charge. The excavated material was returned to the shaft as stemming, and compacted approximately to the original density. The three charges were placed at depths 80 ft, 17.1 ft and 34.2 ft, corresponding to 2.3 lambda, 0.5 lambda and 1.0 lambda. The three charges were functioned at intervals of about one week in this order.

For each charge a single seismic line, using three instruments, was established, instruments being at 3000, 4000 and 5000 ft in each case, and the azimuth being kept constant. A trial record covering the operation has been issued (Jones and Winfield, 1960). The records obtained are included herein as 80N to 88N, and are discussed elsewhere in this dissertation.

2.43 Records at Longer Distances from SES Charges

Many records have been obtained at distances from the SES charges greater than those discussed in the previous sections. Generally, these are not relevant to the present dissertation, but certain records are of interest in showing the existence of air-coupling at quite long ranges.

During the 1960 trial of 40,000 lb, the writer had the use of a Texaco seismic truck belonging to the University of British Columbia. This equipment was used at a nominal distance of 56,000 ft from GZ on an extension of the main seismic line. The ground between GZ and the recording site was mainly flat, but some rolling country intervened. The site consisted of a shallow saucer-shaped depression below a feature known as the Hogback. The site lies in a generally sandy area, but is itself a silt deposit not unlike that at Watching Hill.

Twenty-two geophones of 25 cps type were available, and these were used in a spread some 2000 ft long, with the recording truck in the centre of the spread. No pre-suppression was used, and the filter circuits were inoperative, so that the low frequency cutoff was dependent upon the geophones. The gain was set approximately equal on each channel, and was approximately the maximum available, since the area was found to be generally quiet. In view of the anticipated record length, the paper was allowed to run freely from the camera and was processed immediately before opening the (stifflingly hot) cab.

A few preliminary shots, with 1/2 lb charges air-burst a few hundred yards from the spread, produced typical records showing refraction arrivals well separated from distinct air-coupled waves of the type recorded by Dobrin et al. in their investigation of air-coupled waves (loc cit).

The radio count-down from the control bunker was monitored at the site, and a zero-time accurate within the operator's reaction time was recorded by releasing two held down 'line test' switches,

one in each bank of recorders. Visual observation of the monitor panel detected the passage of a refracted wave which was later found to be barely above the noise level. An approximate velocity of 15,000 fps was calculated for this arrival. The precision is low, and beyond assuming that this probably represents a refraction from the Mississippian Limestone, little can be said of it.

Approximately 45 seconds after zero, the first geophone detected an arrival, and the others picked it up in succession. As the signal transferred from the inside bank to the outside bank, the airblast arrived at the recording vehicle. An assistant outside heard the detonation distinctly, and the writer inside was somewhat startled by the violence of the arrival. The vehicle acted as an efficient seismoscope. The relevant portion of the record is included herein as Fig. 8. The velocity of the arrival over the spread length turns out to be $2.808/2.52$, or about 1120 fps, a reasonable value for the sound velocity. The typical period of the early part of the train was 0.03 sec., but in view of the high frequency geophones, this is not significant. The record length for this phase was around ten seconds before the signal dropped to noise level. This indicated an aircoupled train of at least 11,000 ft - a fifth of the epicentral distance.

The writer, both from the record and from his physiological sensations at the time, is in no doubt that this was classical Press-Ewing coupling. The pressure pulse at this distance would be no more than a few hundredths of a psi, and the front would be of essentially constant speed. At the time this was the most distant

positive identification of air-coupling from a surface burst explosive charge. However, records which may show air-coupling were obtained by G. Frannti at Hays, 100 kms from the 200,000 lb GZ. Benioff, Ewing and Press (1951) also give evidence of the arrival of an air wave at 265 km from a natural earthquake, which they interpret as being an air-coupled wave produced in a track length of 55 km over low velocity sediments, and then refracted down to the recording site from a vertical height of 40 km. An interesting illustration of the duration of the seismic effects, and of the large surface area undergoing disturbance simultaneously, is provided by the fact that the Sprengnethers at 10,000 ft were still recording quite strong motion while these effects were being recorded at 56,000 ft.

The records shown in Fig. 8 indicate two distinct bursts of energy of greater intensity than the mean value. The data are not sufficient to allow positive interpretation of this effect, but it is probable that the second burst is an indication of atmospheric focussing at some point in the track.

During the same trial, records were made by Imperial Oil Ltd., at Calgary*.

As mentioned in para. 2.37, a team from the University of Michigan made recordings of the seismic effects of the 200,000 lb charge, using Benioff equipment near the village of Hays, 100 km

* A. Mair, Imperial Oil Ltd., personal communication: "We heard two distinct arrivals and recorded three". (See also, Mair (1960)).

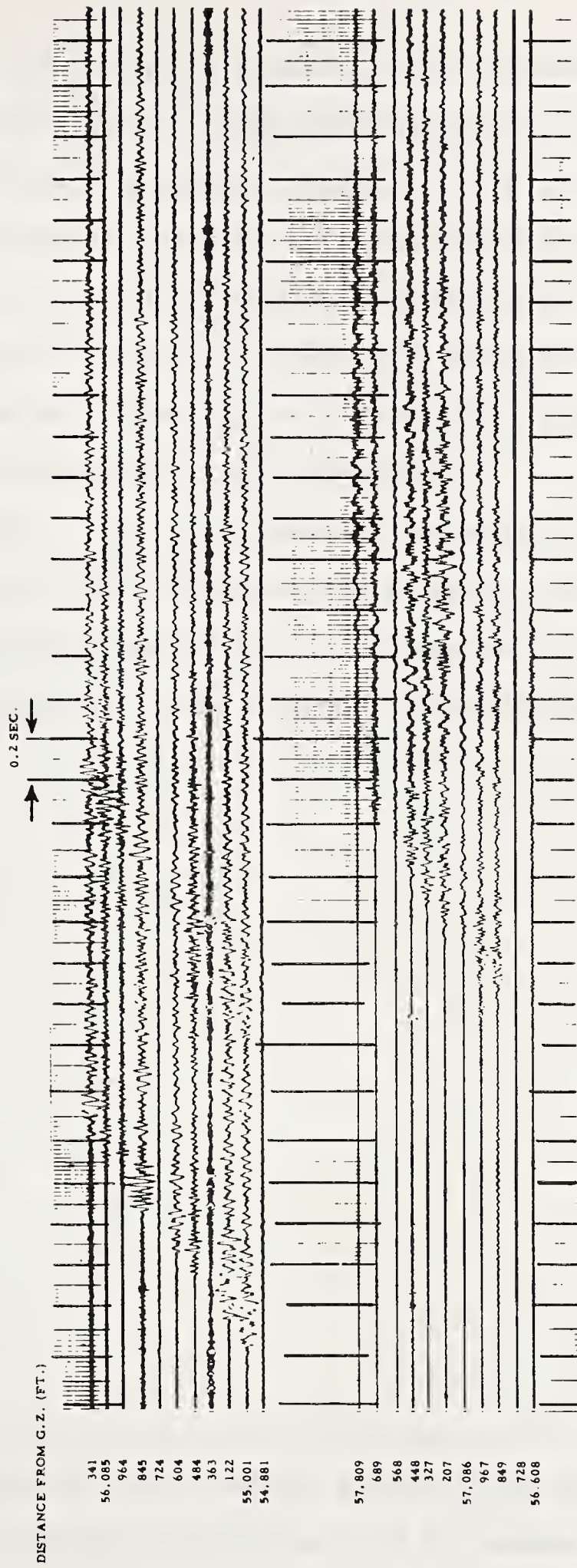


FIG. 8

AIR - COUPLED GROUND ROLL 55,000 FT. FROM 40,000 LB. CHARGE

from the test site. Some interpretation of the records has been given by Frantti* (1962). An air-coupled ground roll, presumably of classical Press-Ewing type was detected, but it is interesting to note that Frantti was able to show close similarities between these waves and the general microseismic background in the plains areas. Whether or not this is an indication that much of the microseismic noise in these regions is produced by coupling to wind is outside the scope of this dissertation.

Partly at the writer's request, and partly to provide data for another study**, equipment used by the U. of A. MOHO project was allowed to run in various locations until times consonant with the arrival of the airblast from certain surface bursts.

* Paper presented at S.E.G. meeting, Calgary, 1962. (See also footnote p. 90).

** E. Reinelt, Doctoral Dissertation, U. of A., Edmonton, Alberta.

3.00 GENERAL ANALYSIS

3.10 Zero Time and the Arrival of the Airblast

The correlation of zero time, and the time of arrival of the airblast, is of importance in the interpretation of the seismograms. In some cases these data are available directly from the impressed marks on the records. In all cases other than the very small charge records, the arrival of the airblast is also indicated by a distinct 'blip' on the records caused by the action of the airblast on the case. If the travel time of the airblast is known, zero may thus be obtained even in the absence of a zero marker. Where the refracted P wave is detectable as a first arrival, zero time may also be estimated from the known travel-time curve.

Table 5 gives the airblast data abstracted from the seismograms, the same data corrected for ambient conditions, and the corrected data scaled according to Hopkinson's Law to a 10,000 lb charge. Corrections for ambient conditions are not wholly satisfactory with the type of data available. No correction was made for ambient pressure, since the changes about the standard of 13.69^{*} for the site were small. If data from other sites are to be correlated with these, however, conversion to sea level would be appropriate. Corrections were made for the mean wind by using local measurements at two metre height, the measurements being taken close to GZ and as near zero time as practicable. Similarly, corrections for the mean temperature at two metres were made to convert the readings to a standard of 32°F.

* psi.

After preparing Table 5, the writer attempted to obtain, for comparison, a 'standard' travel time curve. It appeared that, while ample data exist out to about 600 ft from a 10,000 lb charge, few data are available beyond this distance. The data given herein are, therefore, the best available experimental data, and an expansion of previous data by a factor of nearly fifteen. It will be seen that, for these moderately short distances, the velocity of the front is well in excess of the sonic velocity, and errors would be involved in assuming a constant velocity front even at the out-stations.

3.20 The P Wave and Postulated S Wave

At points sufficiently remote from GZ, the first arrival will be a refracted longitudinal body wave, or P wave. This statement is true provided the seismic velocity increases in some way with depth, and provided the gain of the instrument is sufficient to detect the low energy arrival. In the present dissertation, analysis of the P wave is restricted to identification and the abstraction of incidental information, since the experimental system was quite unsuitable for a study of this event.

The P wave may be identified as the short train visible in the vertical component of Seismogram 35D, starting about 0.4 sec. after zero. From this point it is possible to trace the event forward and back in the various records. Table 6 gives the travel time data abstracted for the event. No P wave data are quoted for the small seismograms (before 12D) since, in the interpretation of the writer, the airblast arrival is the first recorded event.

This could be disputed, but confirmation may be obtained by comparing the amplitude of the P wave in 11-13D with the amplitude of the first arrival in 4-7D. The arrival times quoted for the P wave in the 200,000 lb trial are based upon the calculated zero (see Jones, Kisslinger and Cyganik, 1961).

Since there are two test sites involved, the P data are not necessarily reconcilable between the sites, and are therefore plotted separately in Fig. 9. Actually, the Watching Hill data agree well with the Drowning Ford data for the high velocity layer. Although not very suitable for a refraction analysis they may be interpreted in the standard way (see, for example, Dobrin, 1960). This is worth doing in view of the normal seismic survey conducted by Century (see Appendix B).

For the Drowning Ford Site the data indicate a three layer system consisting of unconsolidated sediments with a velocity of less than 2000 fps down to 70 ft. A velocity of about 6900 fps between 70 ft and 300 ft represents the horizontal Foremost beds of soft shales and sandstones. Below this level the velocity rises to about 8400 fps, possibly indicating the somewhat more competent Basal Foremost. This interpretation may be compared with the Century data given in Appendix B, which give 2200 fps to 75 ft, 6000 fps down to 225 ft and 7700 below this depth. The agreement is satisfactory considering that the present analysis is based upon a large variety of seismograms, taken at different times with instruments of low gain. The P wave amplitude is barely above the recording threshold of the instruments, and the strong motion region has signal strengths at least an order of magnitude greater.

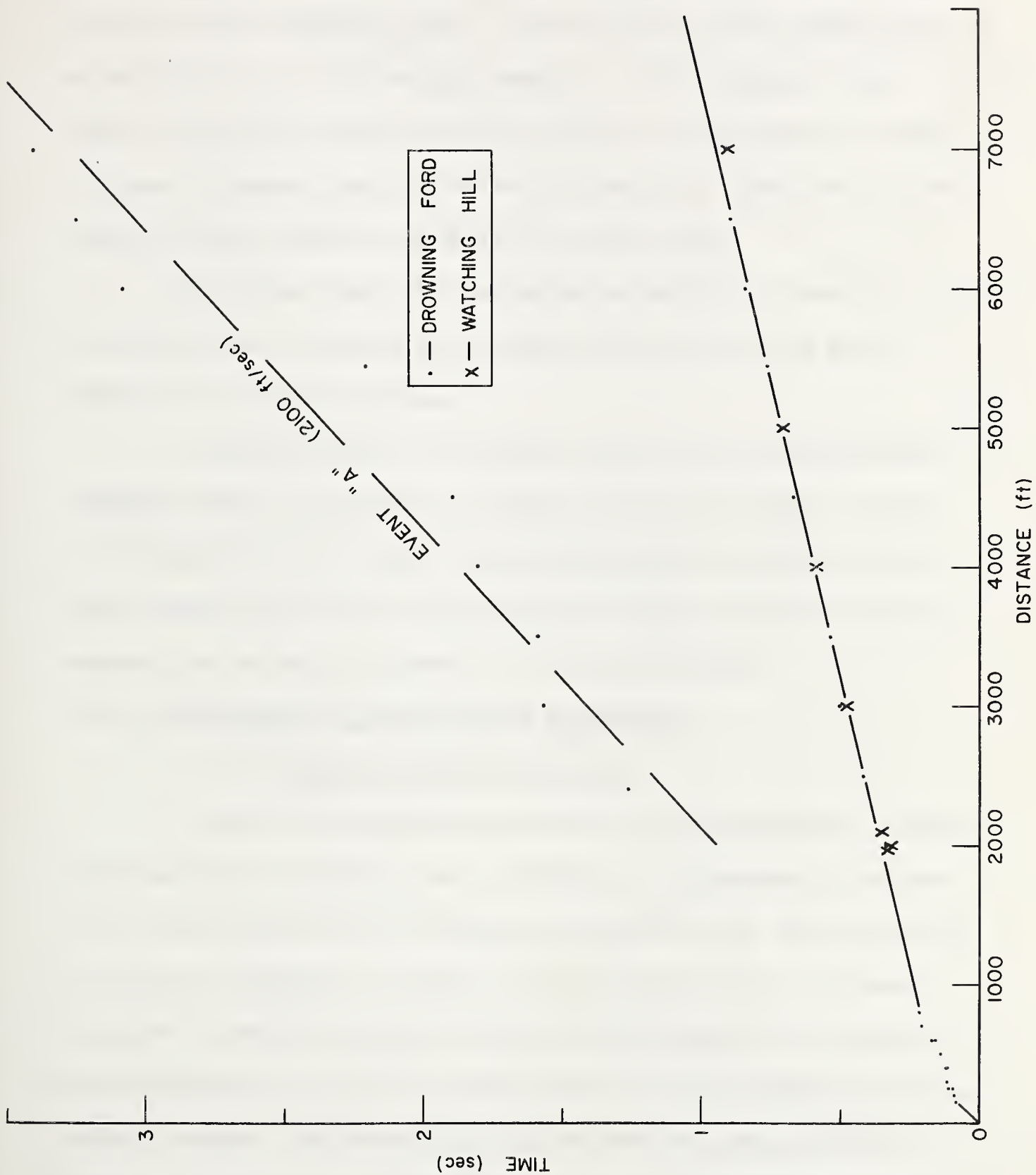


FIG. 9
TRAVEL - TIME CURVES

An event, marked A in 36D, is occasionally to be seen as an abrupt arrival in the radial trace, associated with a synchronous arrival in the transverse trace. The amplitude is low, about that of the P wave, and precise measurements are not possible. The travel time plot is shown in Fig. 9, but the scatter tends to show that some erroneous identifications are included. The mean step out velocity between 2000 ft and 6000 ft is about 2160.

This event could be interpreted as merely the start of the surface wave discussed in the next section, but it is more likely to be a distinct phase.

The event may be a refracted S wave, as in unconsolidated sediments there is no reason to suppose that the α/β ratio is that of a "Poisson" solid. Most of the seismologists who have looked at these records favour this interpretation, despite the fact that this requires the sub-surface layers to be unconsolidated.

3.30 On Dispersion in Strong Motion Seismograms

3.31 On Group and Phase Velocity

Despite the apparent simplicity of the relationship between Group and Phase velocities, much confusion is introduced by the fact that the phase velocity is frequently identified with the velocity of the physical wavelet or 'crests' in the recorded train. It seems expedient, therefore, before discussing the strong motion regions of the seismograms, to clarify precisely what is to be understood in the present context. The essential point is that the common practice among seismologists of equating wavelet velocity and phase velocity is acceptable only in regions remote from the source.

Let us define Phase velocity in the usual way as the velocity of propagation of an infinitely long constant frequency constant amplitude sine or cosine wave - essentially a Fourier component. We bear in mind that only in rare circumstances is this wave directly observable. In a non-dispersive medium the Fourier components will have the same constant velocity independent of frequency. Hence if we compound several components, with different amplitudes and in a given initial phase relationship, the compound wave will be an infinitely repeating train of amplitude groups. The train of groups will propagate without change of form, in the common velocity. If, by some means, we can produce a single group from the train, that is a packet starting and ending with zero amplitude and in isolation, we may represent this group, within its space time interval only, by the same set of Fourier components by introducing the fiction that the group repeats indefinitely outside its interval. Two situations may arise in such a case, depending upon the actual form of the isolated packet. In some cases it will be possible to replace the group by a finite number of components, to the necessary accuracy in any practical situation. On the other hand, in the case common to explosion waves, we may have an abrupt change in profile at some point within the group. In such a case a strictly infinite number of components is required to describe the wave packet, and even in practice the packet cannot be described by a small number of components. The difficulty can be overcome by replacing the Fourier component by the Heaviside function if this technique is acceptable for other reasons. (For a reasonably full

discussion of this aspect, see Pekeris, 1959).

Now let us consider the case in which the medium is dispersive - that is to say each frequency of Fourier component propagates at its own, distinct velocity. We assume in all that follows that the attenuation of the Fourier components with distance is either zero or at a rate common and constant for all frequencies. We combine several such components in a given amplitude and phase relationship at time zero (as each component is assumed of infinite length we need not specify the location of the space origin). This superposition of Fourier components is our initial condition, and is the situation considered in a similar way by Lamb (1932, p. 380). The subsequent motion is in general made up of a system of component waves, each travelling at its own velocity, moving in either direction, independently of each other. The result will be a compound wave which will exhibit gross maxima and minima of amplitude, the envelope of which may enclose many individual physical wavelets. The shape of the envelope and of the individual wavelets will continuously alter, so that if, for example, we fix our attention upon a given amplitude maximum in the envelope, and move with it, we shall see the envelope curve lengthen with time, and the shape of the individual wavelets within the envelope change in keeping with the envelope. In the case of surface waves on water, for example, we see amplitude groups move across the surface, each amplitude group being made up of wavelets which form at the rear and die away at the front, the wavelets travelling through the group with a velocity greater than the gross velocity of the group. The wavelet velocity is the velocity with which these wavelets travel, and this

is not the same as the phase velocity of any of the individual Fourier components into which the group may be analysed. In many circumstances, however, common in long range seismology, where we are observing the wave packet well removed from the source region, dispersion has already acted to such an extent that a given region of a wave packet contains only a very narrow range of frequencies in the Fourier components. In this case, little error is introduced by equating phase and wavelet velocity. This is emphatically not the case in the strong motion region where active dispersion is changing the wave profile.

We may, after Lamb, consider the group obtained by superposing two equal amplitude Fourier components. Each component will, of course, have a definite wavelength independent of whether the wavelength is measured as the wave passes a fixed point at the phase velocity, or whether we look at the actual wave profile in space. Summing the two components we get:

$$\begin{aligned}\eta &= a \sin(kx - wt) + a \sin(k'x - w't) \\ &= 2a \cos \left\{ \frac{1}{2}(k - k')x - \frac{1}{2}(w - w')t \right\} \sin \left\{ \frac{1}{2}(k + k')x - \frac{1}{2}(w + w')t \right\}\end{aligned}$$

where $k = \frac{w}{c} = \frac{2\pi}{cT} = \frac{2\pi}{\lambda}$ for the single "k" component,

and $k' = \frac{w'}{c'} = \frac{2\pi}{c'T'} = \frac{2\pi}{\lambda'}$ for the single k' component.

Now if k' is very nearly the same as k, the cosine term varies but slowly with x. The surface therefore has a sine wave profile in which the amplitude changes periodically between the values 0 and 2a.

The distance between the centres of two successive groups is $\frac{2\pi}{k - k'}$, and the system will shift through this space in a time $\frac{2\pi}{w - w'}$.

We may then define as the group velocity the value $\frac{w - w'}{k - k'}$.

In the limit as we bring k and k' together, this reduces to $b = \frac{dw}{dk}$.

If we wish, in this limit, to put the group velocity in terms of the phase wavelength for small perturbations about a fixed component, we have

$$b = \frac{d(kc)}{dk} = c + k \frac{dc}{dk} = c - \lambda \frac{dc}{d\lambda} \quad (1)$$

In this limiting case, we have the usual situation for a dispersed train well removed from the origin. The wavelet profile at any point in the group is almost exactly a sine wave, while the whole group merely looks like a sine wave train which is being progressively 'stretched' as we go along the train. In this circumstance, the velocity of propagation of the wavelets is, to all practical intents and purposes, the phase velocity for a sine wave of the local period

Consider, however, the case where active dispersion is taking place in a complex waveform. Individual wavelets will not be of sine wave form, but we may nevertheless assign a 'period' and a 'wavelength' to any given wavelet. In this case it is more instructive to consider two expressions as below:

First we express the rate at which two successive wave crests are separating due to the dispersion.

$$\frac{\partial \lambda}{\partial t} + c \frac{\partial \lambda}{\partial x} = \lambda \frac{\partial c}{\partial \lambda} \frac{\partial \lambda}{\partial x} \quad (2)$$

Secondly, by definition we have that the group velocity is the velocity at which a given wave profile moves. Thus in the region of a geometrical point travelling with the group velocity b , the 'apparent period' or 'group period' or 'group wavelength' is constant

$$\frac{\partial \lambda}{\partial t} + b \frac{\partial \lambda}{\partial x} = 0 \quad (3)$$

In general, there is a difference in interpretation between the two 'wavelengths' used in (2) and (3). In the limiting case, we are again led to (1) by combining (2) and (3) and submerging the difference in the meaning of λ .

Brillouin (1960) has shown that, if we wish to be precise in our discussions, we should distinguish between signal velocity, front velocity, group velocity, wave velocity and phase velocity - all are distinct.

Evidently, as stated by Stoker (1957) it is important for the usual discussion of group velocity that the motion discussed should consist of a superposition of waves differing only slightly in frequency and amplitude. In practice, particularly for the strong motion region, the motions obtained are the results of the superposition of waves whose frequencies range from zero to infinity and whose amplitudes also vary widely.

As Stoker points out, although it is usual to describe the transmission of energy in terms of the group velocity, this is logical only in the limiting case, and the kinematic concept of group velocity is of primary significance.

Inspection of a seismogram may easily lead to wrong impressions about the actual 'ground profile', in the case of a seismic surface wave, even in the case of a perfect displacement seismograph. For example, a constant period in the seismogram does not of necessity imply a constant wavelength in the ground profile. The effective wavelength of the profile, considered as an entity passing the seismograph, is given by the product of the period and the group velocities at individual parts of the train. If we assume the duration of the train is short compared with the travel time to the seismograph, the group velocity decreases monotonically as we move along the train. In the strong motion region the effect is complicated by the fact that the travel time is usually not long compared with the duration of the source motion. For example, at 2000 ft we may have a train with two to three seconds duration, with a travel time to the start of the train of about two seconds. If we treat the whole train as a 'wave packet' we may talk of a group velocity of about 800 fps. We would not be justified in quoting group velocities for the start and end of the train, calculated as the epicentral distance divided by the travel time from zero to the start and end of the train. This would be acceptable for the front of the train, but the travel time to the end of the train is unknown, since the duration of the originating motion is unknown, and may well be of the same order as the train duration.

Obviously, in such a discussion we must ignore the source motion, at least in the first instance. We must consider the seismogram at the seismograph closest to the source as the signature of the ground

motion at that point, and then investigate the transmission of this motion from this point outwards. Of course, having at a later stage succeeded in describing the change in profile with distance, we can work backwards to the source. This is essentially Sato's method of analysing dispersed surface waves. Care should also be taken to distinguish the 'profile', worked out from a seismogram at a fixed range r , from the ground profile existing at time t , equal to the arrival time of the first motion. Where dispersion is slow, the two profiles are virtually identical, but they differ quite markedly in the case of a rapidly dispersing train.

In many practical cases there is an additional complication, due to the fact that the recorded motion may be compounded of more than one mode, travelling according to different dispersion curves. Close to the source the 'wave packet' will appear to be a single entity. As we proceed outwards, however, we note that the wave packet separates into two or more groups, possibly similar in character, which diverge more and more. The quiescent region between the groups is actually composed of a superposition of short-period waves being shed by the leading pulse and long-period waves being shed by the following pulse. Seismograms 89D-92D furnish the first example of this type of effect recorded in the present research.

In the special case where air-coupling is occurring, additional complications are introduced by the fact that two essentially different wave groups are being superimposed one upon the other.

We may use this to illustrate our discussion graphically.

Let us assume a hypothetical medium in which the phase velocity varies with phase period in the way shown in Fig. 10. Provided we are considering groups in which only a small range of frequencies is involved, we may derive a group velocity-period curve from this phase velocity curve by differentiation. This, however, presupposes that the actual group is approximately sinusoidal in wave form, so that we can assign a 'group period' to the wavelets. The physical reason for the difference between the phase velocity of a given period and the group velocity of the particular region in the wave packet in the region of this period is that the amplitude only of the wavelets change sharply through the group. In a region where the train is of reasonably constant amplitude and only slowly varying period, the phase velocity, wave velocity and group velocity are very closely similar. In the strong motion region this is not the case. Rapid dispersion is taking place, and the wave group is neither approximately sinusoidal in form nor constant in amplitude, even from one crest to the next adjacent. Thus, close in there is little meaning in assigning a 'period' to a specific group velocity. Let us, however, move rather farther out so that some appreciable velocity sorting has occurred, so that the individual wavelengths look roughly sinusoidal, and we can assign a period to each wavelet. Generally speaking, we shall see that the early part of the train shows longer periods than later parts. If we consider two seismograms from stations sufficiently close together that there is a recognizable

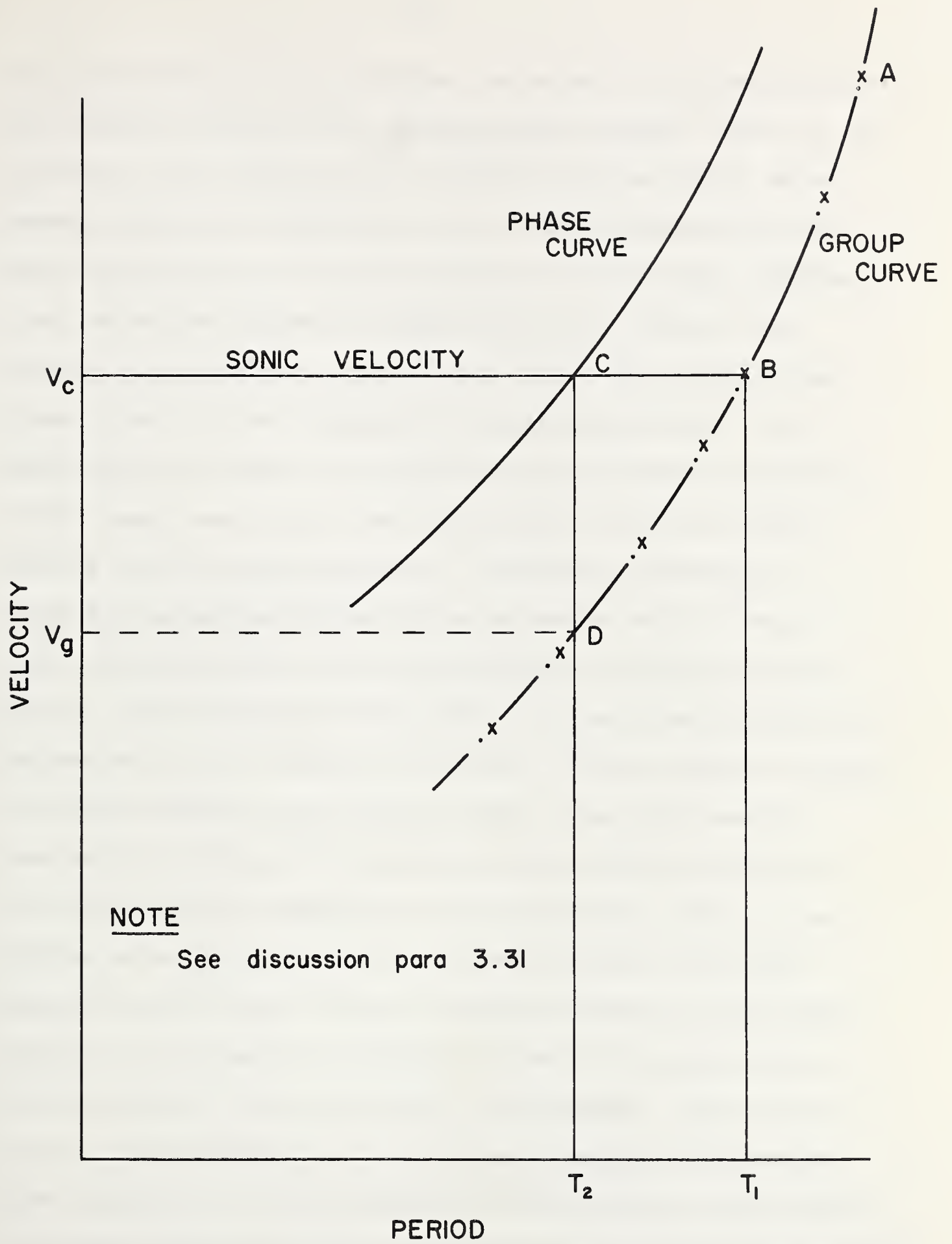


FIG. 10

relationship between the two profiles, we see that the periods associated with comparable regions of the seismograms have changed. Thus it is not feasible to derive 'phase velocity' directly from the record. We can, however, assign group velocities to the comparable regions, but the group velocities for the comparable regions will be slightly different, since the assigned periods are slightly different. From two such seismograms we could plot a curve such as that in Fig. 10, where the crosses refer to values calculated at one station and "dots" values calculated at the other. Each pair of crosses and "dots" is calculated for the 'same' wavelet, but, due to dispersion, the values of group velocity and period will both differ. A practical illustration is afforded by seismograms 59W and 60W, in the region ahead of the air-blast. The first surface wave crest in 59W has a 'group velocity' of 1600 fps, while the "same" crest in 60W has a group velocity of 1800 fps. The wavelet has a wave velocity of 2560 fps - but this cannot be assigned as the phase velocity of any specific period. What can we mean by 'wavelength' in this case? Obviously, we can contrive to compute at least three different wavelengths, at any one station. First, we can consider the wavelength defined by the wavelet speed at that point multiplied by the period. This has a distinct physical interpretation. Similarly, we can compute a wavelength for the actual ground profile when the wavelet is just at its peak at the seismogram. This will be the group velocity multiplied by the period. Finally, if we knew the phase velocity of a Fourier component with this period, we could compute a wavelength given by multiplying the measured period by the phase velocity. Does this latter have any physical meaning? The writer appears to differ

sharply in opinion here with Dobrin et al. (1954), also quoted in EJP page 208, who show a group wavelength computed in this way. It is, of course, merely a matter of presentation, but it appears devoid of physical meaning to the present writer. We may avoid this difficulty - which is really only semantic - by confining our attention to the periods as actually measured on the seismogram. If we do this, we may interpret physically precisely what happens in the case of air-coupling to a rapidly dispersing wave packet. It should be stressed that in the following discussion we are dealing with the coupling of an 'air-induced' train of waves to a dispersed train of waves which is physically present in the ground. This differs quite markedly from the case where the only train existing is the air-coupled, or air-induced, train itself.

Referring again to Fig. 10, let the horizontal line marked 'sonic' be the constant sonic velocity in the air above the medium, and let us assume that a pressure pulse moves in the air above the surface at this velocity, starting simultaneously with the generation of a strong motion pulse in the ground at the same origin. We attempt to predict what will happen at two points, one comparatively close and one comparatively far from the source (illustrative examples will indicate the interpretation of close and far).

Consider first the point close to the origin. The seismograph will first detect long period waves arriving at high velocity, corresponding to point A in the group velocity curve. Successively shorter period waves will arrive with successively lower velocities,

the periods and velocities following the group velocity curve. When we reach point B of the group velocity curve, however, the airblast wave arrives at the seismograph. The period in the dispersed wave is then T_1 . However, there is a phase wave of period T_2 which has the same phase velocity (point C in Fig. 10). The air blast will have been generating this phase wave continuously as it passed over the surface, and therefore an almost pure sine wave of this period will begin passing through the seismometer position simultaneously with the arrival of the airblast. Thus in the region immediately after the arrival of the airblast, the seismogram will be a composite waveform of two apparent periods, T_1 and T_2 , with the added period T_2 considerably shorter than the period of the original ground wave. Seismogram 66W furnishes a good example of the abrupt arrival of a relatively short period wave in this way. The nature of the wave form in the succeeding time interval will depend upon the relative amplitude, periods, and phase relationship of the two superimposed wave groups. If the air-induced wave is dominant, a virtually constant period wave, of period close to T_2 and virtually constant amplitude will persist until a time corresponding to the point D in Fig. 10, which represents a point in the normal dispersed wave which has a group period equal to the period of the phase wave of the sonic velocity. The actual duration of the train will thus depend upon the distance from the source and be proportional also to the intercept CD. Thus, at a range R the duration of the train will be given by

$$\frac{R}{V_c} - \frac{R}{V_g} = R \left\{ \frac{1}{V_c} - \frac{1}{V_g} \right\}$$

At this time the air-induced wave will stop, and the dispersed train will continue with successively shorter periods along the group velocity curve. The situation is clearly evident in seismogram 66W.

Now consider a point considerably farther from the source. The duration of the dispersed train ahead of the airblast will be much longer, since the long period waves will be continually gaining ground on the airblast. The situation at the arrival of the airblast will be similar to the previous case, but the duration of the composite train will be longer. The situation changes if we care to consider an air pulse of decreasing velocity. In this case the airblast will be associated with gradually decreasing periods in the dispersed train, that is to say, the airblast will suffer phase retardation compared with the dispersed train. Also, of necessity, the intensity of the airblast, and thus of the air-induced train, will decrease with distance. Eventually we shall approach the true sonic velocity, and the previous situation will be restored, with the exception that the effect of the airblast may be either the sole remaining effect, or alternatively, may be negligible compared to the amplitude of the dispersed wave. As we shall see in the more detailed discussions of the individual seismograms, these situations are, in fact, met in practice.

Finally, provided we have seismograms from at least two positions on a radial line from the epicentre, we may apply Sato's method and calculate the actual phase velocities for various components. In Appendix E a modified version of Satô's method, suitable for our present purposes and adapted to the Stantec Zebra computer

is described in detail. The method is applied to certain of the seismograms from the present series in Section 3.50 and elsewhere.

3.40 The Surface Wave Preceding the Airblast

We may now consider the strong motion region of the seismograms, bearing the above discussion in mind. We deal first with that part of the surface wave which is recorded before the arrival of the airblast at a given seismograph. In 36D and 37D the main trough of this phase is marked 'B', and we confine our attention to the region between the dubious event mentioned earlier and the arrival of the airblast. This region has been discussed in some detail in a preliminary report (Jones, Reiniger and Cyganik, 1962) and the descriptive part of this section is based to some extent upon that report. The report includes a digitization of this region for the 10,000 lb, 40,000 lb and 200,000 lb seismograms, which is too voluminous to include here.

We start with a phenomological description of the region, based upon the data quoted in the cited report.

Obviously, from the geometry of the situation, the records represent surface waves travelling outward from the source, with a gradual decrease in group velocity towards the local air-pressure-pulse velocity. Insufficient cycles are available for a detailed dispersion analysis, but the trend may be seen in Figs. 11 and 12 for the two larger charge sizes. These are plotted for the vertical component only, since this component is somewhat more sinusoidal than the radial and gives a more consistent picture. Group velocity and periods for this purpose were calculated for each crossing of

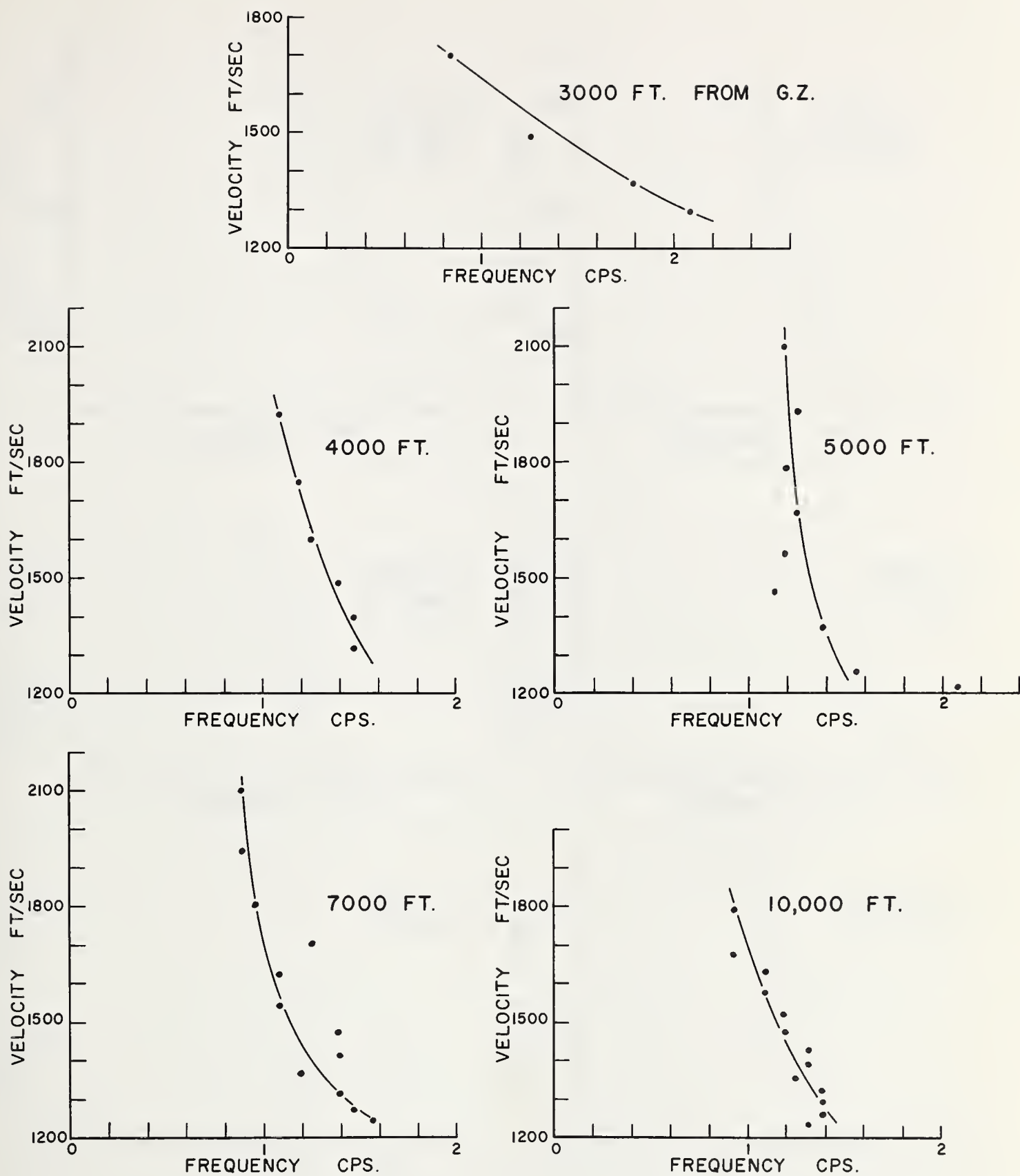


FIG. II

VERTICAL DISPERSION — 20 TON CHARGE

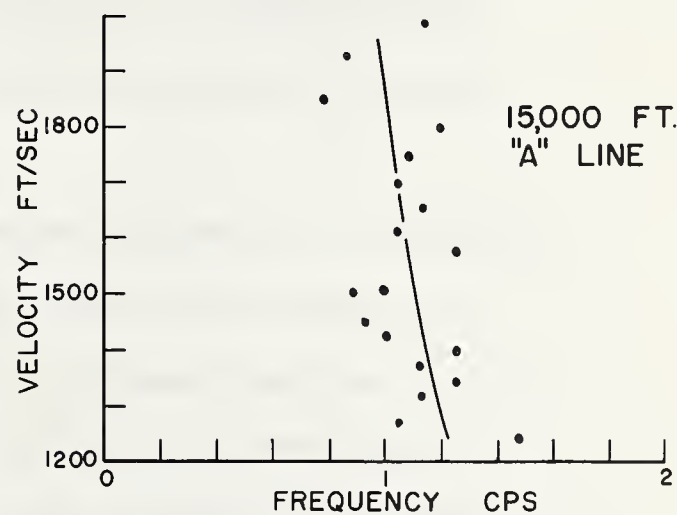
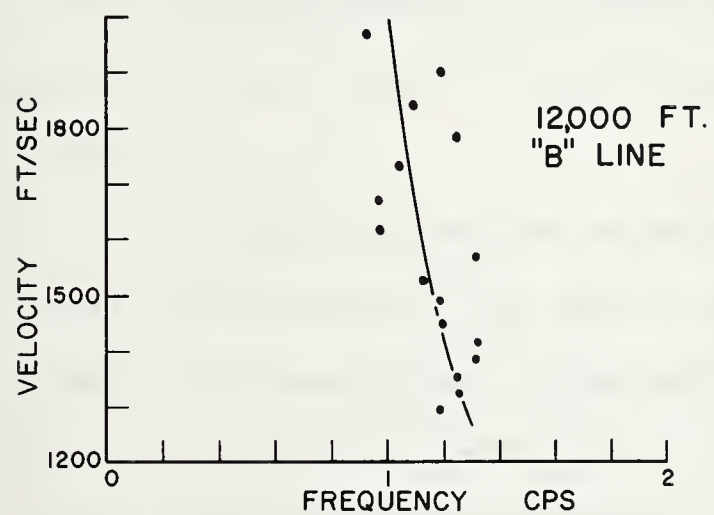
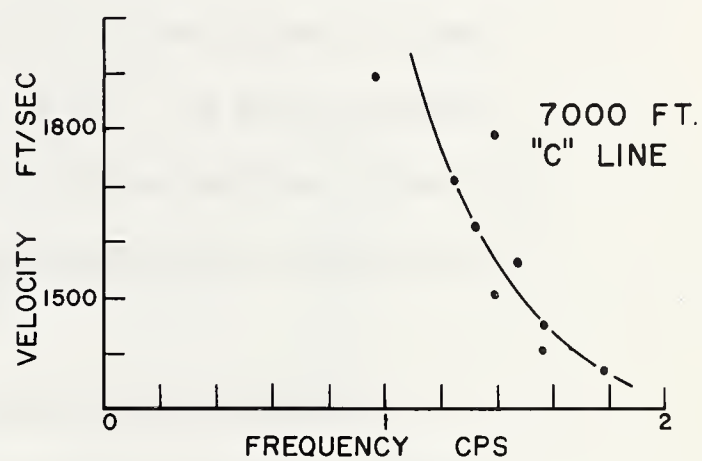
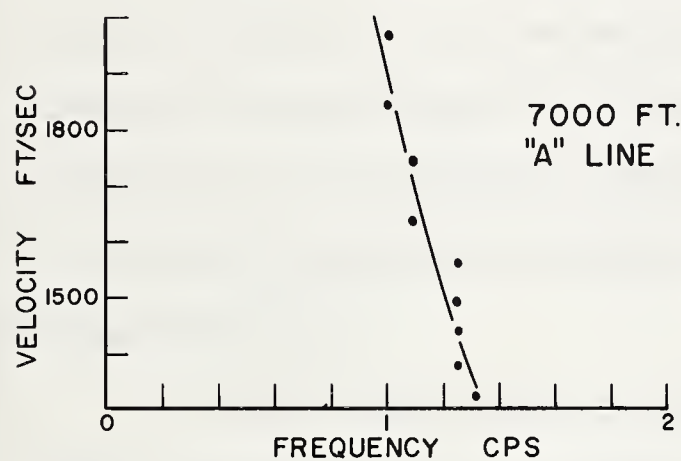
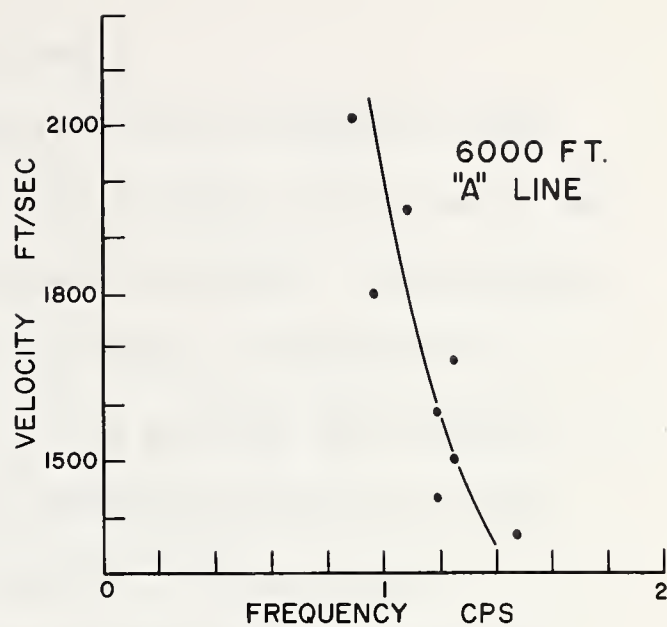
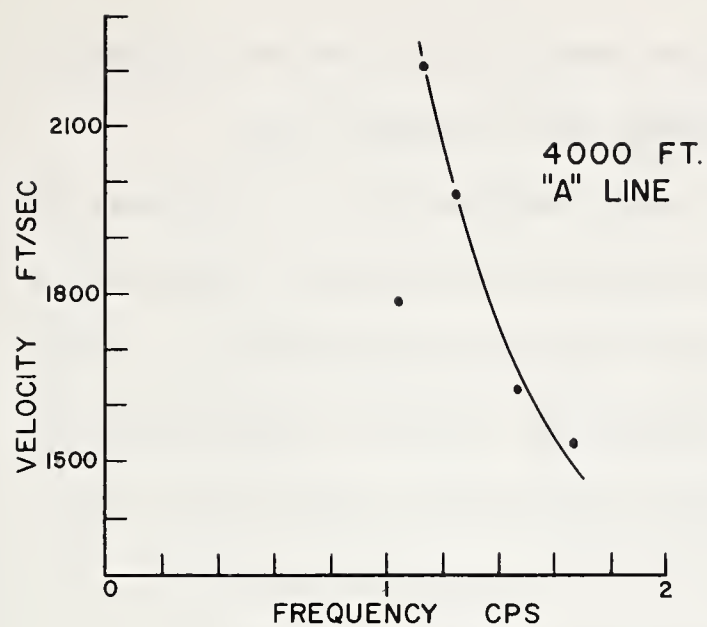


FIG. 12

VERTICAL DISPERSION — 100 TON CHARGE

the base line and for each crest and trough.

3.42 Turning to the trajectories for the region, it will be seen that, in the vertical trace, there is first a slow rise in the ground level, followed by an abrupt downward movement. In the radial trace, a slow initial movement towards the charge is followed by a strong movement away from the charge. It is possible that the true start of the surface wave is the strong down-away motion, and that the up-towards motion is associated with the previous event.

Figs. 13 and 14 show the nine trajectories obtained from 10,000 lb trials on the Drowning Ford site. The arrival of the airblast is the last point on the trajectory. In every case the trajectory is a horizontally elongated prograde ellipse, about $3/4$ of a cycle at the shortest distance and about $1\ 1/2$ cycles at the longest distance.

Fig. 15 shows the trajectories from two 10,000 lb trials on Watching Hill. The orbits are not so clearly defined as the previous ones, but they do indicate a prograde elliptical orbit.

Fig. 16 shows five trajectories obtained with a 40,000 lb trial on Watching Hill. At 3000 ft and 4000 ft the orbits are single retrograde cycles, approximating horizontal ellipses with a 2:1 ratio horizontal-vertical axis. At 5000 ft and 7000 ft, the orbit is still generally retrograde, but the ellipse has narrowed and tilted so that the motion is approximating to an oscillation at an angle of 30° , the high point being away from the charge. At 10,000 ft the orbit has changed radically into a single prograde

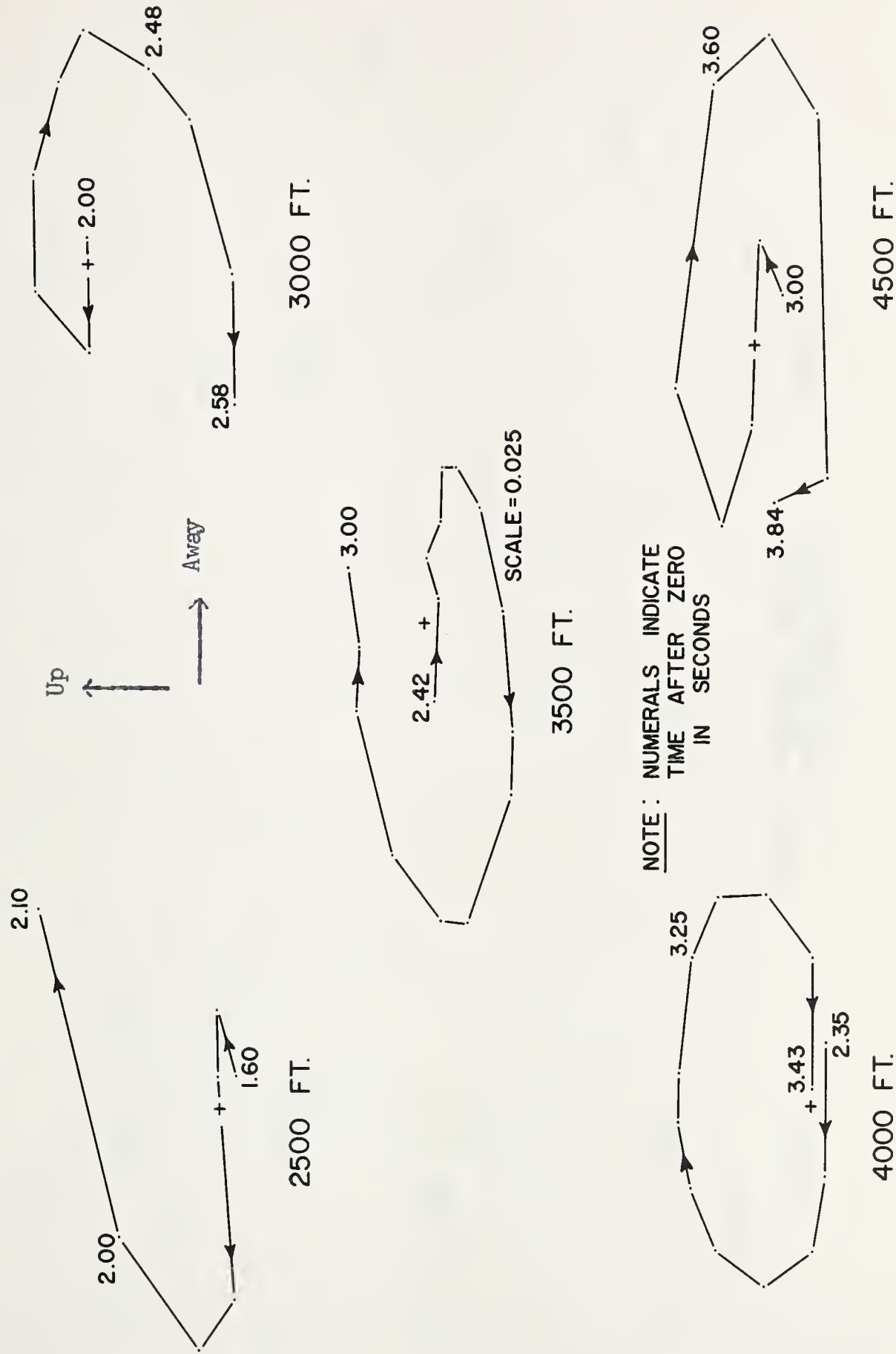
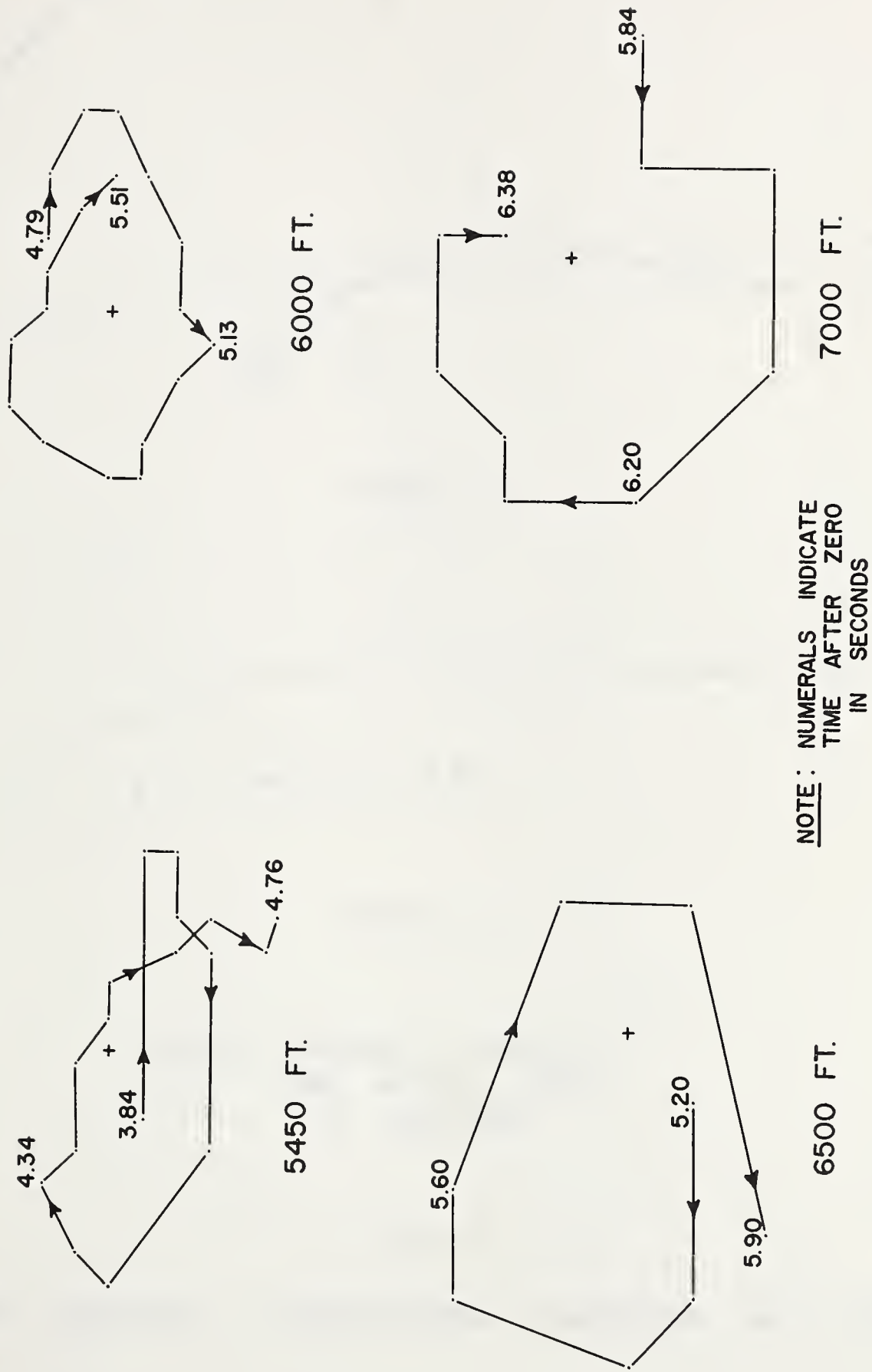
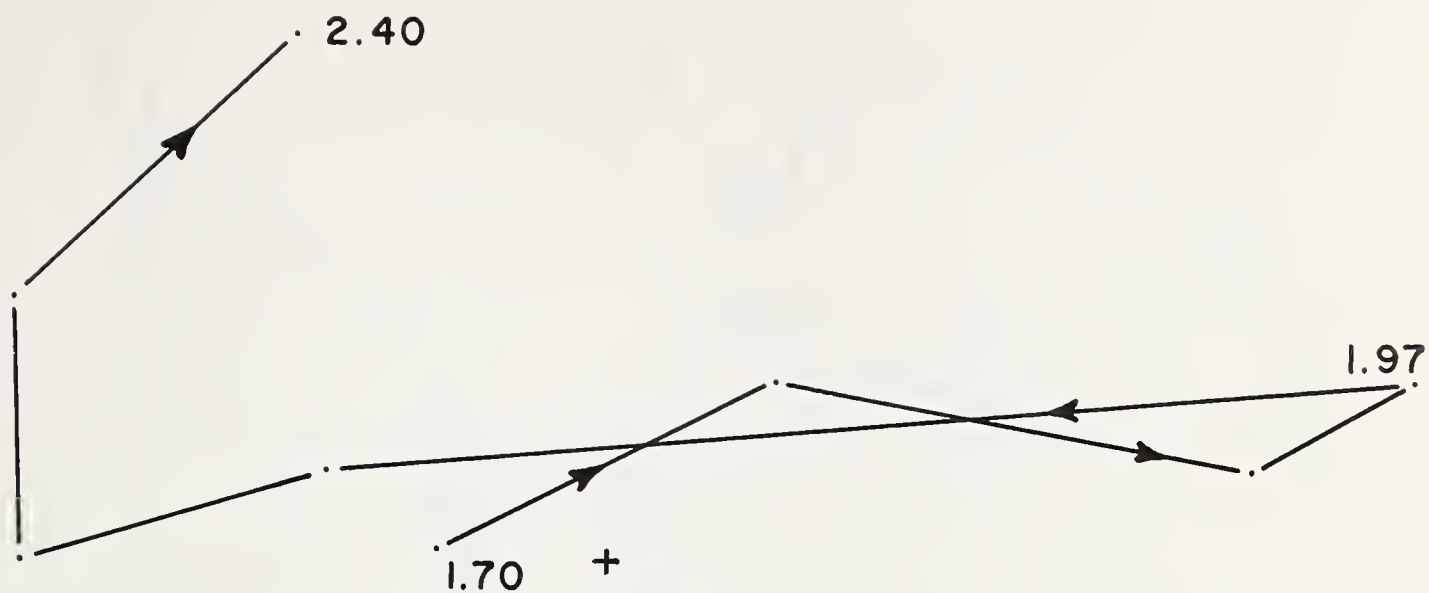
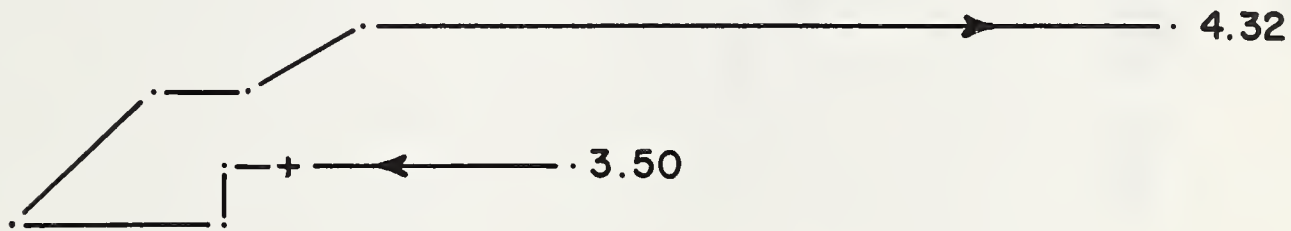


FIG. 13.
5 TON PARTICLE TRAJECTORIES — DROWNING FORD SITE





3000 FT.

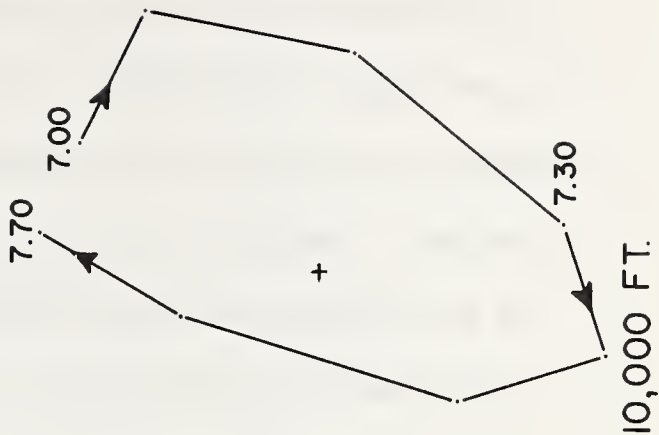
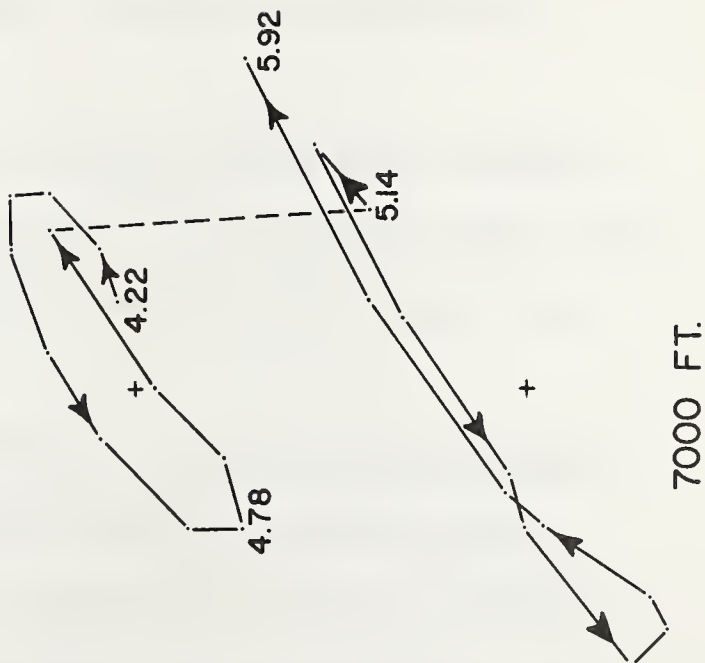
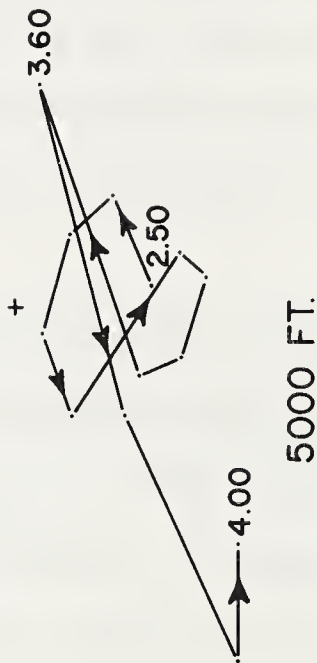
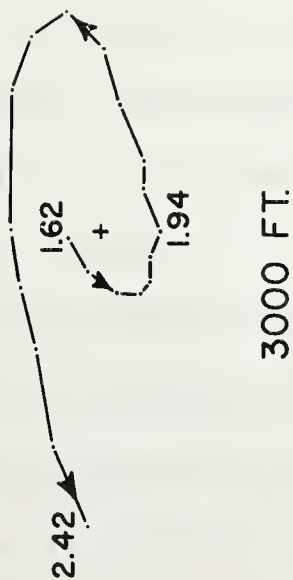
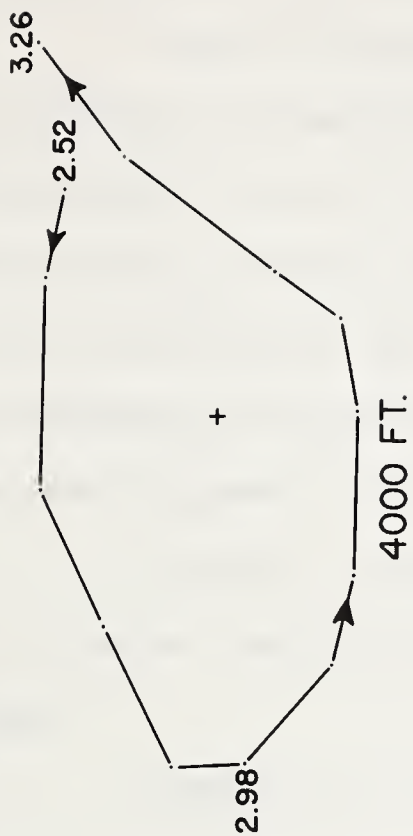


5000 FT.

NOTE : NUMERALS INDICATE
TIME AFTER ZERO
IN SECONDS

FIG. 15

5 TON PARTICLE TRAJECTORIES — WATCHING HILL SITE



NOTE : NUMERALS INDICATE
TIME AFTER ZERO
IN SECONDS

FIG. 16

cycle similar to those obtained with the smaller charges.

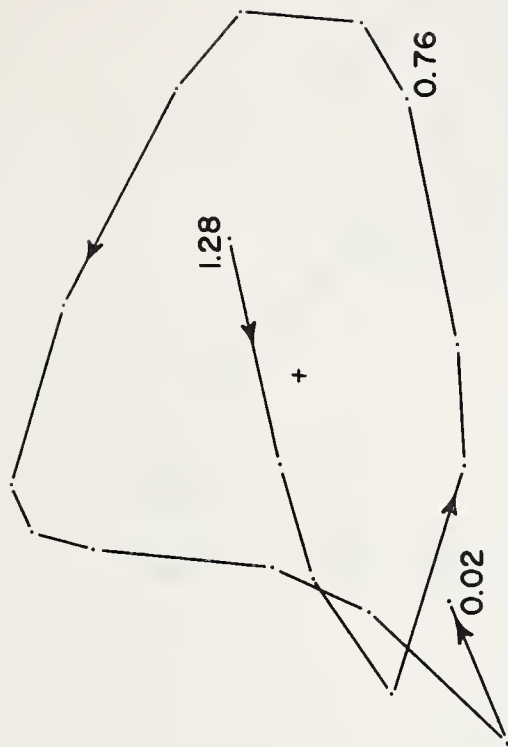
Figs. 17, 18 and 19 show ten trajectories obtained with the 200,000 lb charge on Watching Hill. The 2000 ft trajectory is that obtained with the 7.5 magnification instrument, and is possibly from as high a pressure level as any hitherto obtained. The orbit is by no means clear, and it is probably best to interpret it as two independent components, a general trend towards elevation of the ground together with an oscillatory radial motion.

At 4000 ft a distinct retrograde cycle occurs, rather more circular than those at 3000 ft and 4000 ft from the 40,000 lb charge.

At 6000 ft the orbit is basically retrograde, but has narrowed to an almost linear 45 degrees motion similar to that at 5000 ft from the 40,000 lb charge. At 7000 ft three trajectories are available from instruments disposed in azimuth. All three give a consistent picture of a narrow, elliptical orbit sloped away at 45° from the charge, and with a faint tendency to convert to prograde motion.

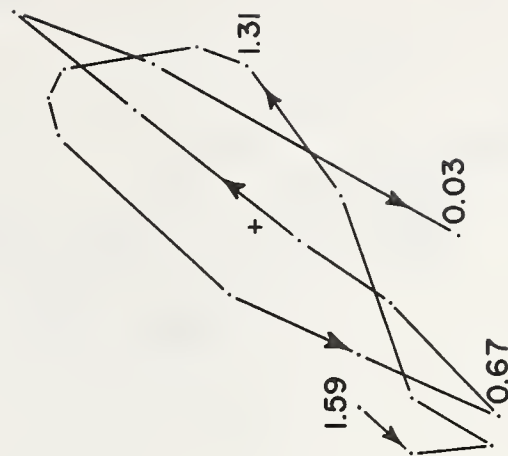
At 10,000 ft, the orbit is definitely circular, prograde motion, about 2 1/4 cycles being present. The early part still shows a tendency to a 45° slope, but by the end of the motion the orbit is almost circular.

At 12,000 ft, two trajectories from instruments disposed in azimuth are available. Both show distinctly prograde motion, but the one instrument indicates a rather flat ellipse, while the other shows an initially circular motion becoming elliptical with



4000 FT.

2000 FT.

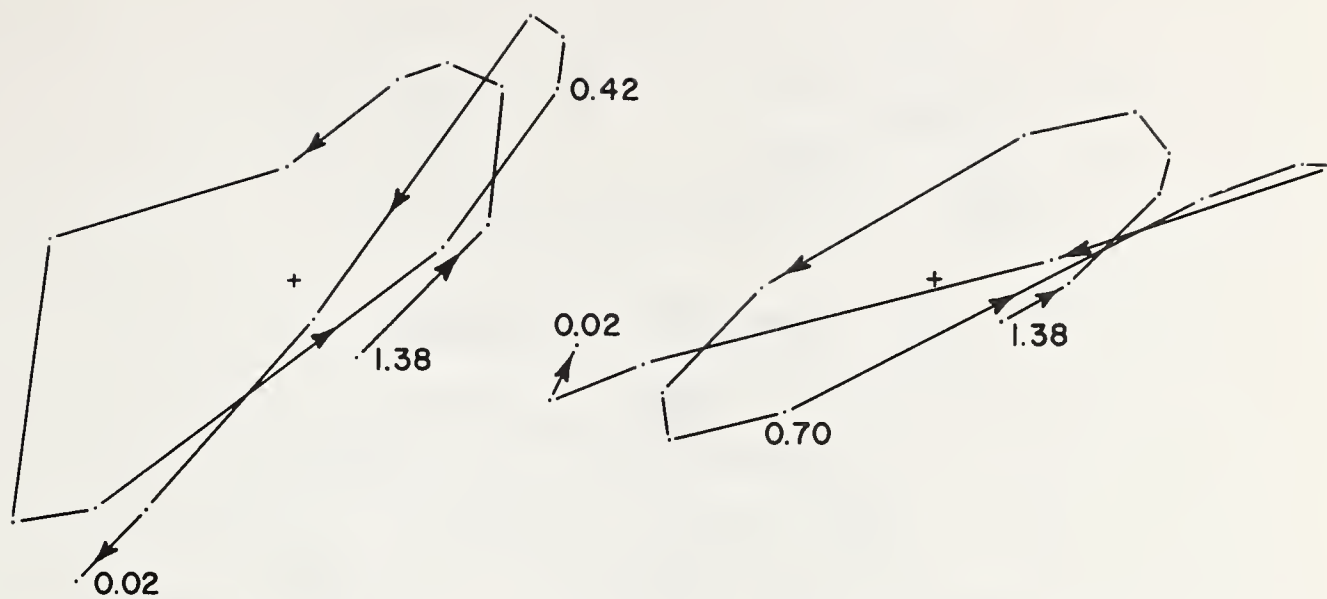


7000 FT.

6000 FT.

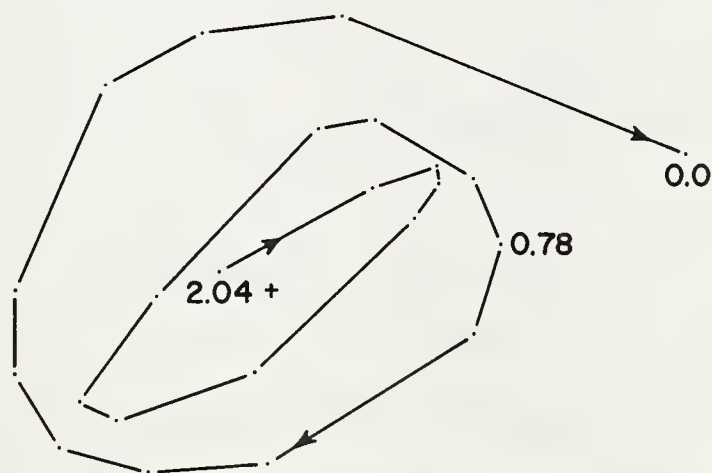
NOTE: NUMERALS INDICATE TIME BEFORE ARRIVAL OF AIR BLAST IN SECONDS

FIG. 17
100 TON PARTICLE TRAJECTORIES — WATCHING HILL SITE "A" LINE



7000 FT. "B" LINE

7000 FT. "C" LINE

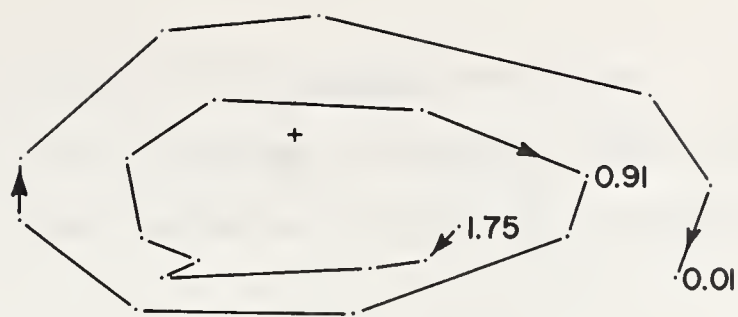


10,000 FT. "A" LINE

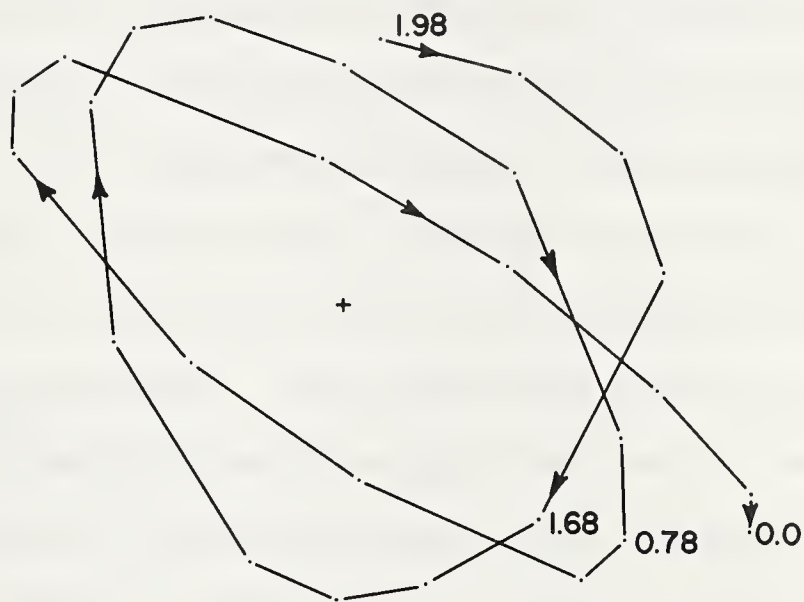
NOTE : NUMERALS INDICATE TIME
BEFORE ARRIVAL OF AIR
BLAST IN SECONDS

FIG. 18

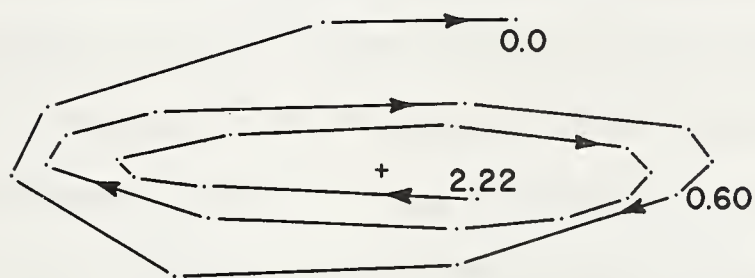
100 TON PARTICLE TRAJECTORIES — WATCHING HILL SITE



12,000 FT. "A" LINE



12,000 FT. "B" LINE



15,000 FT. "A" LINE

NOTE: NUMERALS INDICATE TIME
BEFORE ARRIVAL OF AIR
BLAST IN SECONDS

FIG. 19

100 TON PARTICLE TRAJECTORIES — WATCHING HILL SITE

a tilt of 45° , the high part being towards the charge.

At 15,000 ft the trajectory consists of three flat lying prograde cycles, a natural extension of the orbit at 12,000 ft on the same line.

Fig. 20 shows the particle trajectories plotted from the seismograms obtained at distances of 3000, 4000, 5000, 6000 and 7000 ft from a charge of 40,000 lb on the Drowning Ford site. These may be compared with the trajectories obtained from the similar charge on the Watching Hill site (Fig. 16). Although the two test sites are not identical, it is obvious that a very similar sequence of events is indicated by the trajectories. The trajectories at short ranges again indicate a retrograde mode, and the trajectories from the region 5000 - 7000 ft indicate a transition zone, with a tendency to prograde motion. No seismogram is available from a range of 10,000 ft on the Drowning Ford site, where we would expect pure prograde motion.

In summary, it may be said that these trajectories indicate that close to the charge the motion is retrograde-elliptical. At intermediate distances there is a transition zone where the orbit narrows to a linear trajectory sloped away from the charge. Beyond this point, the orbit 'crosses over' and becomes prograde, initially a narrow ellipse which opens out into a circle and then reduces to a flat lying ellipse which continues undisturbed and becomes more clean in character up to the arrival of the airblast at the site.

3.43 Sezawa and Kanai (1935a, b) showed that there are generally two dispersion curves for Rayleigh Waves in a stratified body, and in 1939 they reconsidered the subject and showed that the

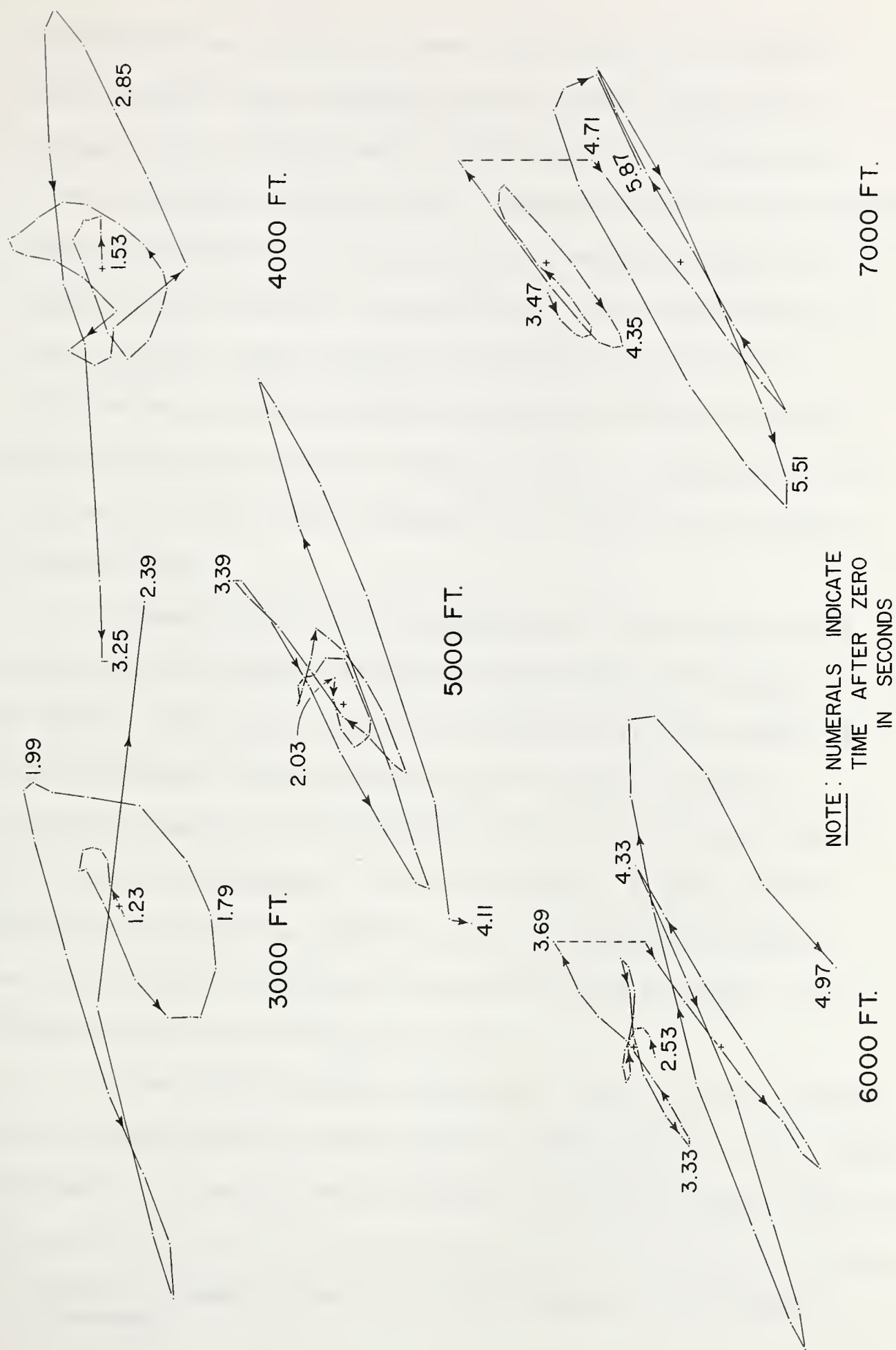


FIG. 20

20 TON PARTICLE TRAJECTORIES — DROWNING FORD SITE

orbital motion was reversed between the two cases. The fastest travelling (M2) wave, according to these authors, should show a prograde orbit, while the normal (M1) Rayleigh waves should show the characteristic retrograde orbit. Nagamune (1956), however, while agreeing with Sezawa and Kanai in general, does not agree that a prograde orbit is typical of the M2 branch. His calculations for several specific cases show that the M2 branch may itself be characterized by either prograde or retrograde orbits, though the M1 branch will always show a retrograde motion. A reversal in the M2 branch may occur, due to changes in the detail of the layering along the path.

Howell (1949), in an investigation of the surface waves from very small charges, divided his record into three regions C, H and R. His region C appears to correspond with the region now under discussion. Howell measures what he terms the 'group' velocity of the end of the C region (and the start of the H region) and quotes 345 metres/sec., the sonic velocity. Haskell (1951) discusses this paper in connection with air-coupling and points out that, in fact, Howell was measuring the phase velocity*. The R region is stated to be the Airy phase.

Leet (1939 and 1946) discusses a surface wave with prograde orbital motion, which he termed the Hydrodynamic wave, H. Care should be taken to distinguish between the Leet and Howell H waves, which are

* Neither statement appears to be quite correct - see previous discussion.

quite distinct. Leet's recording of prograde orbital motion is believed to be the earliest in the literature, but apparently Leet has at no time suggested that this might be the Sezawa and Kanai M2 wave.

In 1953, Howell, Neuenschwander and Pierson, in an investigation of surface waves in the Gulf Coast, showed that their records could be divided into two regions, in the first of which the motion was prograde and in the second, retrograde, as called for in the Sezawa and Kanai theory.

The M1 and M2 waves are frequently termed the symmetric and antisymmetric branches, by analogy with the vibrations of a plate. Tolstoy and Usdin (1953), noting Pekeris's (1948) interpretation of normal mode propagation in a layer as an interface or 'wave guide' phenomenon, developed a very elegant treatment by ray theory. The M1 and M2 branches appear quite simply as a consequence of this theory, and the theory confirms the generality of Sezawa and Kanai (and Nagamune's) numerical treatment. They show that the frequency equation can be derived from ray theory in a far simpler way than from the usual method of expanding the determinant (illustrated in Appendix A). In the Tolstoy and Usdin method, the form of the equation is entirely physical, and each coefficient may be interpreted in terms of the reflection coefficients at the boundaries.

A superficially similar set of trajectories, with directional reversal following a linear transition phase, may be obtained in the case of the normal (M1) wave simply by tracing the trajectory changes with depth at a given point. This has been done, for example, by Dobrin, Simon and Lawrence (1951). This similarity is, of course,

quite superficial and the mechanism is entirely different in the two cases.

None of the orbits obtained in this section has the canonical form of a Rayleigh orbit with the radial axis about two-thirds of the vertical. This departure from the canonical form is usually explained by departures from the Poisson condition (in which the two Lamé elastic constants are numerically equal) and possibly by visco-elastic effects. Horton (1953) has investigated Rayleigh waves on a visco-elastic solid and has shown that, while there is a tendency to convert from a vertical ellipse to a Lissajous figure tilted towards the source, the magnitude of this effect is, in theory, very much less than the experimentally observed departures from the canonical state.

Attention is also drawn to the theoretical treatment of Kuo (1958) of the propagation of Rayleigh-type pulses on a visco-elastic solid. He showed that competent rocks may be treated as purely elastic, but that unconsolidated sediments should be treated as visco-elastic. However, his treatment does not allow for a departure of the orbit from the canonical retrograde elliptical form. Kuo also discusses the experimental verification of the existence of M1 and M2 waves, and confirms that the major axes of the two modes are tilted relatively to each other. In the present region of the seismograms (that is, ahead of the airblast), it is difficult to compare the results with the limited results of Kuo, and it seems to the writer that the gradual rotation of the major axes in these cases is merely due to the proximity of the transition zone between the pulses. Well removed from the transition zone, the trajectories appear to be consistent in form, as may be seen by comparing the

200,000 lb trajectories at 12,000 and 15,000 ft. As will be seen in a later section, however, the results of Kuo are confirmed and extended for buried charges.

To summarize the discussion of this section, we may therefore say that the region encloses an M2 vibration, with a prograde orbital motion. However, contrary to the theory of Sezawa and Kanai, for a single model, the prograde M2 branch arrives after a retrograde branch. It would appear that this retrograde branch cannot be identified as the equivalent mode of the M1 branch in the same system, since this branch would arrive after the M2. It is possible that we are dealing here with a transition between modes of different systems, one of which has retrograde and the other prograde motion. Should this be indeed the case, we would expect that the prograde orbit would, in due course, suffer a transition into a retrograde orbit. However, the prograde M2 mode is interrupted by the arrival of the airblast and we must therefore defer investigation of this point until after a discussion of the event associated with the airblast.

The discussion of this section has concentrated on the three larger charge sizes. It will be seen that this is a necessary restriction, since in the next size down (30D and 32D) the epicentral distance is too small to allow this train of events to be separated from the preceding P wave and the following airblast.

Attention is drawn to the work of Kisslinger (1959), (and Appendix D), using similar instrumentation, and small charges, at Saint Louis. There is a close similarity between his buried charge records and the region presently under consideration, and he obtained a similar separation into prograde and retrograde orbits.

3.50 The Surface Waves From Contained and Venting Charges

3.51 It is convenient at this point to discuss the Rayleigh and Sezawa-type surface waves produced by charges detonated in a geometry different from that of the main series. These charges enable us to look at the dispersed surface waves and the air-coupled waves separately, and thus study the sequence of prograde and retrograde phases and the method of coupling to the airblast.

3.52 Records were obtained from four charges of 1000 lb TNT fully contained at a depth of 50 ft on the flank of Watching Hill. All these charges were in the form of cased cylinders, 6 ft long by 18 ins in diameter, inserted in 20 inch diameter wells 53 ft deep. Two of the charges were water-tamped, and two fully tamped with silt. No appreciable difference was detected which could be attributed to the method of tamping, either in the source region or at remote points where the waves were monitored by U. of A.-SES MOHO project teams.

We consider first a pair of charges (F.E. 549-1 and F.E. 549-2) which were buried at 50 ft and on the surface respectively. Records 100H-103H were obtained at distances of 4000, 6000, 8000 and 10,000 ft from the GZ of the buried charge. Attention is drawn to the close-in record, 100H. cursory examination shows that, in the vertical trace, several phases are present, and the train ends with a dispersed train of decreasing amplitude. With the exception of the final region, the phases show up with almost equal clarity in the radial and transverse traces.

The second charge, a 1000 lb sphere of TNT, was detonated on the same seismic line, on the surface, but some 150 ft from the GZ of the buried charge, and records 122H-126H obtained at the same recording

sites as 100H-103H. Comparison of the two sets of seismograms indicates that this charge did not feed sufficient energy into the ground to excite the dispersed surface wave phases with measurable amplitude. Immediately following the airblast, however, we see a wave train of approximately constant period, though not of particularly sinusoidal form. The vertical components of the two seismograms at a nominal distance of 4000 ft from these two charges are re-plotted in Fig. 21. If we assume that, in the case of the surface-burst charge, the whole of the record is a Press-Ewing coupled wave, we may estimate the phase velocity from the duration by using the relationship $V_c = \frac{R}{T} + V_g$ given earlier (section 3.31, p. 49). The values obtained in this way are, from the 2000 ft seismogram, 122H: $T = 2.60$, $V_g = 1280$ and hence $V_c = 2050$ fps. From the 4000 ft seismogram, 123H, we obtain $T = 6.14$, $V_g = 1200$ and hence $V_c = 1855$ fps. It will be seen later in this section that these velocity pairs are reasonable values for Press-Ewing type coupling to an M2 mode on this test site. The distance of 4000 ft corresponds to a distance of 24,000 ft from the 200,000 lb charge, as far as the airblast is concerned, and so is well outside the strong motion region investigated in the case of the larger charges. It is of interest to note that the form of the air-induced train obtained in this case is very similar to the records obtained at the greatest distances from the larger charges, where the pre-airblast wave has fallen below the recording capability (cf 42D, 43D and 122H). Anticipating the dispersion curves discussed later in this section, we may say that Press-Ewing coupling occurs at points well removed from the charge.

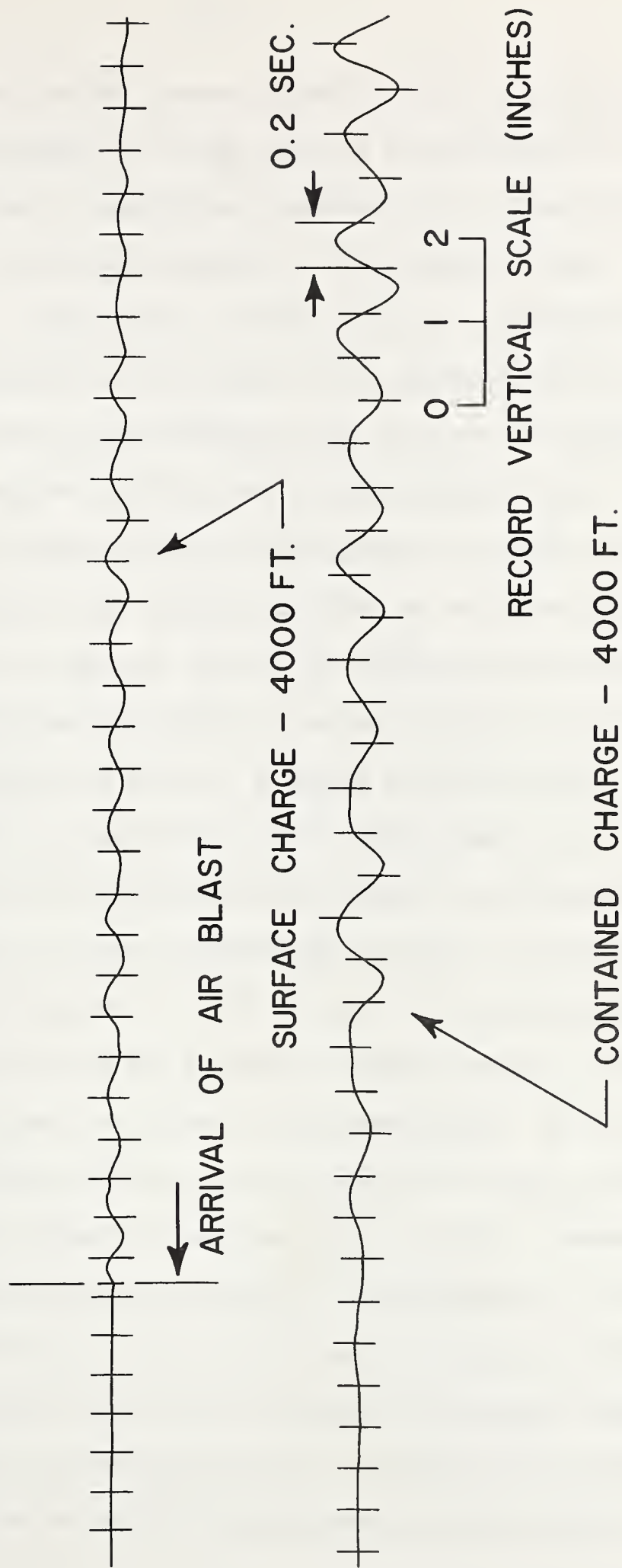


FIG. 21

SEISMOGRAMS (VERTICAL COMPONENT) AT 4000 FT.
FROM BURIED AND SURFACE 1000 LB. CHARGES

We may use the two traces plotted in Fig. 21 to illustrate graphically the appearance of a wave which is a combination of a Press-Ewing train and a pre-existing dispersed train, though of course we cannot in this way demonstrate a 'resonating' effect. The air-coupled train is superimposed directly onto the dispersed train at a point corresponding to the arrival of the airblast at the given distance. The process is then repeated with the time of arrival shifted in phase relative to the crest of the dispersed train. Three examples of the resulting 'synthetic seismograms' are shown in Fig. 22, which is a photograph of the computer printout of the trace amplitudes added at intervals of 0.02 sec. Due to the comparatively low amplitude of the air-induced train, the effect is not so striking as in the multi-ton charge seismograms, but there is a marked similarity which indicates that we may attempt to interpret the actual seismograms in this way.

3.53 We may now with advantage consider the seismograms obtained from charge F.E. 549-4 (seismograms 94J-98J). This charge was a 1000 lb sphere buried at a depth of 23.5 ft in a low sandy hill on the main seismic line of the 200,000 lb charge (see para 2.41). Several distinct phases are visible in the seismograms. If only the vertical component were available (as is usually the case in exploration work) one might judge that only two phases existed. However, when one correlates the radial and vertical components as a particle trajectory, one finds that there are, in fact, at least five distinct phases, which alternate between the retrograde and prograde habit. Each of these phases has associated with it a phase in the transverse trace. Fig. 23 shows the particle trajectories for the radial-vertical

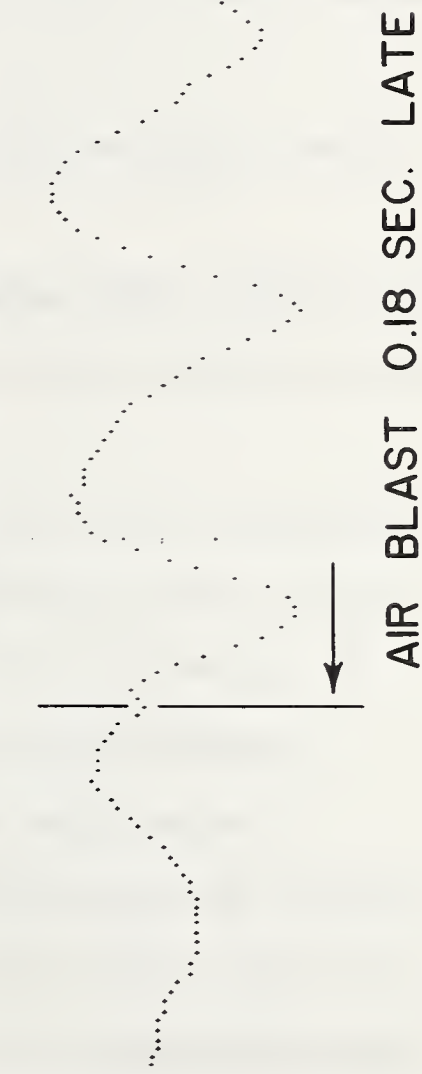


FIG. 22

components of seismogram 97J, in which the five phases are clearly evident. At points closer to the charge, this separation is incomplete, and the interpretation of such seismograms must always be complicated and of doubtful validity. Where a phase is clearly separated, it is possible to identify it by its particle trajectory at various distances and then obtain the spectrum and analyse the dispersion by Satô's method. Where the phases are not separated, however, one can be led into serious difficulties by blind attempts to apply such methods. In extreme cases we may see the attempt made to apply a Satô-type analysis to a complete seismogram, despite the fact that none of the fundamental assumptions is valid.

At the degree of separation shown in Fig. 23 we may select the following phases:

Phase One. Three-quarters of a cycle, retrograde habit, flat lying ellipse.

Phase Two. (a) Four cycles, prograde habit, fairly narrow ellipse tilted forward 60 deg. from the vertical. This breaks into

(b) which may or may not be the same physical phase. This is one complete cycle, which retains the prograde habit but whose tilt is nearer 45 deg. forward of the vertical.

Phase Three. Two cycles, retrograde habit, narrow ellipse tilted back 25 deg. from the vertical.

Phase Four. Two cycles, prograde habit which retains the same general shape and the same backward tilt as the retrograde phase three.

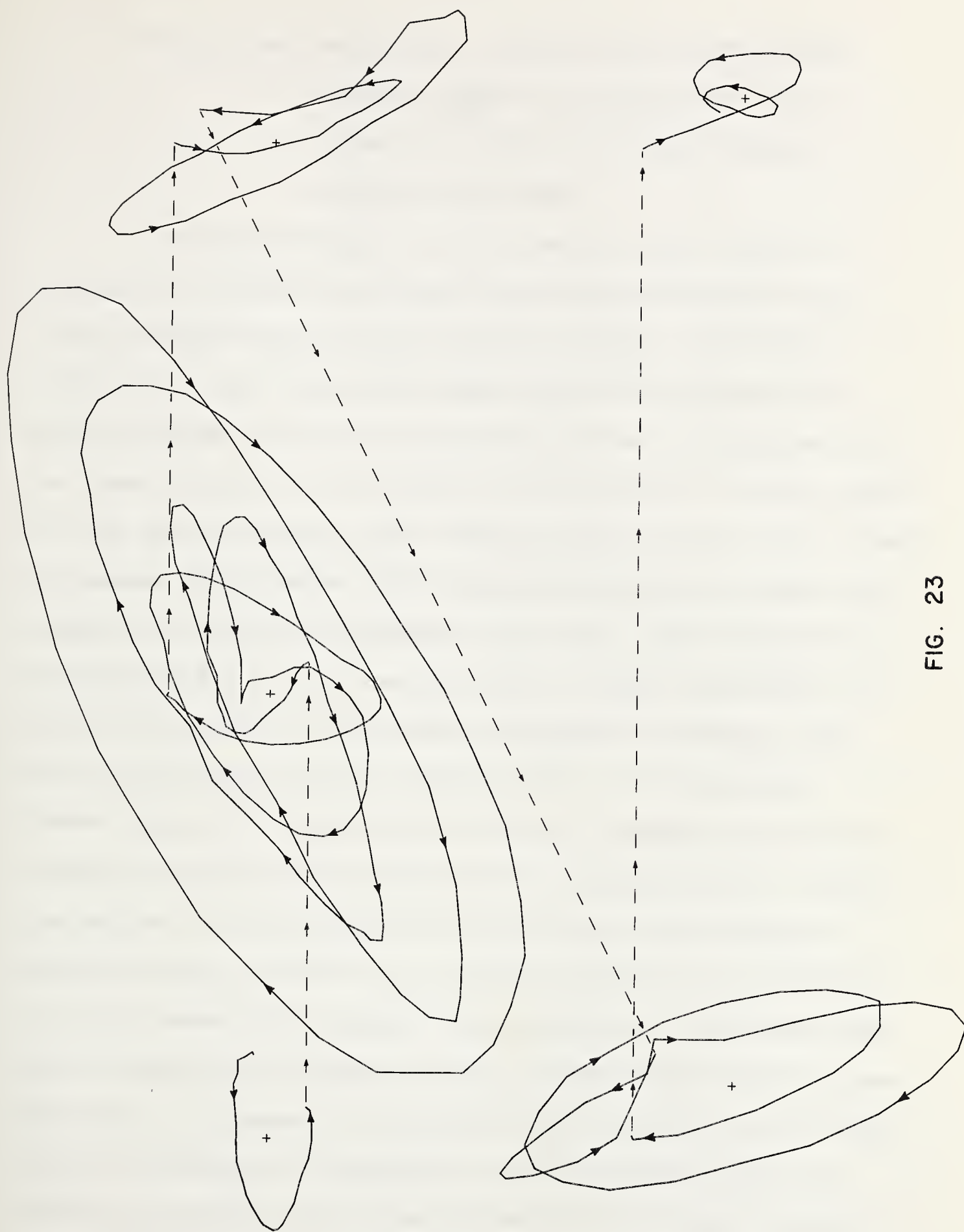


FIG. 23

PARTICLE TRAJECTORY
SEISMOGRAM 97 J — 4000 FT.

Phase Five. Four cycles, retrograde habit, approximately vertical ellipses of classical form. This phase is very small in amplitude compared with the other phases.

The dominant phases are the second and third, which are prograde and retrograde and tilted forwards and backwards from the vertical respectively, so that the included angle is approaching a right angle. There can be little doubt that these two phases constitute an M2-M1 pair for the same layering system. The agreement with the system discussed by Kuo (1958) is virtually exact. The other phases are less easy to identify, since changes of habit can occur for a variety of reasons. The M2 motion itself may become retrograde for short wavelengths in a fixed layering system, but in such a case, following Kuo, we would expect the tilt of the major axis to remain consistently forward of the vertical. In the present seismogram no retrograde orbit has the same forward tilt as a prograde orbit. It is noteworthy, however, that in the trajectory illustrated, a retrograde orbit tilted backwards from the vertical transforms into a prograde orbit of similar inclination. At first sight one might think that this represents a prograde M1 wave, but there is no evidence whatsoever in the literature or in the present work to justify such a conclusion. The Rayleigh (M1) mode is essentially retrograde in habit, for every system which has been calculated. It appears to be generally agreed that the M2 and M1 orbits tend to be orthogonal, independent of the fact that the M2 mode may itself be retrograde. Kuo states that the M2 wave is tilted forward of the vertical, and the M1 backward, and this conclusion is generally confirmed by the present work. However, Howell (1948) observed that in

his experiments the two phases, while orthogonal to each other, were tilted in the reverse direction - M2 backward and M1 forward. Thus the backward tilted prograde wave of phase four is almost certainly M2, but it is not clear why this phase should depart from the common forward tilt for the site. As no theory exists to explain the tilted orbits, it is premature to draw conclusions. It is eminently possible that the direction of tilt is governed by fortuitous elements (as is the direction of rotation of a bath tub vortex). Once established there will be a tendency for a given habit to hold, even though a new transient is driving the motion, provided a smooth transition is possible from one habit to the other. It is noteworthy that the tilt of the orbit does not remain constant for a given phase as it proceeds outwards from the source. Kuo indicated that the tilt changes linearly with distance, and there is some indication of a similar effect in the present results for the prograde phase. The retrograde phases are less clearly developed and conclusions would be premature, but no linearity is obvious. There is room here for a definitive investigation.

We may proceed to examine the dispersion curves for the two dominant phases according to the method described in Appendix E. It is necessary to make a subjective selection of the equivalent regions in the seismograms from two different distances. Seismograms 97J and 98J were selected, and the corresponding regions defined from the particle trajectories. These regions were then digitized, and the Fourier Integrals calculated separately for each phase at each station. The dispersion curves were then deduced as a 'sheaf' of curves for each phase, due to the indeterminate multiplier in the equations (see Satô, 1955b).

The resulting sheaves for the first attempt are illustrated in Fig. 24. The curves for the prograde mode are well separated, and it is comparatively easy to select the correct curve. This is particularly important since the airblast arrival is usually associated with the dominant prograde mode. Selection of the curve may be made on the basis of the wavelet velocity (as defined in para 3.30), thus defining the dispersion curve with precision. A full analysis of the records from this 1000 lb charge is being prepared by Hastrup (1963) in which each phase is analysed separately and in detail. The basic conclusion is unchanged in this more detailed analysis, but there is some evidence that the spectra become more peaked as the distance increases and this effect is more marked for the prograde phase than for the retrograde phase. Hastrup also discusses the change in the peak frequency with charge size for the 10 lb, 296 lb and 1000 lb* charges. Considerably more work is required in this area and use will be made of later shots in the U. of A. --SES MOHO programme to define the dispersion curves and the spectra of the phases in detail. The preliminary analysis is sufficient to show that the conditions for Press-Ewing coupling exist, and that the group velocity -- phase velocity bracket obtained experimentally with the surface-burst charges is compatible with the dispersion curve deduced from the buried charges.

* Records 89D-93D, 94J-98J and the buried 10 lb charges functioned at SES for Dr Kisslinger, Saint Louis University.

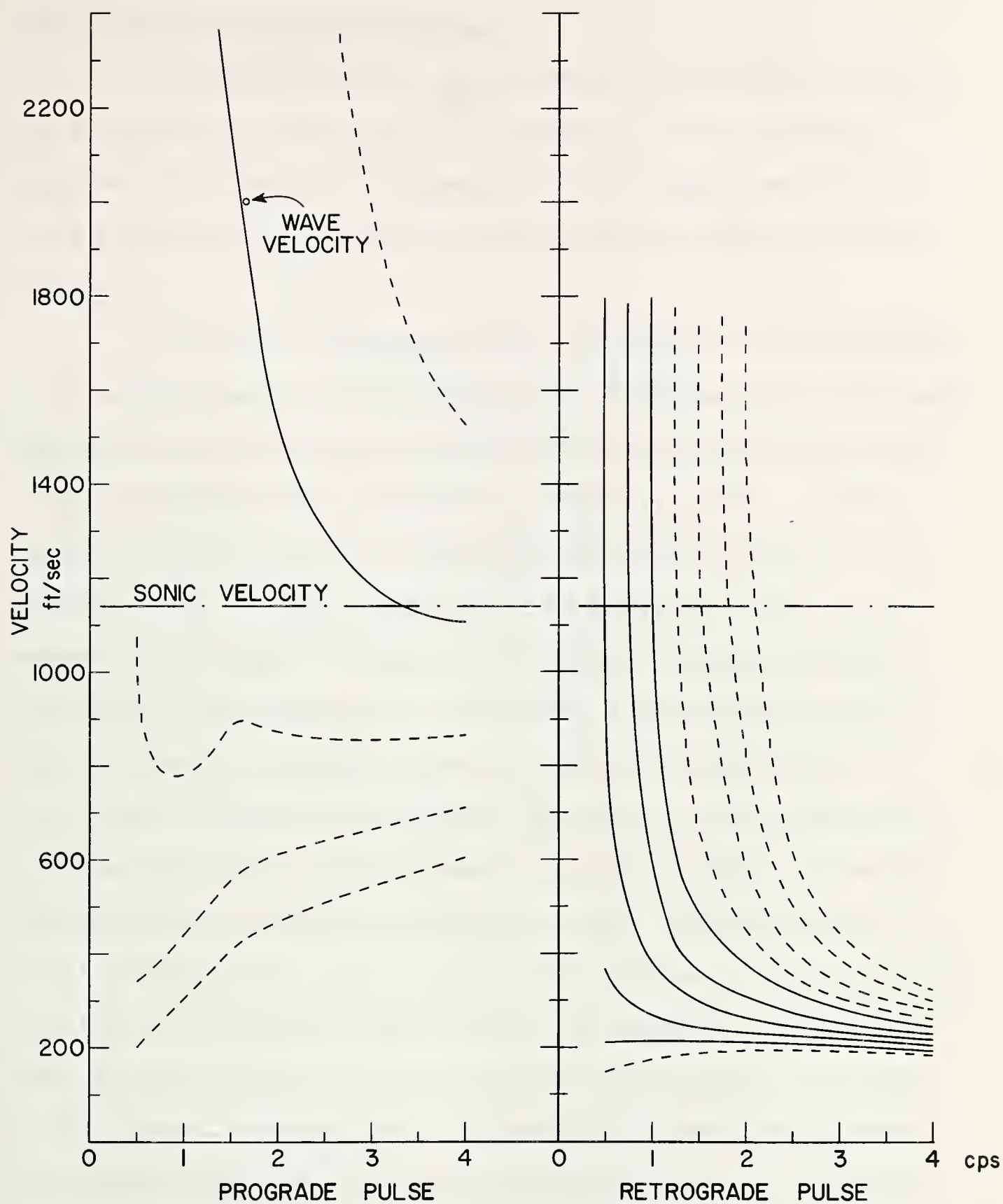


FIG. 24
EXPERIMENTAL DISPERSION CURVES FOR PROGRADE
AND RETROGRADE PHASES OF A 1000 LB. BURIED CHARGE

3.60 The Waves Following the Airblast

Following the arrival of the airblast, we may expect to find (a) an indication of the action of the airblast on the instrument, together with either (b) a continuation of the virtually unaffected surface wave or (c) an aircoupled wave followed by uncoupled surface waves.

The theory of aircoupling, and a discussion of the appearance to be expected when an air-coupled wave is superimposed upon a dispersed wave, is given elsewhere in this dissertation. Attention is also drawn to the experimental work of Anderson and Henriksen (1962). In this section we need only look at the experimental results obtained on the Suffield sites. It may be said immediately that in all the close-in records there is some indication of the airblast coupling to either a prograde or retrograde wave. In all cases except the most distant records, there is a distinct change in the record at the arrival of the airblast. Preceding the airblast, the record is either below the recording capability of the instrument, or, alternatively, is a smooth, sinusoidal wave train showing slight dispersion. After the arrival of the airblast there is, in all cases where a smooth train has preceded the airblast, a disturbed train following the airblast. In cases where there is no preceding wave, there is a wave recorded after the arrival of the airblast. In many cases (for example seismograms 65W and 66W) the airblast arrival is followed by many cycles of virtually constant amplitude, constant period waves, which in the vertical component looks like classical air-coupling. We have also shown (in para. 3.50) that the experimental phase dispersion curve for a prograde mode on the

Watching Hill test site crosses the sonic (and blast) velocities, so that Press-Ewing-type coupling may exist. The amplitude of the air-coupled wave cannot be predicted, and in individual cases it is possible to have either a small amplitude air-coupled train superimposed upon a pre-existing surface wave, not necessarily the same mode, or the pre-existing surface wave mode driven into large amplitude resonance.

We may use, as our first illustrations, selected records obtained with the 200,000 lb charge. We start at 12,000 ft along the A line, seismogram 69W, in which the apparent effect of the airblast arrival is negligible in the record. The arrival coincides with a high frequency disturbance which is rapidly damped - a typical effect at all distances, which is attributed to the direct action of the airblast on the case. After this high frequency effect has died out, there is a relatively large amplitude surface wave which has departed from the pre-airblast sinusoidal wave form. The particle trajectory is shown in Fig. 25. As indicated earlier, the pre-airblast orbit is a very clean ellipse, with the major axis horizontal and a ratio between the axes of about two. The actual arrival of the airblast does not modify the orbit instantaneously, but shortly afterwards the orbit is distorted from its elliptical form, with a tendency to indicate a tilting of the major axis toward the vertical. This orbit then breaks sharply into an approximately orthogonal tilt, and then settles down again into a smooth, almost circular prograde orbit. One concludes that there is no direct evidence of Press-Ewing coupling, but evidence of two successive prograde habit phases, modified or induced by the airblast.

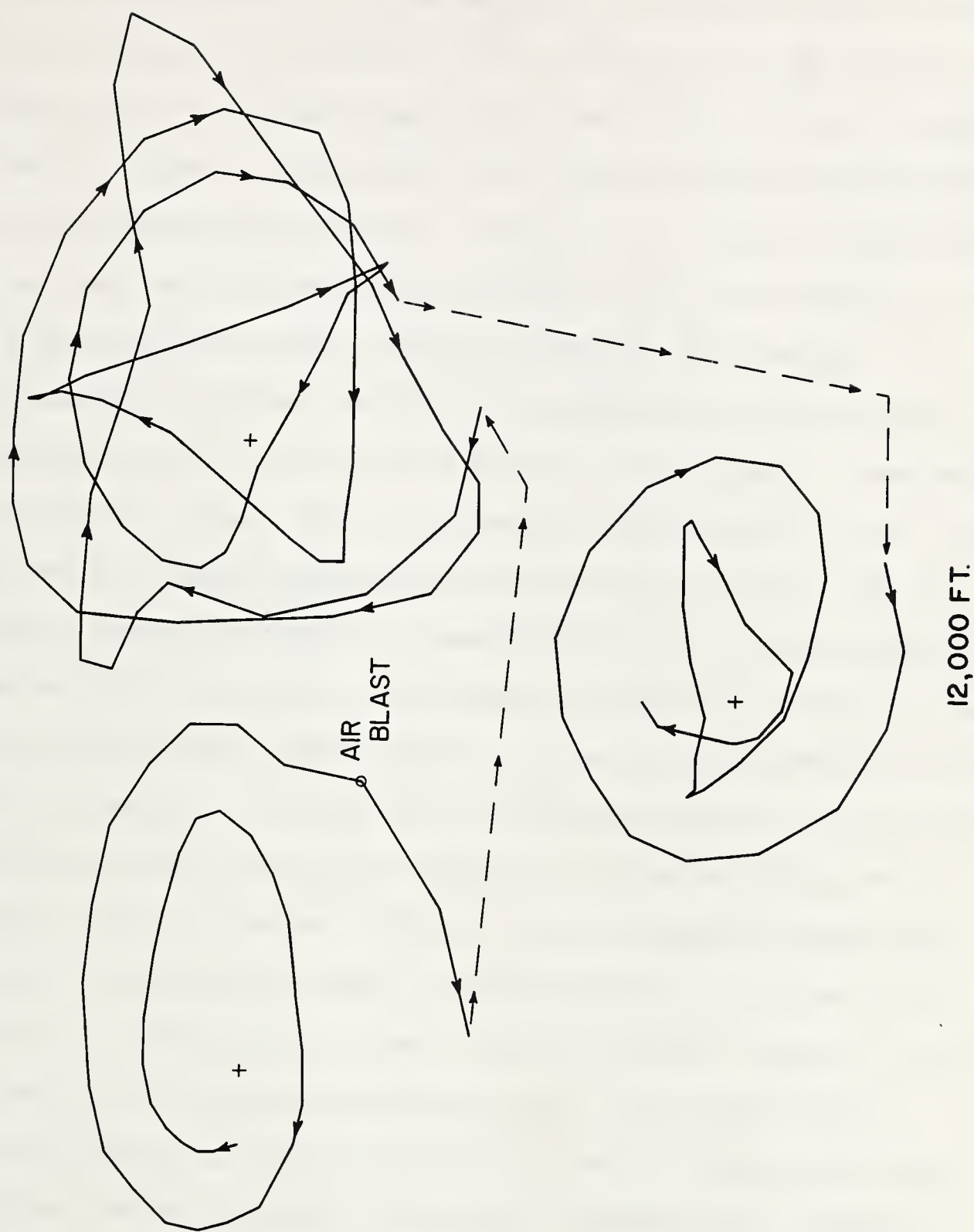


FIG. 25
100 TON PARTICLE TRAJECTORIES — WATCHING HILL SITE

Moving closer to Ground Zero, we look at seismogram 68W. In this seismogram there is distinct evidence of a change of phase in the radial component at the arrival of the airblast, but in the vertical component there is no abrupt change in the wave profile, though the region after the arrival of the airblast is of larger amplitude and less smooth than that preceding the airblast. Turning to the particle trajectories, we see that the orbit preceding the airblast (Fig. 18 and start of Fig. 26), is a smooth prograde orbit, initially elliptical with the major axis approximately four times the minor, and tilted forward of the vertical, but becoming virtually circular by the arrival of the airblast. Immediately following the airblast there is horizontal movement towards ground zero, followed by a large amplitude orbit which is almost circular, but has a tendency towards the form of a forward-tilted ellipse. After slightly more than two cycles, this orbit breaks sharply towards the vertical and then sets into an almost linear oscillation tilted backwards from the vertical, almost orthogonal to the tilt of the pre-airblast orbit. In the confused transition region there is some tendency to retrograde motion, but the dominant motion is prograde. Thus, in this seismogram we again have evidence of two prograde modes, generally circular in form but with a tendency to orthogonality in their elliptical regions. There is little evidence of a superimposed Press-Ewing train. The sharp motion in towards ground zero cannot be explained in terms of the action of the airblast upon the instrument itself, and is without doubt due to the influence of the airblast on the ground.

Moving still closer to GZ, we look at seismogram 65W. This, with 66W, constitutes a pair of seismograms which apparently show very

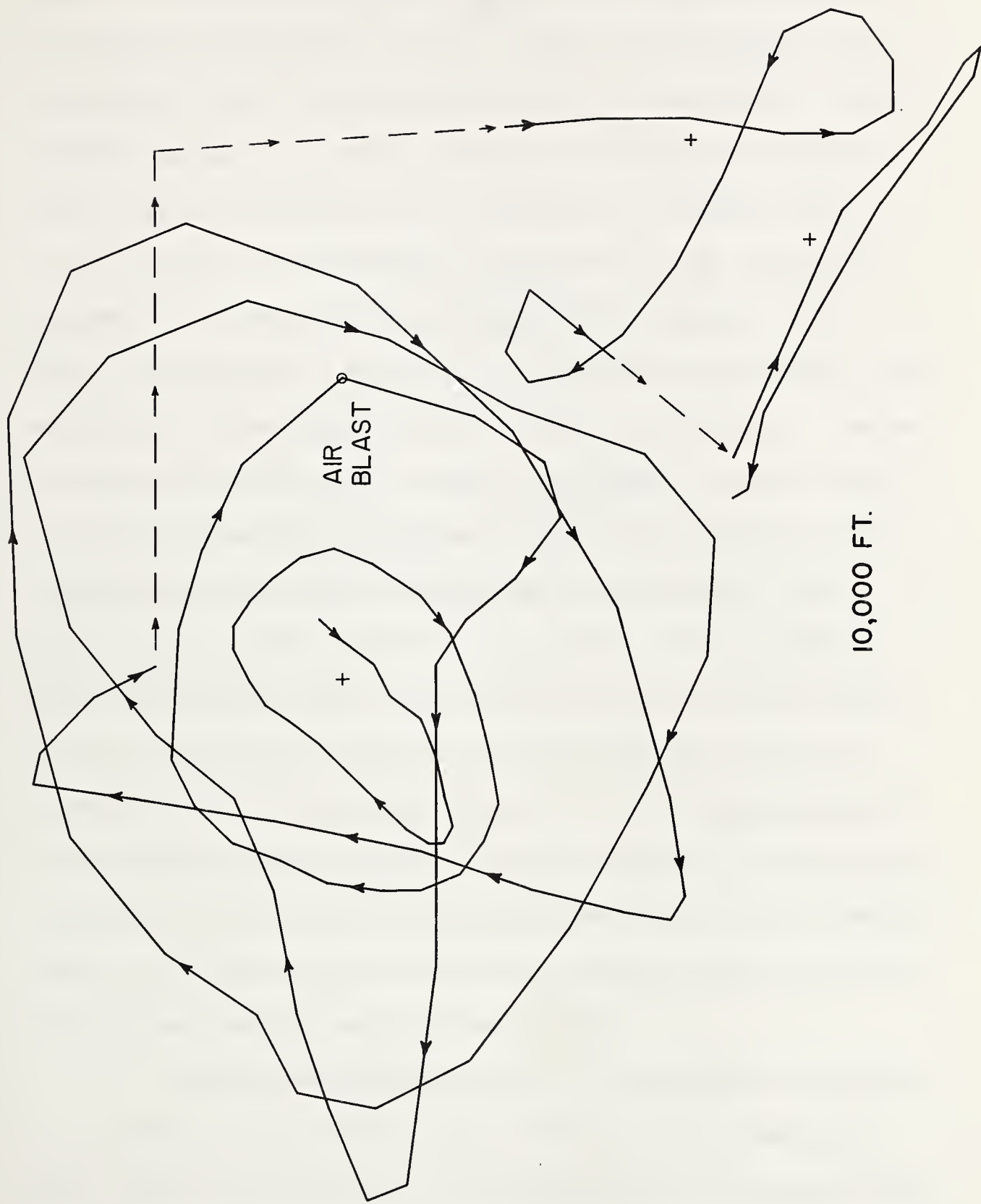


FIG. 26
100 TON PARTICLE TRAJECTORIES — WATCHING HILL SITE

marked air-coupling. In 65W we see that, ahead of the airblast, there is a strong surface wave, which shows a change of phase in the vertical approximately 0.3 sec. ahead of the airblast, and a very marked change of phase at the arrival of the airblast. The particle trajectory is shown in Fig. 27. The main pre-airblast phase shows a retrograde orbit, breaking into a prograde orbit 0.3 sec. ahead of the airblast. The arrival of the airblast is followed by a large amplitude, forward tilted prograde orbit. There are approximately three and a half cycles of this orbit, with evidence of a superimposed effect at the top of the orbit. The orbit finally narrows down to a linear oscillation, and then breaks sharply in the vertical and becomes a new orbit orthogonal to the previous orbit, but still retaining the prograde habit. At a later stage this orbit becomes circular, then, after a confused region, settles down into a retrograde orbit tilted forward of the vertical. Thus, with the exception of the final phase (which is presumably below the recording capability at the distant stations) and the initial phase, both of which are retrograde, this seismogram indicates that the pair of orthogonal phases were already a dominant effect at this distance, where there is strong coupling to the airblast in the immediate post-airblast region.

At the closest distance, 2000 ft, seismogram 64W, we have a record from a low gain instrument. The particle trajectory is shown in Fig. 28. Once again, the strong motion is associated with the arrival of the airblast. The first motion after the arrival of the airblast consists of a single elliptical, backward tilted orbit

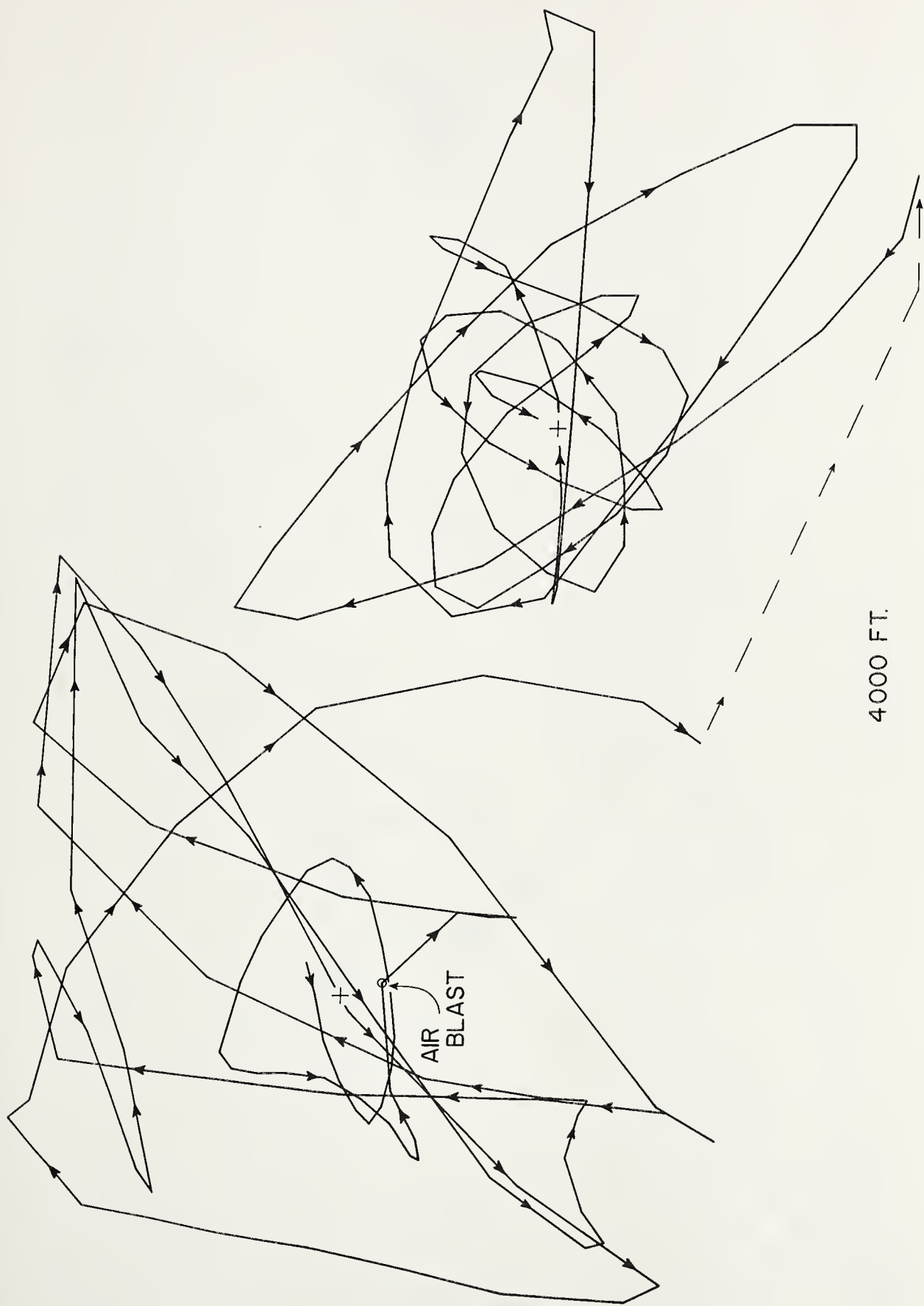


FIG. 27

100 TON PARTICLE TRAJECTORIES — WATCHING HILL SITE

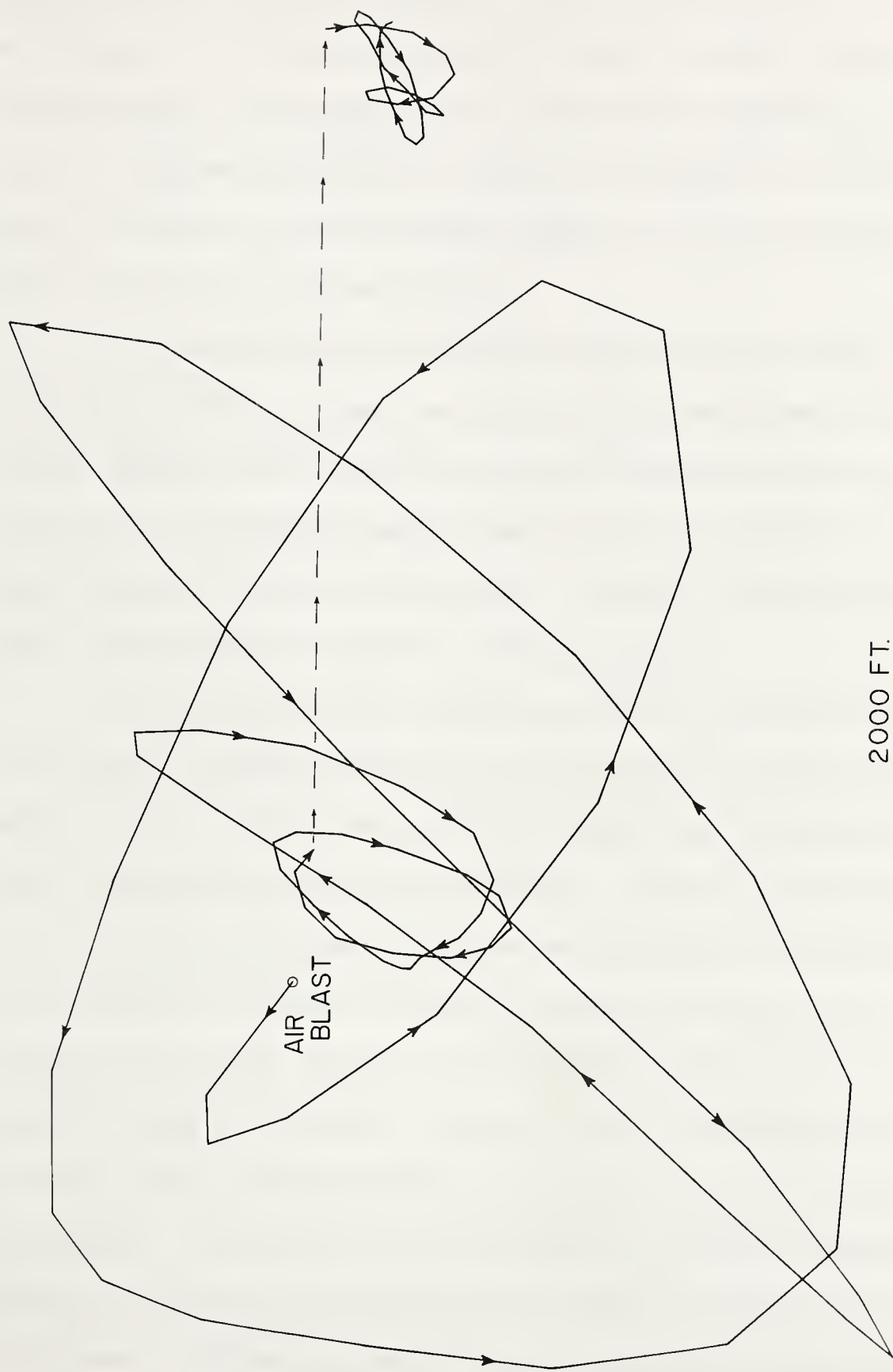


FIG. 28

100 TON PARTICLE TRAJECTORIES — WATCHING HILL SITE

with a retrograde habit. This widens out into a large amplitude, almost circular orbit before changing abruptly into a forward-tilted, narrow elliptical orbit, converting into a prograde phase. Presumably, by a comparison of this record and the record at 4000 ft (65W), the retrograde mode is that equivalent to the first prograde mode at 4000 ft. The retrograde mode at 4000 ft is indicated in the 2000 ft record by the low amplitude signal visible in the radial trace between the P wave and the airblast arrival.

We see that these 200,000 lb seismograms show quite clearly a succession of four phases, an initial retrograde phase followed by the two dominant phases which are usually prograde and orthogonal to each other. The prograde habit, however, is not invariable, and these phases may adopt the retrograde habit. Finally, the strong motion ends with a relatively low amplitude retrograde phase.

The arrival of the airblast is at all times associated with the (normally prograde) second phase. The actual motion in this phase tends to start slightly ahead of the airblast, but at the short epicentral distance the association is close. Classical air-coupling in the Press-Ewing sense does not appear to be dominant. Nevertheless, it would appear that the air blast is driving a surface wave - or waves - with large amplitude. This is made abundantly clear in the 20 ton seismograms 59W, 60W, 61W and 62W. Before we look at the particle trajectory for these waves, it is rewarding to compare the vertical phases of these seismograms. These are re-plotted in Fig. 29, with the airblast arrival aligned. Clearly, the arrival of the airblast is driving the post-airblast wave. A dispersive wave is gaining ground upon the airblast, as

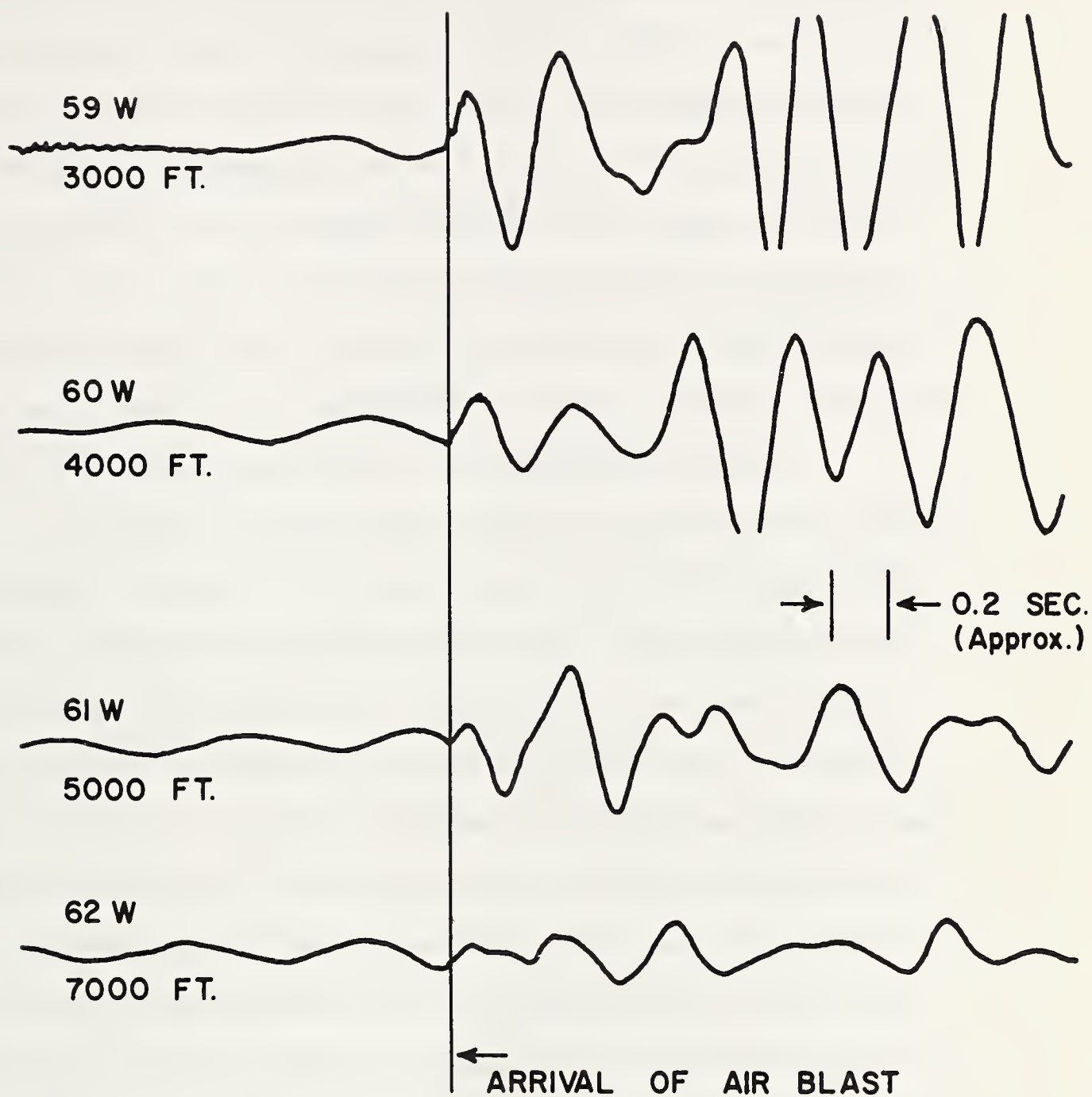


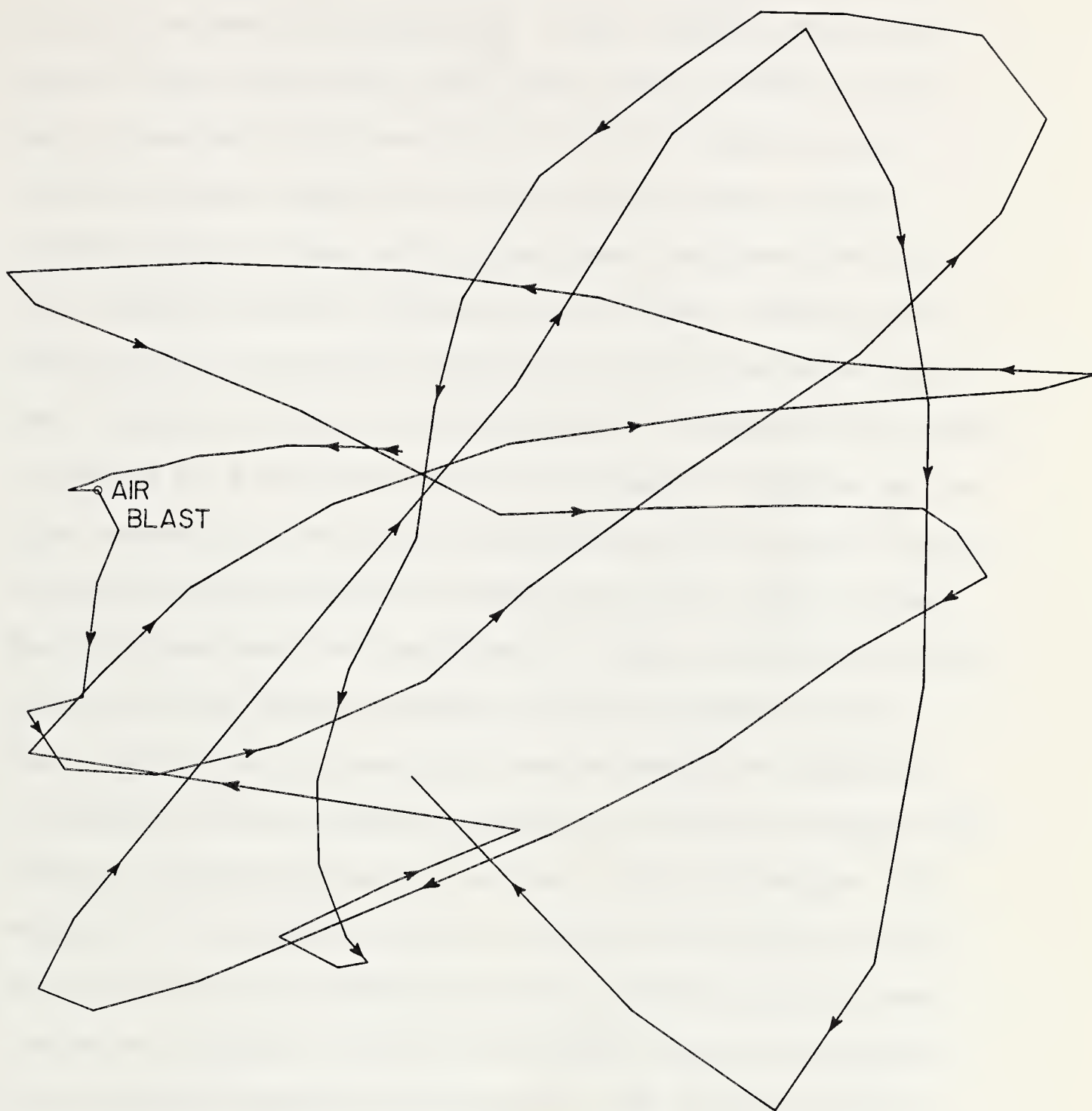
FIG. 29

VERTICAL COMPONENTS FROM 20 TON SEISMOGRAMS
SHOWING EFFECT OF AIR BLAST

a smoothly dispersed train, but, despite this 'shedding', due to dispersion, there is no indication whatsoever that the large amplitude post-airblast train at the shortest distance (59W) is gaining on the airblast even at the greatest distance (62W). A simple dispersive train would certainly have done so. The particle trajectory for the 3000 ft seismogram is shown in Fig. 30. The impulsive action on the instrument case is clearly evident in the right-hand side of the orbit. The orbit again shows a retrograde-prograde-retrograde-prograde succession, but the phases are neither so clearly separated nor so well formed as in the 200,000 lb records - possibly due to the shorter epicentral distances for a given airblast pressure.

Precisely the same association of the airblast and a strong post-airblast surface wave is demonstrated by the seismograms from 10,000 lb charges on the Watching Hill site. Typical examples are 50W and 51W, at 2000 and 3000 ft respectively on the same azimuth. The association is repeated in the 2000 - 3000 ft pair from another charge and different azimuth and ground zero in 44W and 45W, and many examples at 2000 ft in different azimuths (e.g. 47W et seq) indicate that the association is quite invariable. There can be no doubt of the reality of the phenomenon on the Watching Hill test site, even though, due to the pre-existing surface wave and the multiplicity of phases, the classical Press-Ewing form is not clearly evident.

The theoretical dispersion curves given in Appendix C indicate that Press-Ewing coupling may be expected for the layering system of the test site, for waves in the period bracket excited by the multi-ton charges. Small charges, which excite high frequency



3000 FT.

FIG. 30
20 TON PARTICLE TRAJECTORY — WATCHING HILL SITE

waves (4-10 cps) will produce seismograms with low group velocities and little evidence of air-coupling. Larger charges, which excite waves of longer period, will exhibit wave trains in which the air-blast is associated with wave groups of the same velocity due to the flat 'plateau' region in the group velocity curves. Group periods of about 0.5 sec. will be associated with phase waves (and hence Press-Ewing waves) of about 0.3 sec. period. Detailed interpretation of the interaction requires that all the individual phases from a variety of surface and buried charges be analysed by the methods of Appendix E. For this purpose it is necessary to digitize the complete records, plot the particle trajectories, and then select regions of each phase which are free of interference by the adjacent phases. The digital data must then be corrected to allow a 'smooth' start and end to the phase, before proceeding with the dispersion analysis. Since there are several steps which require subjective judgment, it is essential that the analysis be repeated on several seismograms from different epicentral distances, and from a variety of charges. The mechanics of the operation have been reduced to the technical level, but, due to the very considerable labour involved, it will be some time before sufficient analyses of individual phases are available for a scientific appraisal of the results. The report by Hastrup (1963b) may be taken as the first step in this direction for a single buried charge. A similar analysis has been undertaken on the immediate post-airblast phase of seismograms 60W, 61W and 62W. Details are given in Appendix F, as a typical example of the process of reduction.

The fact that the post-airblast record is strongly influenced by the phase relationship of the airblast and the pre-airblast seismic

wave is illustrated by three seismograms at different azimuths, but the same range, from the 200,000 lb charge. In seismograms 67W and 71W the airblast is associated with the crest of the pre-airblast wave, and the immediate post-airblast record in both cases is strikingly similar, and of large amplitude. Seismogram 74W, in contrast, is from the same distance but a radically different azimuth. In this case the airblast is associated with a point well below the crest of the pre-airblast wave. The post-airblast region is entirely different in form from the common pattern of 67W and 71W, and is of comparatively low amplitude. The correspondence between these effects and the effects shown in the 'synthetic seismograms' of Fig. 22 leaves little doubt that the explanation given is adequate. An air-coupled wave has been superimposed upon the pre-airblast strong motion. The classical form of constant period train in the post-airblast region is hardly to be expected. An additional illustration of the effect may be seen in a comparison of the 40,000 lb seismograms from Watching Hill, which show marked evidence of the influence of the airblast, and the records from the 40,000 lb charge on Drowning Ford, a test site in which the evidence of airblast-coupling is less marked. In both these pairs of records the interval between the P wave arrival and the airblast arrival is constant, indicating that the phase change is not due to variation in the wind, but to slight differences in the dispersion curves.

It was noted by Press (1963)^{*} that reversal of polarity occurs between the main shock surface wave and the collapse shock surface waves. It is possible that we should look to crater re-bound to explain some of the features of the multiple phases in both the

* see also Smith, S.W., J.G.R. Vol. 68, No. 5, 1963.

buried and surface charges.

3.61 It is possible to follow the close association of the airblast and the ground shock into the very high pressure regions, but, at the present time, it is not possible to do so with instrumentation comparable to that used at more moderate pressure levels. At Suffield comparisons have been made between the arrival time of the air blast and the ground shock along lines reaching to within a few feet of the charge itself. The arrival time of the airblast was measured by foil-contactor-type switches and by piezo-electric gauges mounted just above the surface. The ground shock arrival was detected by ground shock switches in which a seismic mass actuated the closure. These ground shock switches respond to radial acceleration by design, but may have some cross-axial sensitivity. It is not at present certain what the time resolution or the threshold acceleration is for actuation. The switches have almost 'dead beat' damping, and a natural period of between 1 and 3 cps*. Table 7 gives the travel time data obtained for the 40,000 lb 1963 trial (F.E. 556). The data are also plotted in the form of a travel-time curve in Fig. 31.

It is clear that there is very close association between the airblast and the ground shock right in to the crater area, with the two effects decelerating according to very similar curves. In the very high pressure region the airblast leads the ground shock, as indicated by the ground shock switch. It is not certain that the switch detects the first onset of the ground shock, but certainly the first

* A report on the design of these gauges (and additional results) is in preparation but no publication date can be given (S.T.N. No. 88). The development is being undertaken by the Instrumentation Group of the Physics and Meteorology Section, SES.

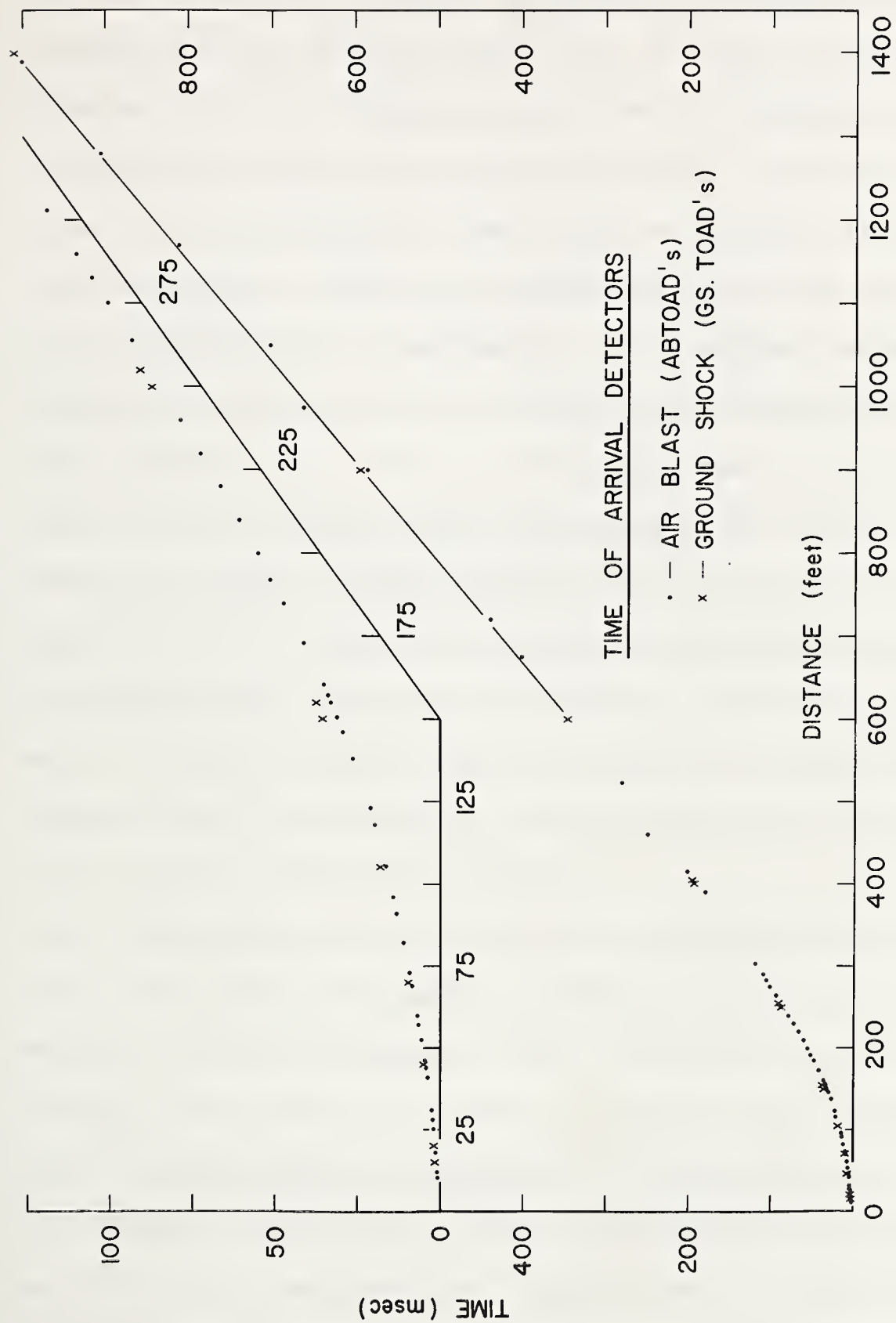


FIG. 31

TIMES OF ARRIVAL OF THE AIR
AND GROUND SHOCK FRONT

ground shock with sufficient amplitude to operate the switch follows very closely upon the airblast. At intermediate pressure levels, the two effects become virtually synchronous. A stage is finally reached where the airblast is lagging a ground wave of sufficient amplitude to trigger the switch, and thereafter the travel time curve for the ground shock is effectively linear, while the airblast continues to decay in velocity. This may be compared with the events recorded by the Sprengnethers at close ranges. At the shortest ranges the Sprengnethers indicate that the airblast is synchronous with the large amplitude event, but as one moves away from GZ a moderately large amplitude dispersed train gains ground on the airblast, even though the airblast is still associated with the largest amplitude. In nuclear effects studies the early region is sometimes divided into the 'superseismic' region where the airblast precedes the seismic event, and the subsequent sub-seismic region. The ground shock 'precursor wave' may explain the 'precursor air shock' occasionally seen in advance of the main air shock.

3.62 During several of the large trials at Suffield, attempts were made to record the electromagnetic radiation associated with the detonation (Dobbie and Hamilton, 1963). No definite success was achieved in this phase of the work, but consequent upon the attempt, it was considered worth investigating the possibility that the electrical potential between various parts of the test site could change in association with the detonation. Evidence from the Nevada Test Site indicated that potential changes synchronous with a surface wave could occur. No evidence is known to the writer of similar changes in association with H.E. detonations, and the effect was therefore looked for in

the 1963 multi-ton detonations.

Potential probes were installed at a depth of 20 ft, at a spacing of 200 ft, in pairs radial to GZ and tangential to GZ, at 4000 ft from GZ. The intersection of the two probe lines coincided with the position of a Sprengnether seismograph.

The data available up to the present time are not conclusive. No short period variation was detected which could be associated with the surface wave periods. However, a definite change in the potential difference between the probes was detected synchronous with the arrival of the airblast. This was a long period effect (order of seconds), and there is no conclusion possible at this stage. At the present time the effect appears to be real, and cannot be traced down to the recording equipment itself. Fig. 32 illustrates the type of record obtained without further comment*.

A second attempt to record this effect, using a 10,000 lb charge, in August, 1963, did not confirm the existence of potential change. Thus the effect may be spurious, or may be associated with large charges or specific soil conditions. Definitive experiments will be carried out on the 1963 Bell Telephone 40,000 lb trial and the 1,000,000 lb trial in 1964.

.....
NOTE. The BTL 40,000 trial was carried out 15 August, 1963. A record similar to that from the previous 40,000 lb trial was obtained, thus justifying further effort to investigate the phenomenon.

* The writer records his appreciation of the effort being made by the Physics and Meteorology Section's Instrumentation Group in this work.

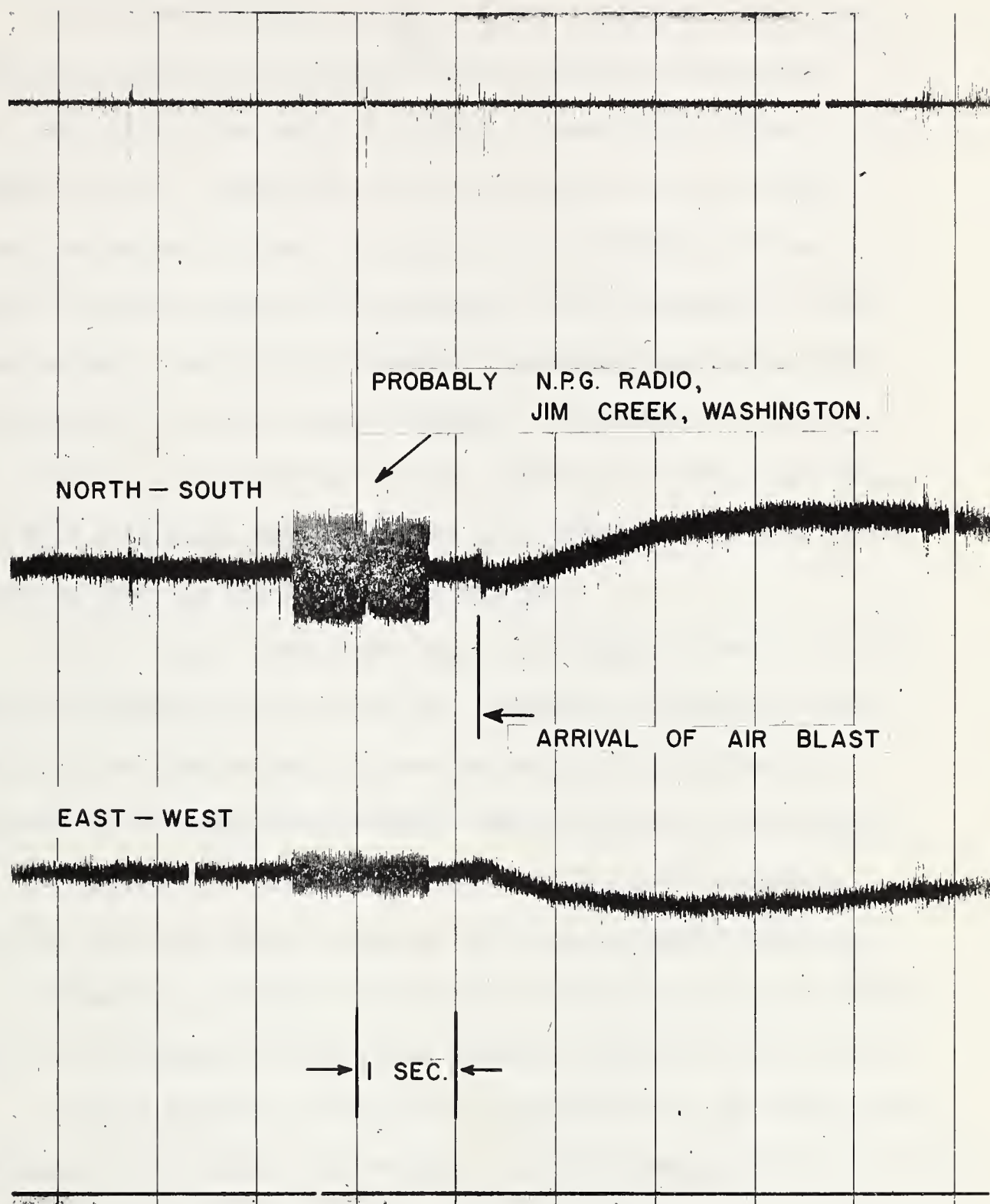


FIG. 32
TELLURIC PROBE RECORDS

3.70 The Transverse Motion

One of the dominant features of the seismograms from the Suffield test sites is the relatively large amplitude transverse motion. Such transverse motion is almost automatically dubbed "Love Wave Motion". Surprisingly few data appear to be available on transverse motion for short periods, or for explosive sources. Virtually the whole of the EJP discussion, and the references cited by these authors, deal with continental and oceanic Love waves with periods greater than about eight seconds. An exception is the Lg phase, a short period transverse motion coupled to a vertical motion, but, in this case also, the discussion is reserved for the continental phase with periods in the range 1 - 6 seconds.

Love's theory treats the transverse motion as being strictly independent of motion in the other two components. Numerical computations have been undertaken of Love-type motion by Harkrider and Anderson (1962) and others for specific cases relevant to long period waves. Horizontal anisotropy in the medium will lead to coupling between the body wave modes, removing the division into P and S type waves. Presumably a similar coupling will occur in the case of surface waves but no satisfactory theoretical analysis appears to be available.

In this section, attention is concentrated on the experimental observations by the writer. These data are more extensive than any hitherto available for the range of periods below one second, for a range of charge sizes. Strong motion studies of the transverse wave for a limited charge size have been undertaken by the Saint Louis explosion seismology group (Kisslinger 1959, 1961, 1962 and Kisslinger et al 1961). Discussion of

some of the Suffield results have been given by Jones (1962b, c).

We consider first the evidence for repeatability of the wave form in a given azimuth from repeated charges on the same GZ. This is a matter of some importance as several of the theories dealing with the origin of transverse motion (see, for example, Press and Archambeau, 1962) suggested that we must look to the crater region itself. These theories cannot account for a consistent radiation pattern on a given ground, and must fail if there is evidence of such consistency. The F.E. 536 series of 10,000 lb shots provides a direct check on this point. Seismograms 47W, 52W and 58W were all obtained at a distance of 2000 ft from 10,000 lb charges detonated on the same GZ, the craters being excavated, filled, and partially re-consolidated between shots. The transverse surface wave portion of these records is re-plotted in Fig. 33(a) on a common time scale. Virtually exact duplication of the wave form is evident, both in amplitude and frequency. Two records were also obtained on another common bearing, but unfortunately one of these records is the only known instance of a recorder being run with batteries too weak to bring the time mark motor up to speed. However, it is possible to match two recognizable peaks and so correct the time scale in this case. The corrected and uncorrected record, together with the record from the other trial, are shown in Fig. 33(b). It is quite evident that there is virtually complete matching. Even one case of matching is sufficient to prove the point, without labouring the issue. Kisslinger et al (1961) have also detected a similar repeatability on another test site, so that the 'radiation pattern' appears to have a distinct geographical orientation, presumably

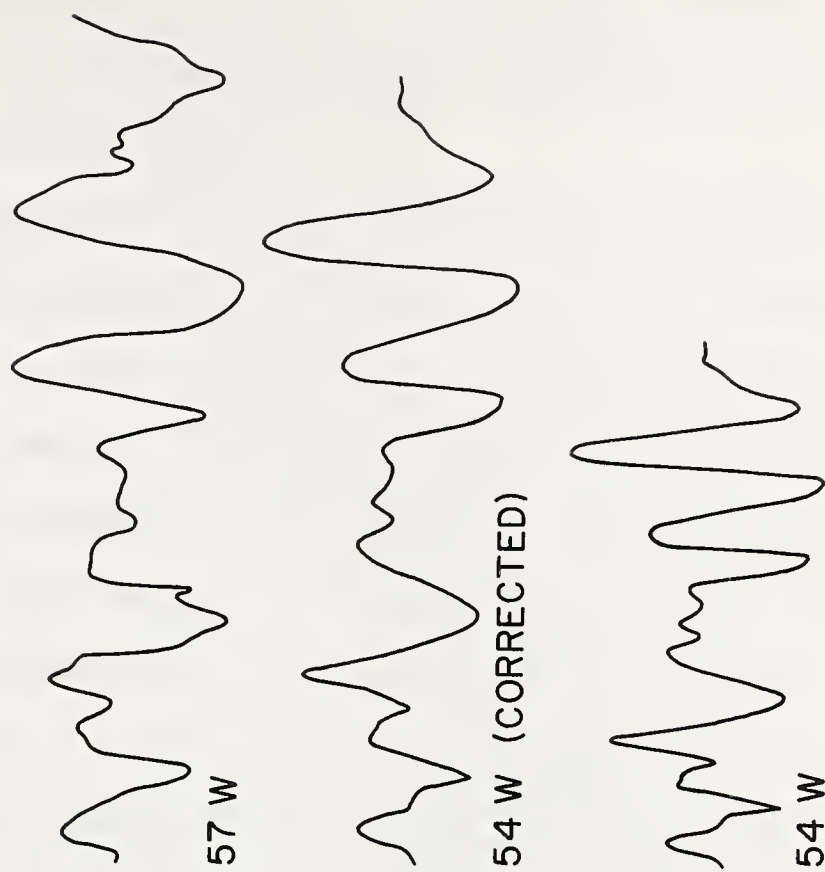
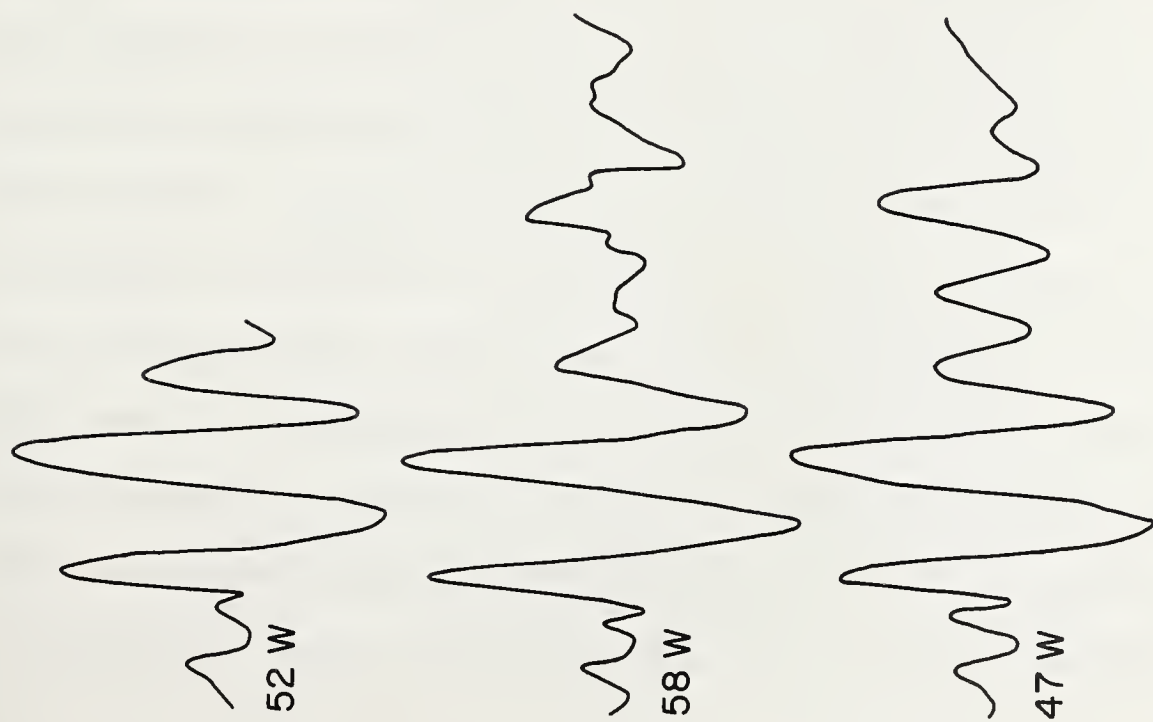


FIG. 33

REPEATED TRANSVERSE MOTION

based upon sub-surface features. A similar repeatability is evident in the records from the Nevada Test Site (Seismograms 80 - 88N), where there is no air-blast effect.

Kisslinger et al, using very small charges which resulted in short and comparatively simple seismograms, were able to demonstrate a lobed radiation pattern similar to that predicted on the Knoppoff and Gilbert Model (Knoppoff and Gilbert, 1960). Nodal lines, of the type demonstrated by Kisslinger et al, must exist for any transverse motion which is not a pure rotation. Nevertheless, the present writer is not convinced that these nodal lines are permanent in direction. The few azimuthal variation data available from the present work are re-plotted in Fig. 34 in the form of a time-displacement plot on seven bearings. It will be seen that, while there is certainly a tendency to larger amplitudes on the 25° line, there is no real evidence of a nodal line. In the experience of the writer, the overall pattern of amplitude in the transverse trace is quite independent of the bearing of the seismic line. The shape of the profile repeats along a given line, and varies from azimuth to azimuth, but the duration of the train, and the mean amplitude, appears to be essentially independent of the particular azimuth selected. Dogmatic statements based upon the few data available on azimuthal variation on the Suffield site would be quite out of order. It is proposed that a very detailed study be undertaken on the Watching Hill test site with moderate size charges (about 100-300 lb) to investigate the radiation pattern at intervals of not more than five degrees. With the limited instrumentation available, this will require a minimum of 100 shots. Due to the cost of such trials, it is essential that the

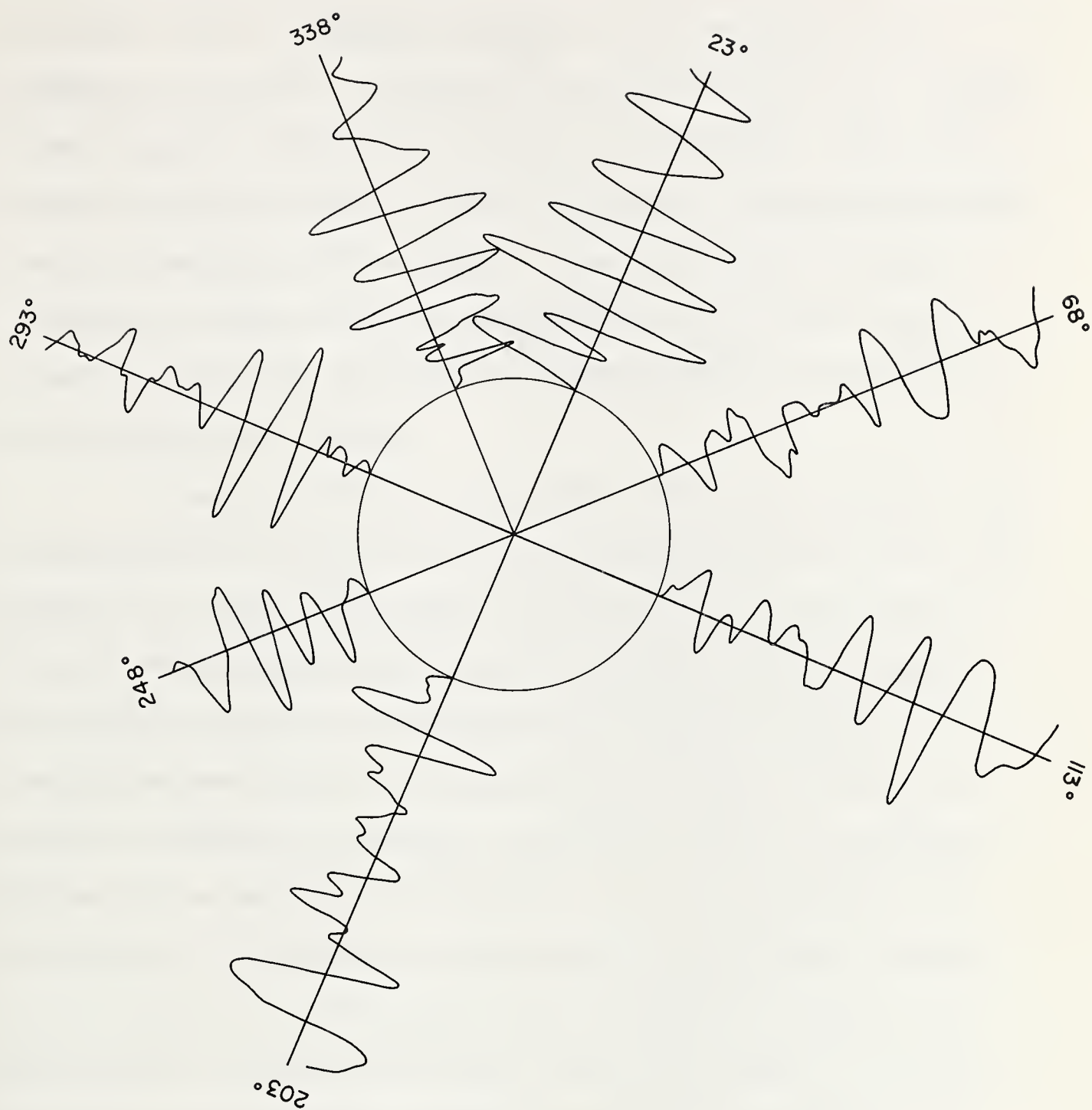


FIG. 34
TRANSVERSE RECORDS AT VARIOUS AZIMUTHS
10,000 LB. CHARGE

programme be linked with other programmes to make full use of the charges, and, until such a coordinated programme can be developed, no time schedule can be given. An alternative method would be to use a simpler form of geophone together with existing tape facilities. This would reduce the required number of shots to about ten, but would require the rental or purchase of new equipment. There are, however, distinct advantages in using mechanical seismographs for this type of study, since this avoids the necessity of analogue studies to determine the true response of the system.

Attention has been drawn (Jones, 1962c) to the apparent coupling between the transverse waves and the radial-vertical waves on the Suffield test sites. With buried charges there is an association of Love and Rayleigh type events, but this association may not amount to coupling so much as a similarity in the dispersion curves. The coupling becomes evident in the post-air-blast region of the seismograms from surface-burst charges. Attention is drawn to seismograms 65W and 71W as examples of this effect, which does not appear to be invariable. It should also be noted that even where direct coupling is not evident, as in the records from the 10,000 lb charges on the Watching Hill test site, the Radial-Vertical wave onset and the Love wave onset are invariably associated, independent of azimuth. It seems unlikely that such an association can be explained by a mechanism of formation which depends upon either a pre-existing or a developing crack structure in the ground. It would appear that some coherent flexure of the surface layers is required.

The initial analyses by Hastrup (1963b) of the two main phases from the buried charges appear to indicate that the transverse

phase associated with the dominant prograde mode in the radial-vertical components may be closely coupled to each other, since both the spectra and the dispersion curves are almost precisely similar to each other. It would appear that this does not apply to the lower velocity phases, but considerable routine analysis is required before definitive conclusions can be drawn.

3.80 Remote Effects

The remote seismic effects produced by these explosions are, generally speaking, beyond the scope of this dissertation. One aspect of remote action, however, is of interest due to the nuisance value. Local areas, comparatively remote from the charge, are occasionally 'shaken' by the explosions, with or without actual damage to structures. This phenomenon is essentially due to atmospheric focussing of the blast wave back to the surface, but it is, in the opinion of the writer, likely that the observed effects are seismic in immediate origin. The essentially acoustic wave is focussed on to a limited area and produces an air-induced wave, possibly described more closely by the Bateman theory than the Press-Ewing theory.

The coupled wave observed by the writer at 55,000 ft from the first 40,000 lb charge (para. 2.43) was almost certainly of Press-Ewing type. However, the first example of interest to the present discussion involved a 10,000 lb charge on the Drowning Ford site. Immediately after the explosion a report was received from a Mr Walker, who farms land East of the river, some fifteen miles from the test site. He claimed that his house and other buildings were badly shaken, with some cracking of the wall panels. As a second 10,000 lb trail was due a week later, the writer and Mr B.J. Perry, Superintendent of Research at SES, arranged to be present at 'Walker's Farm'. An examination was made of the structure of the house, and the alleged 'cracking' investigated. In the opinion of the writer these cracks were not fresh, but may have been made more obvious by dust being shaken out of them. Mr Walker claimed that

previous trials had not bothered the family, though they were always aware when trials were being conducted. The SES representatives, expecting to find the case wildly exaggerated, decided to stand outside the house and observe the arrival from there. The radio countdown was monitored, and a stopwatch started at zero. The cloud was observed within seconds, and at the predicted arrival time (assuming sonic travel for this estimate) the observers were shaken out of their complacency by a loud 'thunderclap' and pronounced shaking of the ground. There were distinct sound effects from within the building, but no additional damage was detected. Mr Walker assured the observers that the effects on this occasion were relatively mild. Since this time great care has been taken to ensure that no large charges are functioned under conditions when focussing is predicted, and in general no complaints have been received, with two exceptions. The first exception involved the Gust farm, some fourteen miles from the test site, where a reaction similar to the earlier one at Walker's farm was obtained. The second exception occurred when a 10,000 lb charge was fired at a point somewhat nearer the village of Ralston. In this case, minor damage (a broken plate glass window) was reported from Medicine Hat, about 30 miles away. It is interesting that in this case people in the street did not hear the explosion, while those within the building assumed at first that a child had broken the window. Whether or not this damage is attributable to the blast is a moot point.

It is very difficult to obtain reliable information on these effects since trials are carried out under conditions which minimize focussing. Attempts have been made to compare normal zones with zones of enhanced pressure, but even with the aid of a helicopter, it is

difficult to arrange for instrumentation to be at the correct locations. From the limited data available, it appears that pressures of up to 0.01 psi are detectable as a rumble like distant thunder, but there is no detectable ground roll. When the pressure level approaches 0.03 the audible effect is like rolling thunder and there is some sensation of the ground shaking. Presumably, effects such as those at Walker's Farm correspond to slightly higher pressure levels, possibly as high as 0.1 psi. This pressure level in itself is too low to cause damage, but may cause sufficient 'air-induced' vibration to cause very minor structural damage. It would be extremely helpful if a serious attack could be made upon this problem, preferably by studying smaller charges detonated under conditions favouring focussing upon uninhabited areas. At the present time it is very doubtful that sufficient data are available to verify the computer programmes used for predicting anomalous blast effects.*

* The investigation of these effects has been undertaken by Mr. J.J. Vesso (in the field) under the direction of predictions made by Messrs Johnson, Gilbert and Clink. At the present time data are being collected and no final report is within sight. Attention is drawn to Johnson et al (1962) which gives some information on the methods.

4.00 CONSOLIDATION OF THE OBSERVATIONS

4.10 The experimental data given in this dissertation will require several man-years of routine technical reduction before the fine details have been elucidated. It is obviously necessary, on scientific grounds, to carry the experimental approach well into the plastic zone in order to determine the mechanism by which the various modes are excited. Similarly, some limited work is required at longer ranges where the modes are well separated. The eventual ramifications of the programme will depend in part upon these scientific considerations, and in part upon economic and political decisions regarding seismological research within the Defence Research Board. It is therefore not irrelevant to quote Wilson and Caless (1963):

"Determination of the precise way in which signals are generated by a seismic source is one of the least explored research areas of seismology".

The proceedings of the Conference of Experts in Geneva indicate quite clearly the need for both experimental and theoretical investigations in this vital area. At the beginning of this research, little, if any, knowledge existed of the form to be expected in the seismograms from the strong motion region close to high yield weapons or other explosive devices in the region of the Western Plains, an area which is not small or unimportant in the field of continental defence. While much of the fine detail remains obscure, the data in the present dissertation are such that a clear picture has now emerged of the general characteristics of the ground-air interaction and the sequence of events to be expected in the strong motion region.

The importance of this as a source of input data in structural effects work cannot be over-estimated.

4.20 We may consolidate what we now know regarding the strong motion effects of large explosions in the plains area into a series of statements, which include the following:

(1) The P and S waves, at ranges where they have separated from the surface waves, may be neglected completely as input parameters in structural damage studies. The amplitudes are far too small to be significant compared with either the direct air blast or the surface waves.

(2) The air blast and the seismic waves are closely associated at all distances within the strong motion region, which we may define for this purpose as the circular area centred on Ground Zero and extending to an airblast overpressure of about one-tenth psi. This definition does not contravene the more usual seismic definition of the strong motion region as being that in which instruments with gains not greater than one hundred produce usable records.

(3) Within the plastic zone, the air shock and the ground shock velocities decay according to similar curves, which indicates that the ground shock is generated essentially by the passage of the airblast over the surface. The transition between this situation and the situation existing in the case of contained charges requires clarification.

(4) At a certain distance, which corresponds with about 1.25 psi peak airblast pressure in the case of a 40,000 lb charge, the ground shock and air shock curves cross each other, so that the ground shock front leads the airblast. In this region the ground shock is of approximately constant velocity, while the air shock continues to decay in

velocity. The ground shock becomes a 'precursor wave' to the events associated with the airblast. The corresponding pressure level from the 200,000 lb charge was monitored by a Sprengnether seismograph and shows a similar pattern of a short precursor wave immediately ahead of the airblast.

(5) The maximum amplitude in all seismograms occurs in the region immediately following the arrival of the airblast.

(6) Surface waves generated at the Suffield test sites (and elsewhere according to the limited data of Kisslinger, Kuo and Howell) exhibit both retrograde (Rayleigh type) and prograde (Sezawa type) orbits. The common pattern at Suffield consists of a large amplitude prograde-retrograde pair, preceded and followed by low-amplitude retrograde phases. In many cases, however, both the large amplitude phases exhibit prograde orbits.

(7) Prograde and retrograde orbits are normally orthogonal to each other. In certain cases, however, both prograde-retrograde and retrograde-prograde conversions may occur with the tilt of the orbit remaining constant.

(8) The prograde orbit is normally tilted forward of the vertical and the retrograde phase tilted backward.

(9) The pre-airblast phase is retrograde at points close to the epicentre. This phase converts into a prograde phase at greater distances, through a transition zone where the orbit is virtually linear and tilted from the vertical.

(10) Both buried and surface-burst charges excite similar sequences of phases showing prograde-retrograde succession, more than one such

pair being evident.

(11) Where a phase continues for several cycles beyond a transition zone, the tilted elliptical orbit tends to become more circular and vertical, indicating that the pure form is a vertical ellipse with a small ratio of minor to major axes.

(12) Both retrograde and prograde phases exist which exhibit dispersion curves which cross the sonic (and blast) velocity, leading to the possibility (and theoretical necessity) of Press-Ewing type coupling between the airblast and the surface waves.

(13) At points remote from the charge, the dominant seismic effect (and the only one detectable by low gain instruments) is a Press-Ewing type air-coupled wave.

(14) At points comparatively close to GZ there is evidence that a Press-Ewing wave is superimposed upon a surface wave excited by a different mechanism.

(15) The precise form of the post airblast seismic wave form in the region where action (14) is occurring depends sharply upon the relationship between the airblast arrival and the phase of the surface wave at the moment of arrival. Very slight changes in this relationship can cause radical changes in the wave form of the seismogram.

(16) In the strong motion region the dominant seismic effect is apparently closely coupled to the airblast. It is probable that this coupling is a direct induction of the surface wave by a 'Lamb' or 'Miles' type mechanism, but at the present stage of the theory this cannot be verified for a multi-layered medium supporting a multiplicity of phases.

(17) The amplitude of the post-airblast surface disturbance does not of necessity decay with distance, but may actually increase, due partly to the combining of independent wave groups in varying phase relationship, and partly due to the rotation of the tilted orbits towards the vertical.

(18) In the seismograms from contained charges, the maximum amplitude in the vertical trace from the retrograde phase decreases with distance fairly uniformly, but there is a tendency for the amplitude of the prograde phase to increase. The length of the major axes, however, appears to decrease with distance in both phases, and it is suggested that amplitude scaling should always be performed upon the axes of the orbit rather than upon a single component of the motion.

(19) The theoretical dispersion curves for models which approximate to the test site conditions all show a common pattern in which Press-Ewing coupling is predicted for the surface waves from moderately large charges, but is not expected as a dominant effect for small charges.

(20) The periods actually excited by the range of charges used up to the present fall within the allowable range for the Rayleigh mode computed by the Anderson programme.

(21) The peak frequencies in the immediate post-airblast phase of the seismograms correspond very closely to the two frequencies associated with Press-Ewing coupling in the dispersion curve for a theoretical model similar to the test site conditions.

(22) Only the layering down to and including the first Upper Cretaceous layer is significant for charges of moderate size (up to the order of 10^5 lb TNT). It is probable that explosions in the

kiloton (and larger) range will excite long period waves which will depend upon the deeper layers.

(23) Very slight changes in the upper layers of the system can produce very large changes in the seismic effects. Thus the system is sensitive to changes in the weathered layer.

(24) In all components, the dominant frequency is sharply dependent upon the charge size. The larger the charge the longer the period of the wave excited as a measurable strong motion effect.

(25) Small charges, of the order of 10 lb TNT excite low velocity waves which show a dominant period of about 0.2 sec. Larger charges do not excite this period as a dominant one, but tend to excite waves in the period range 0.3 sec. to 1 sec. The precise range depends upon the charge size.

(26) Due to the relatively long period waves excited by the larger charges, the commonly available instrumentation is not well suited to the study of the surface waves. The one second period region corresponds to a transition zone in the instrumentation which is commercially available at the present time. This range is of importance in the study of the surface waves from tactical weapons.

(27) At very long ranges the dominant seismic effect appears to be aircoupling, and it is probable that the effectiveness of anomalous blast propagation in causing structural damage depends upon how efficiently the focussed wave excites an air-coupled wave. Attention is drawn to the recent paper by Frantti*(1963) which shows the correspondence between the spectra of the microseismic background and the air-coupled wave at 100 km from the Suffield site.

* "The Nature of High Frequency Noise Spectra", Geophysics, Vol. 28, No. 4, pp 547-562.

(28) The transverse motion in a given azimuth is repeated very closely for repeated shots on the same Ground Zero, indicating that the radiation pattern is governed by sub-surface features of greater scale than the crater zone.

(29) There is strong evidence of coupling between the Rayleigh and Love type waves in the immediate post-air-blast region of the seismograms from surface-burst charges. In the seismograms from contained charges there is an association between the two wave types, but the coupling is not tight. There is some evidence from the spectra and dispersion curves that the prograde radial-vertical mode and its associated transverse mode are coupled. The evidence is against coupling between the retrograde mode and its associated transverse mode. The last two statements are very tentative, being based solely upon the analysis by Hastrup (1963b) of the 1000 lb buried charge records.

(30) Dispersion calculations in regions composed of more than one phase are of doubtful validity even when obtainable in an 'apparently correct' form. It is a pre-requisite of successful dispersion curve calculations that they be performed on a single phase which propagates without spectral distortion. This means, in general, that the analysis of strong motion seismograms must be associated with the analysis of records of the same events at greater epicentral distances. It is necessary therefore to follow the events at successive closely spaced distances out to such a distance that acceptable separation of the phases has occurred. This entails, unfortunately, the use of a variety of recorders of increasing gain as the epicentral distance increases. It is essential that the seismometer spacing be kept sufficiently small to allow wave velocity estimates to be possible, due to the similarity

in the wave forms at successive stations.

4.30 Experimental development of the research into the strong motion seismology of large explosions may be expected to take the course outlined below.

During the twelve months following August, 1963, explosions at Suffield will include about ten charges of 1000 lb TNT buried at a depth of 50 ft on the Watching Hill Site. These charges are designed specifically as energy sources for the SES-U. of A. MOHO programme, but advantage will be taken of them to improve upon the results obtained with the earlier 1000 lb charges. Specifically, close arrays of seismometers will be installed at ranges of between 4000 and 6000 ft, the seismometer spacing being varied between 50 ft and 500 ft. In this way it is expected that close definition of the spectra and the dispersion curves of each phase can be obtained.

In July, 1964, Suffield will be the site of a detonation of 1,000,000 lb of TNT on the surface of the Watching Hill range. During this trial an attempt will be made to obtain a corresponding set of records to that obtained from the 1000 lb charges. That is to say, no attempt will be made to cover the complete strong motion region, and attention will be concentrated instead upon the limits of the region where the phases will be moderately well separated. A minimum of four seismometers will be used at a spacing of 200 ft. One seismometer will be located closer to GZ (at about 8000 ft) where the effect of the airblast will be marked.

These records, and the existing records included in this dissertation, will be the subject of continuous routine analysis

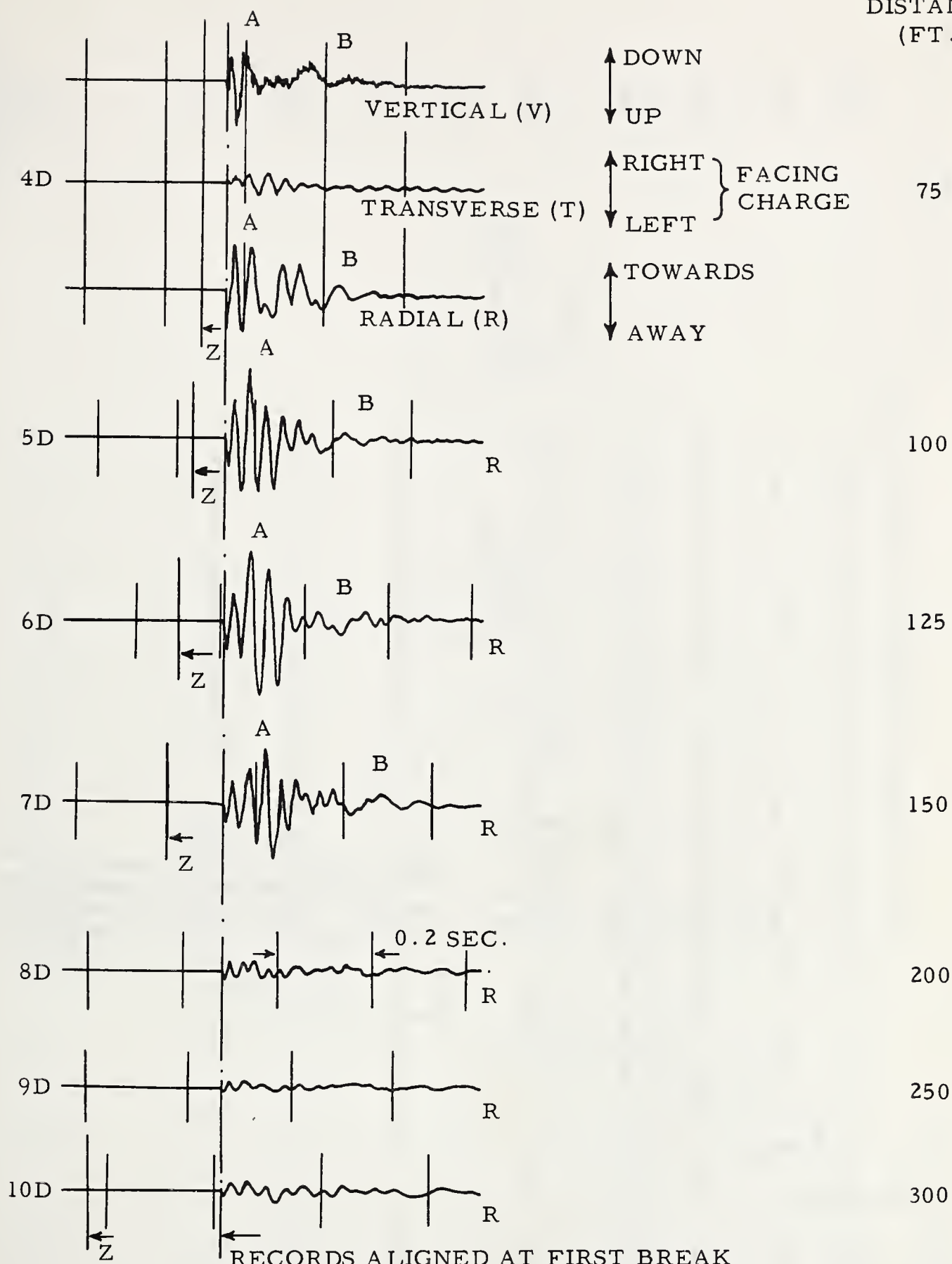
according to the methods of Appendices E and F, a process which may be expected to take about two years.

Theoretical development should proceed by an extension of the Miles formulation of the blast wave problem to the case of a multilayered medium. Due to the complexity of the blast wave propagation and the vicinity of the zone of plastic deformation, it is probable that only qualitative agreement may be expected between the theoretical predictions and the seismograms included herein. It is therefore suggested that a concurrent attempt be made to carry out a model study on the surface waves from airburst charges, which may be expected to fit the theory more exactly. Little model work on surface waves has been reported in the literature up to the present time. It appears, however, that the technology is now sufficiently advanced to justify such work. The model should be of comparatively large size (order ten feet square and correspondingly deep), and modern plastic materials should be used which offer the possibility of approximately correct dynamical scaling, including the scaling of shear velocity contrasts between layers. The use of small airburst charges at about the scale equivalent of a 1 lb charge at 10 ft will prevent plastic deformations and allow the elastic response to be studied by repeated explosions. In order to obtain correct dynamical scaling, it may be necessary to depart from air at atmospheric pressure as the medium for the detonation. This will depend upon the plastic material chosen for the upper layer of the model.

5.00 THE SEISMOGRAMS

The seismograms in the following Section have been prepared by S.A. Cyganik under the direction of the writer. Preparation has included separation of the traces to avoid overlap, removal of the 0.02 second time marks due to the difficulty in reproduction at small scale, and the addition of explanatory captions. The seismograms may be used for all interpretive purposes except those involving very low amplitude or high frequency events. The careful reproduction by the SES Photographic Section and by N. Bonin of the SES Library staff is gratefully acknowledged.

DISTANCE
(FT.)



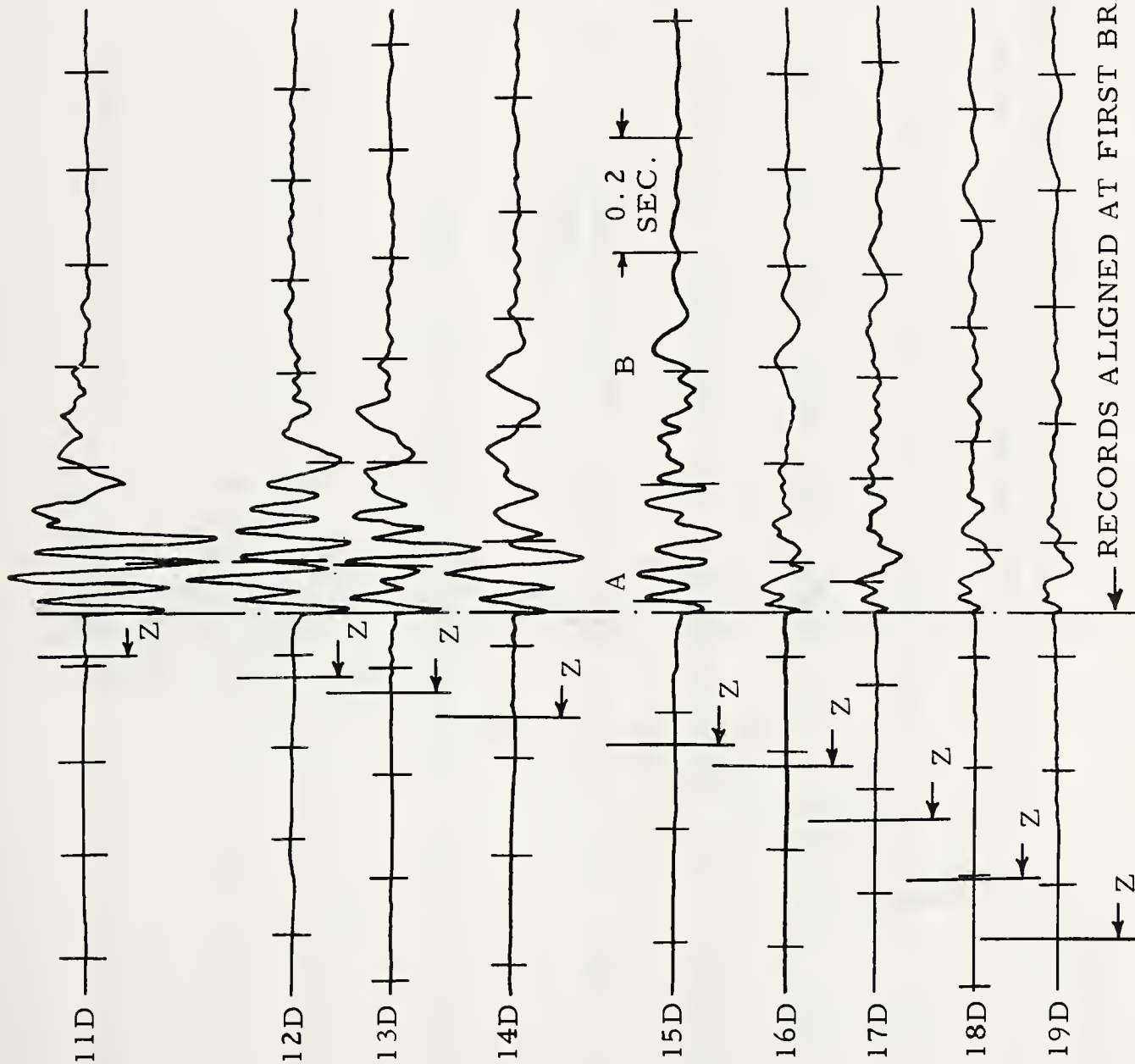
RECORDS ALIGNED AT FIRST BREAK

Z = ZERO TIME

TIMING MARKS = 0.2 SEC.

TYPICAL 8LB. SEISMOGRAMS — DROWNING FORD SITE

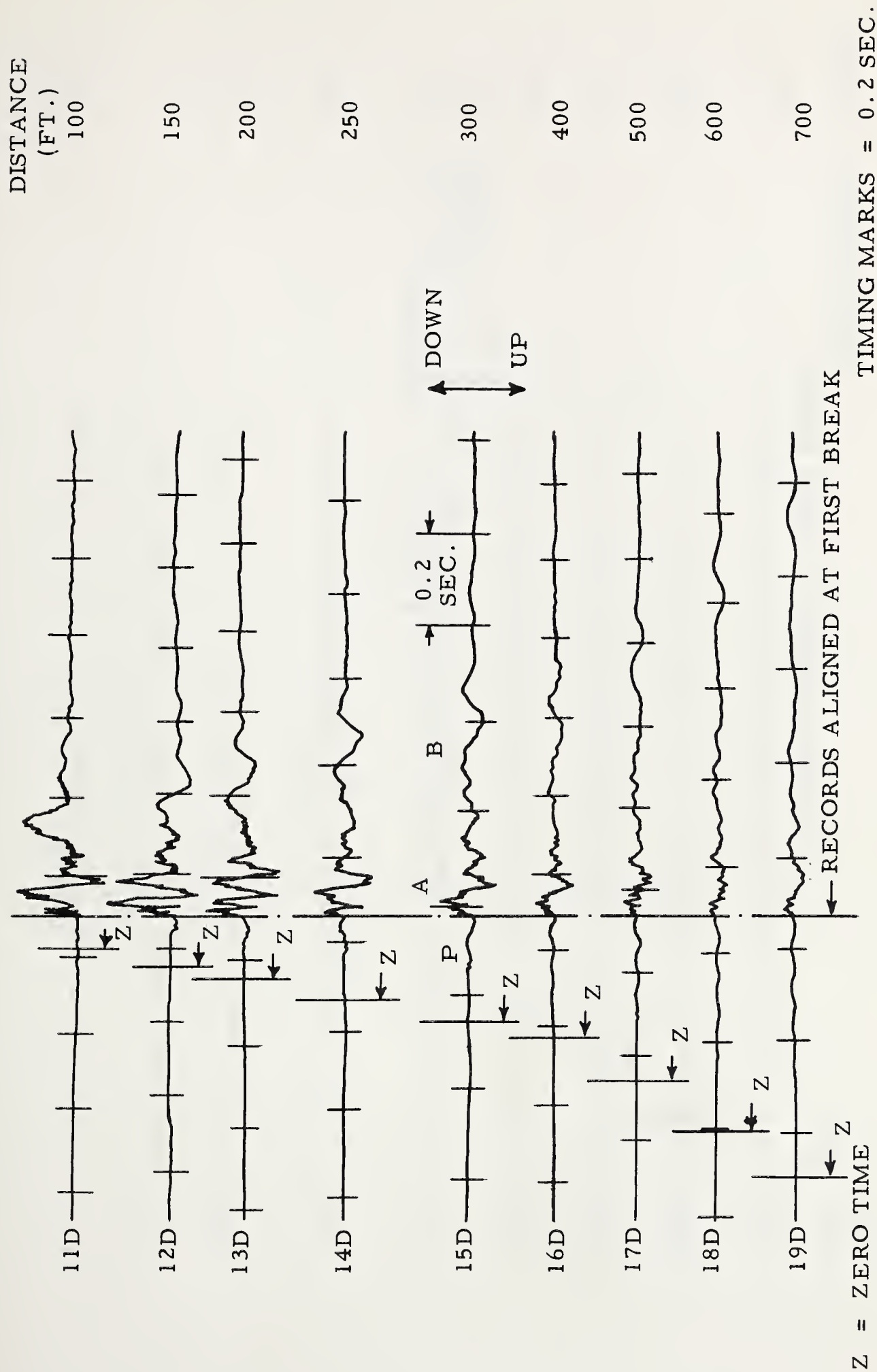
DISTANCE
(FT.)
100



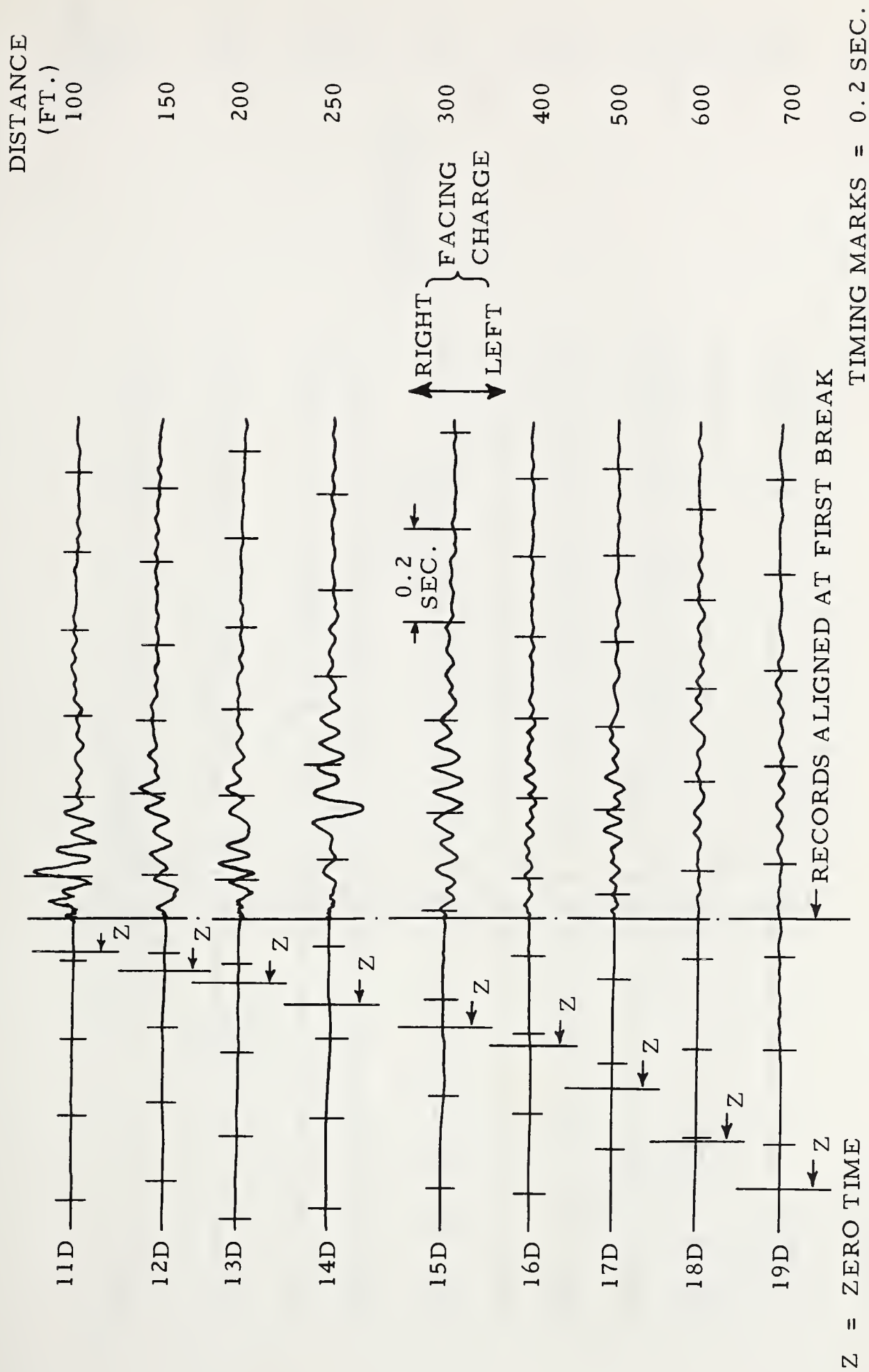
Z = ZERO TIME

TIMING MARKS = 0.2 SEC.

TYPICAL 30 LB. SEISMOGRAMS - DROWNING FORD SITE
RADIAL COMPONENT



TYPICAL 30 LB. SEISMOGRAMS - DROWNING FORD SITE
 VERTICAL COMPONENT



TYPICAL 30 LB. SEISMOGRAMS - DROWNING FORD SITE
TRANSVERSE COMPONENT

DISTANCE
(FT.)

250

400

419

450

480

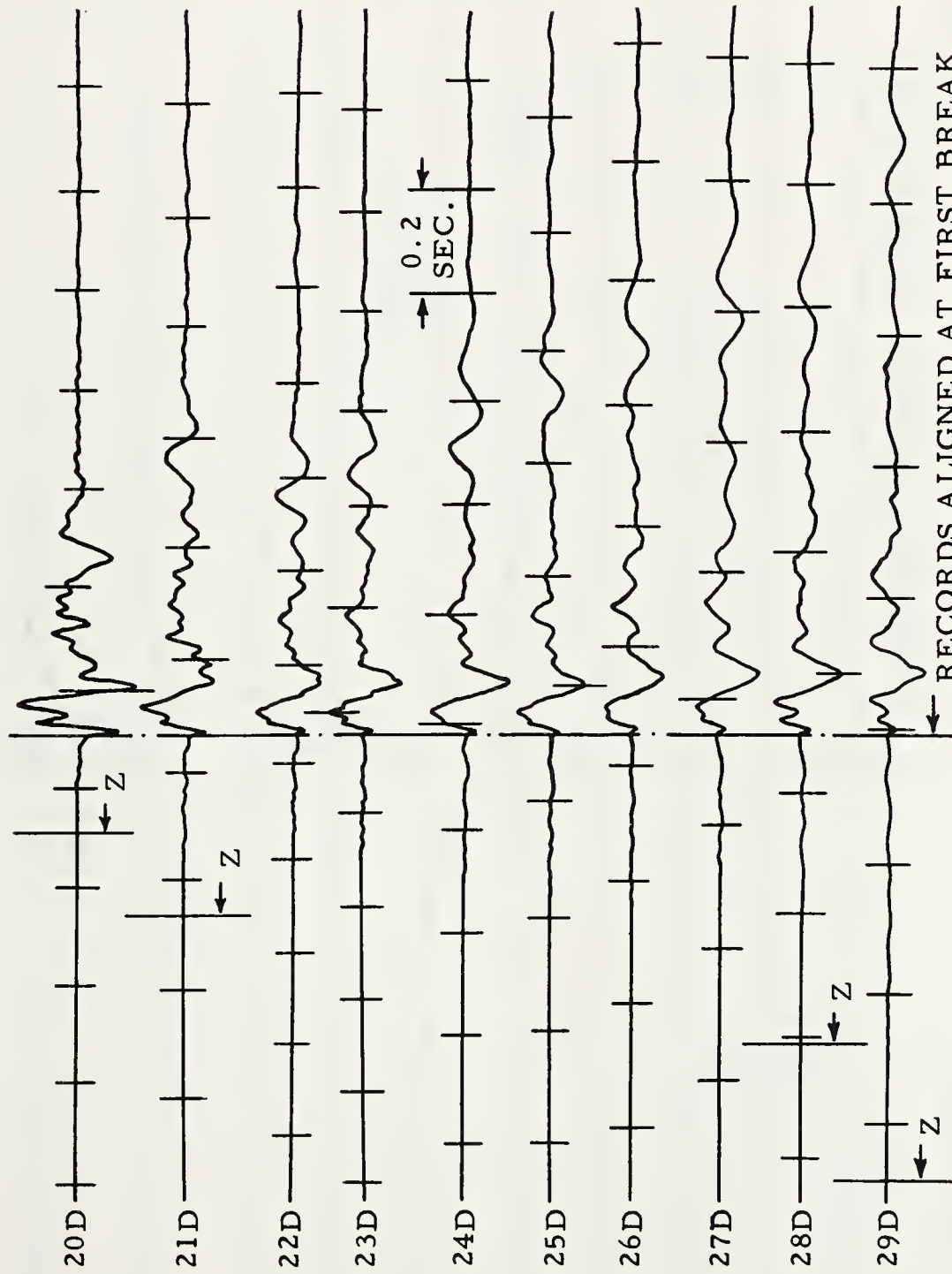
510

541

571

600

800



Z = ZERO TIME

TIMING MARKS = 0.2 SEC.

TYPICAL 60 LB. SEISMOGRAMS - DROWNING FORD SITE
RADIAL COMPONENT

DISTANCE
(FT.)
250

400

419

450

480

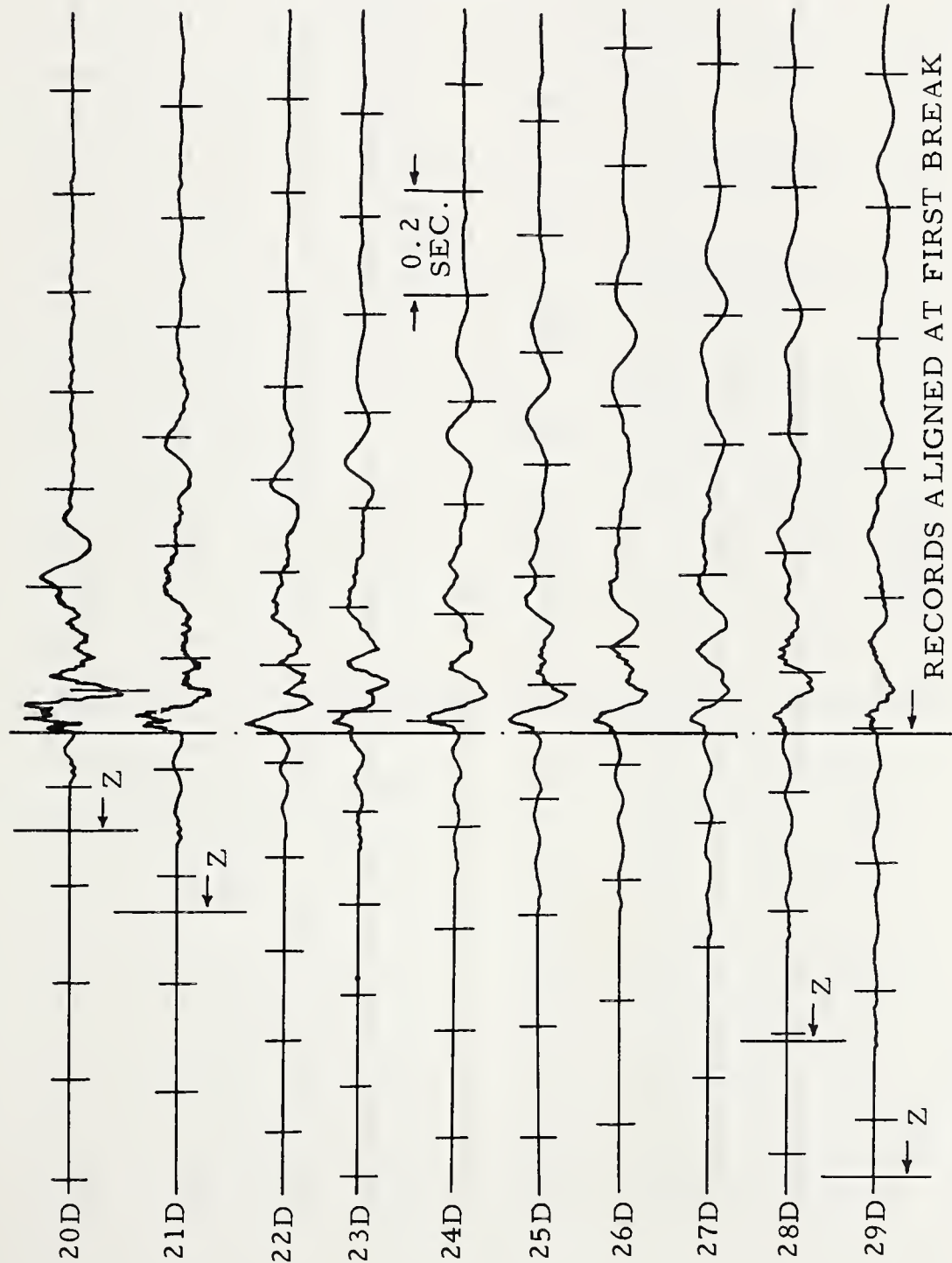
510

541

571

600

800



Z = ZERO TIME

TIMING MARKS = 0.2 SEC.

TYPICAL 60LB. SEISMOGRAMS - DROWNING FORD SITE
VERTICAL COMPONENT

DISTANCE
(FT.)

250

400

419

450

480

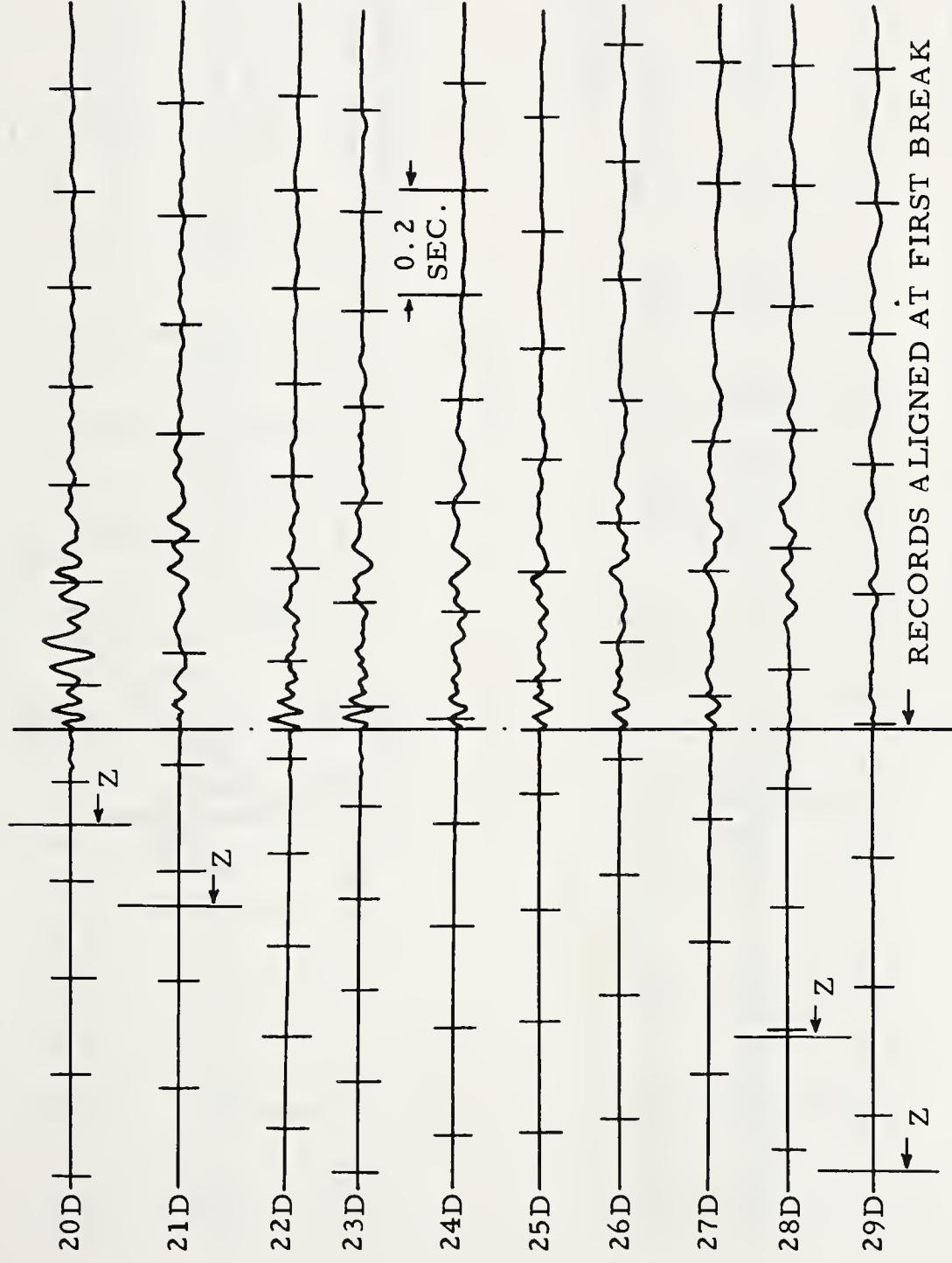
510

541

571

600

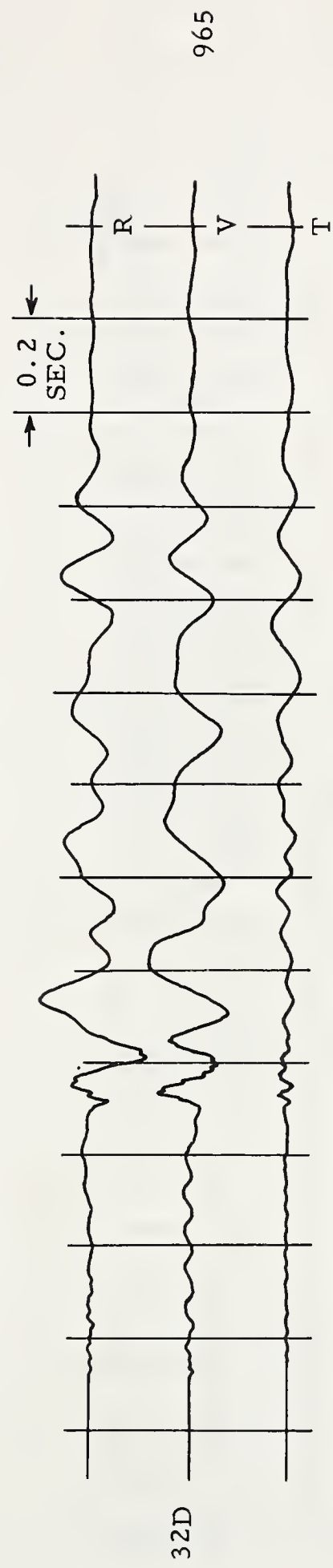
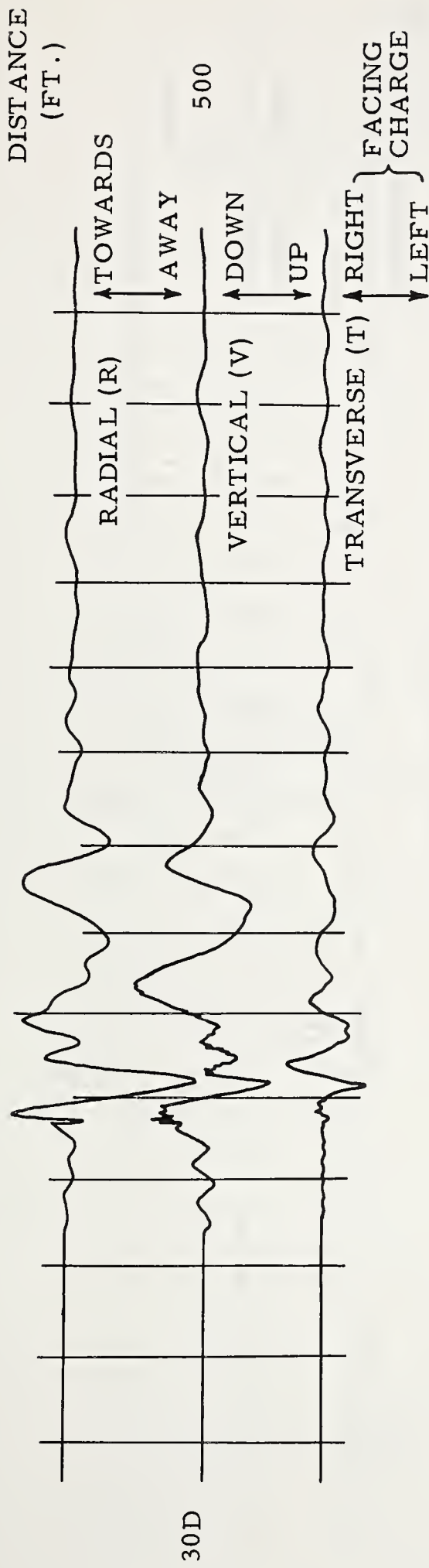
800



Z = ZERO TIME

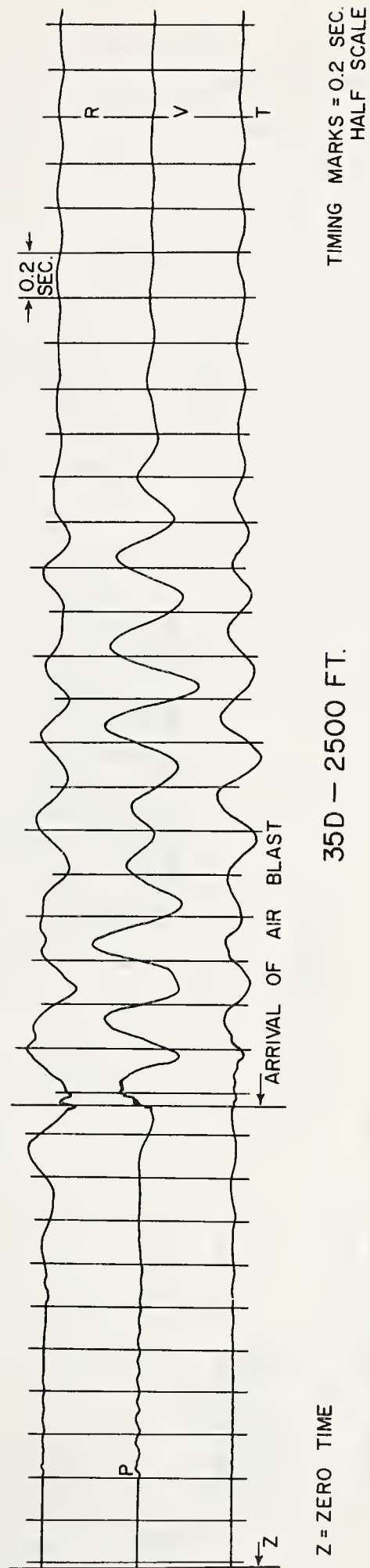
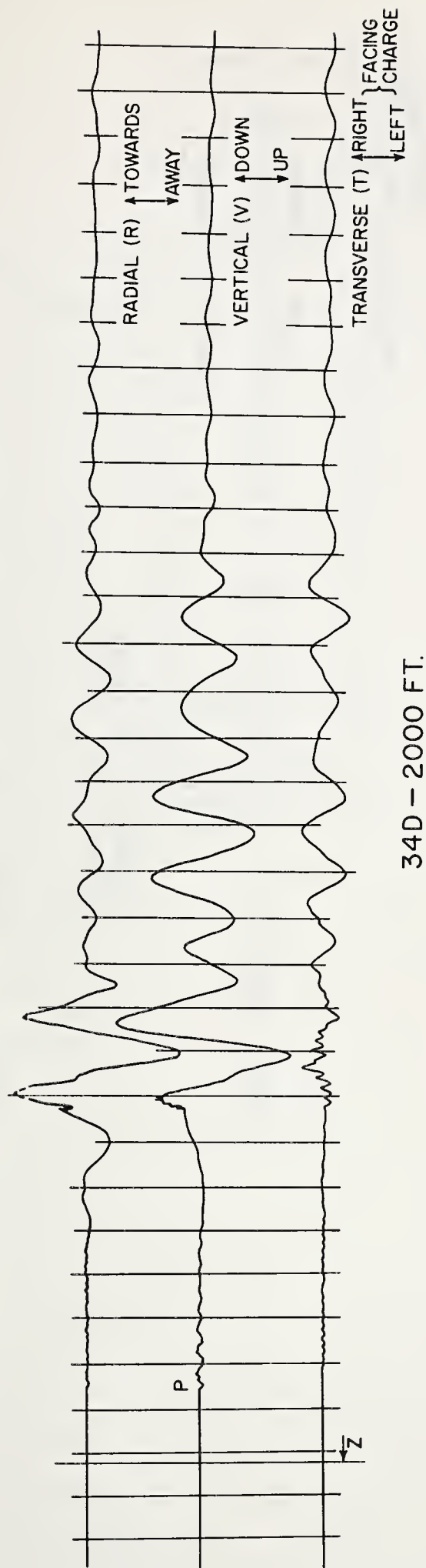
TIMING MARKS = 0.2 SEC.

TYPICAL 60LB. SEISMOGRAMS - DROWNING FORD SITE
TRANSVERSE COMPONENT

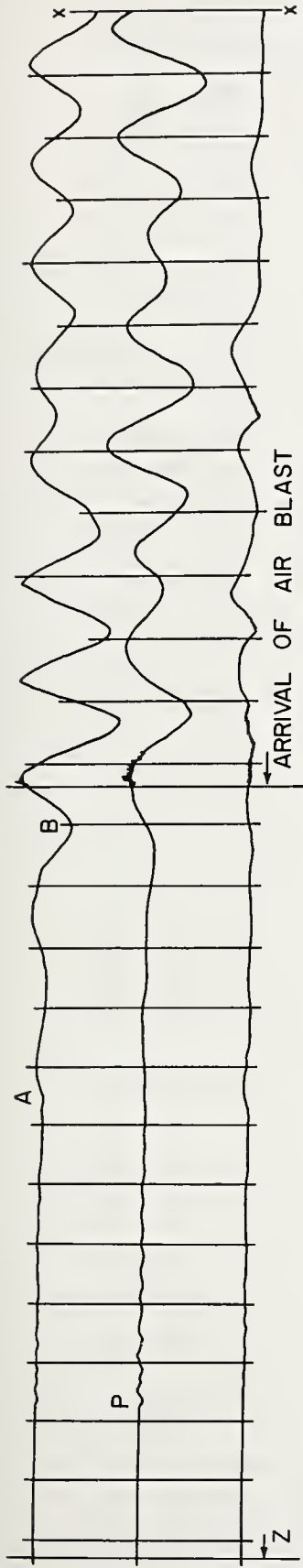


TIMING MARKS = 0.2 SEC.

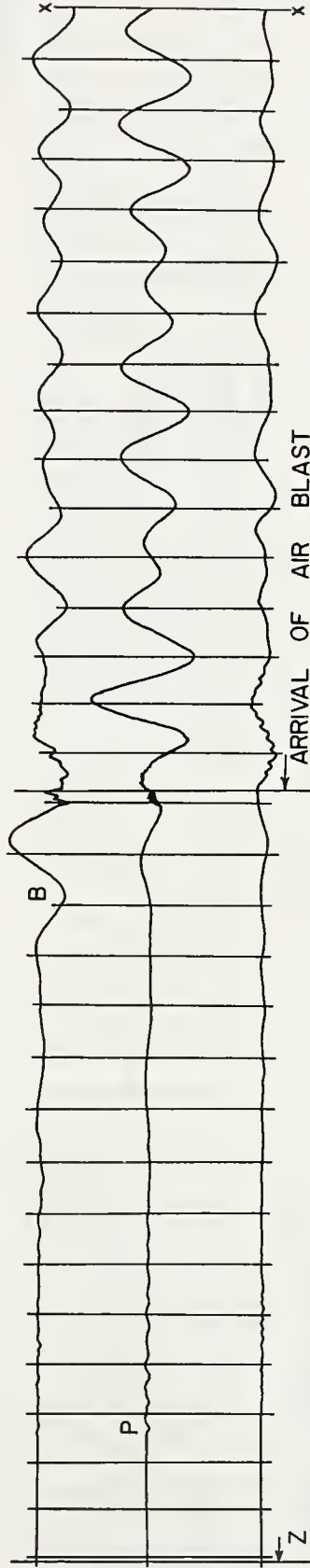
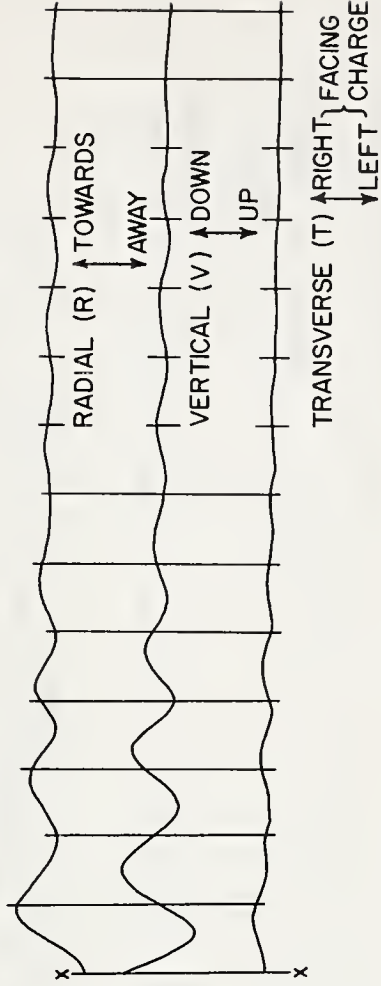
TYPICAL 500 LB. SEISMOGRAMS - DROWNING FORD SITE



TYPICAL 5 TON SEISMOGRAMS — DROWNING FORD SITE



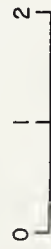
36D — 3000 FT.



TIMING MARKS = 0.2 SEC.

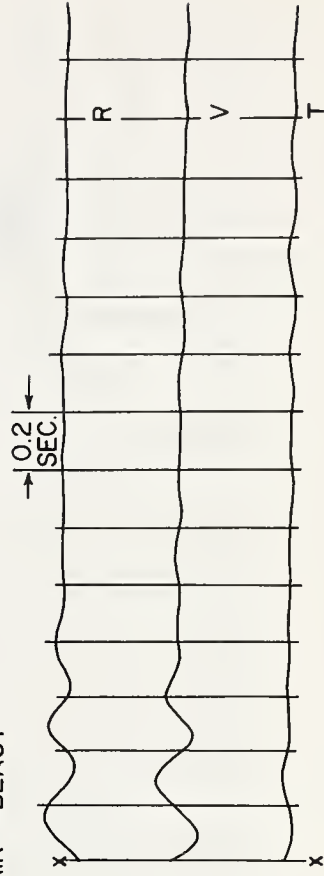
Z = ZERO TIME

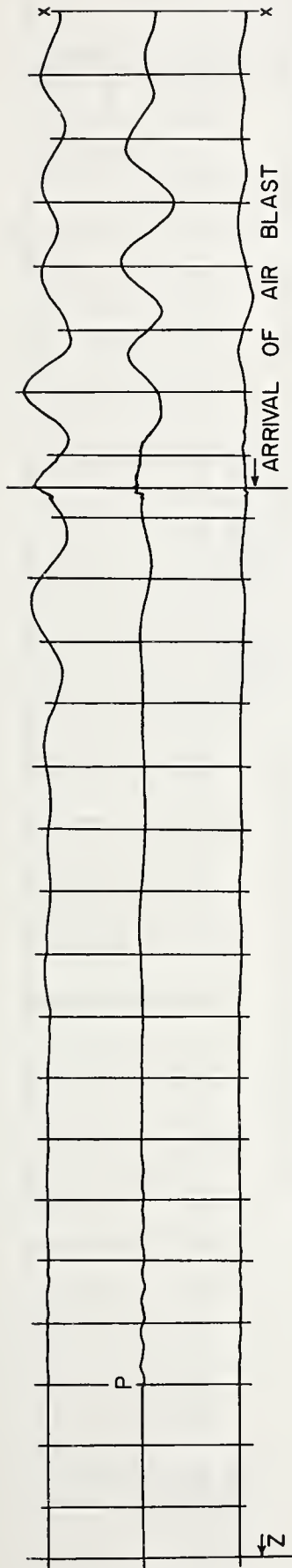
HALF SCALE



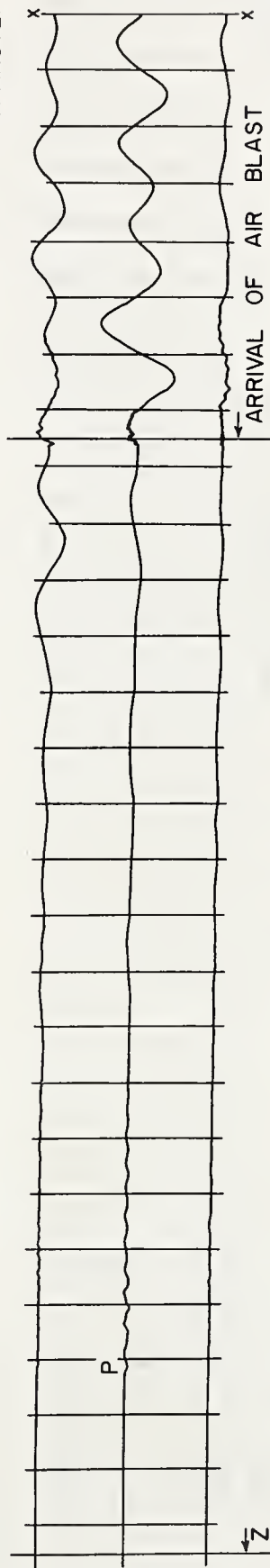
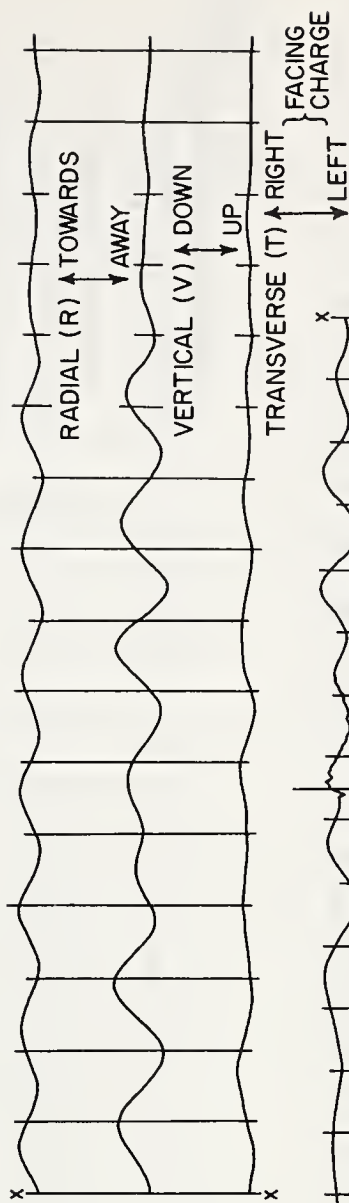
RECORD VERTICAL SCALE (INCHES)

37D — 3500 FT.

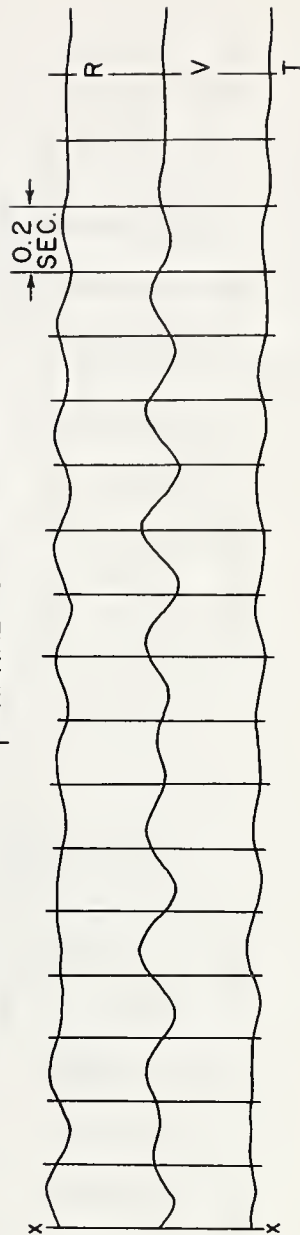




38D — 4000 FT.



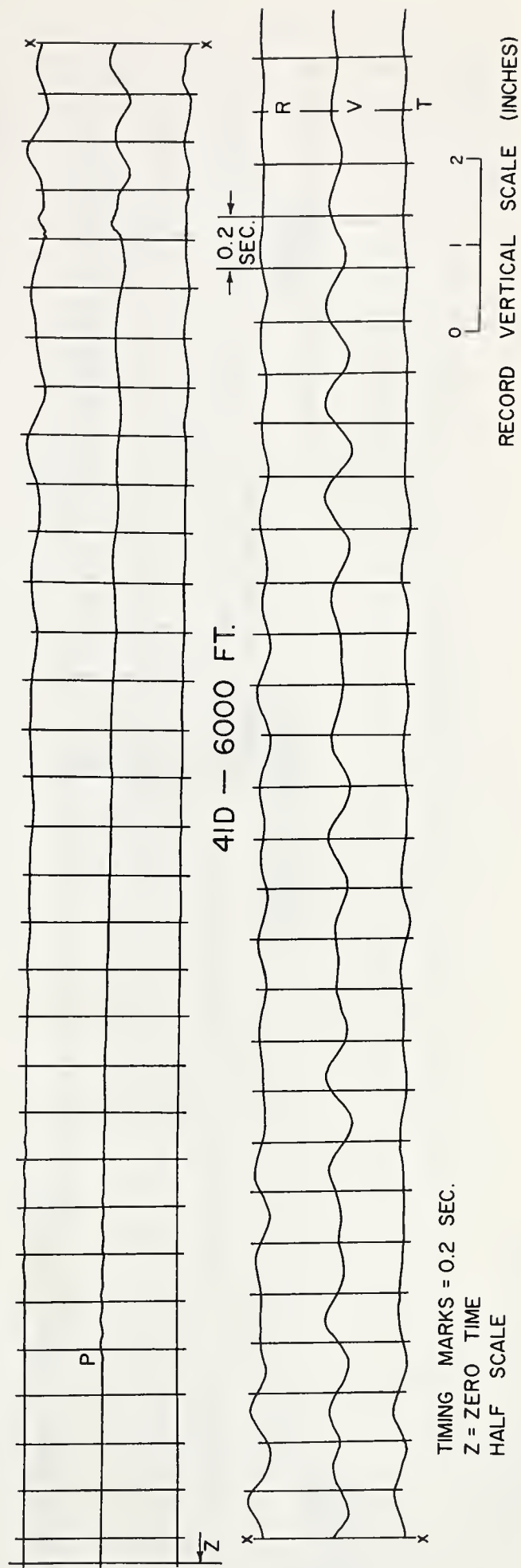
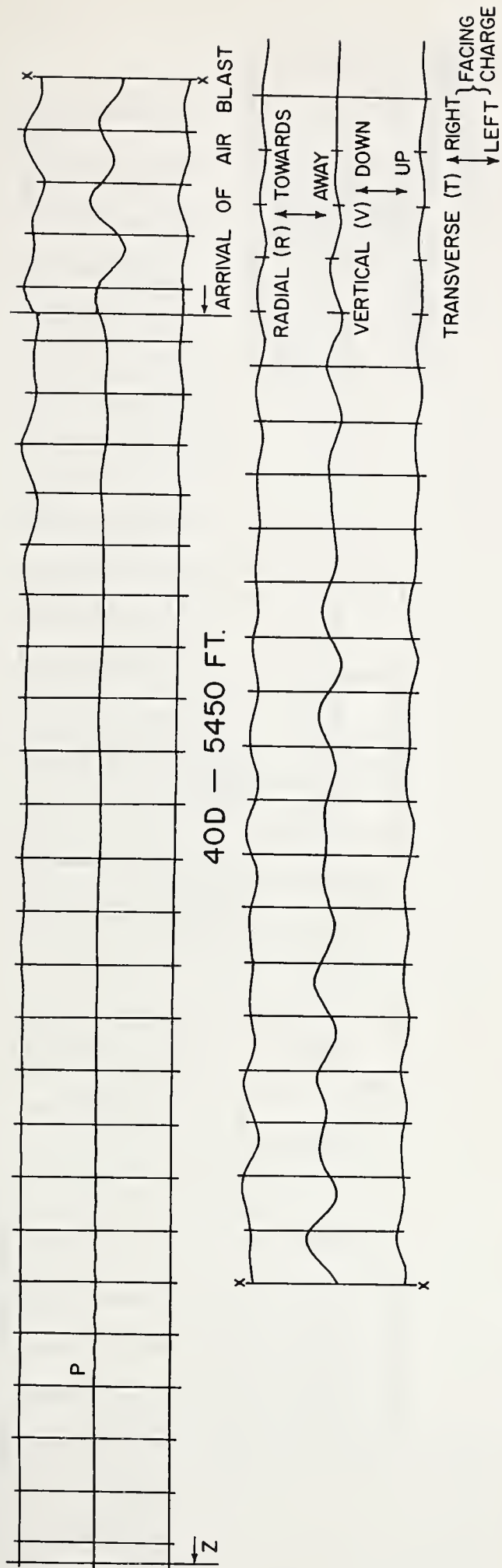
39D — 4500 FT.



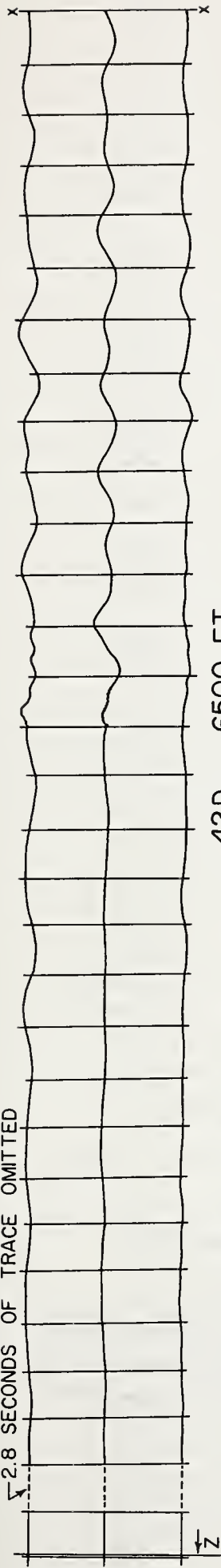
TIMING MARKS = 0.2 SEC.
Z = ZERO TIME
HALF SCALE



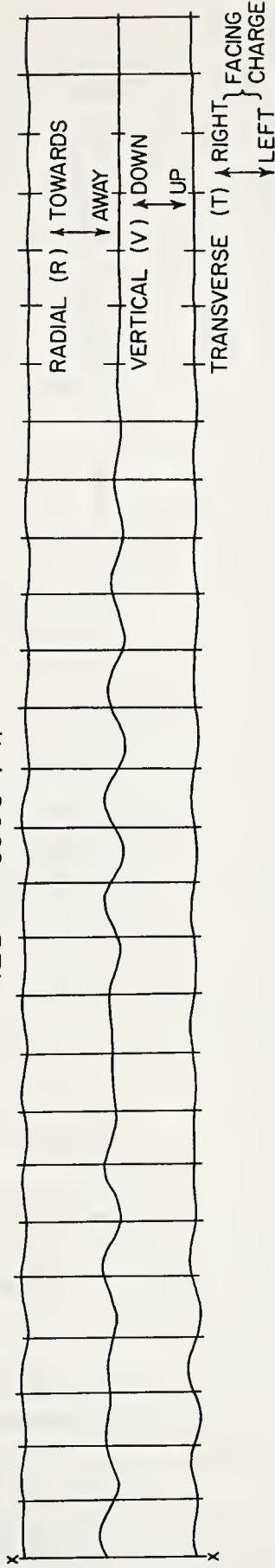
RECORD VERTICAL SCALE (INCHES)



2.8 SECONDS OF TRACE OMITTED

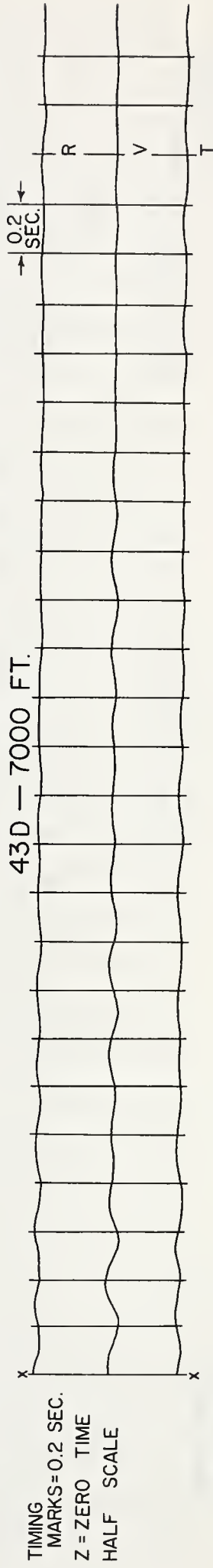


42D — 6500 FT.



ARRIVAL OF AIR BLAST

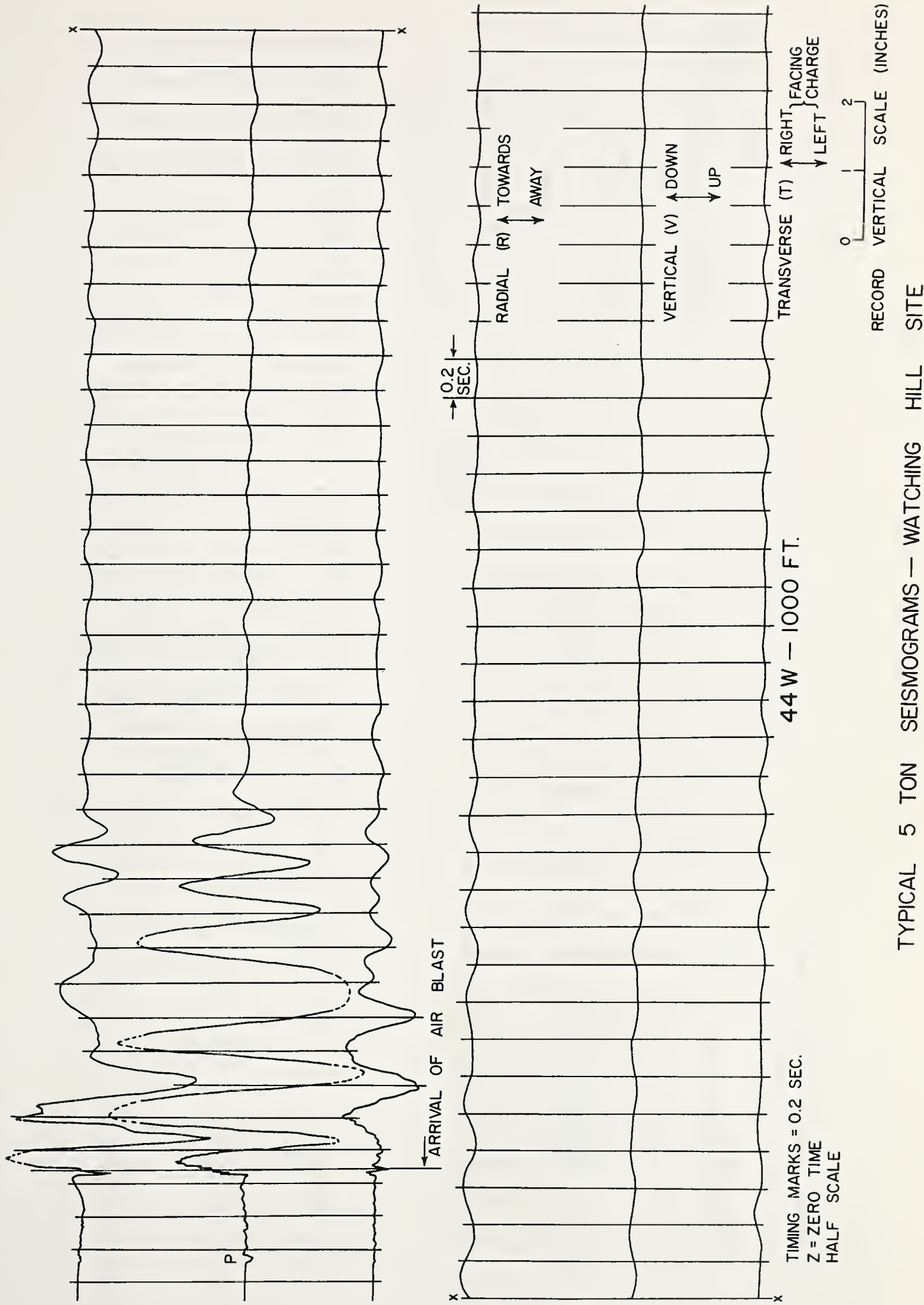
43D — 7000 FT.

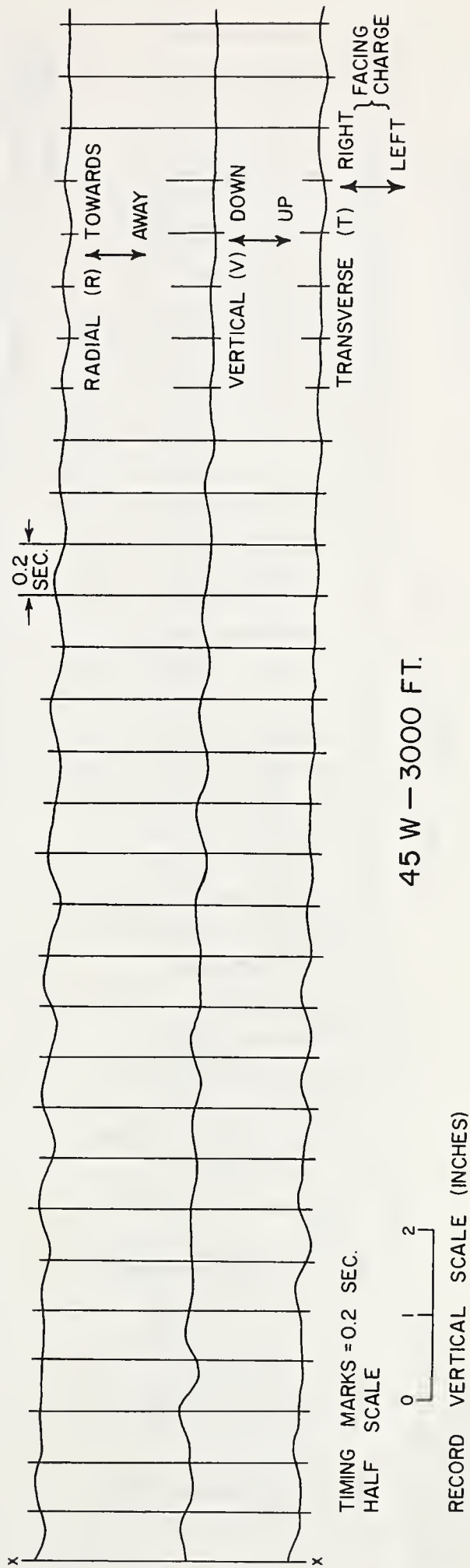
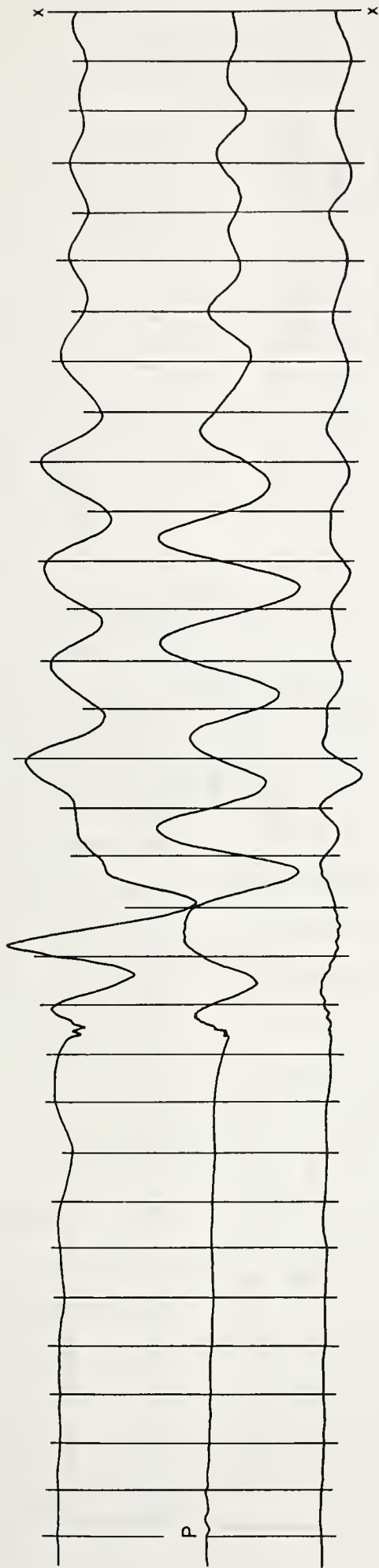


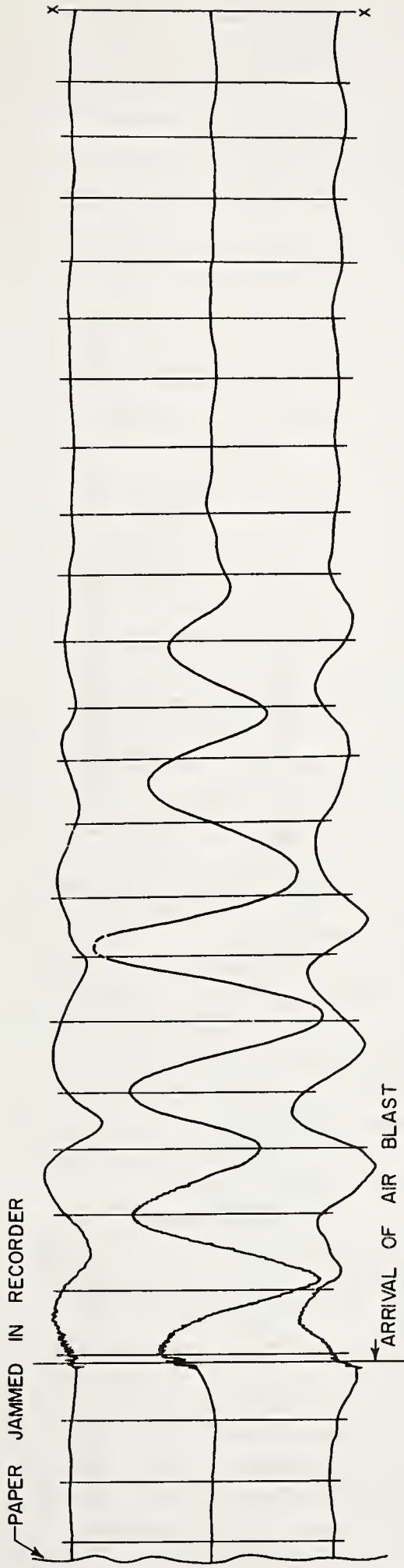
TIMING
MARKS=0.2 SEC.
Z = ZERO TIME
HALF SCALE

0 1 2

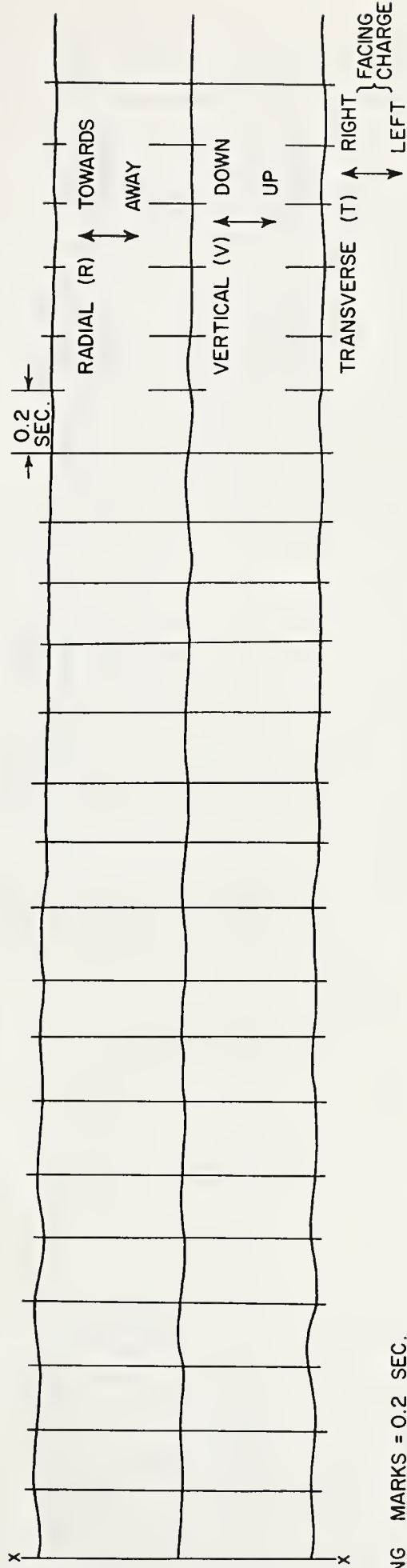
RECORD VERTICAL SCALE (INCHES)







48 W — 2000 FT. NORTH

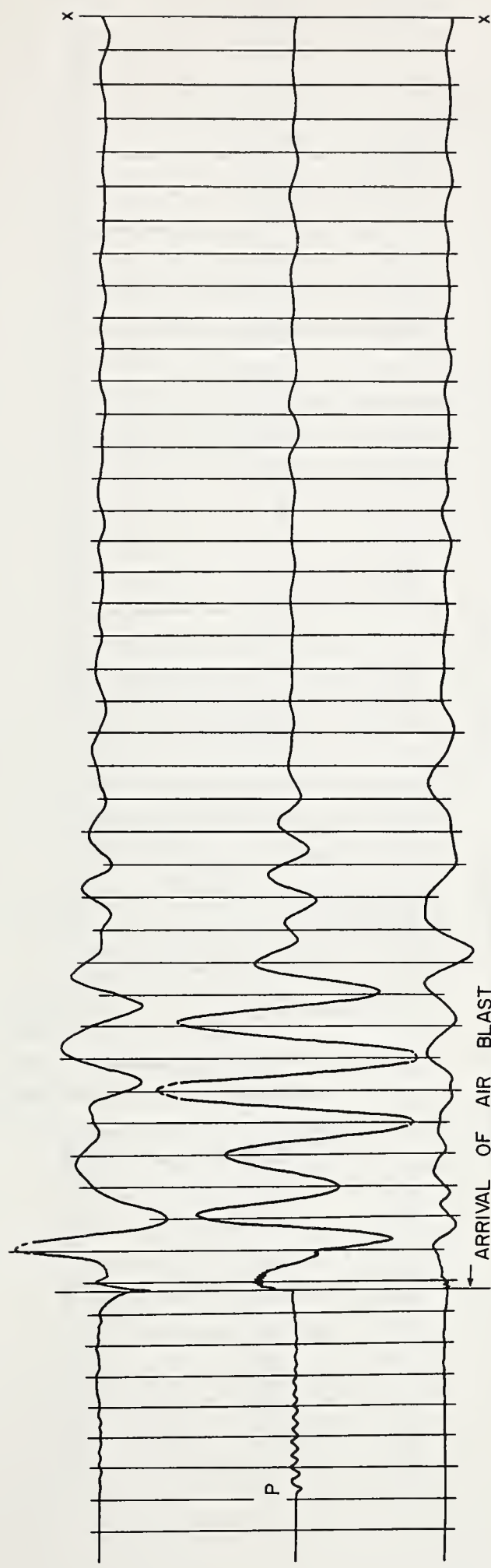


TIMING MARKS = 0.2 SEC.
HALF SCALE

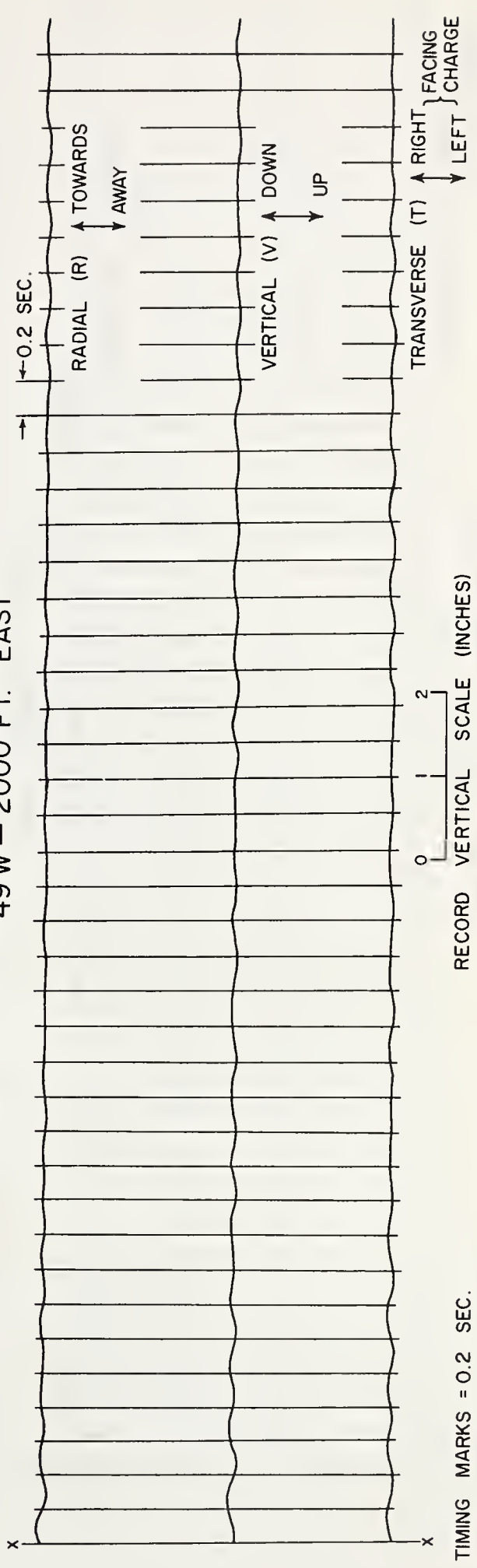


RECORD VERTICAL SCALE (INCHES)

TYPICAL 5 TON SEISMOGRAMS — WATCHING HILL SITE

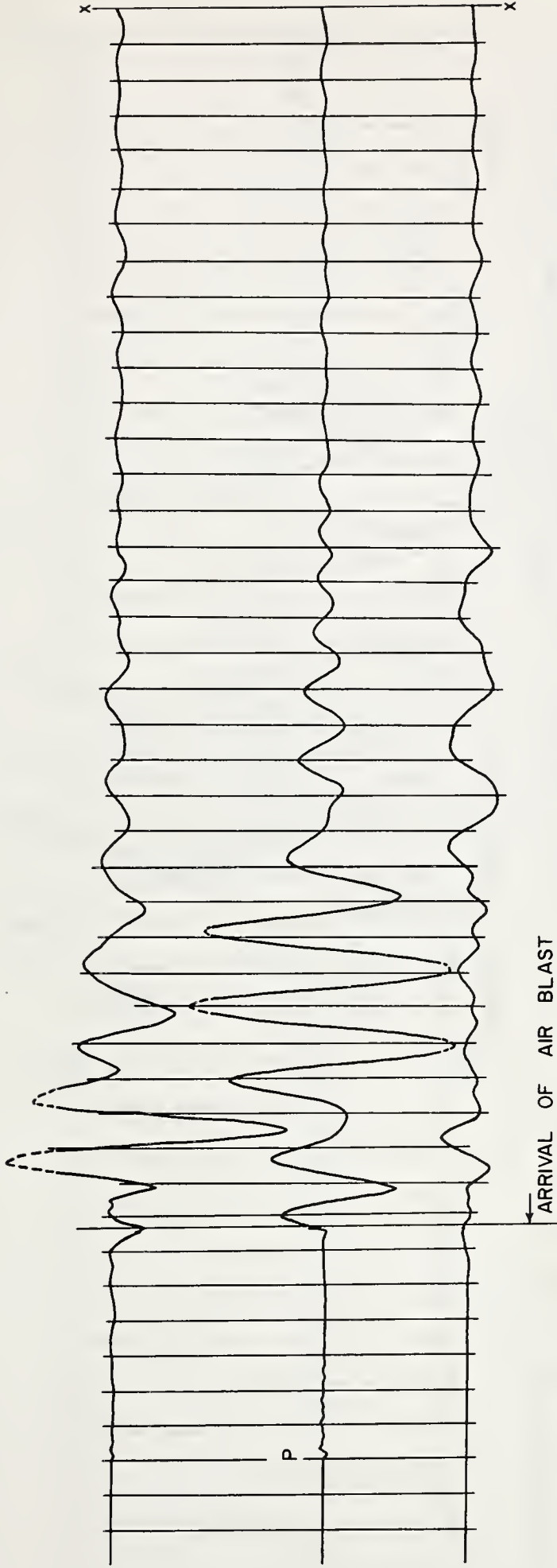


49 W - 2000 FT. EAST

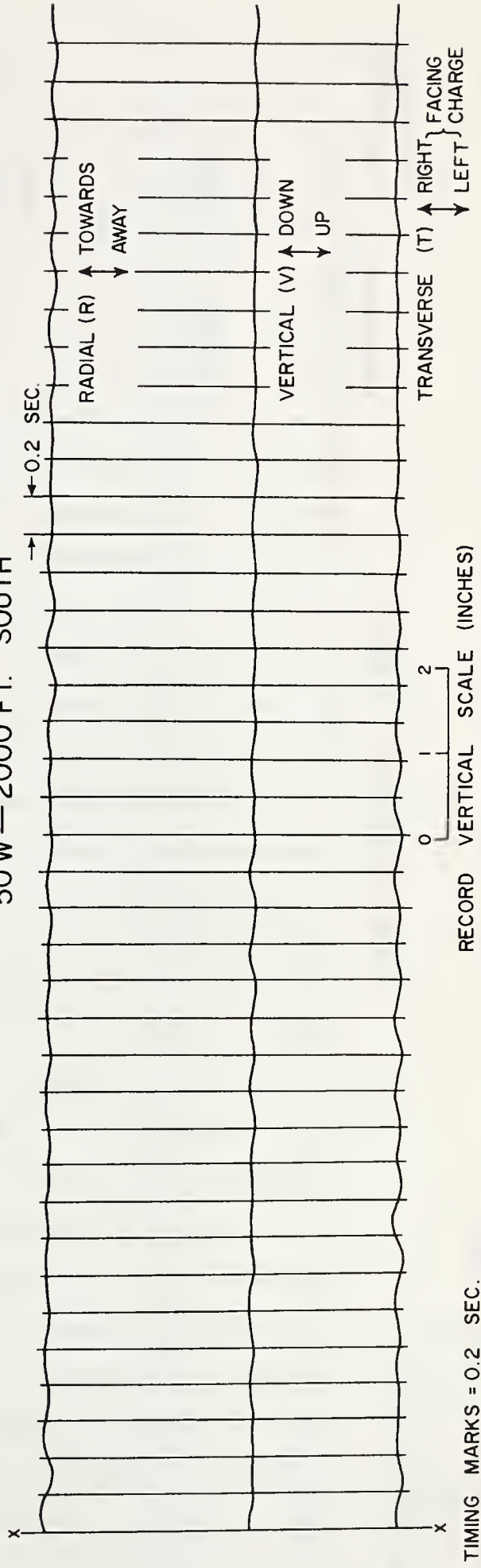


TIMING MARKS = 0.2 SEC.
HALF SCALE

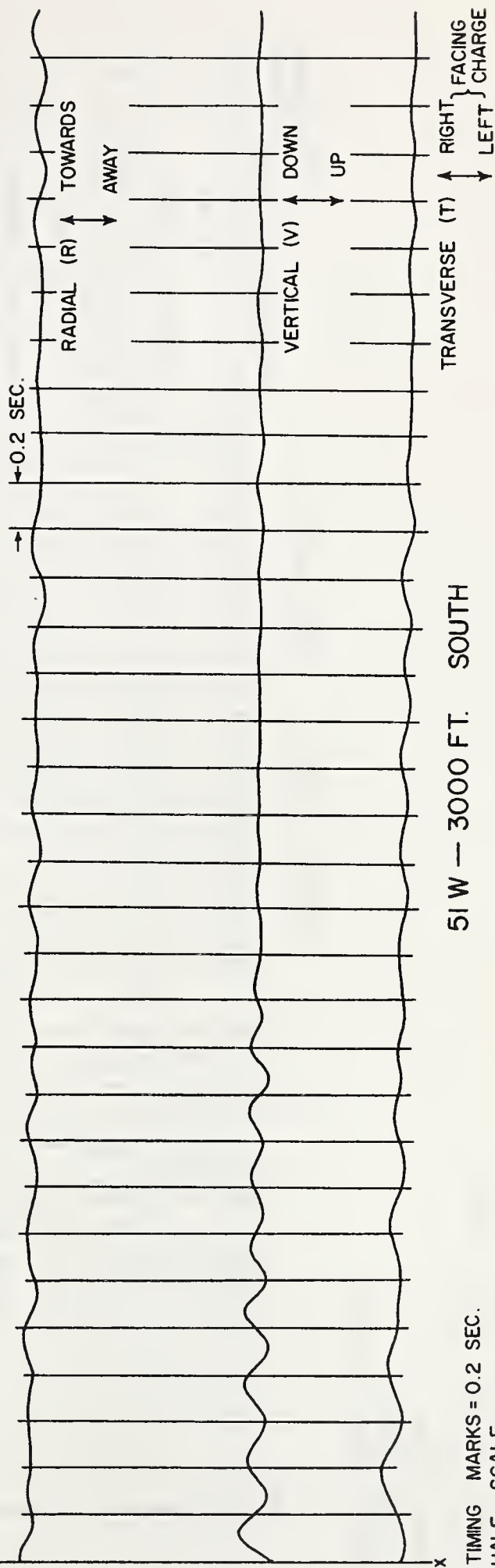
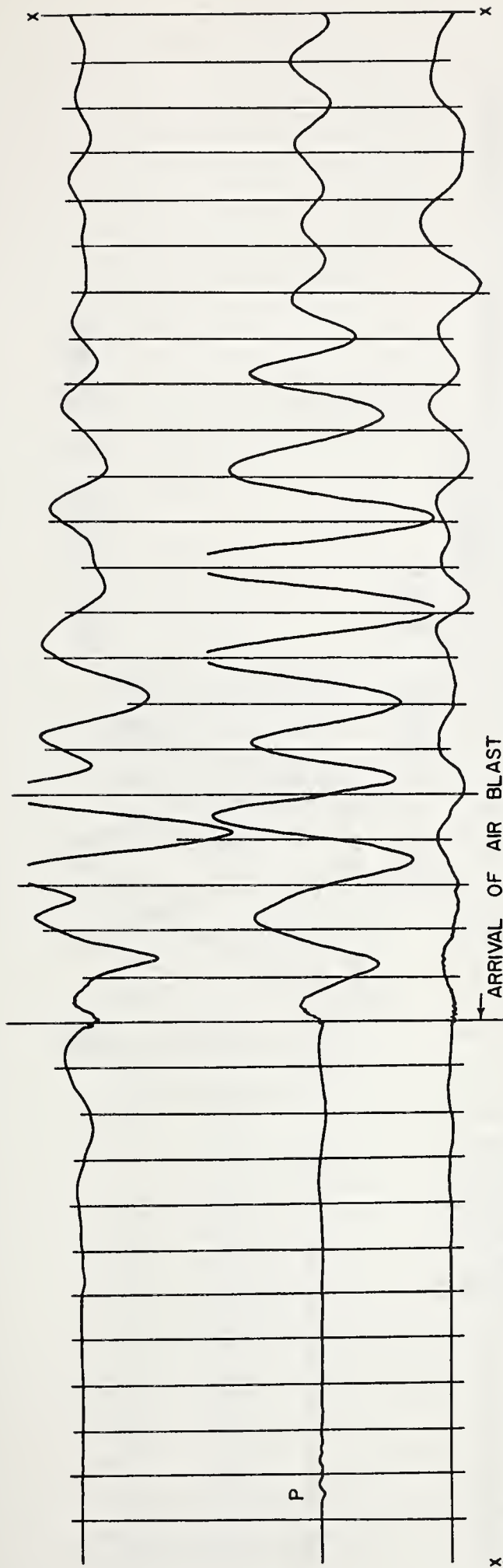
TYPICAL 5 TON SEISMOGRAMS - WATCHING HILL SITE



50 W — 2000 FT. SOUTH



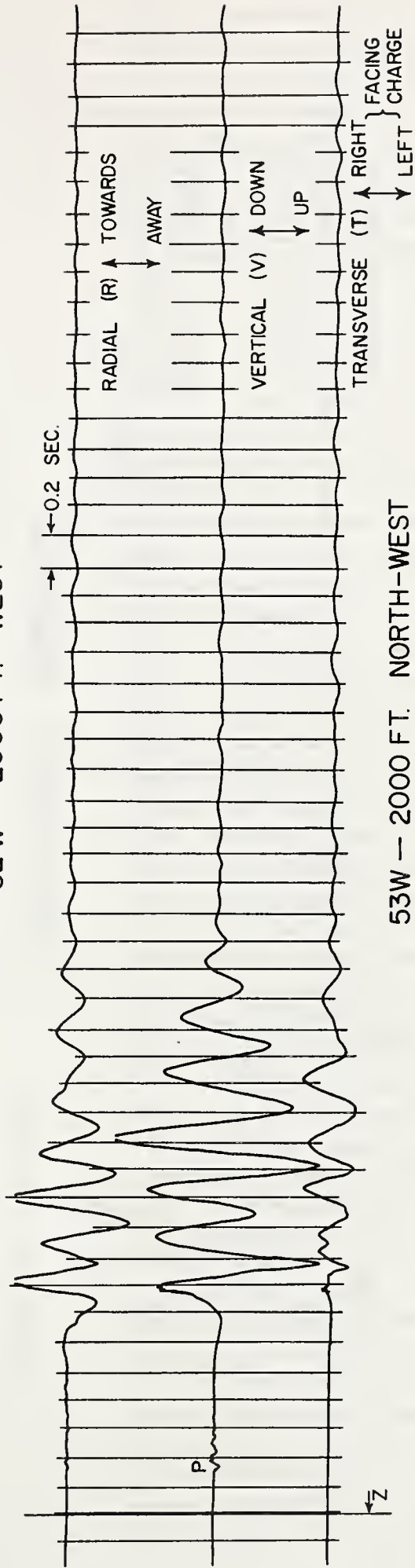
TYPICAL 5 TON SEISMOGRAMS — WATCHING HILL SITE



TYPICAL 5 TON SEISMOGRAMS — WATCHING HILL SITE



52 W - 2000 FT. WEST

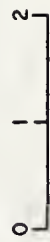


53 W - 2000 FT. NORTH-WEST

TIMING MARKS = 0.2 SEC.

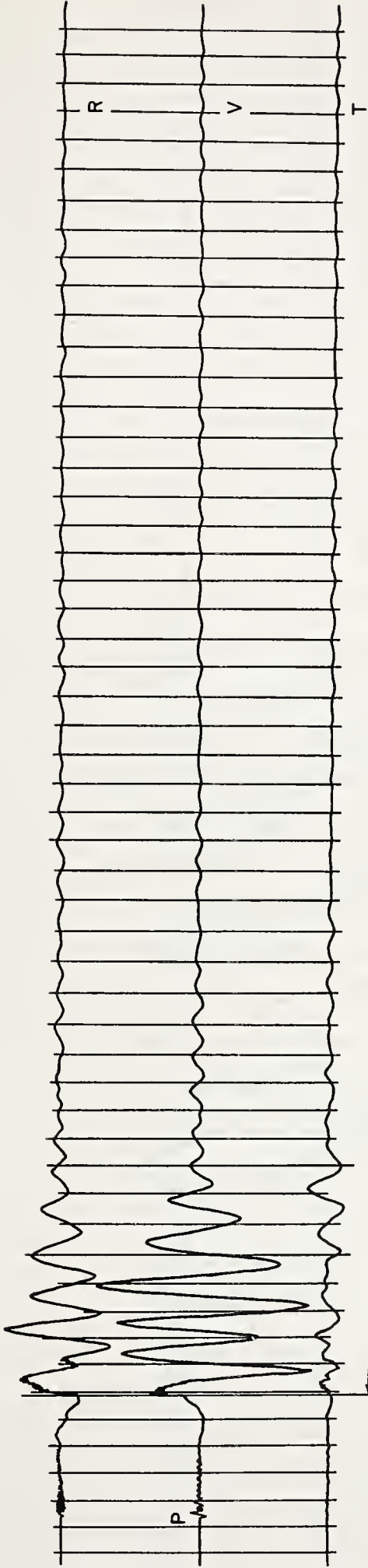
Z = ZERO TIME

HALF SCALE

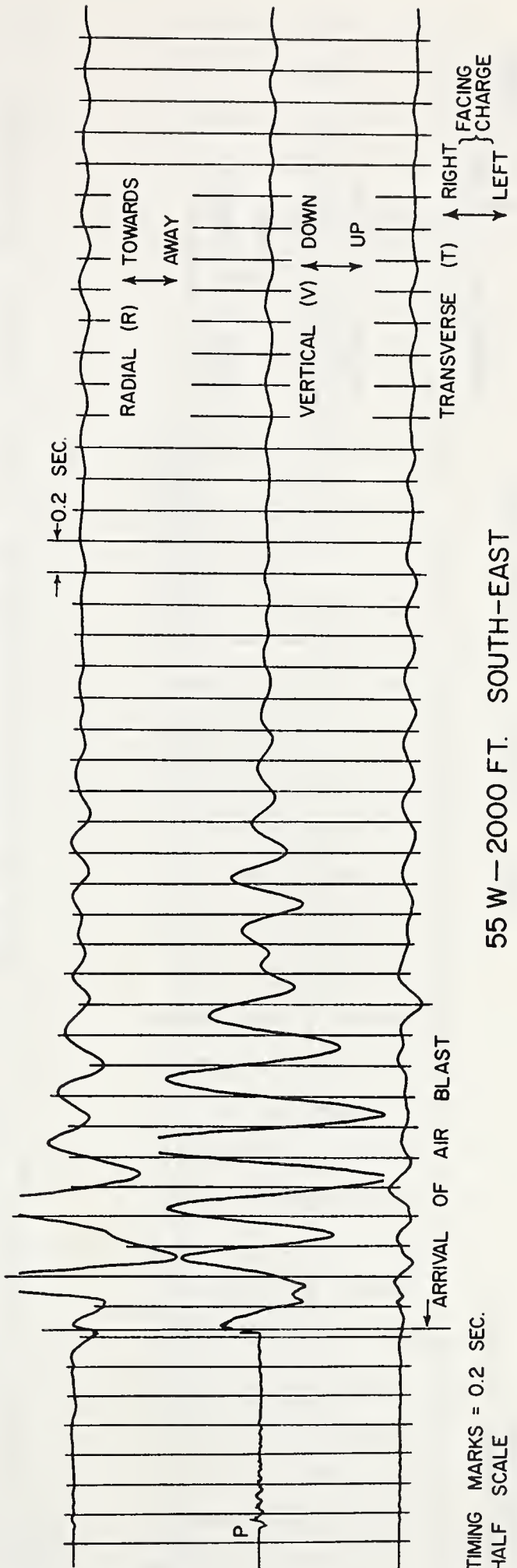


RECORD VERTICAL SCALE (INCHES)

TYPICAL 5 TON SEISMOGRAMS — WATCHING HILL SITE



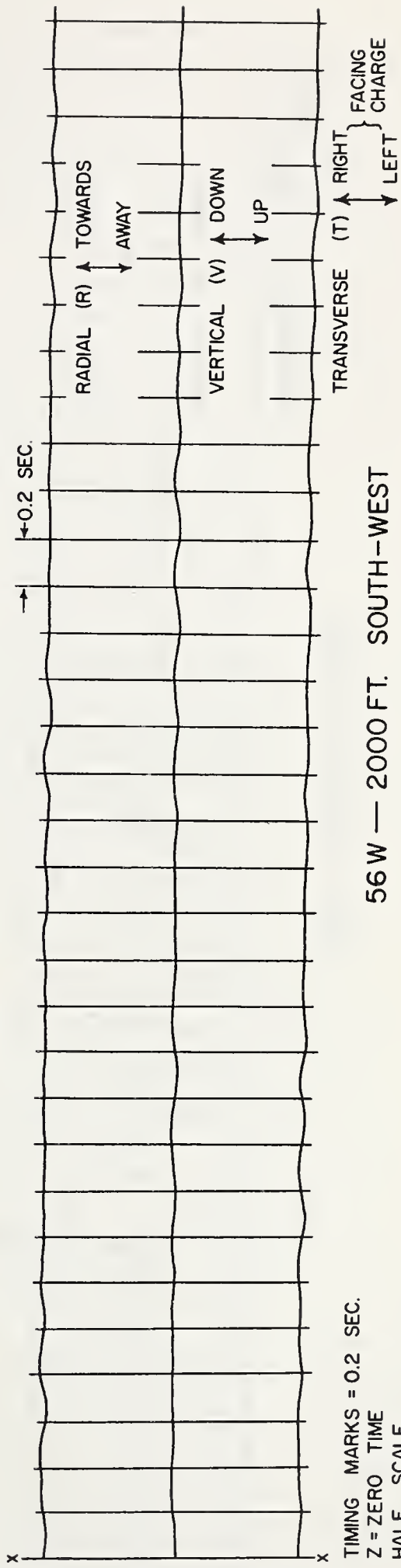
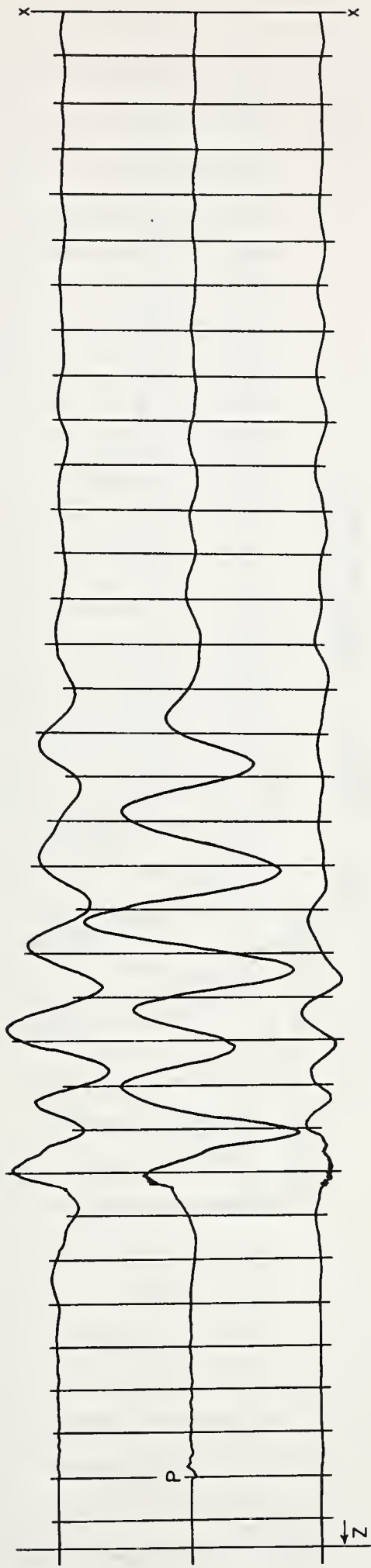
54 W - 2000 FT. NORTH-EAST



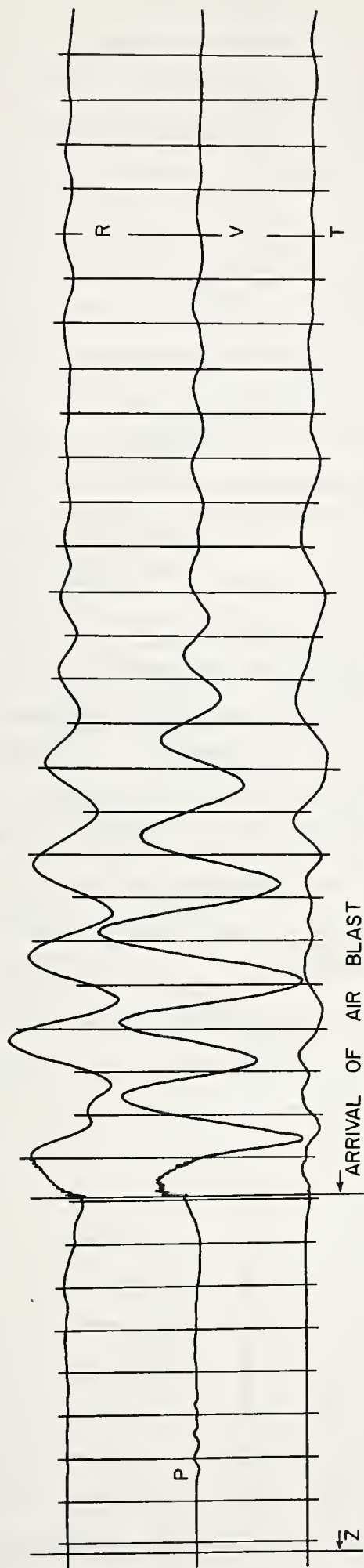
55 W - 2000 FT. SOUTH-EAST

TIMING MARKS = 0.2 SEC.
HALF SCALE

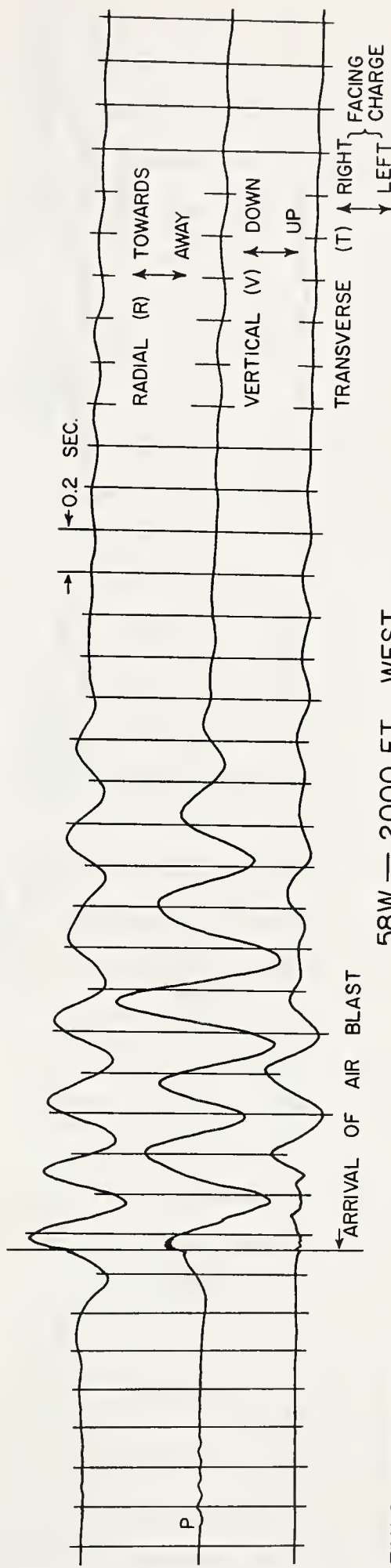
RECORD VERTICAL SCALE (INCHES)
0 1 2



56 W — 2000 FT. SOUTH — WEST



57W — 2000 FT. NORTH-EAST



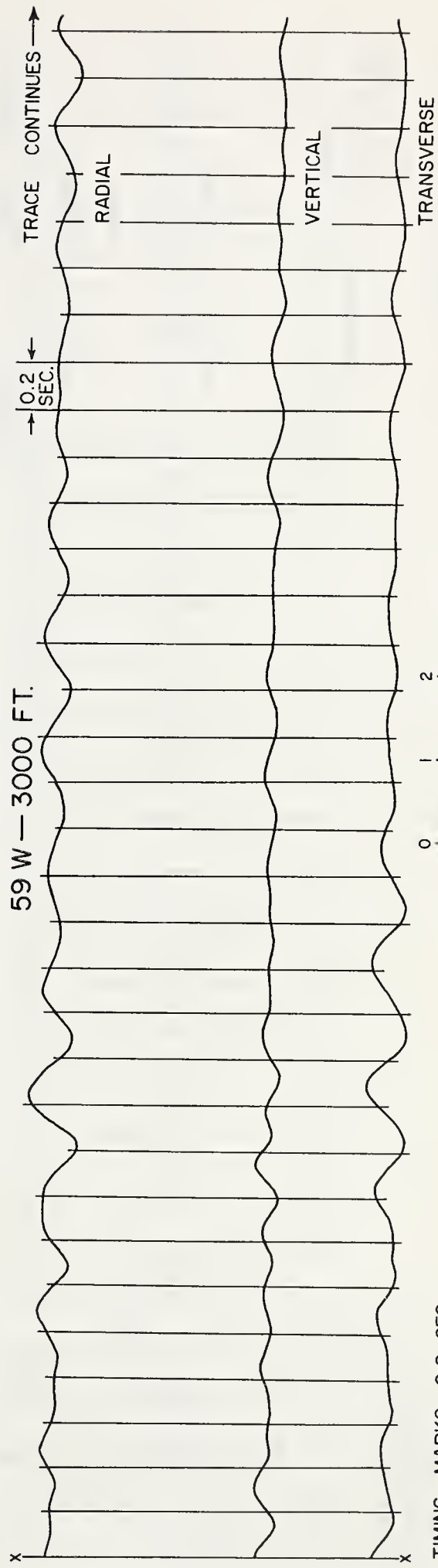
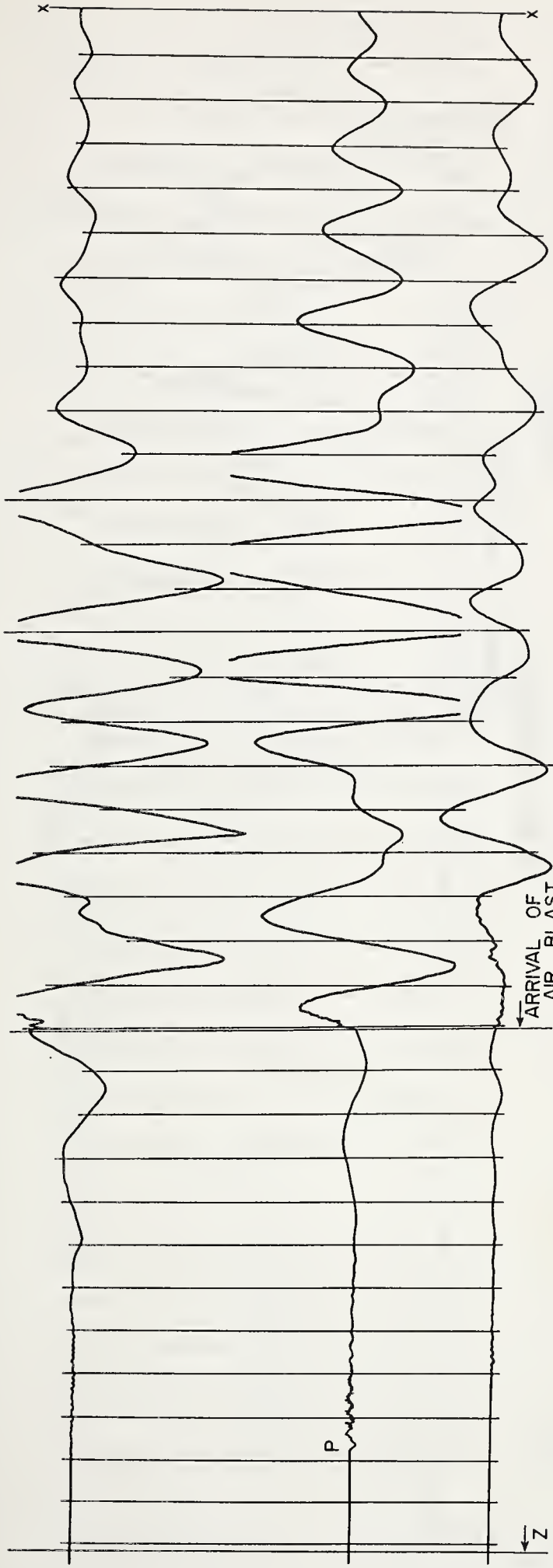
TIMING MARKS = 0.2 SEC.

Z = ZERO TIME

HALF SCALE

RECORD VERTICAL SCALE (INCHES)

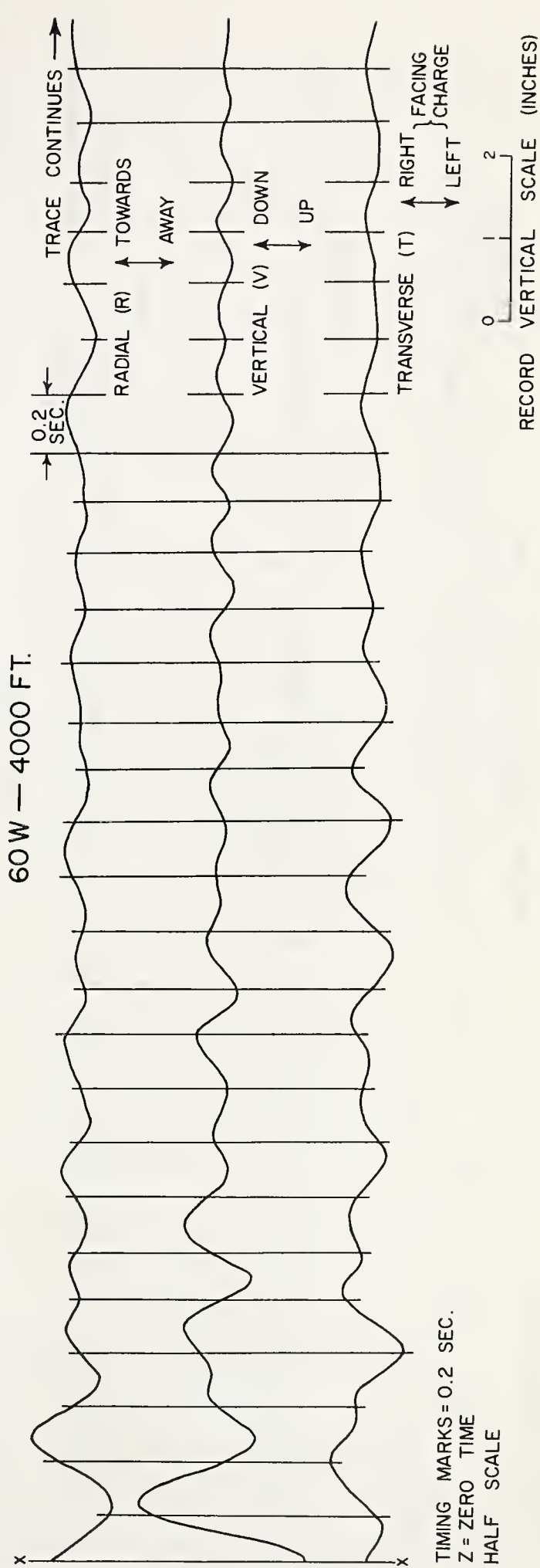
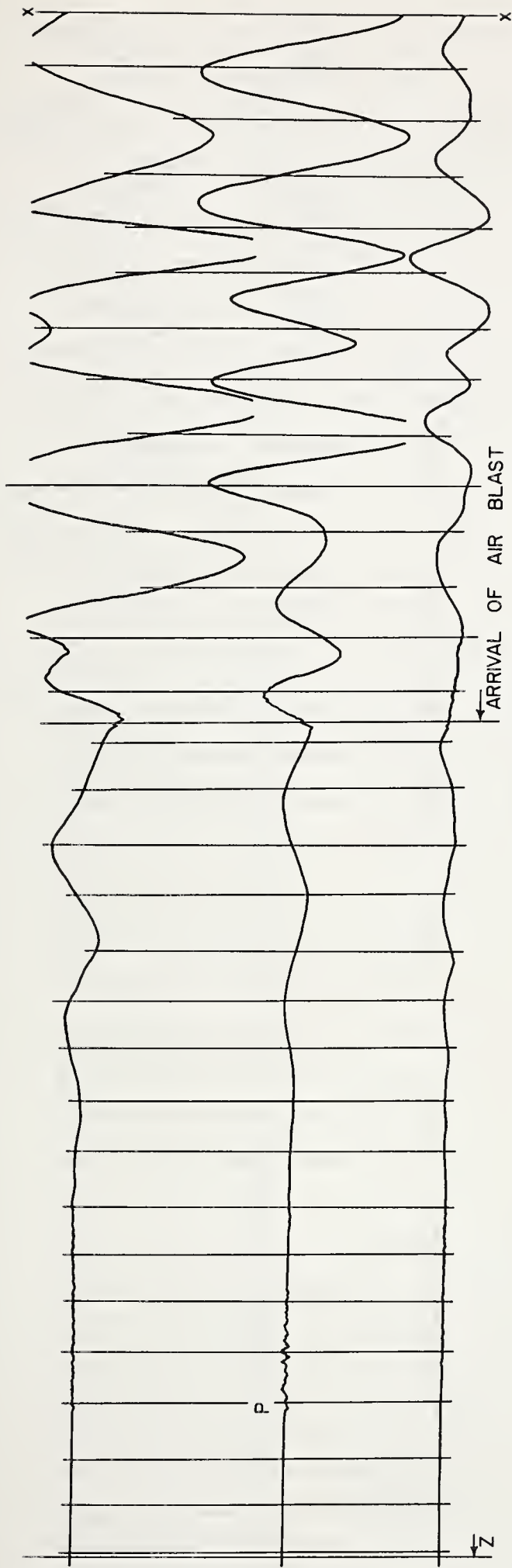
TYPICAL 5 TON SEISMOGRAMS — WATCHING HILL SITE



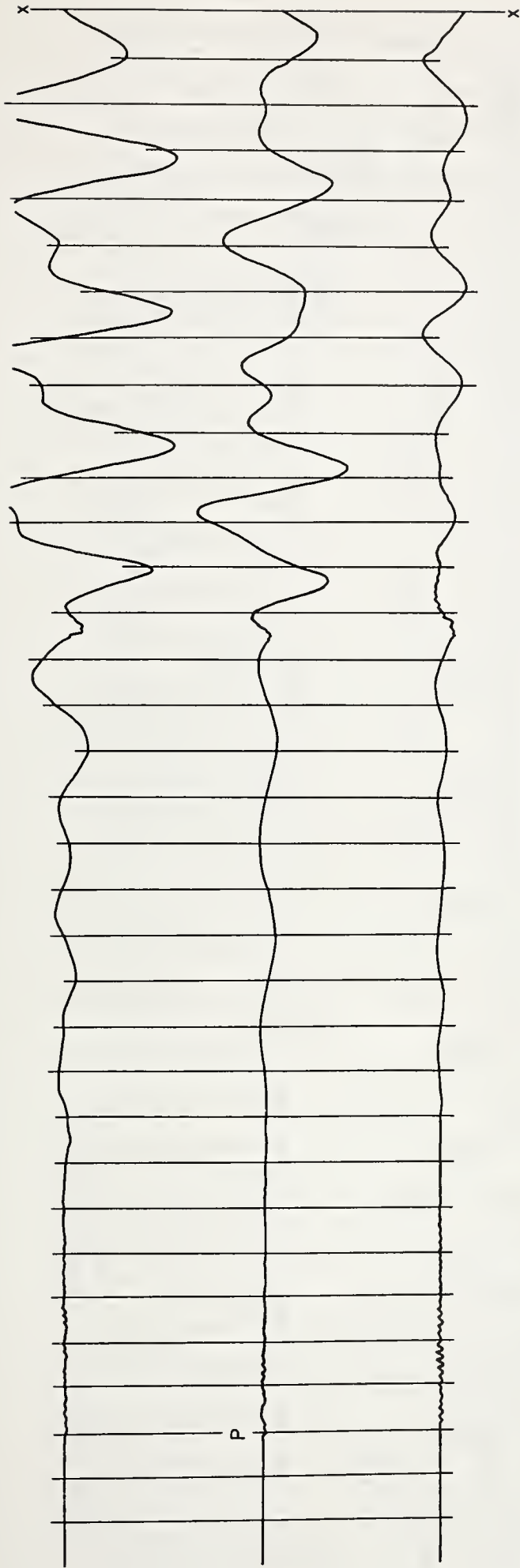
TIMING MARKS = 0.2 SEC.
Z = ZERO TIME
HALF SCALE

59 W — 3000 FT.

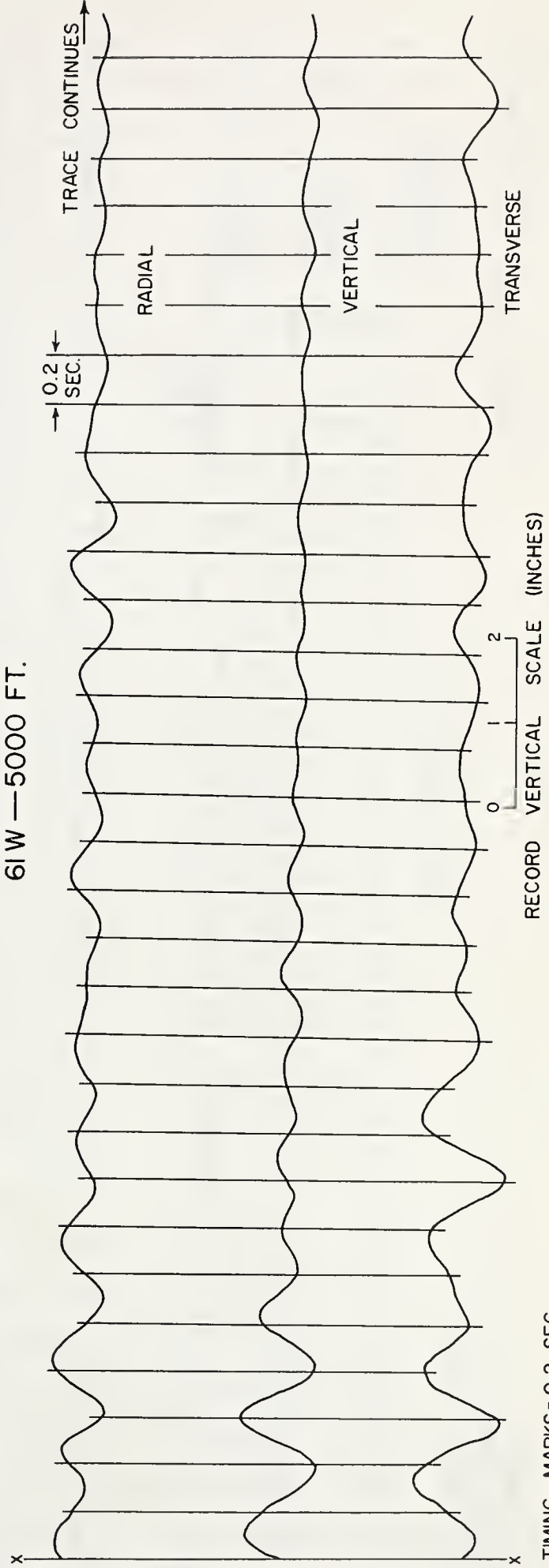
TYPICAL 20 TON SEISMOGRAMS — WATCHING HILL SITE



TYPICAL 20 TON SEISMOGRAMS—WATCHING HILL SITE



61W — 5000 FT.

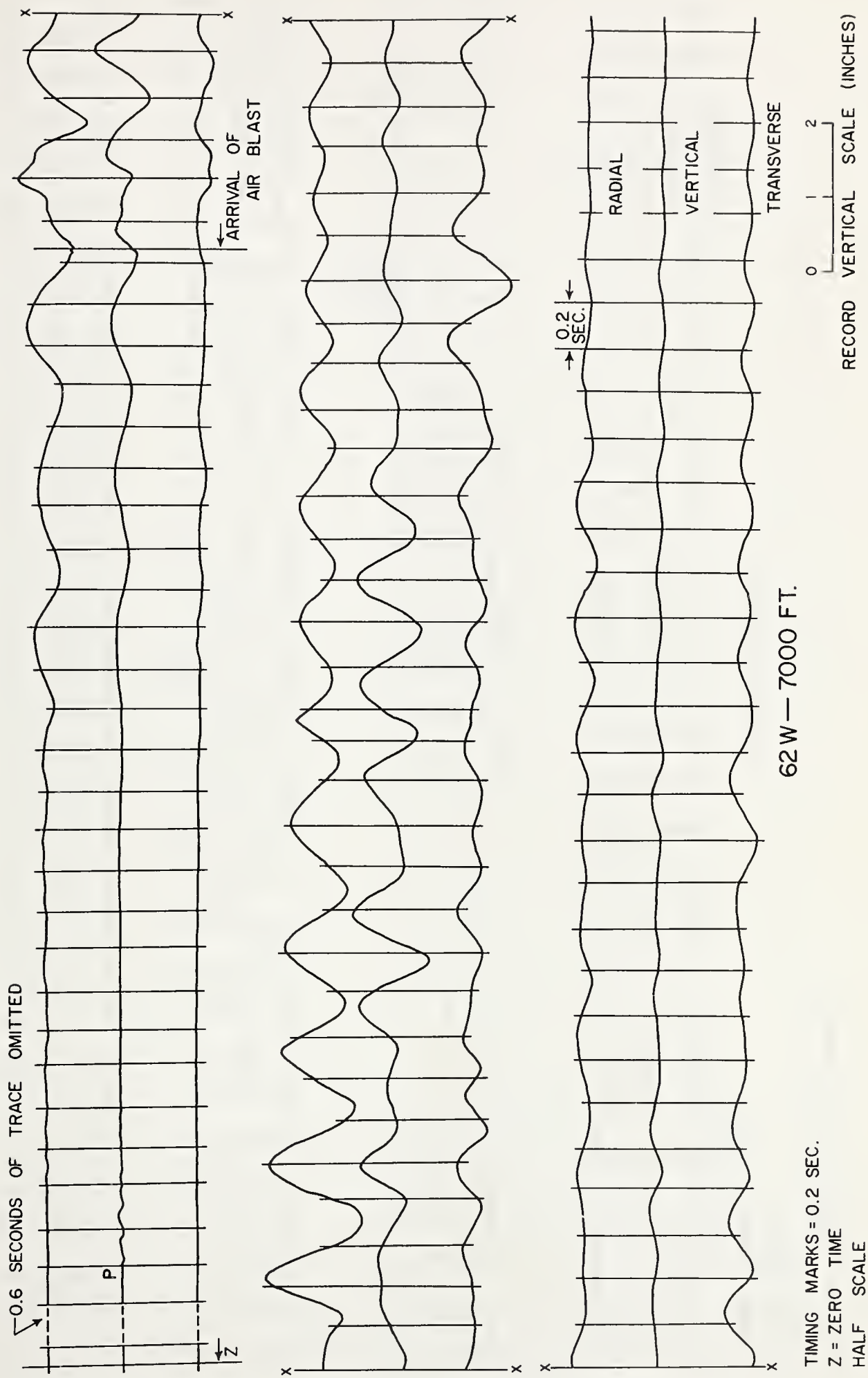


RECORD VERTICAL SCALE (INCHES)

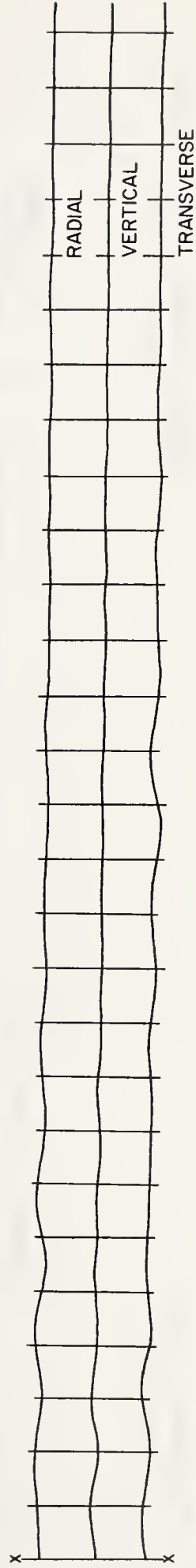
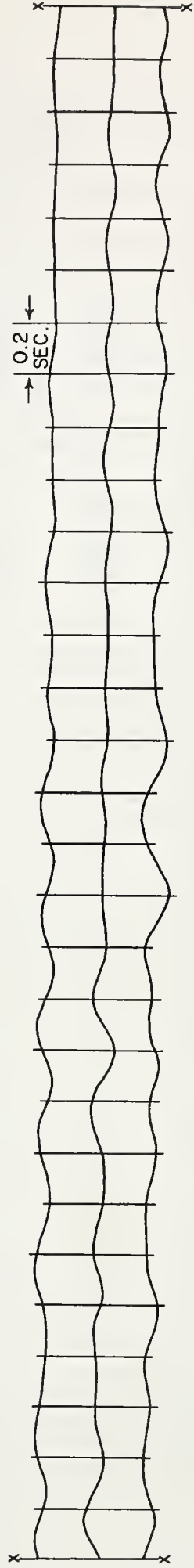
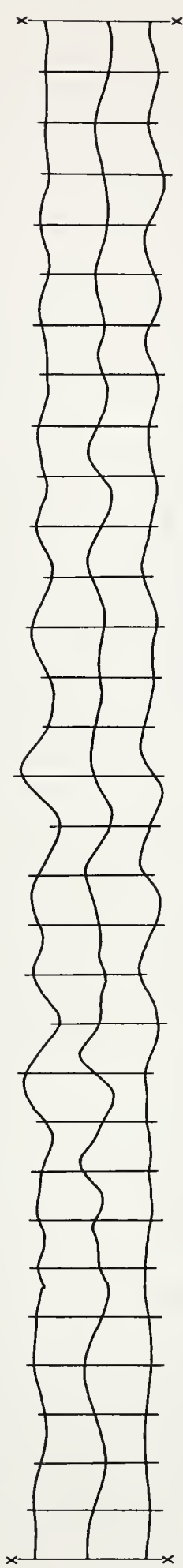
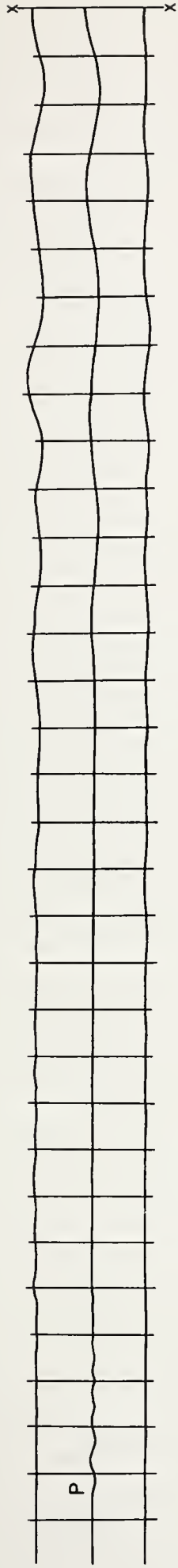
0 1 2

TIMING MARKS = 0.2 SEC.
HALF SCALE

TYPICAL 20 TON SEISMOGRAMS — WATCHING HILL SITE



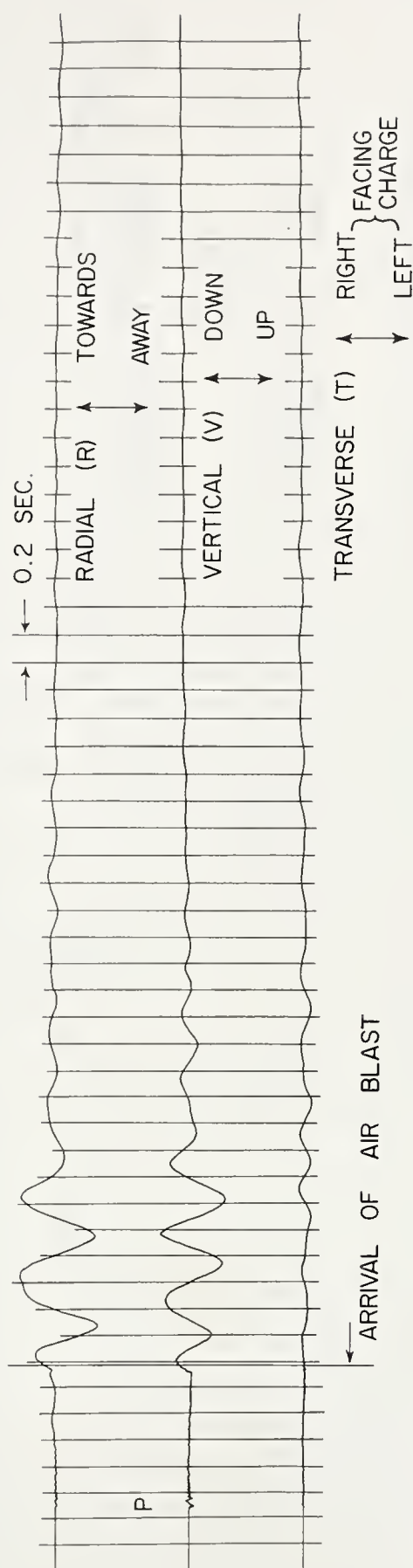
TYPICAL 20 TON SEISMOGRAMS — WATCHING HILL SITE



TIMING MARKS = 0.2 SEC.
HALF SCALE

RECORD VERTICAL SCALE (INCHES)
0 1 2

63W—10,000 FT.



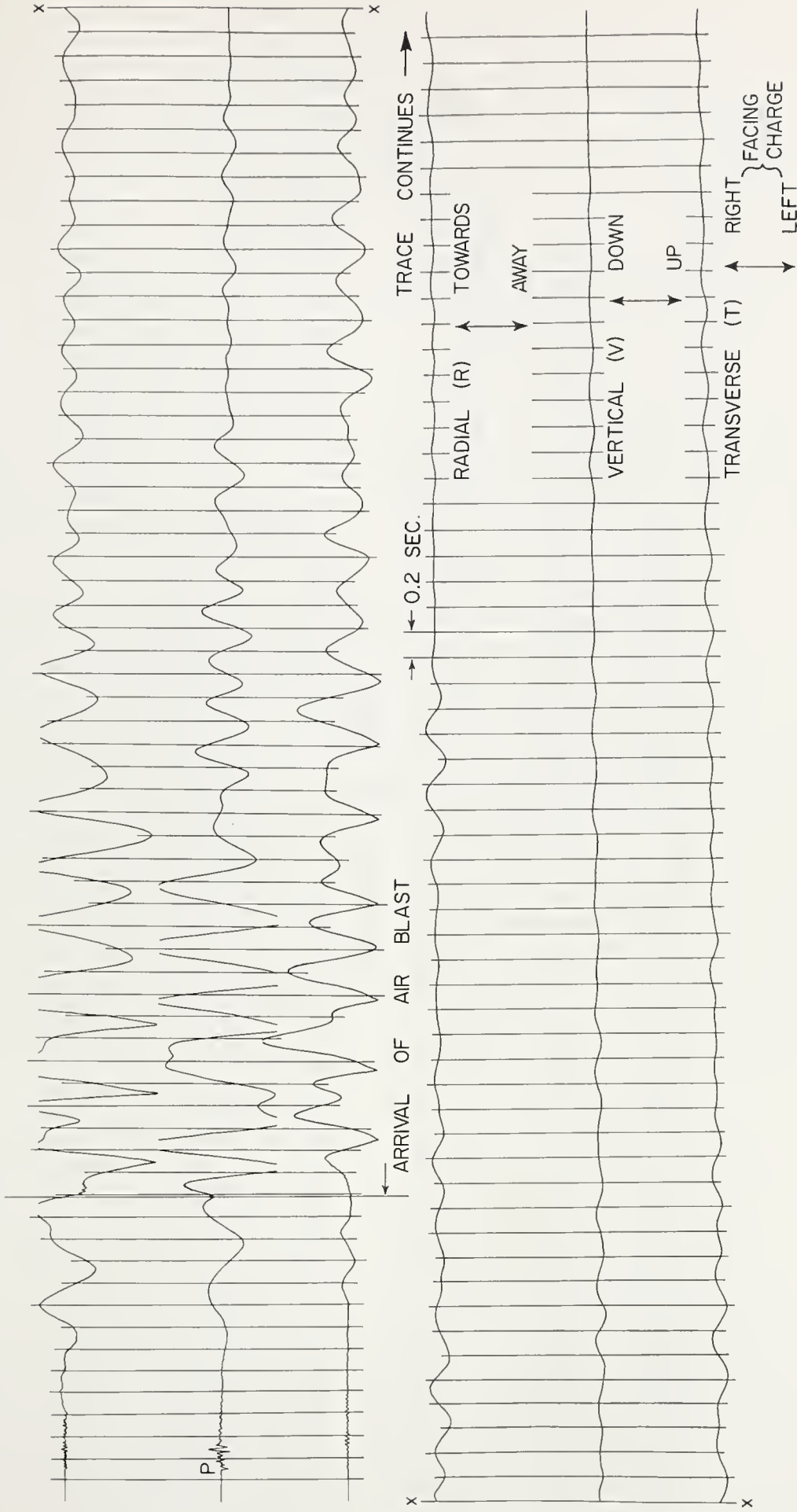
TIMING MARKS = 0.2 SEC.
QUARTER SCALE

RECORD VERTICAL SCALE (INCHES)

0 1 2 3 4

64 W - 2000 FT. "A" LINE

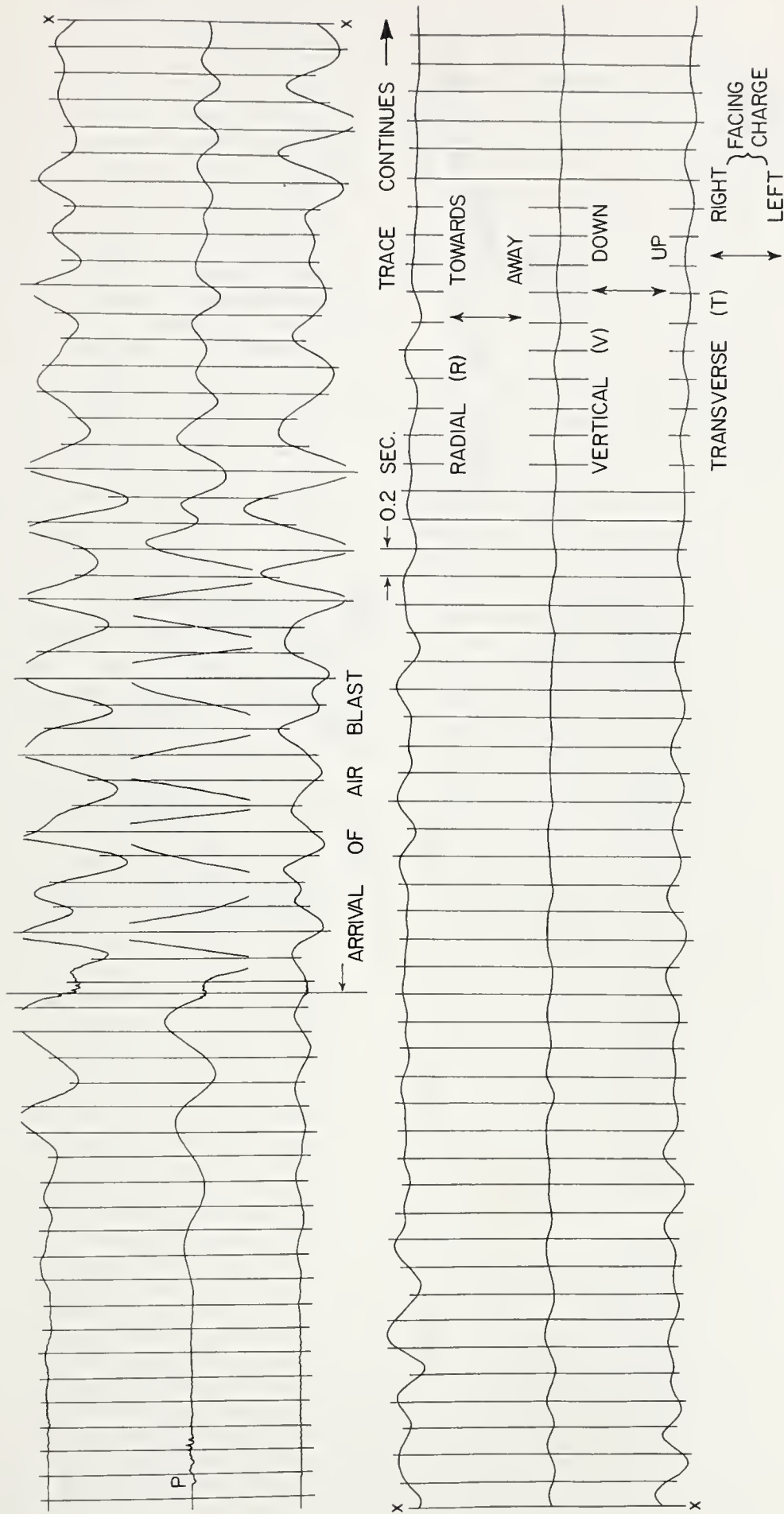
TYPICAL 100 TON SEISMOGRAMS — WATCHING HILL SITE



TIMING MARKS = 0.2 SEC.
QUARTER SCALE

65 W - 4000 FT. "A" LINE

RECORD VERTICAL SCALE (INCHES)
0 1 2 3 4



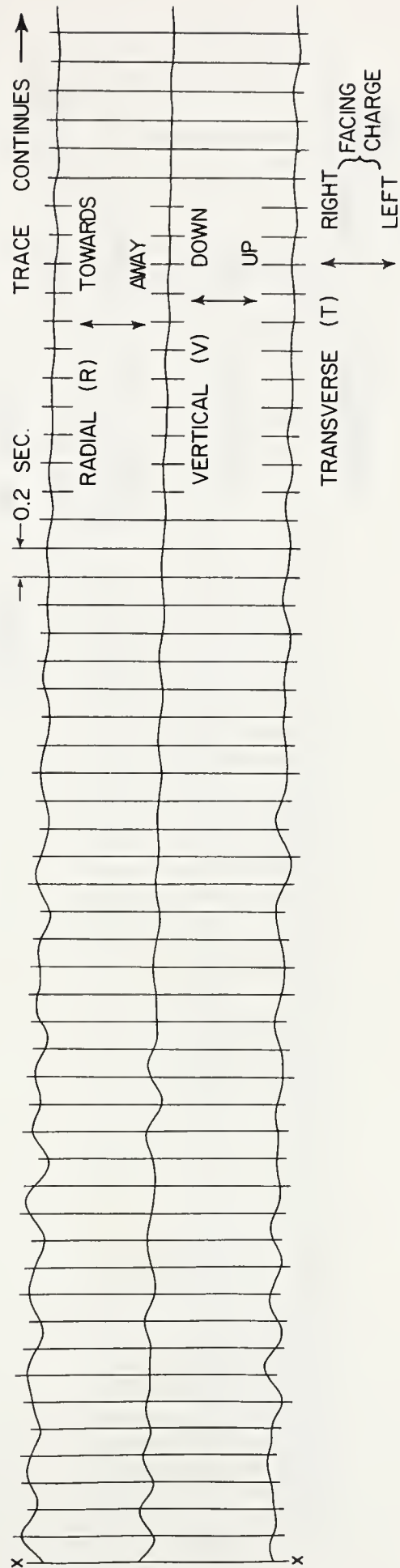
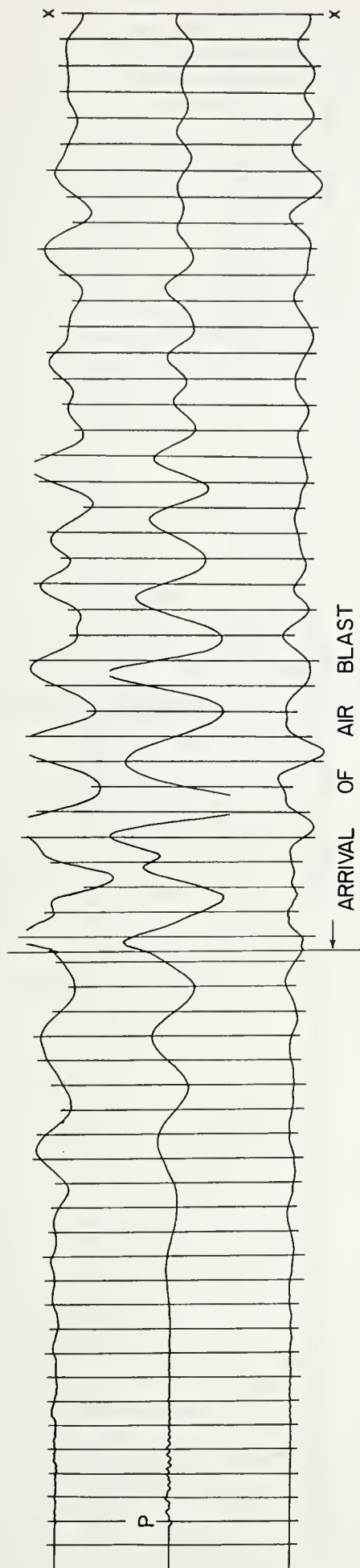
TIMING MARKS = 0.2 SEC.
 QUARTER SCALE



RECORD VERTICAL SCALE (INCHES)

66 W — 6000 FT. "A" LINE

TYPICAL 100 TON SEISMOGRAMS — WATCHING HILL SITE

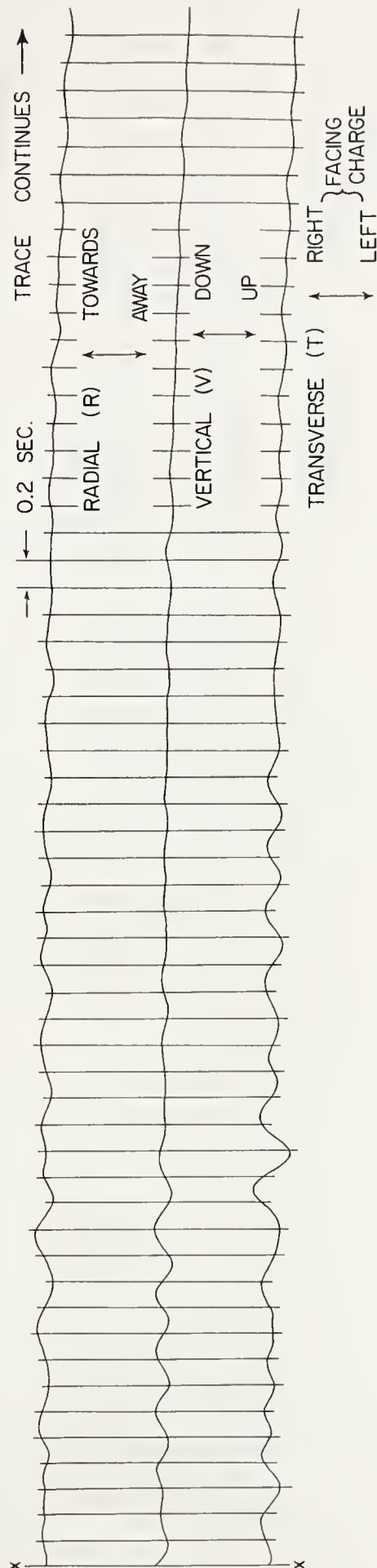
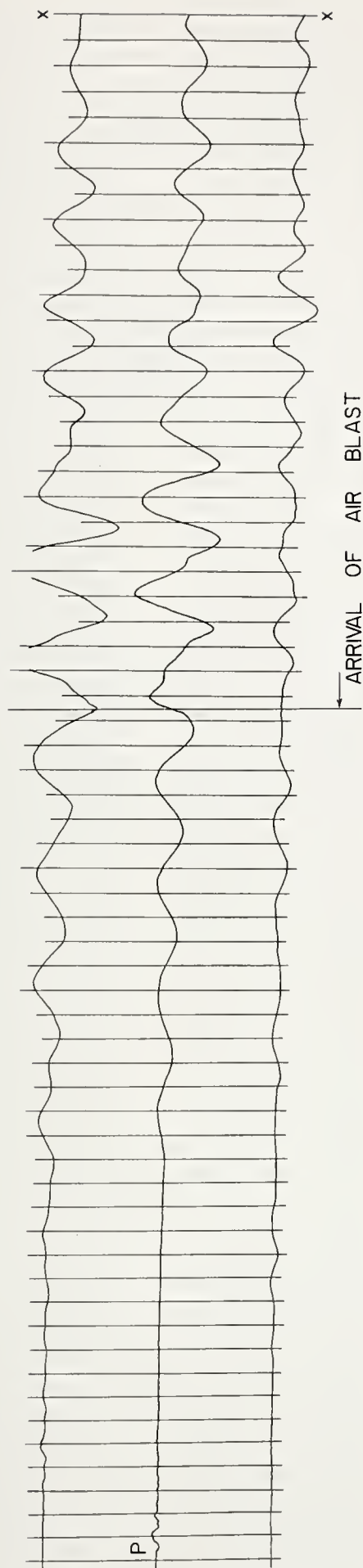


TIMING MARKS = 0.2 SEC.
QUARTER SCALE

RECORD VERTICAL SCALE (INCHES)

67 W - 7000 FT. "A" LINE

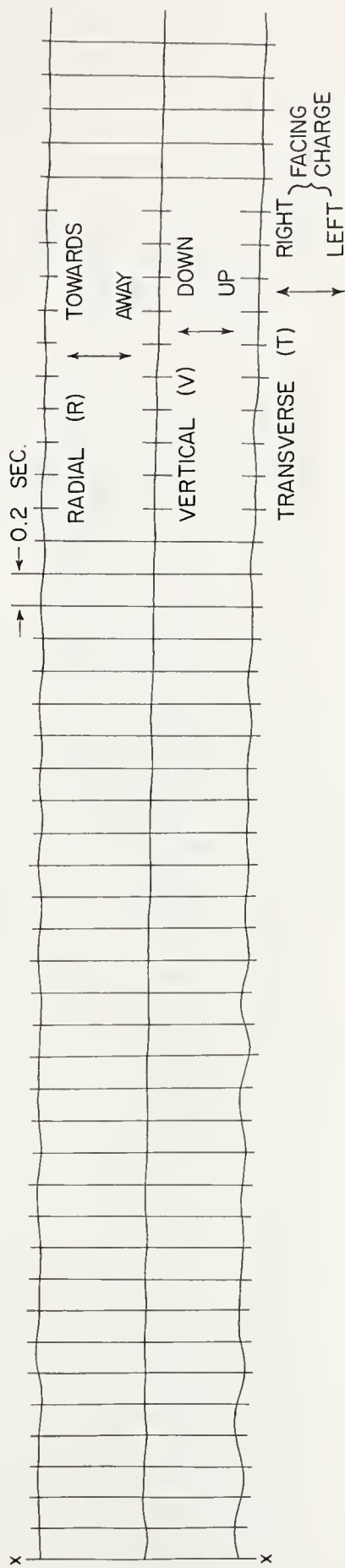
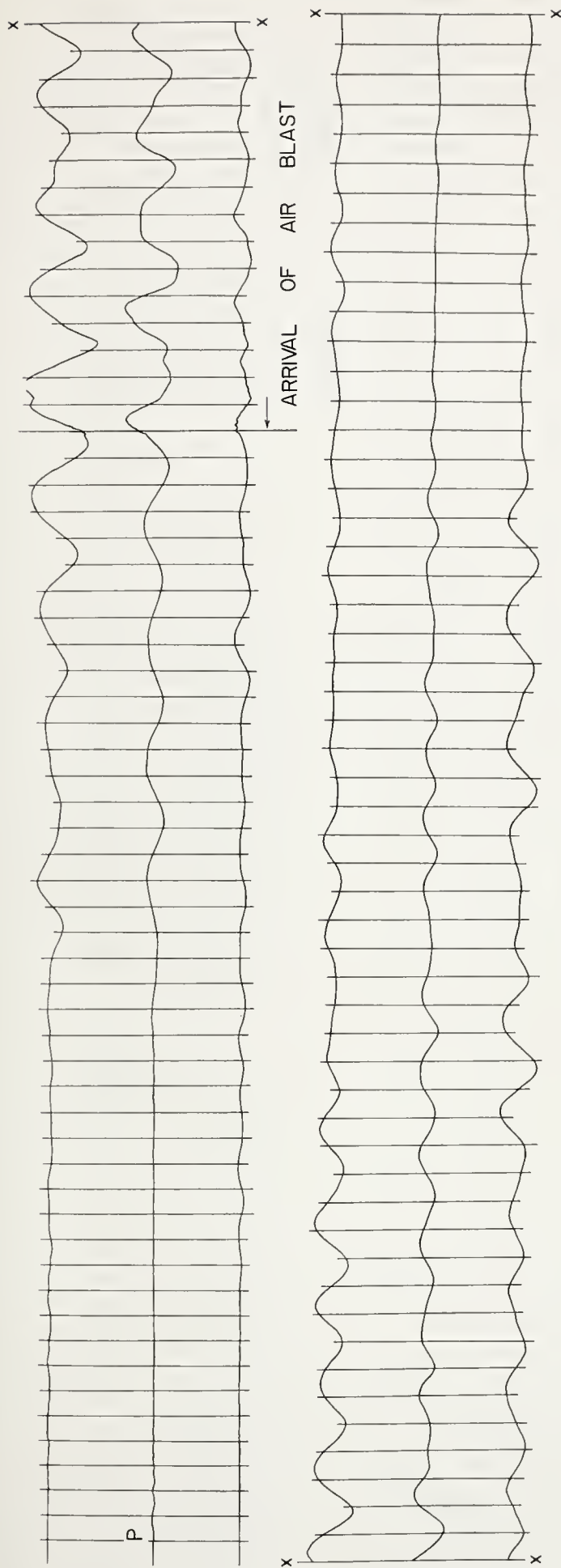
TYPICAL 100 TON SEISMOGRAMS — WATCHING HILL SITE



TIMING MARKS = 0.2 SEC.
QUARTER SCALE

68 W - 10,000 FT. "A" LINE

TYPICAL 100 TON SEISMOGRAMS — WATCHING HILL SITE

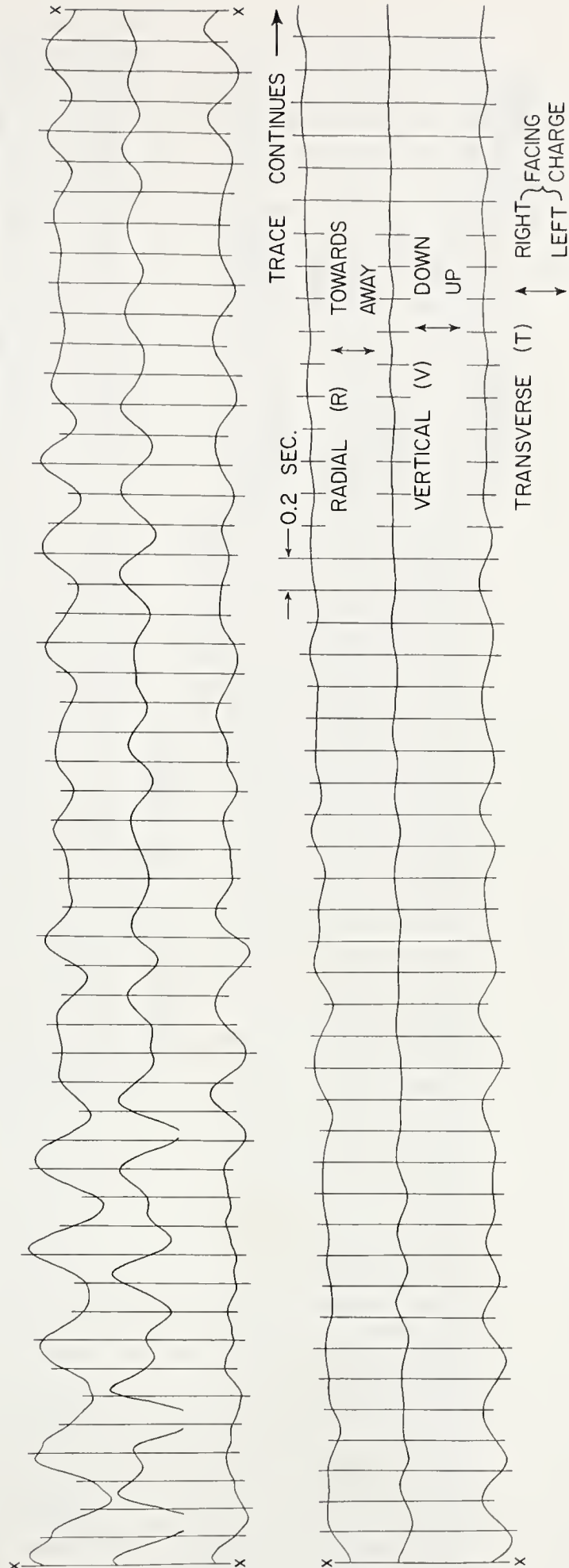
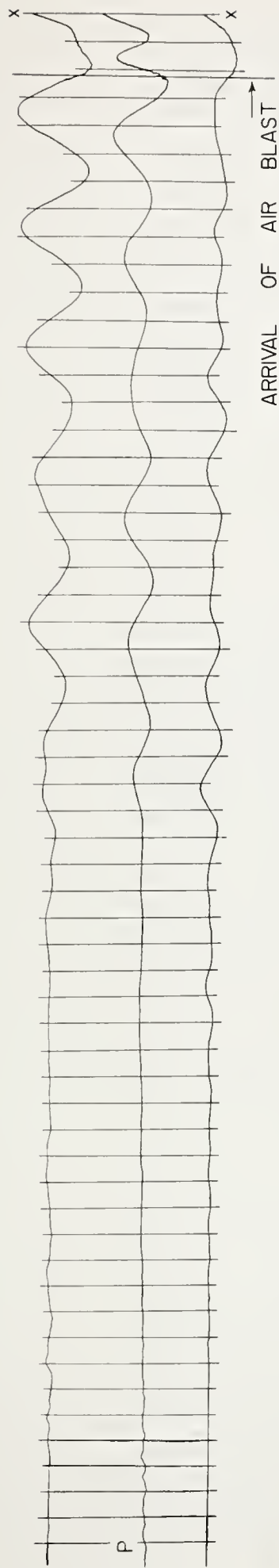


TIMING MARKS = 0.2 SEC.
QUARTER SCALE

RECORD VERTICAL SCALE (INCHES)

69 W - 12,000 FT. "A" LINE

TYPICAL 100 TON SEISMOGRAMS — WATCHING HILL SITE



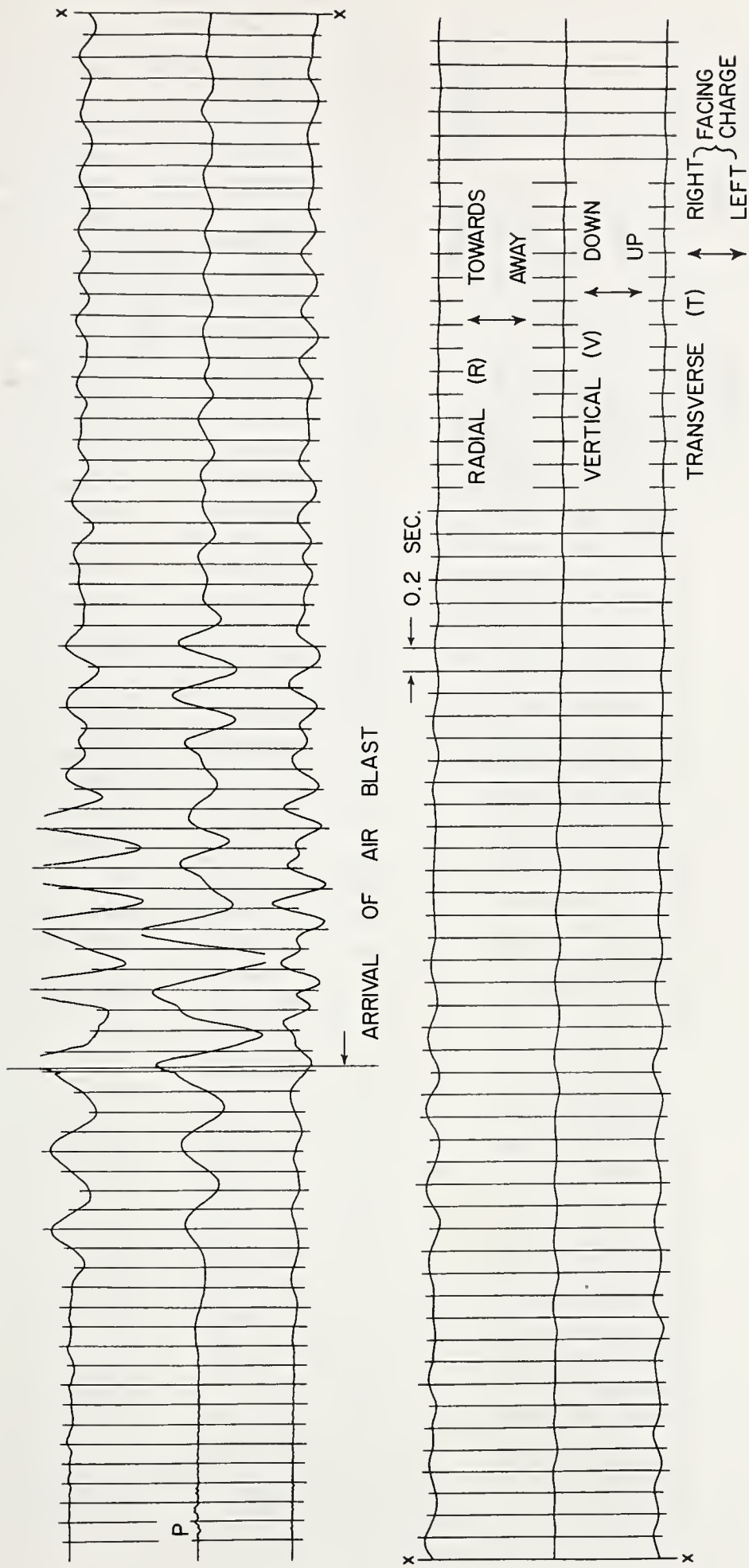
TIMING MARKS = 0.2 SEC.
QUARTER SCALE



RECORD VERTICAL SCALE (INCHES)

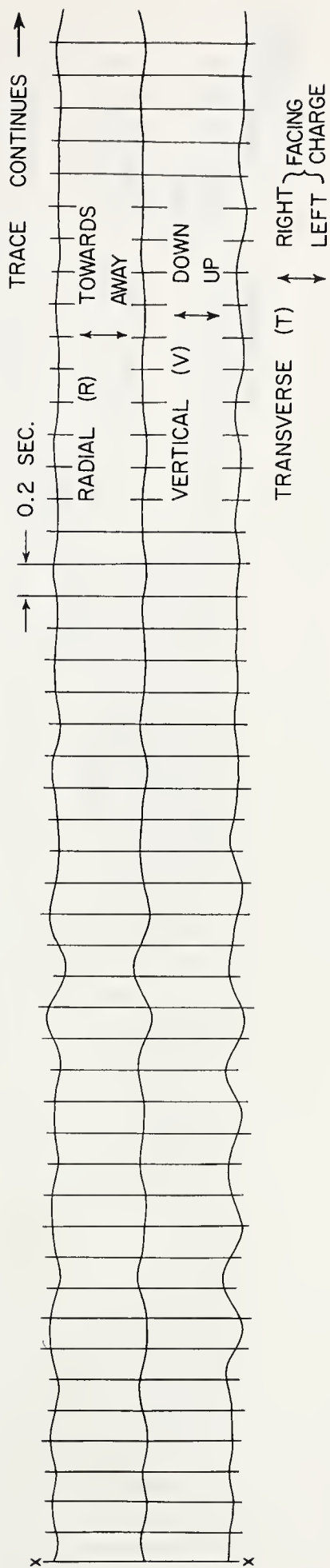
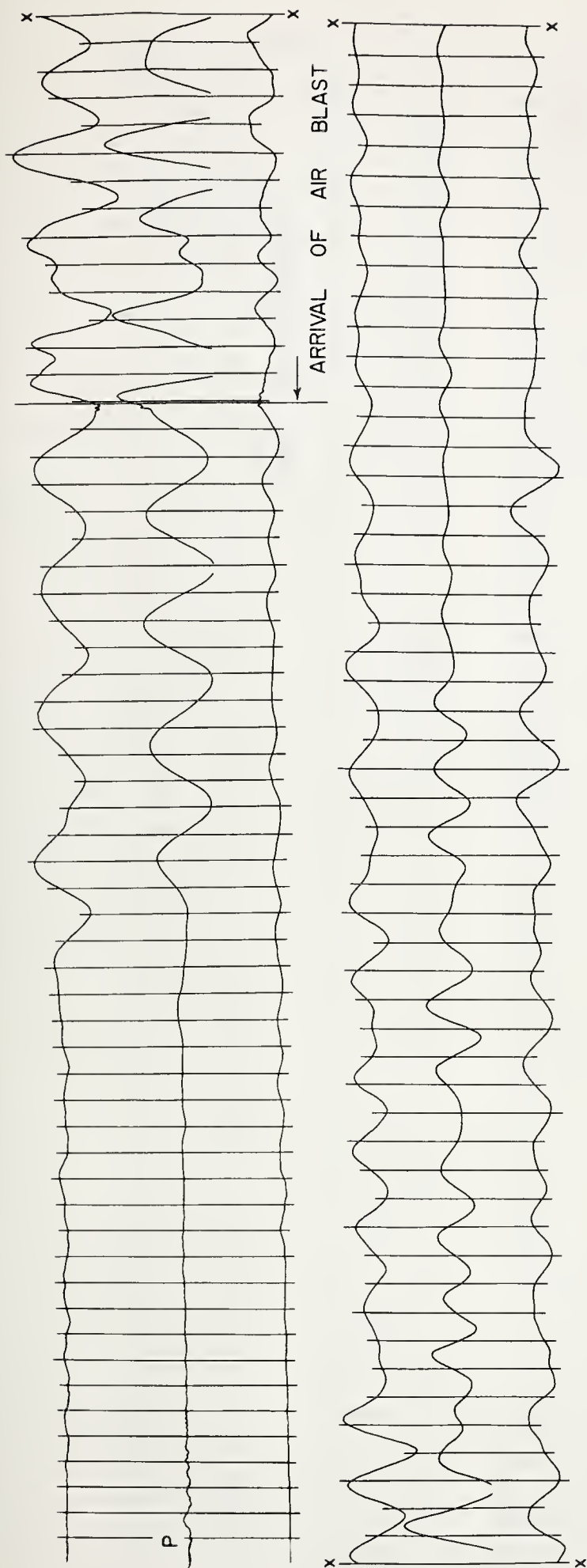
70 W - 15,000 FT. "A" LINE

TYPICAL 100 TON SEISMOGRAMS—WATCHING HILL SITE

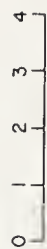


TYPICAL 100 TON SEISMOGRAMS — WATCHING HILL SITE

71 W-7000 FT. "B" LINE



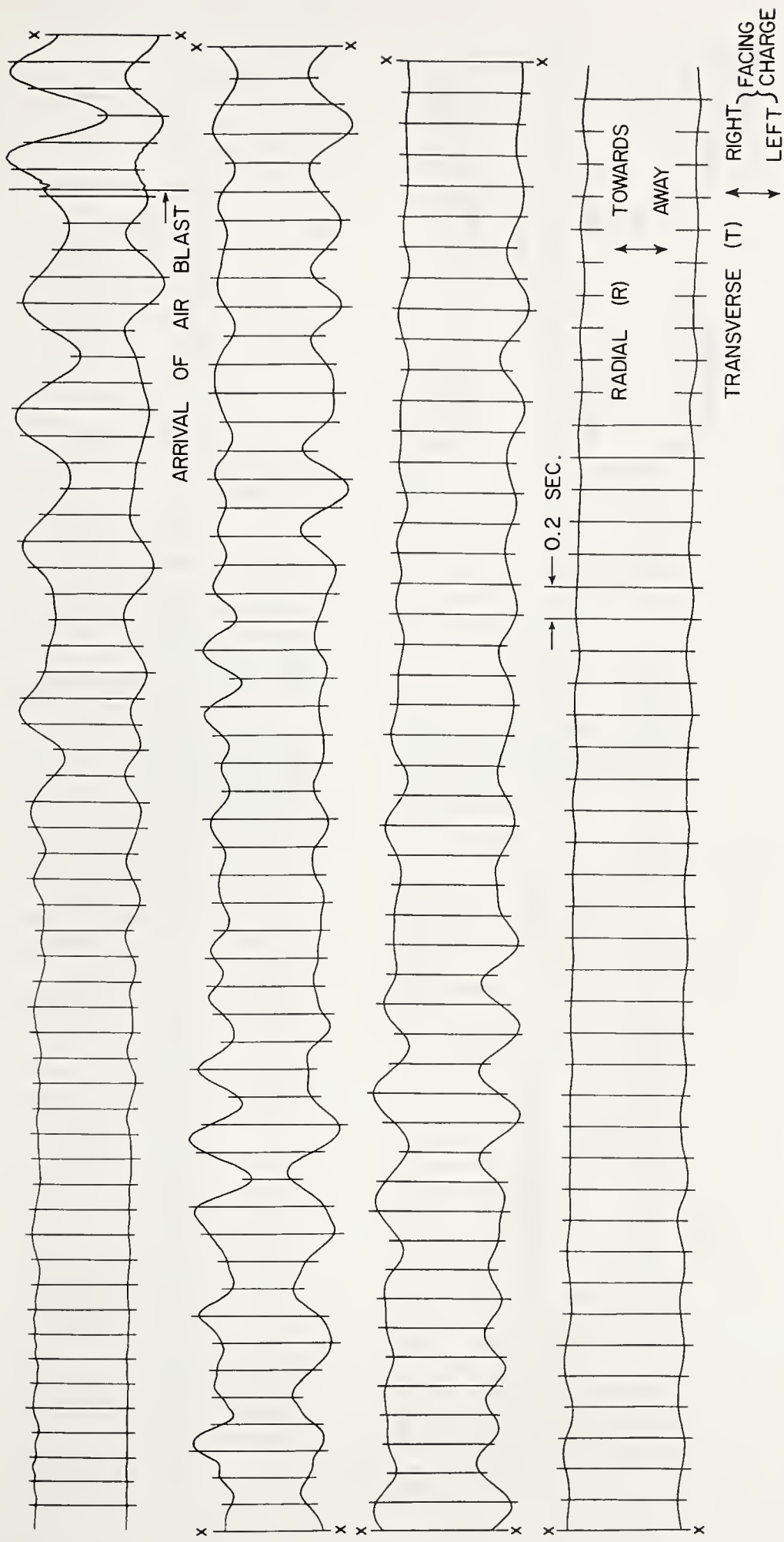
TIMING MARKS = 0.2 SEC.
QUARTER SCALE



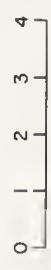
RECORD VERTICAL SCALE (INCHES)

72 W - 12,000 FT. "B" LINE

TYPICAL 100 TON SEISMOGRAMS — WATCHING HILL SITE



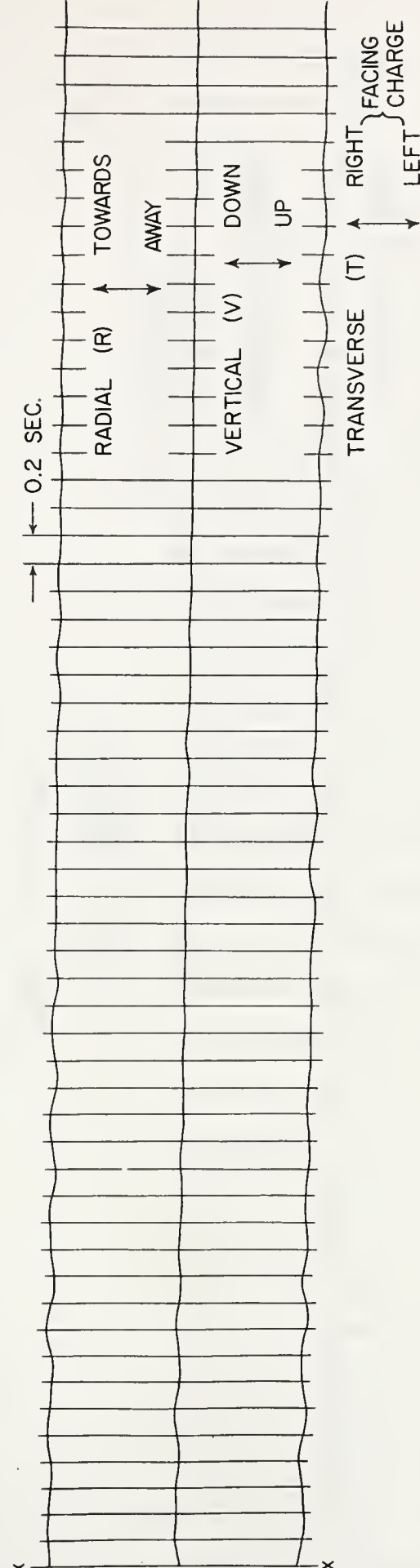
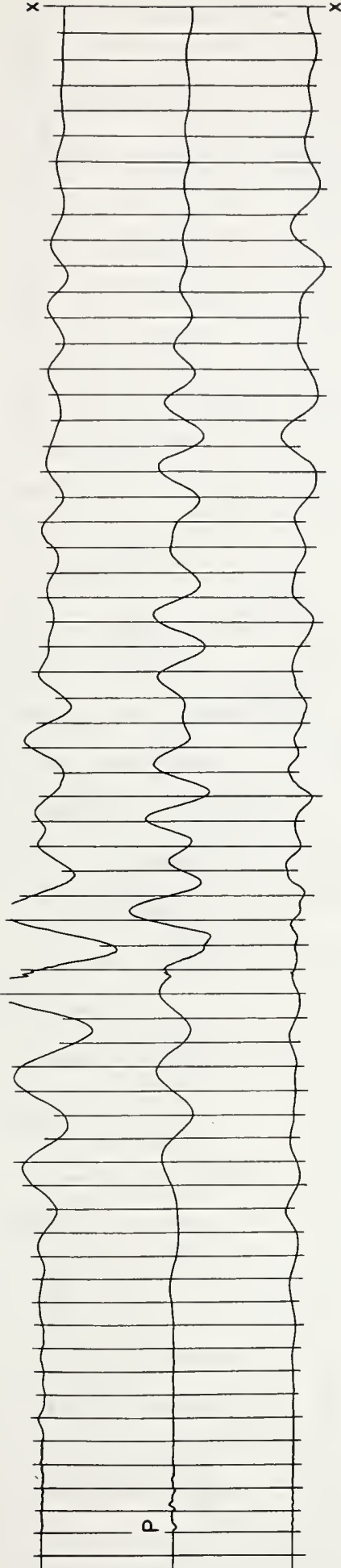
TIMING MARKS = 0.2 SEC.
QUARTER SCALE



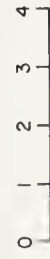
RECORD VERTICAL SCALE (INCHES)

73 W-15,000 FT. "B" LINE

TYPICAL 100 TON SEISMOGRAMS—WATCHING HILL SITE

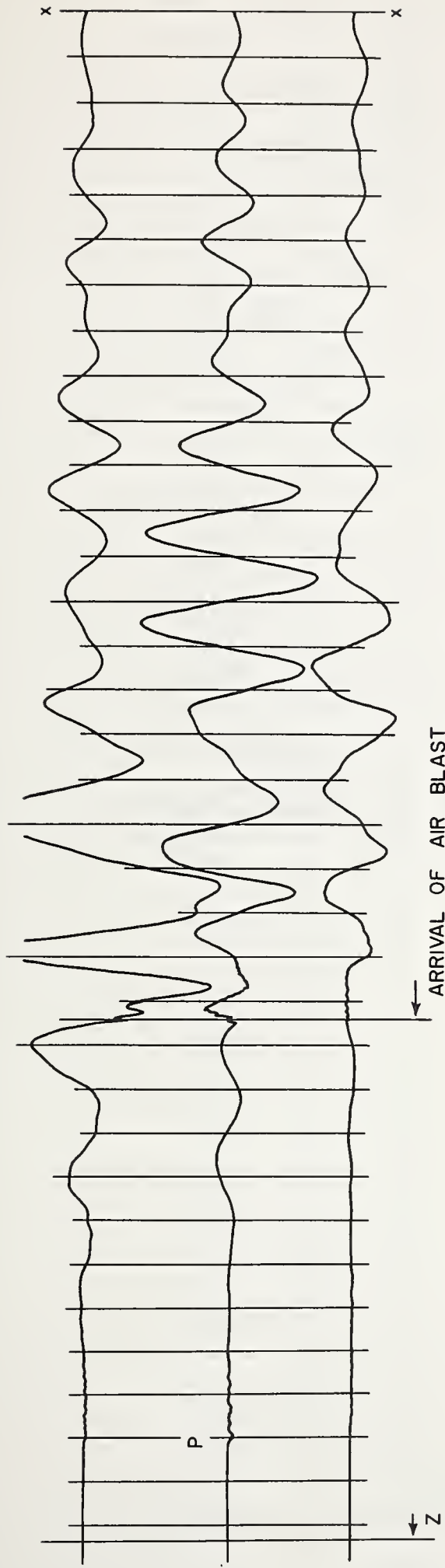


TIMING MARKS = 0.2 SEC.
QUARTER SCALE

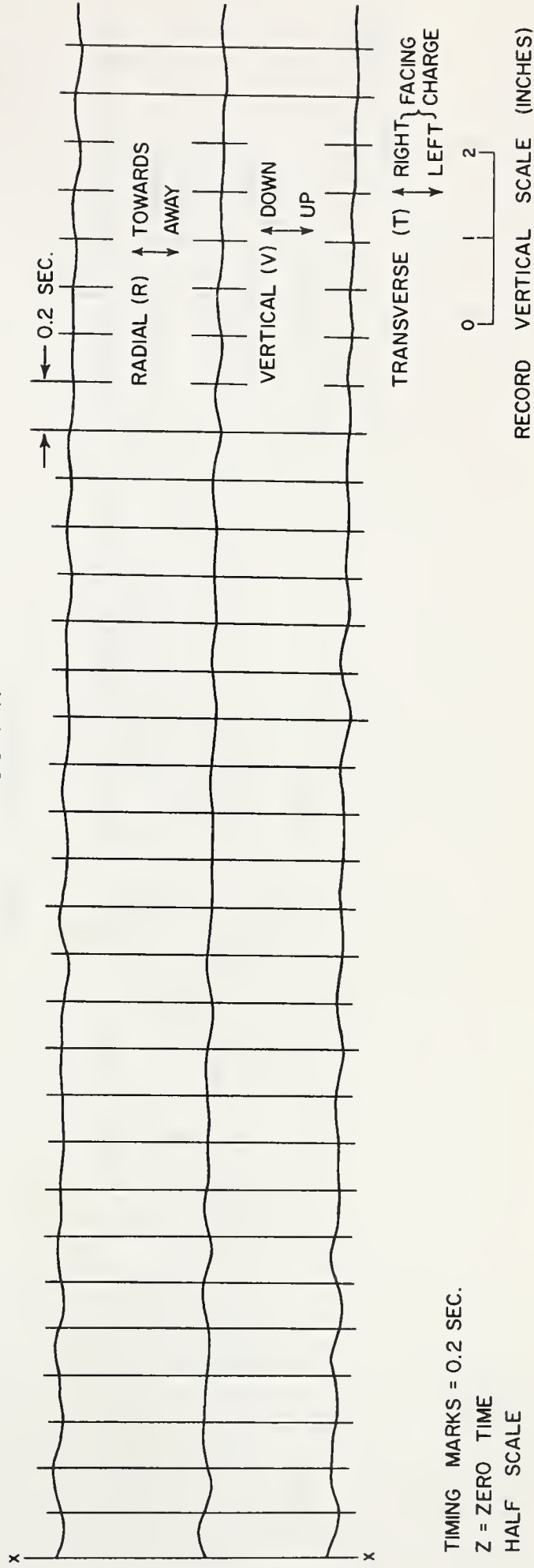


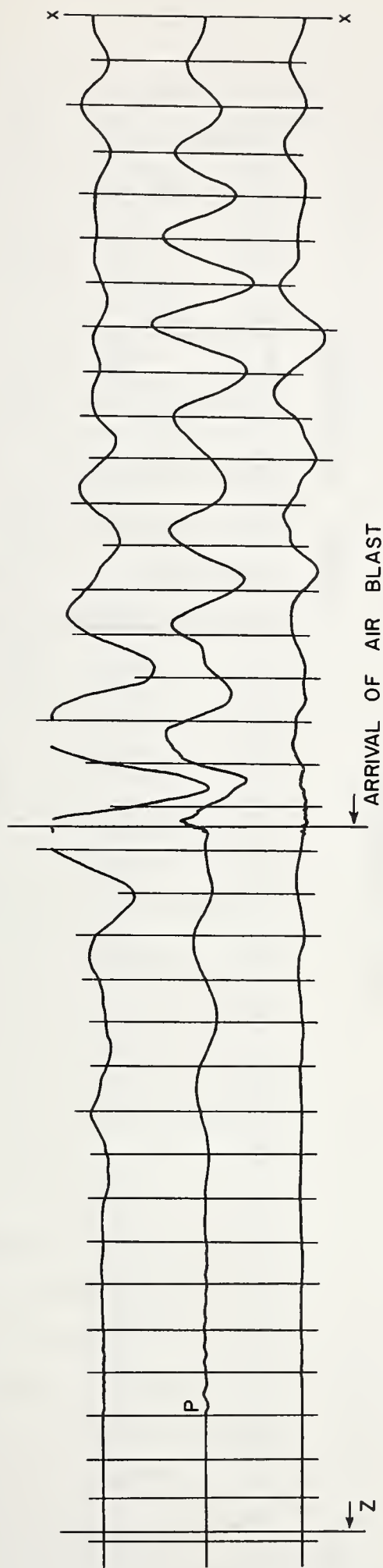
RECORD VERTICAL SCALE (INCHES)

74 W-7000 FT. "C" LINE

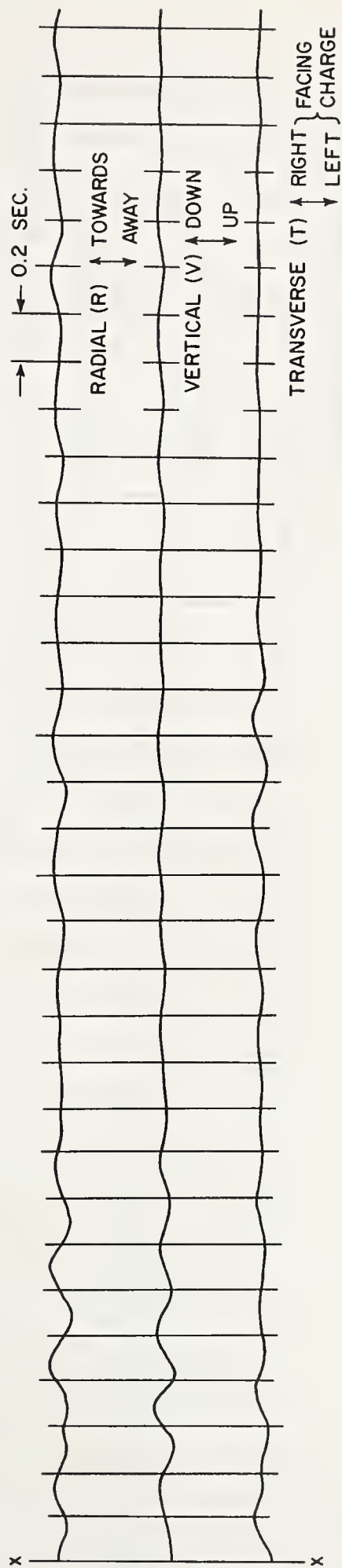


75 D — 3000 FT.





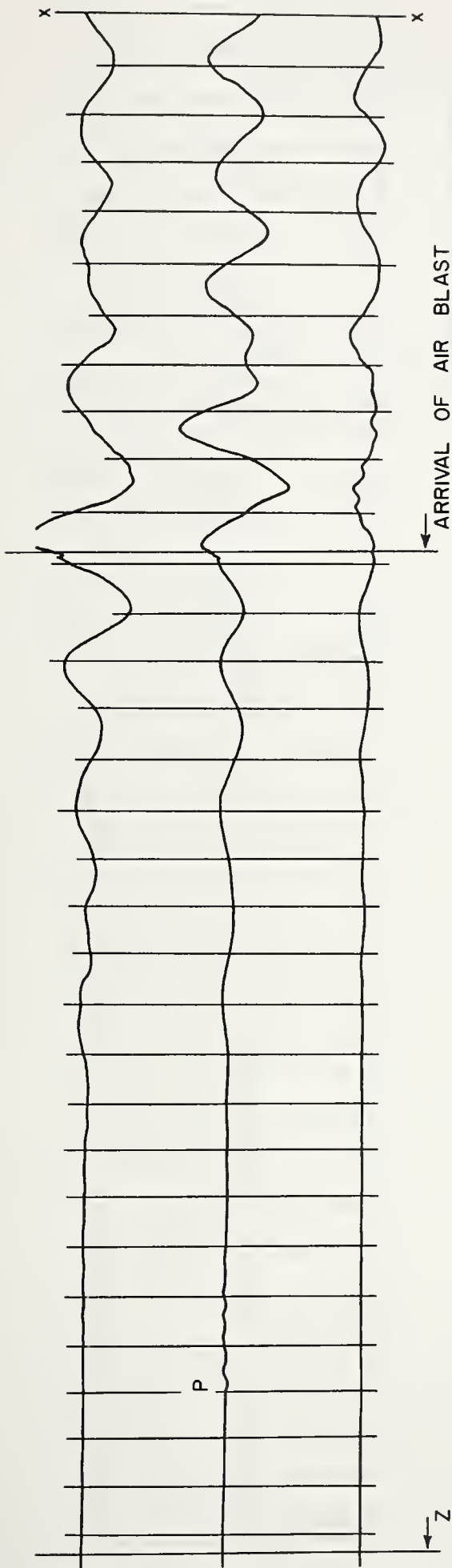
76D — 4000 FT.



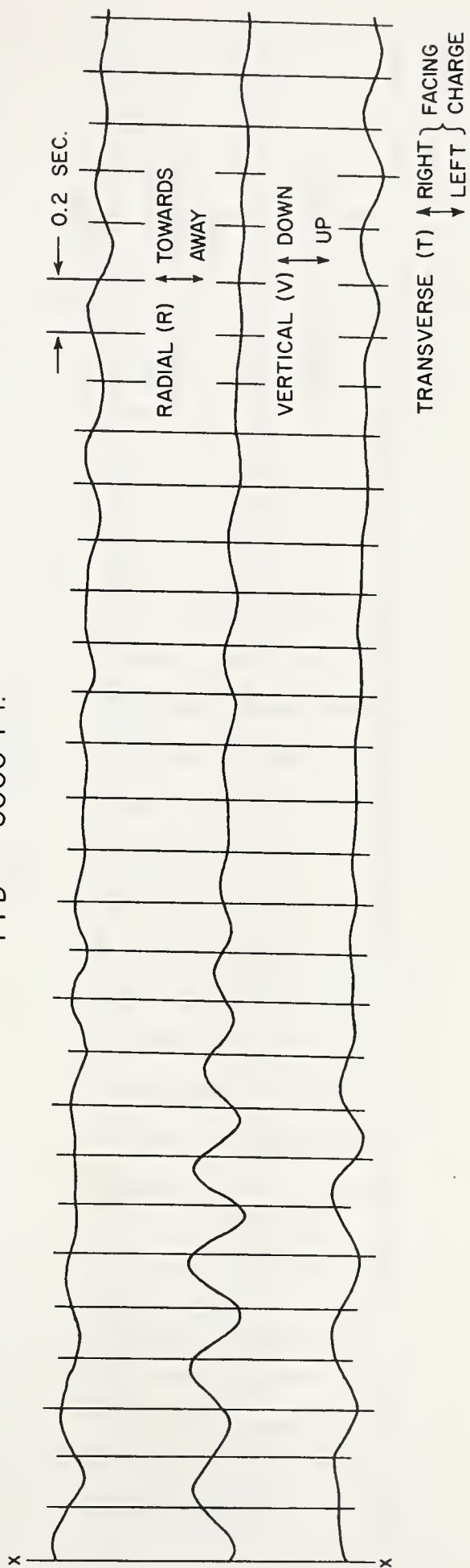
TIMING MARKS = 0.2 SEC.
Z = ZERO TIME
HALF SCALE



RECORD VERTICAL SCALE (INCHES)



77D — 5000 FT.

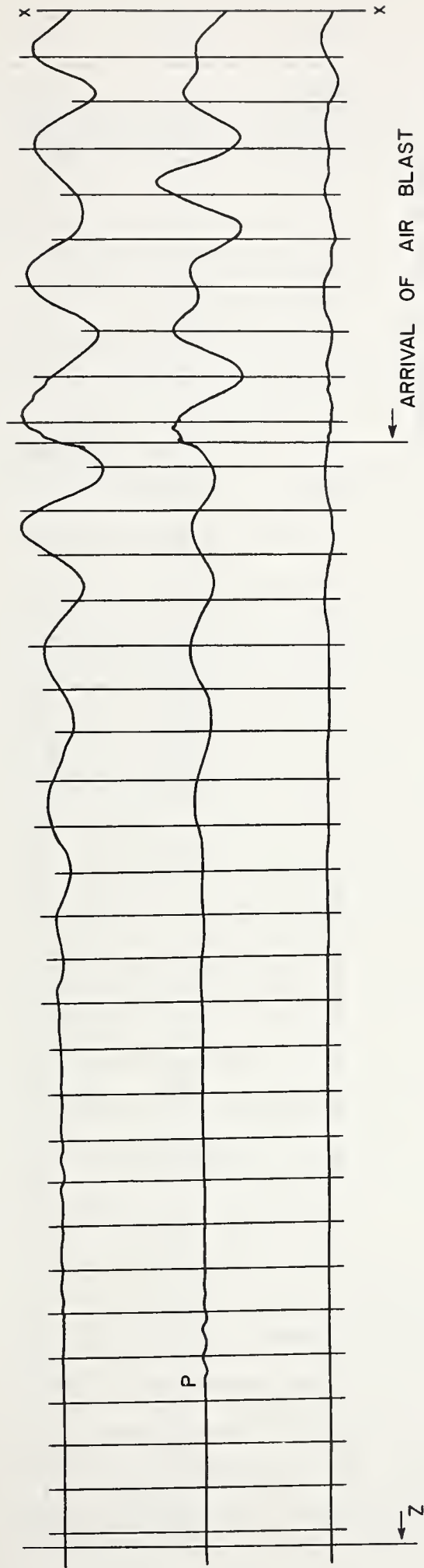


TIMING MARKS = 0.2 SEC.

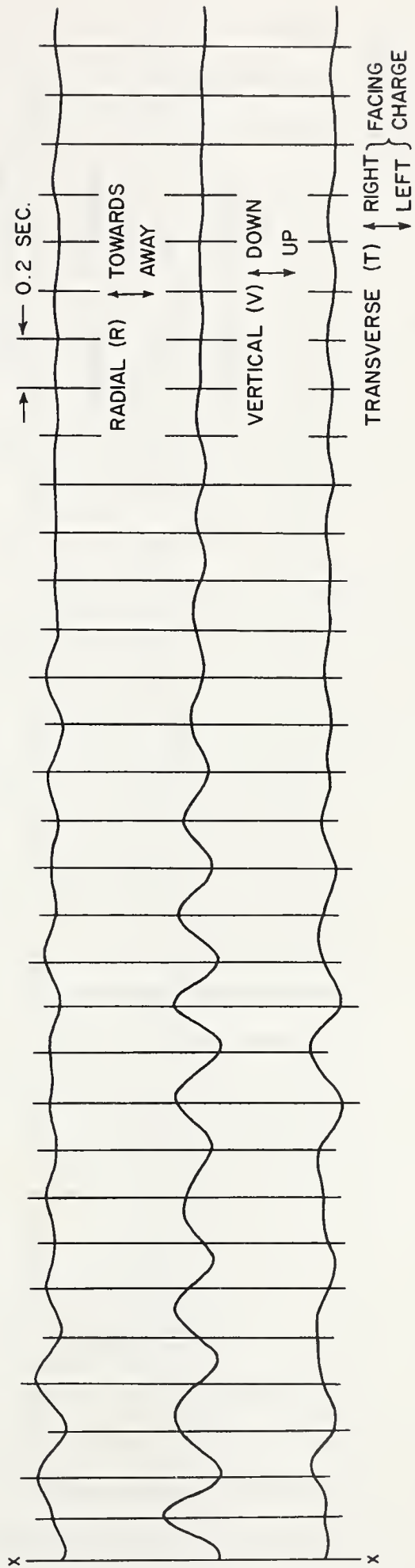
Z = ZERO TIME

HALF SCALE

0 1 2
RECORD VERTICAL SCALE (INCHES)



78D — 6000 FT.



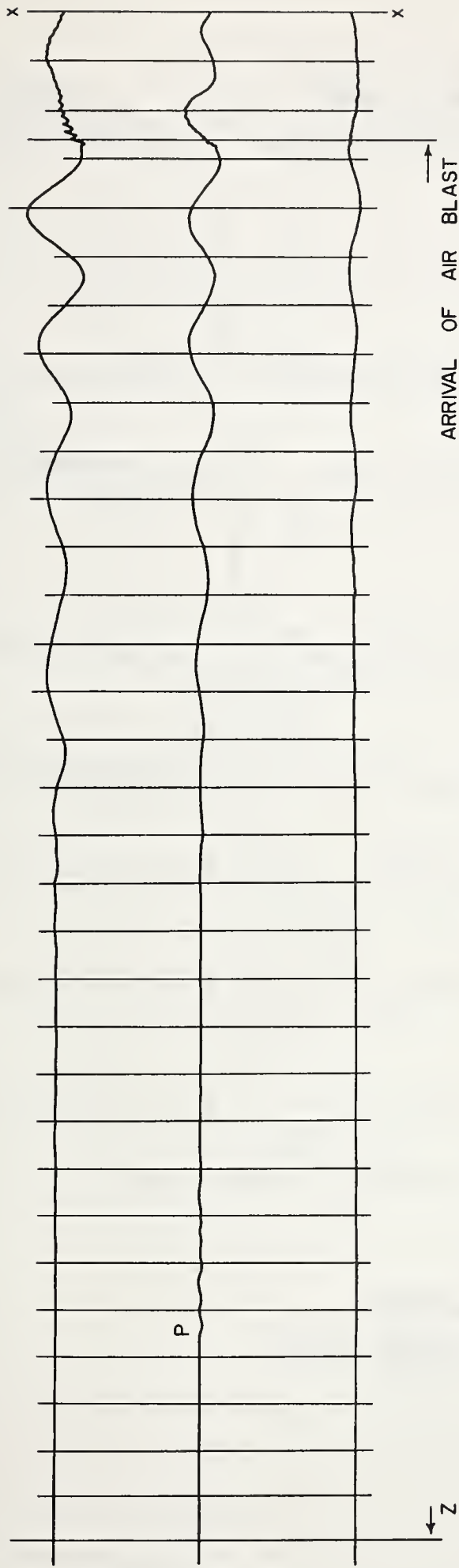
TIMING MARKS = 0.2 SEC.

Z = ZERO TIME

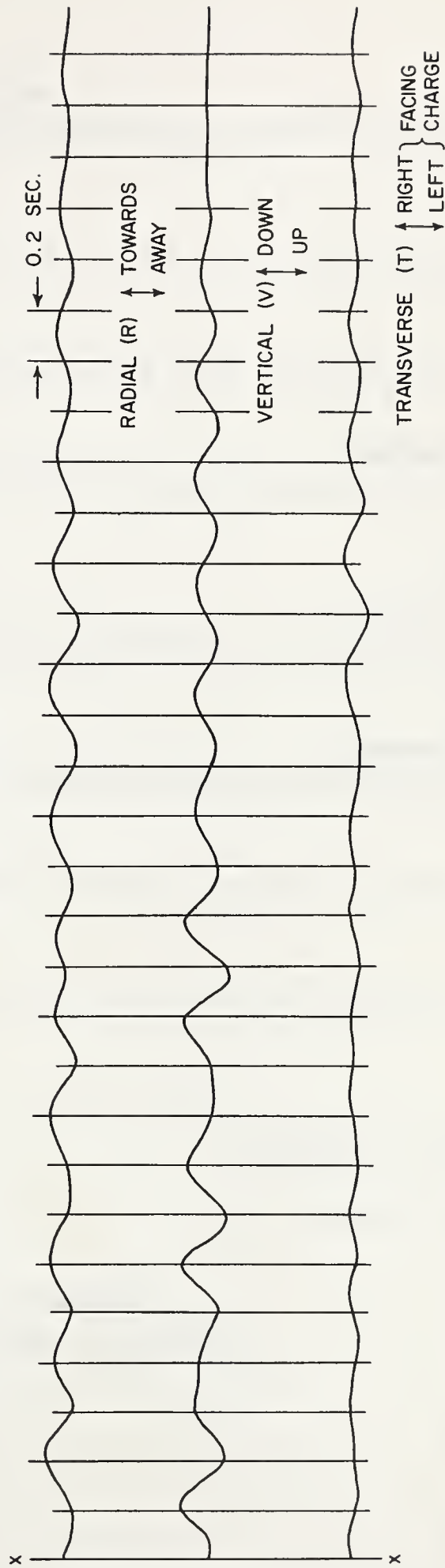
HALF SCALE



RECORD VERTICAL SCALE (INCHES)



79D — 7000 FT.



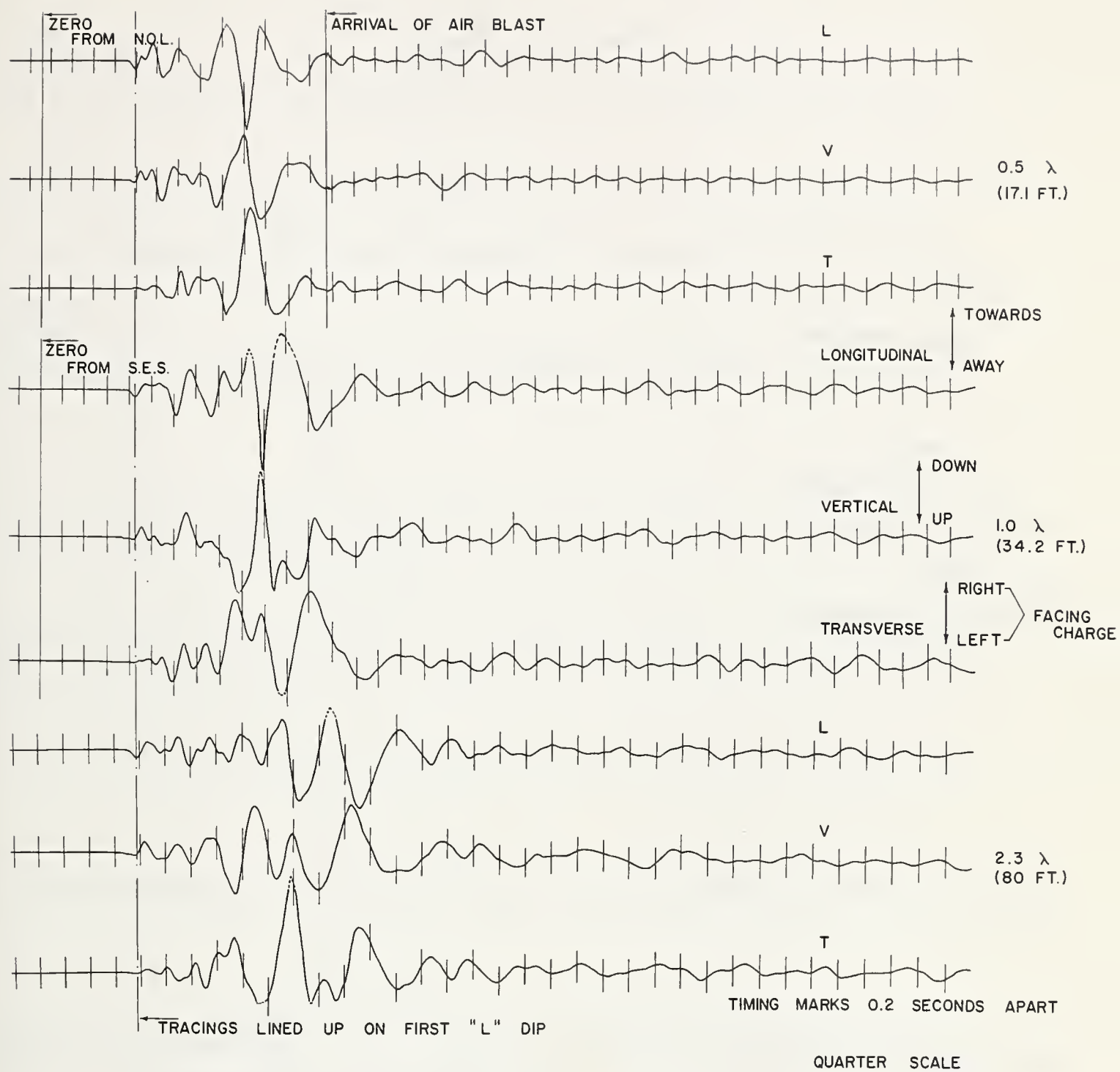
TIMING MARKS = 0.2 SEC.

Z = ZERO TIME

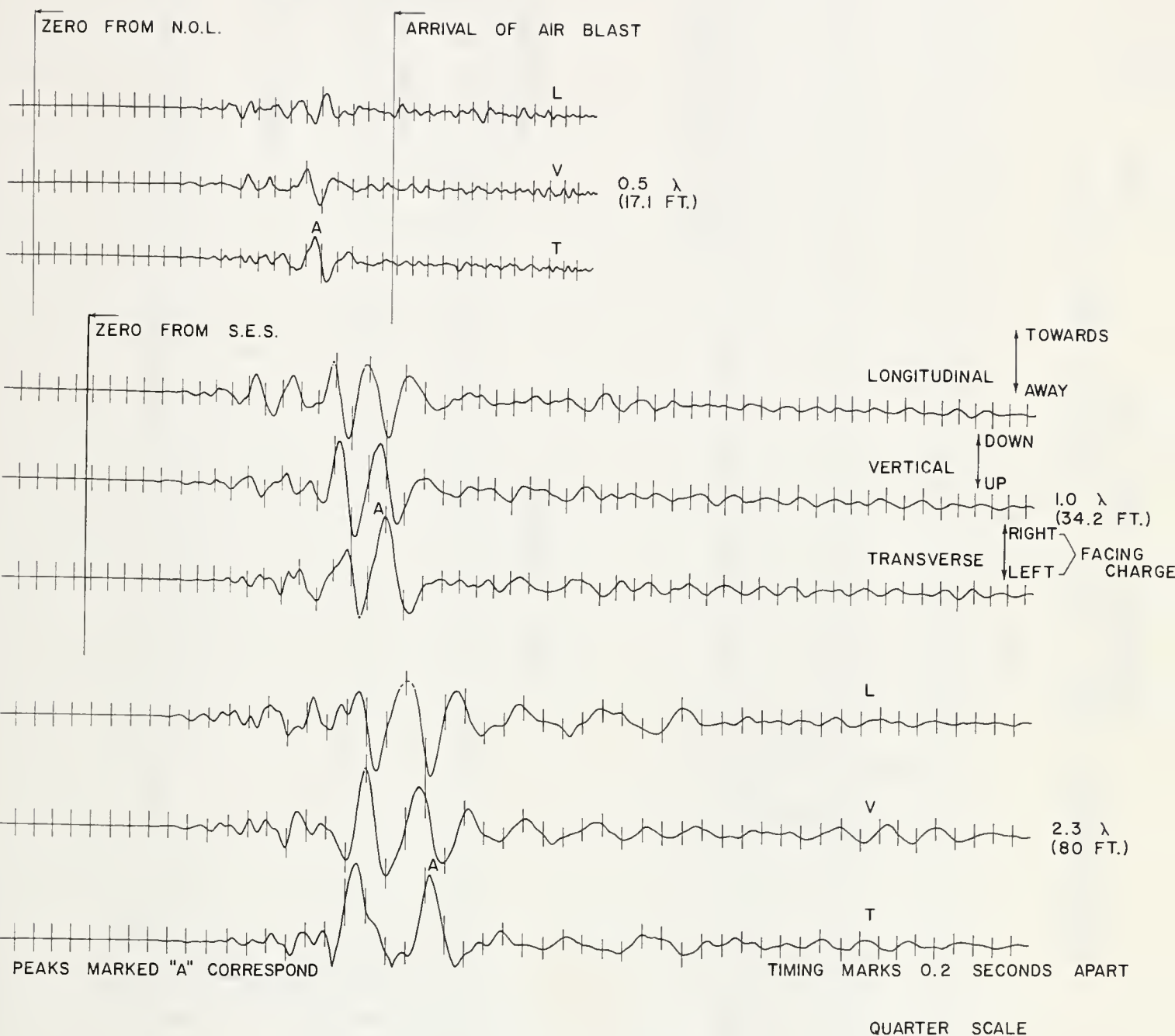
HALF SCALE

0 1 2

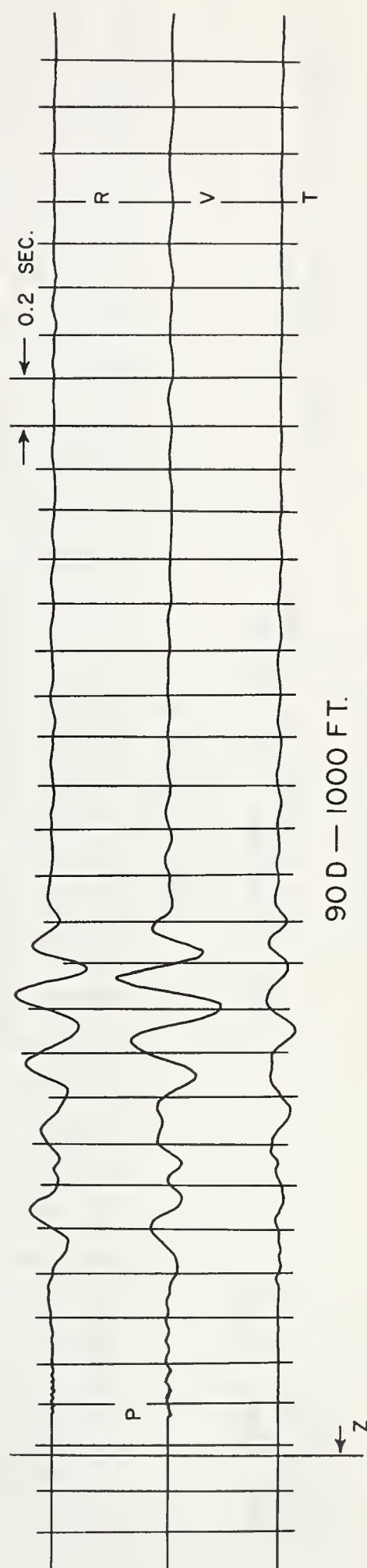
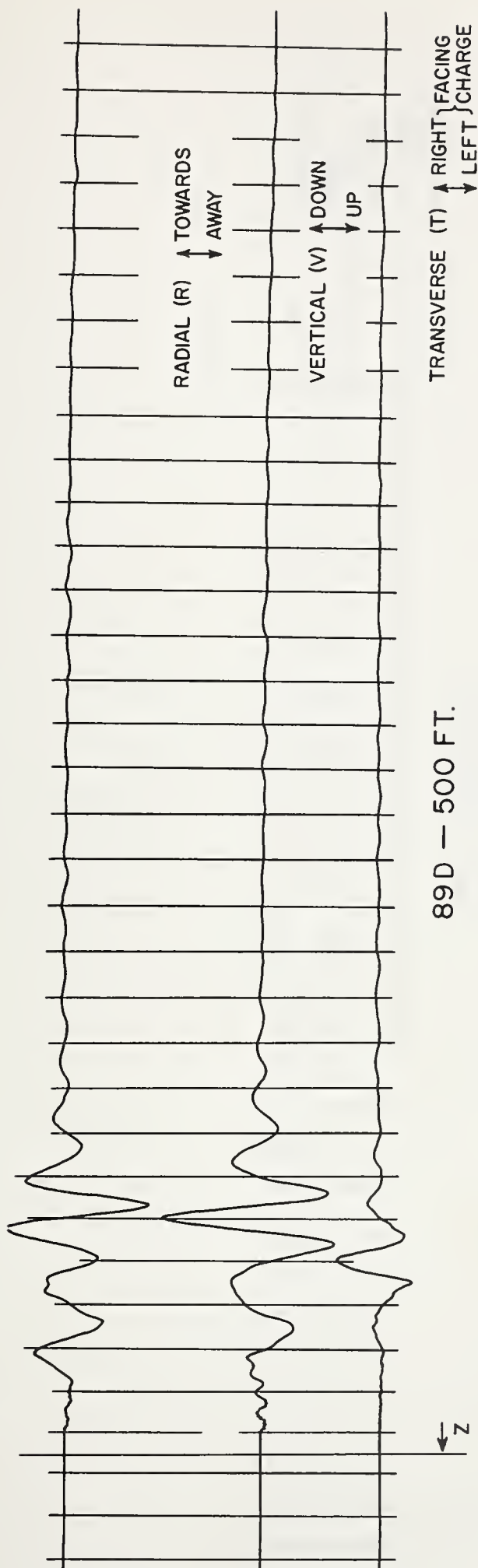
RECORD VERTICAL SCALE (INCHES)



OPERATION STAGECOACH
 SEISMIC RECORDS—3000 FT. FROM G.Z.



OPERATION STAGECOACH
 SEISMIC RECORDS—5000 FT. FROM G.Z.

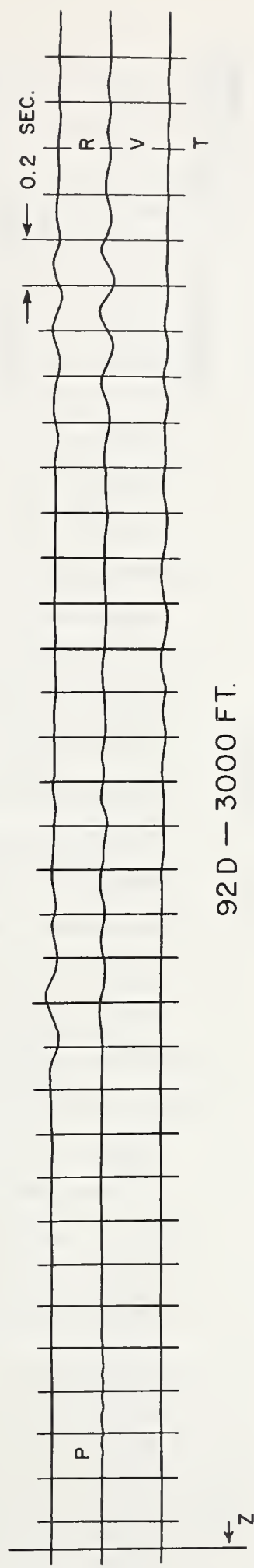
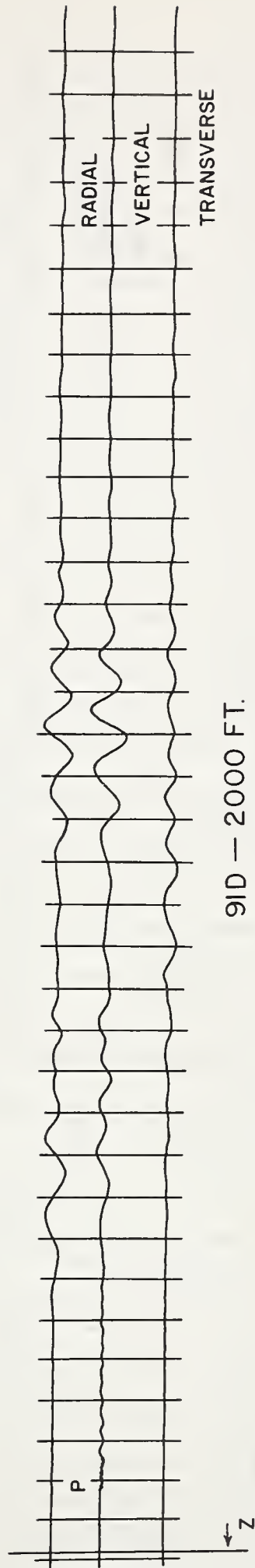


TIMING MARKS = 0.2 SEC.
Z = ZERO TIME
HALF SCALE

SEISMOGRAMS FROM 296 LB. CHARGE BURIED 20 FT.
DROWNING FORD SITE

RECORD VERTICAL SCALE (INCHES)

0 1 2

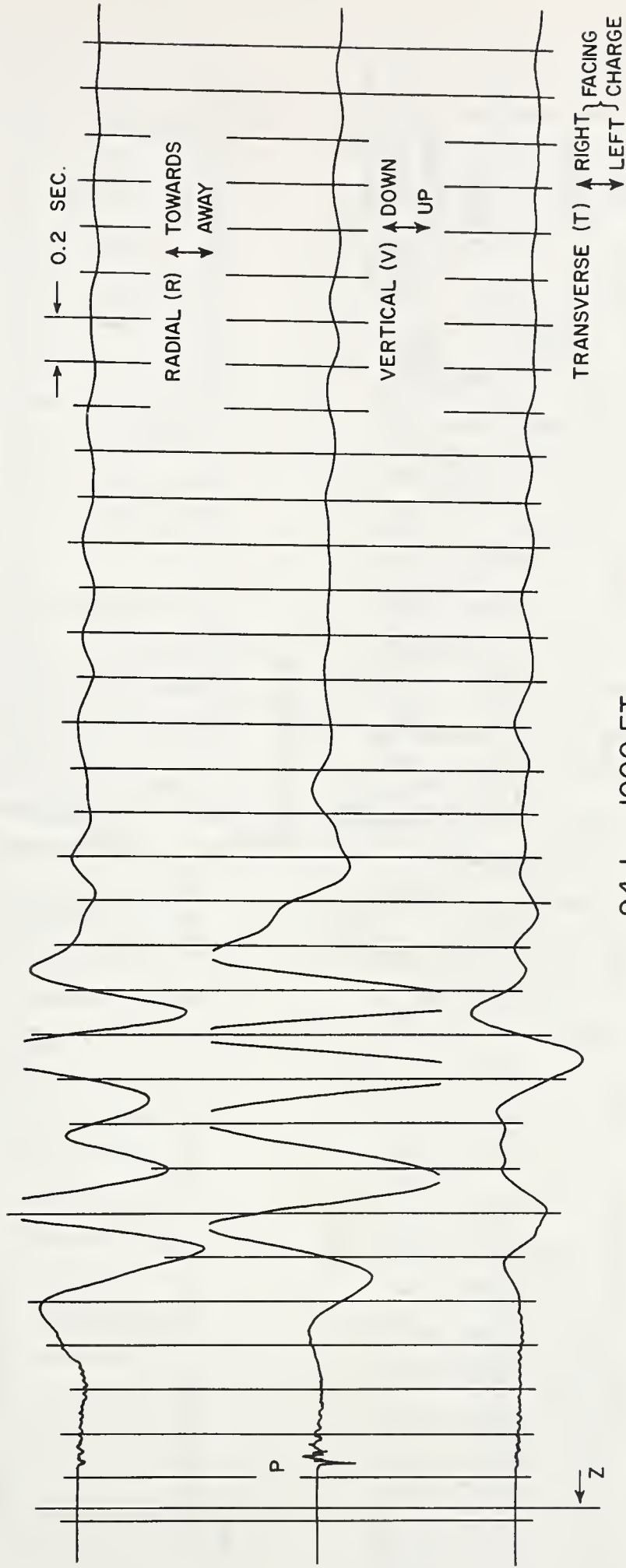


TIMING MARKS = 0.2 SEC.
 Z = ZERO TIME
 HALF SCALE

NOTE : SEISMOGRAM "93D - 5000 FT."
 NOT SUITABLE FOR REDUCTION.

0 1 2
 RECORD VERTICAL SCALE (INCHES)

SEISMOGRAMS FROM 296 LB. CHARGE BURIED 20 FT.
 DROWNING FORD SITE



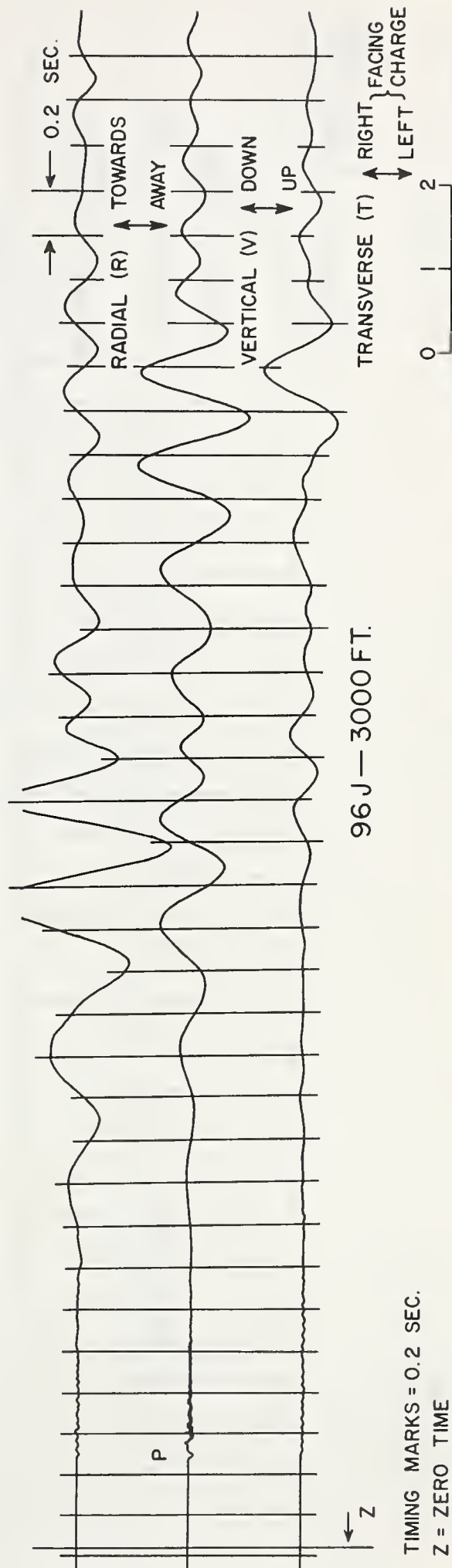
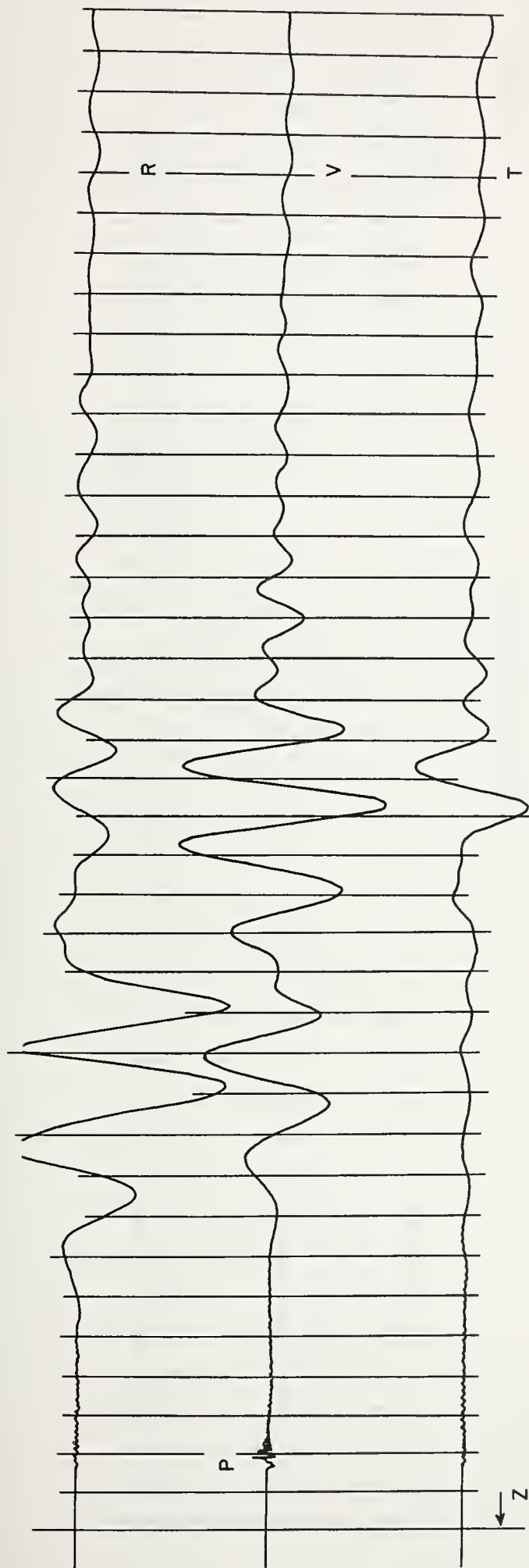
94 J — 1000 FT.

TIMING MARKS = 0.2 SEC.
Z = ZERO TIME
HALF SCALE

0 1 2

RECORD VERTICAL SCALE (INCHES)

SEISMOGRAMS FROM
SPHERICAL 1000 LB. CHARGE BURIED 23.5 FT.
WATCHING HILL SITE



TIMING MARKS = 0.2 SEC.

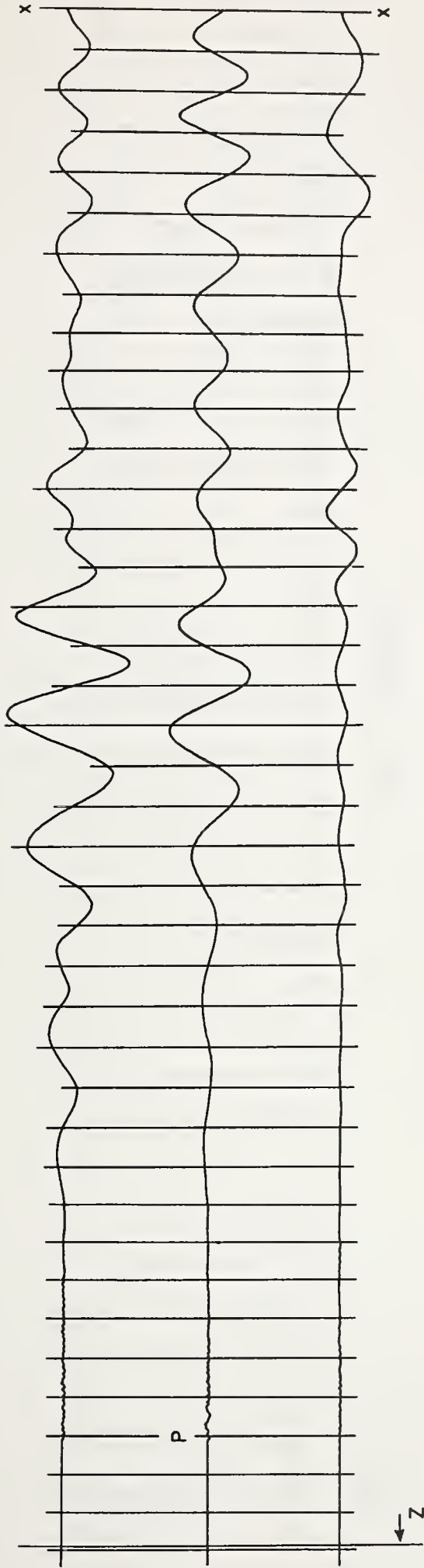
Z = ZERO TIME

HALF SCALE

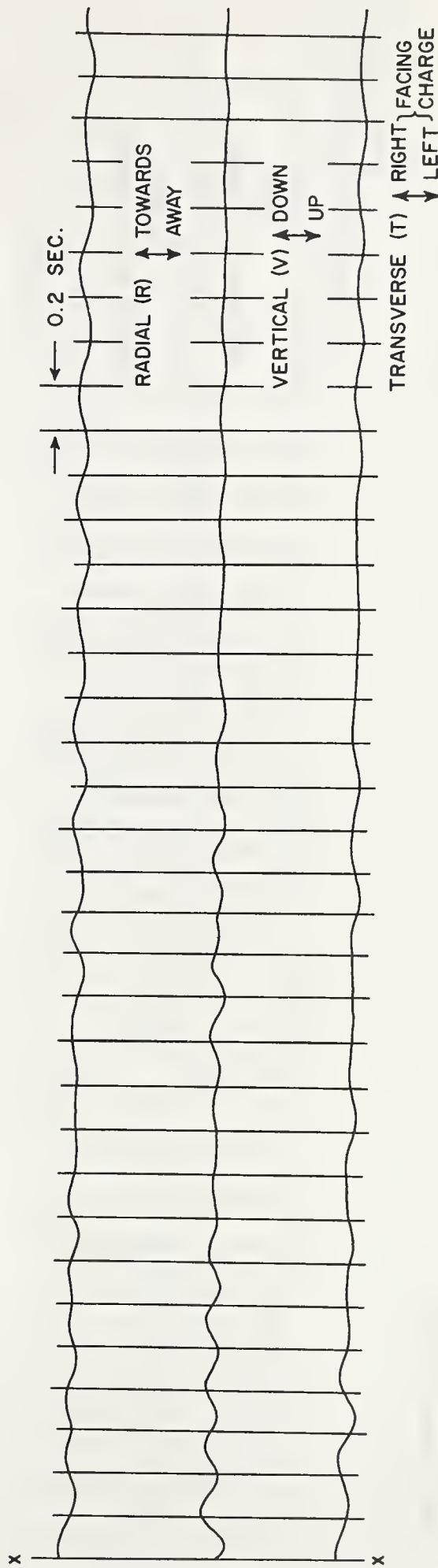
SEISMOGRAMS FROM

SPHERICAL 1000 LB. CHARGE BURIED 23.5 FT.

WATCHING HILL SITE



97 J - 4000 FT.

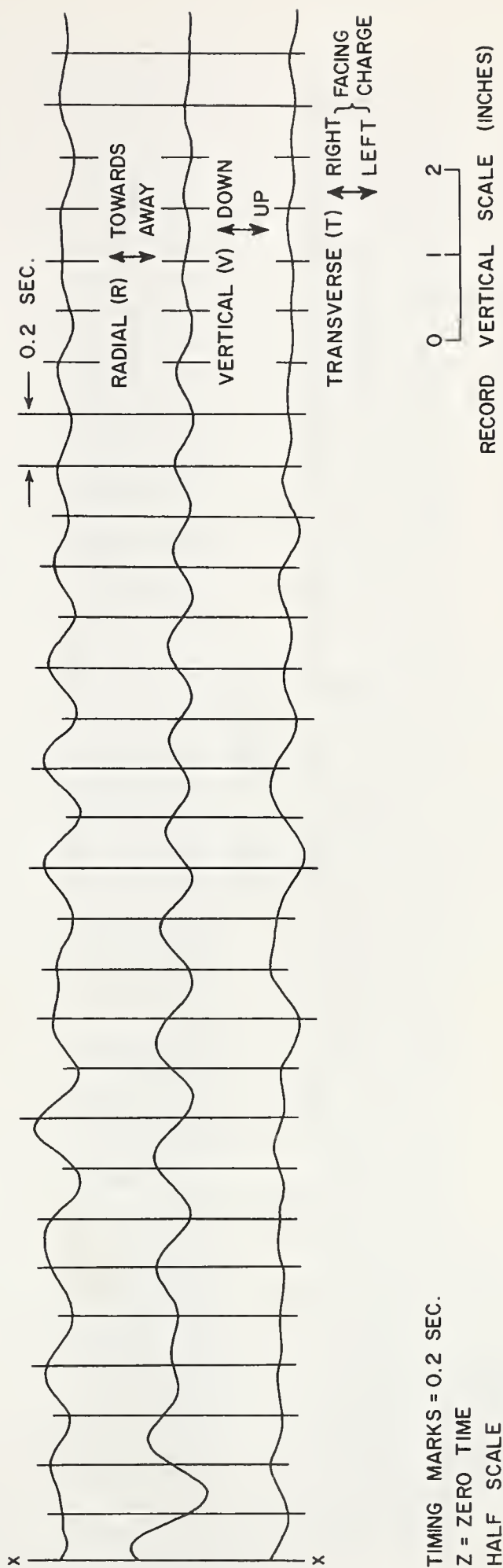
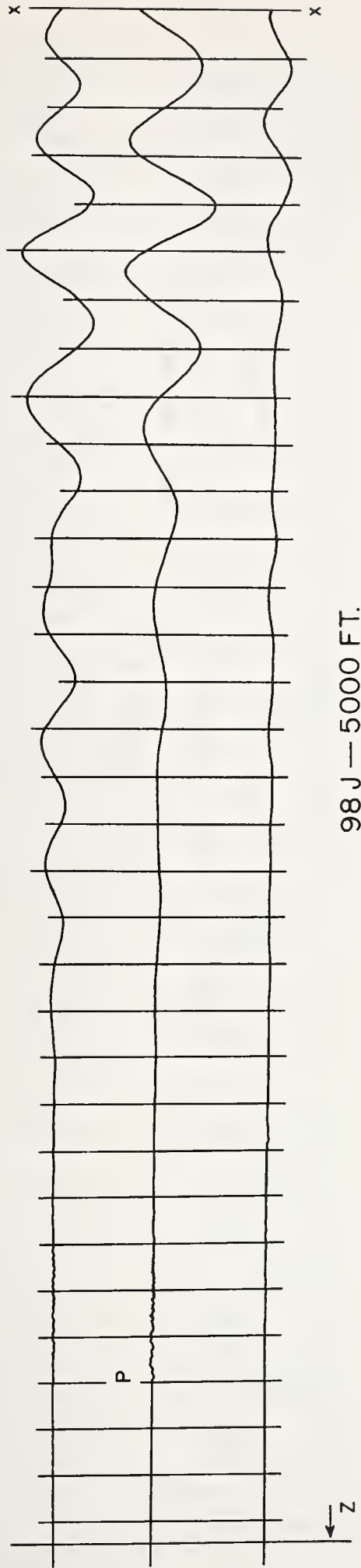


TIMING MARKS = 0.2 SEC.
Z = ZERO TIME
HALF SCALE

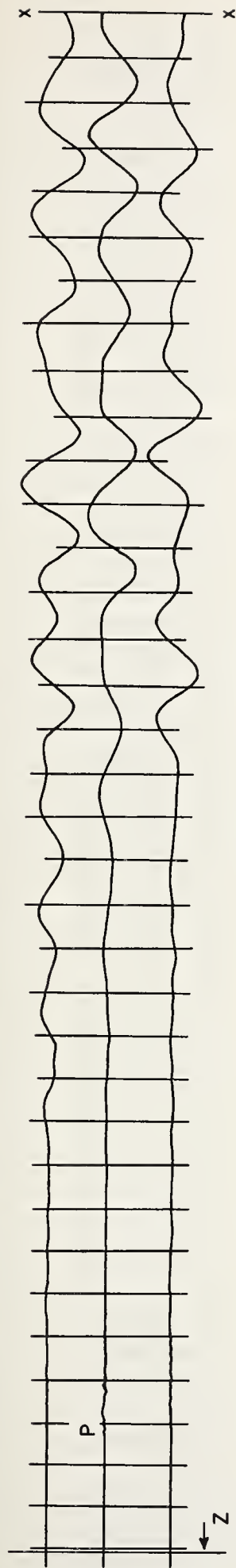
0 1 2

RECORD VERTICAL SCALE (INCHES)

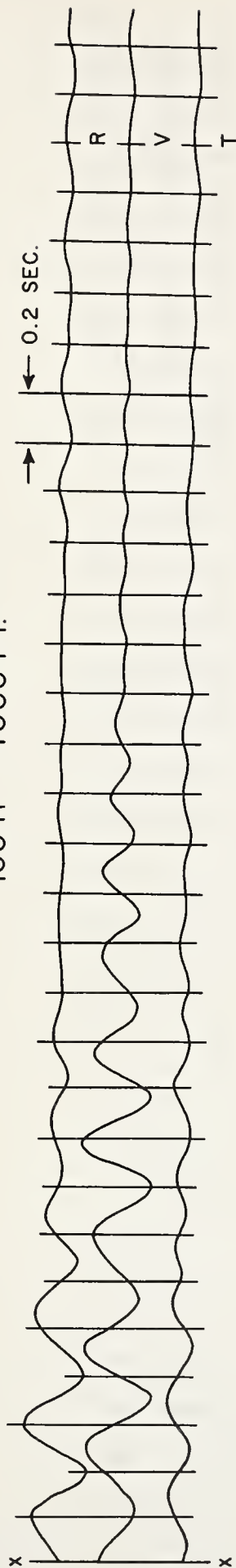
SEISMOGRAMS FROM
SPHERICAL 1000 LB. CHARGE BURIED 23.5 FT.
WATCHING HILL SITE



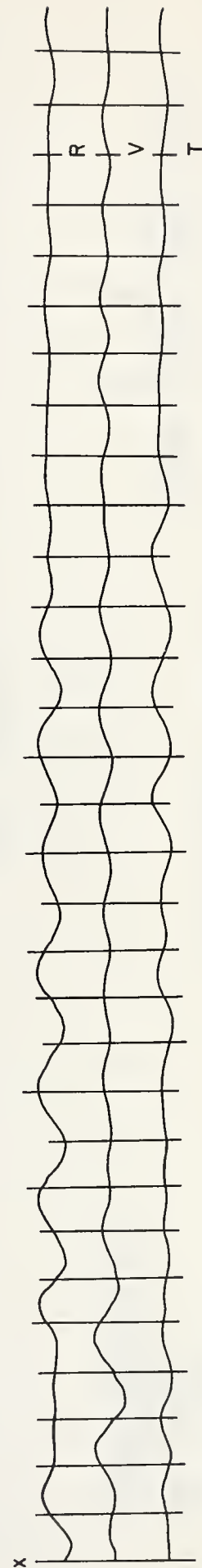
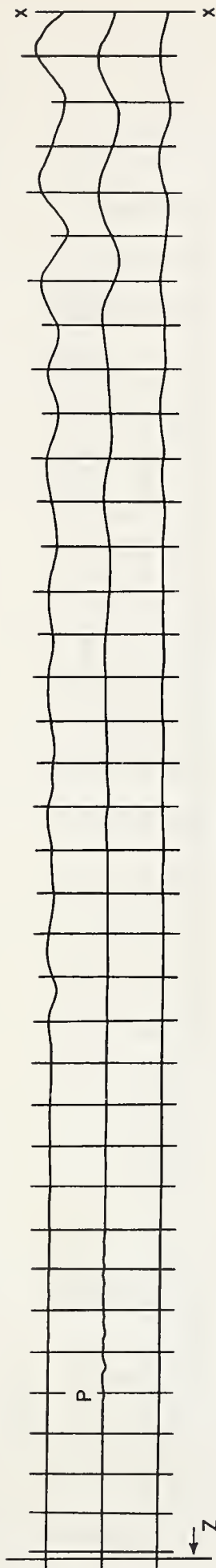
TIMING MARKS = 0.2 SEC.
Z = ZERO TIME
HALF SCALE



100 H — 4000 FT.



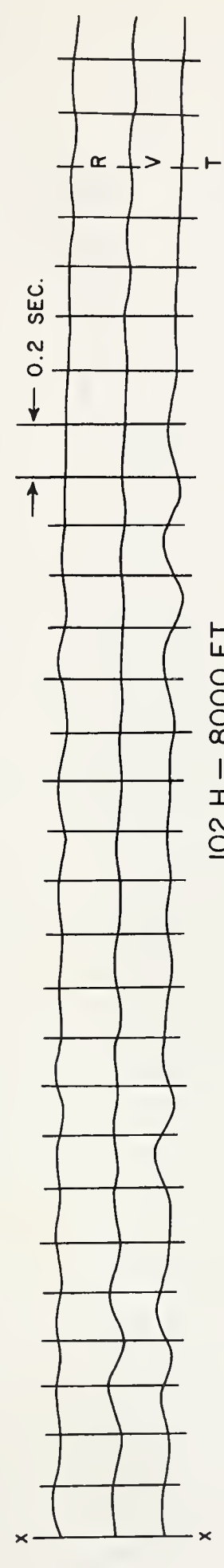
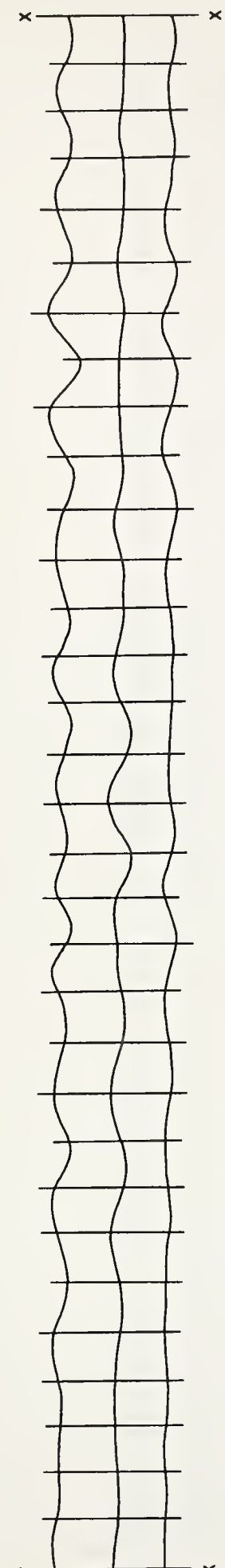
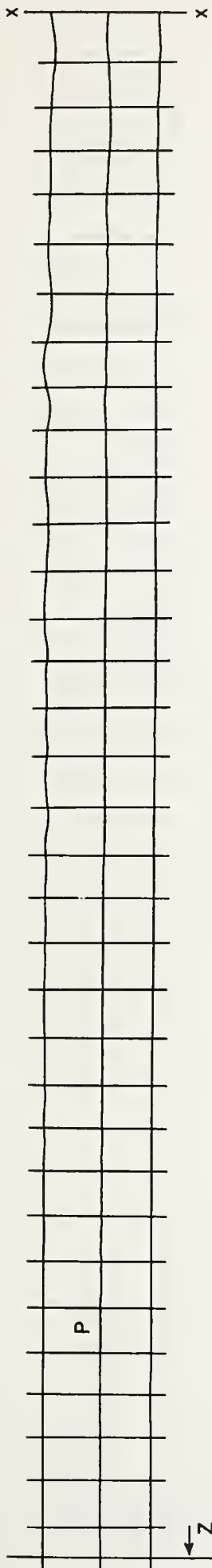
101 H — 6000 FT.



TIMING MARKS = 0.2 SEC.
Z = ZERO TIME
HALF SCALE

0 1 2
RECORD VERTICAL SCALE (INCHES)

SEISMOGRAMS FROM
CYLINDRICAL 1000 LB. CHARGE BURIED 50 FT. — SOIL TAMPED
WATCHING HILL SITE

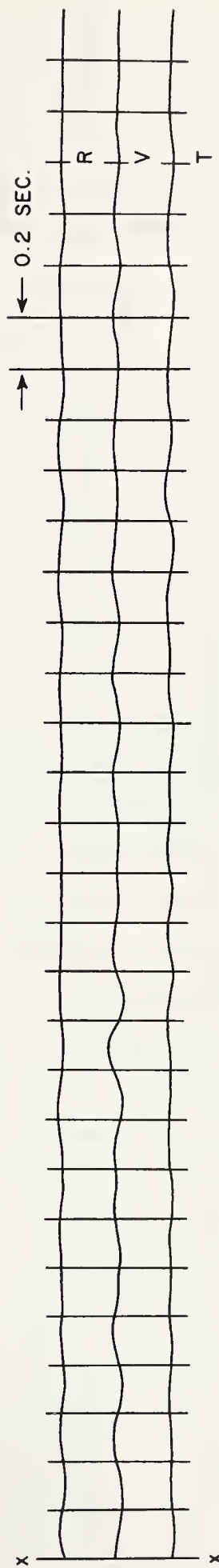
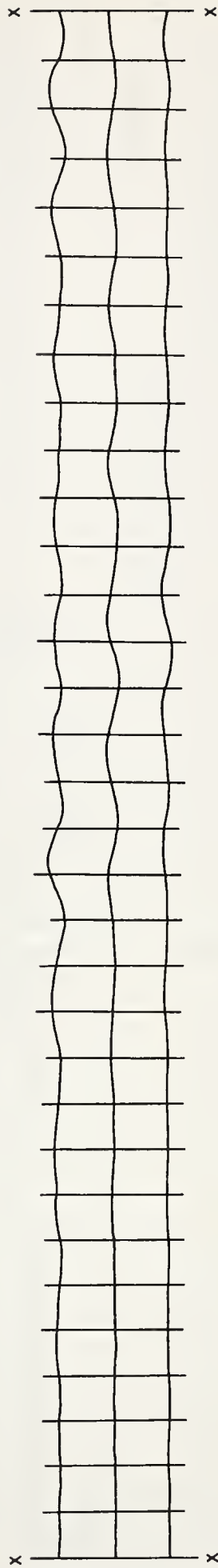
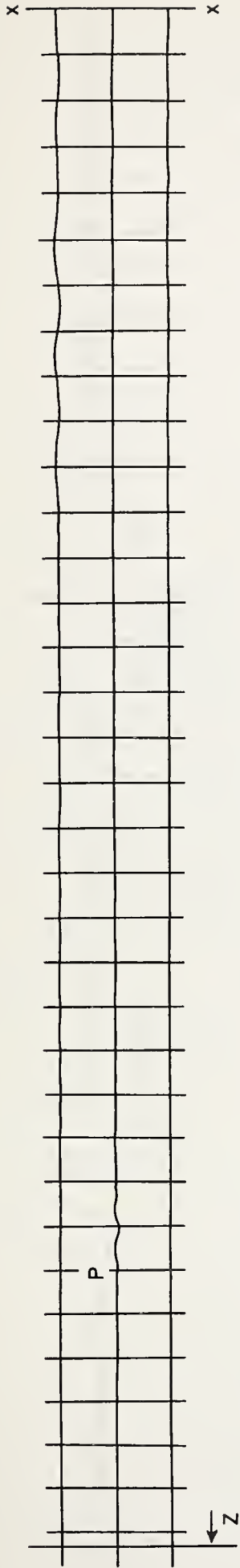


102 H - 8000 FT.

TIMING MARKS = 0.2 SEC.
Z = ZERO TIME
HALF SCALE

0 1 2
RECORD VERTICAL SCALE (INCHES)

SEISMOGRAMS FROM
CYLINDRICAL 1000 LB. CHARGE BURIED 50 FT. — SOIL TAMPED
WATCHING HILL SITE

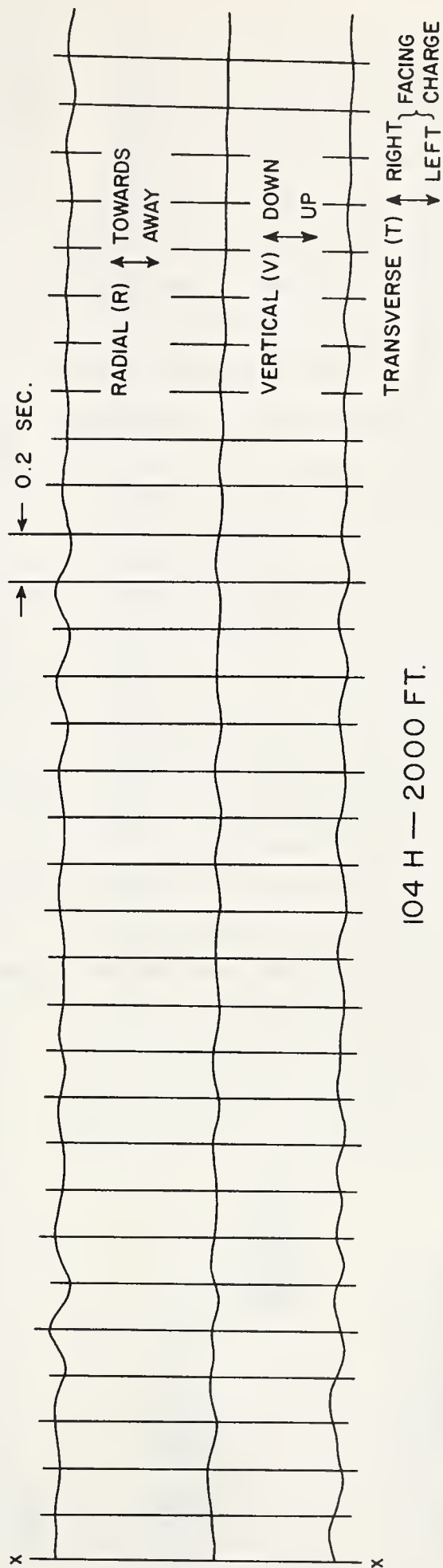
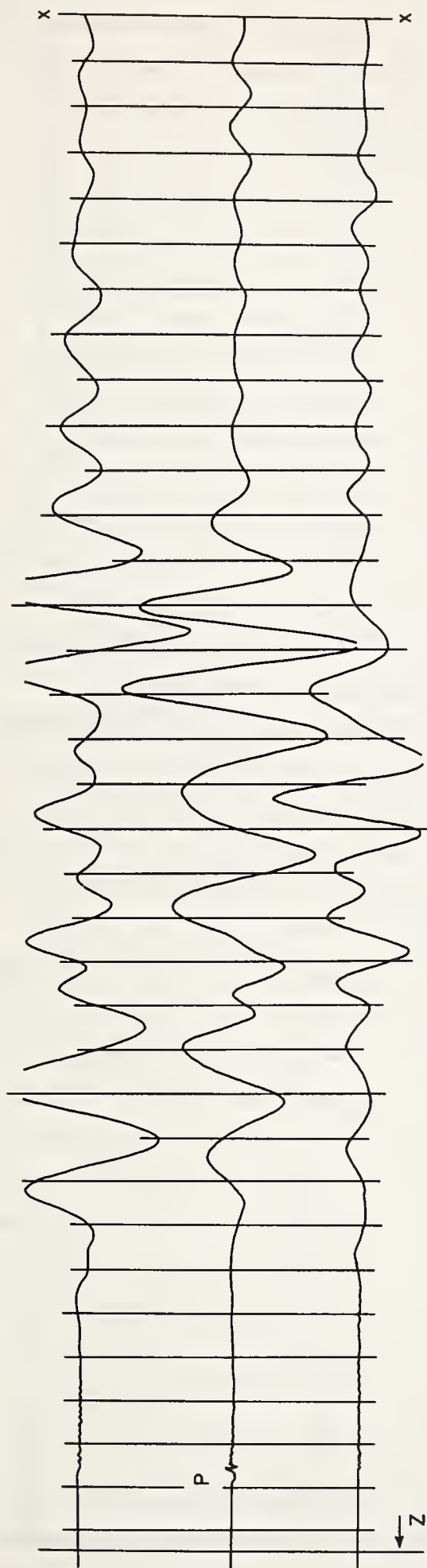


103 H — 10,000 FT.

TIMING MARKS = 0.2 SEC.
Z = ZERO TIME
HALF SCALE

0 1 2
RECORD VERTICAL SCALE (INCHES)

SEISMOGRAMS FROM
CYLINDRICAL 1000 LB. CHARGE BURIED 50 FT. — SOIL TAMPED
WATCHING HILL SITE

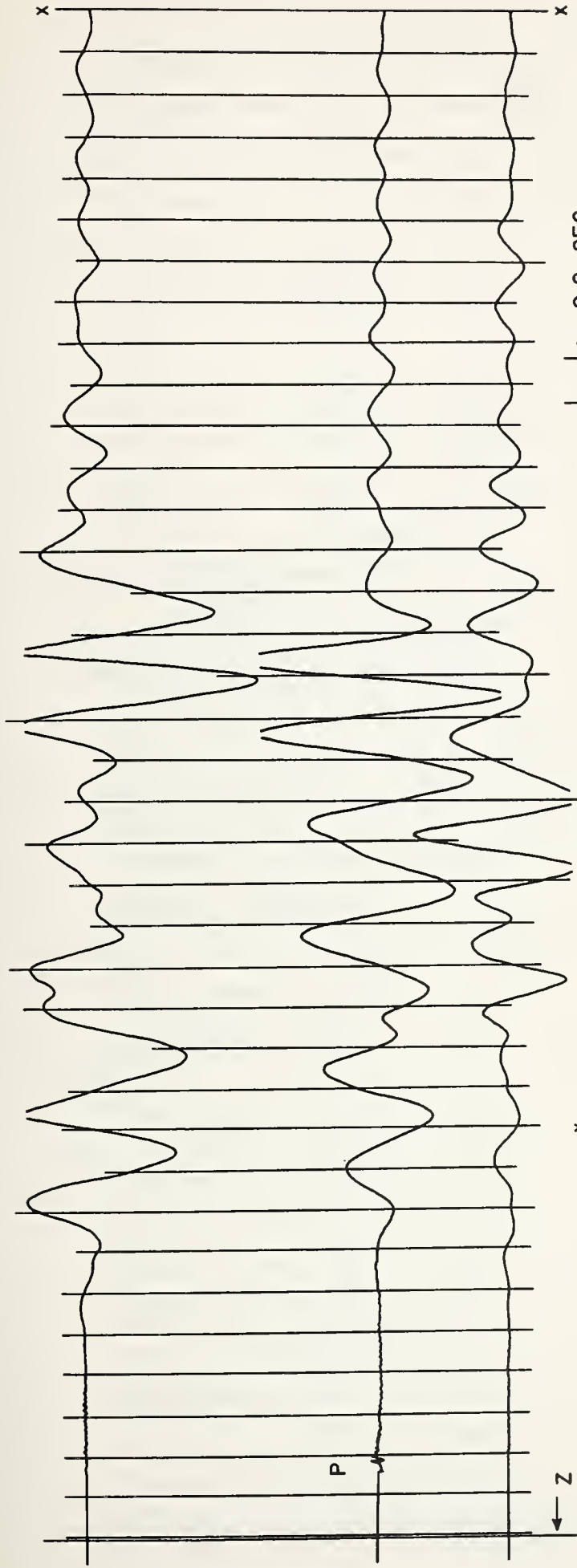


104 H — 2000 FT.

TIMING MARKS = 0.2 SEC.
Z = ZERO TIME
HALF SCALE

0 1 2
RECORD VERTICAL SCALE (INCHES)

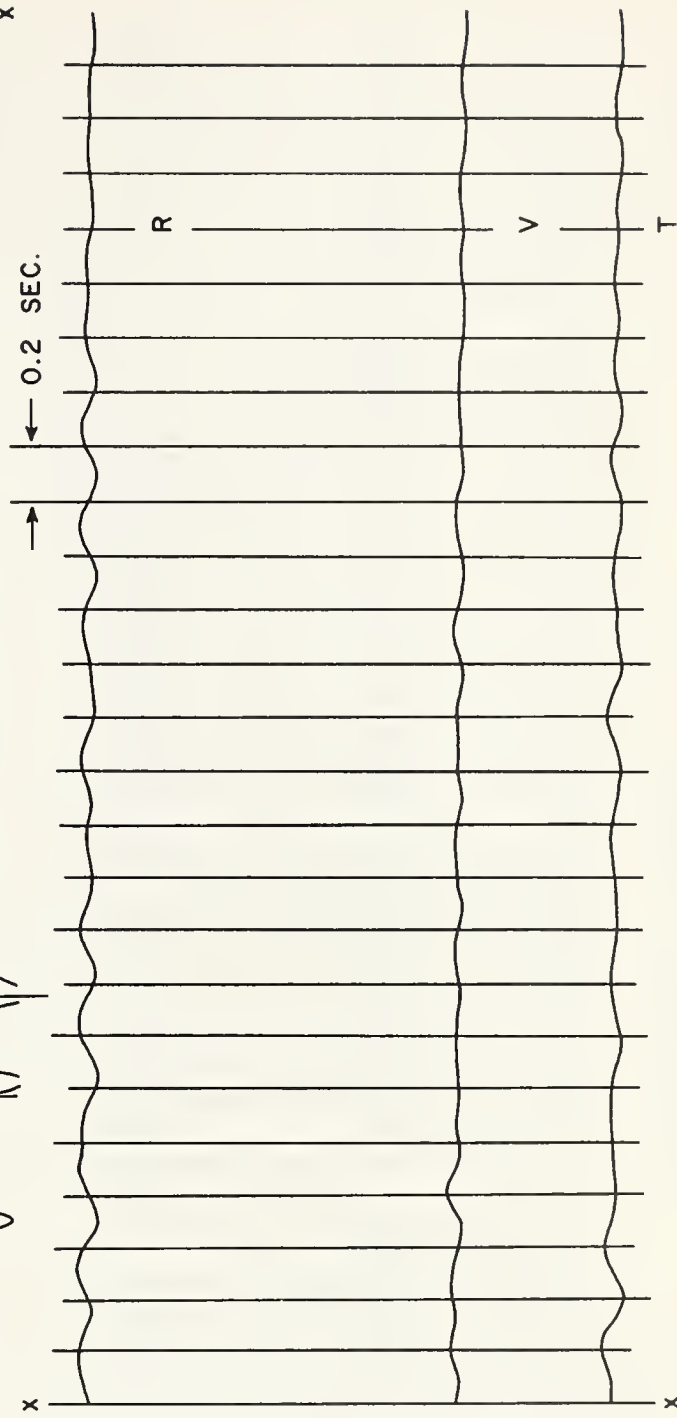
SEISMOGRAMS FROM
CYLINDRICAL 1000 LB. CHARGE BURIED 50 FT. — SOIL TAMPED
WATCHING HILL SITE



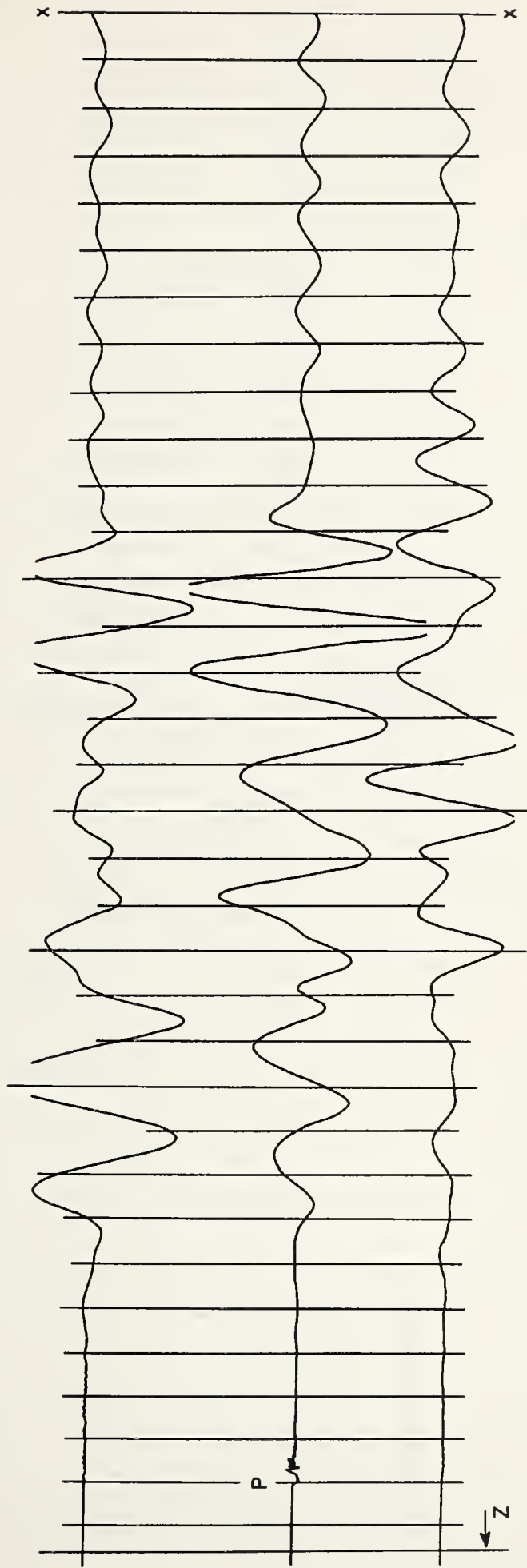
TIMING MARKS = 0.2 SEC.
 Z = ZERO TIME
 HALF SCALE

105 H
 2000 FT.

0 1 2
 RECORD VERTICAL SCALE
 (INCHES)



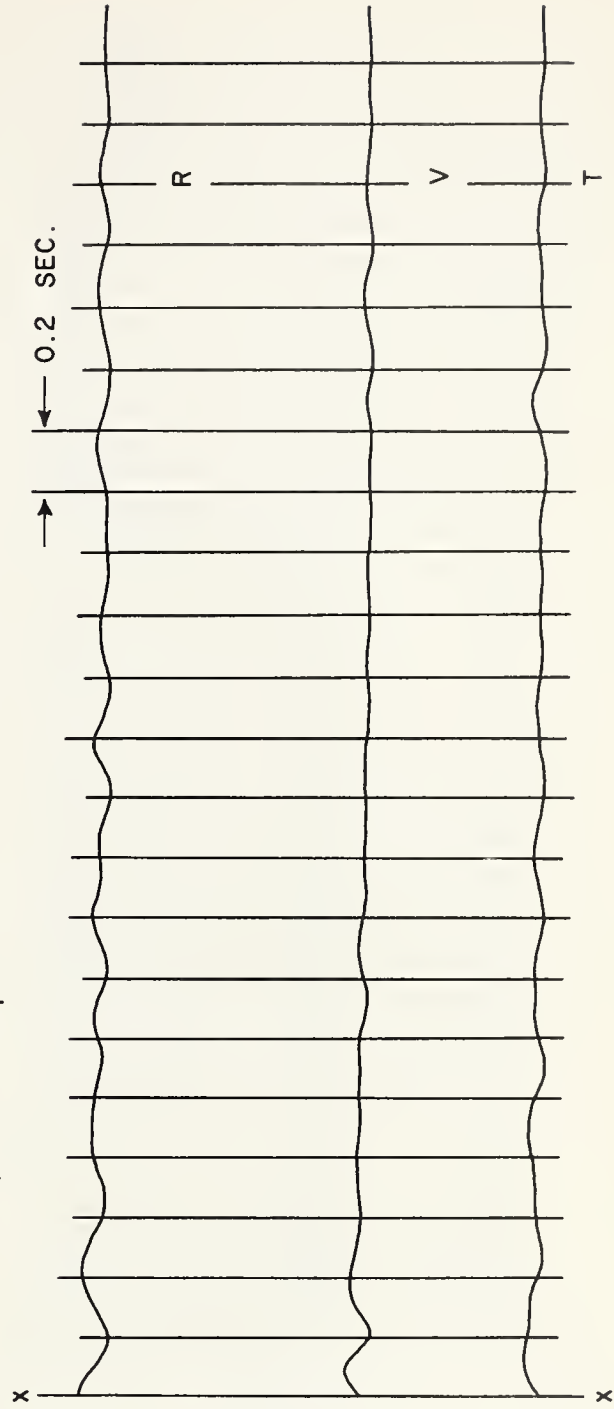
SEISMOGRAMS FROM
 CYLINDRICAL 1000 LB. CHARGE BURIED 50 FT. — SOIL TAMPED
 WATCHING HILL SITE



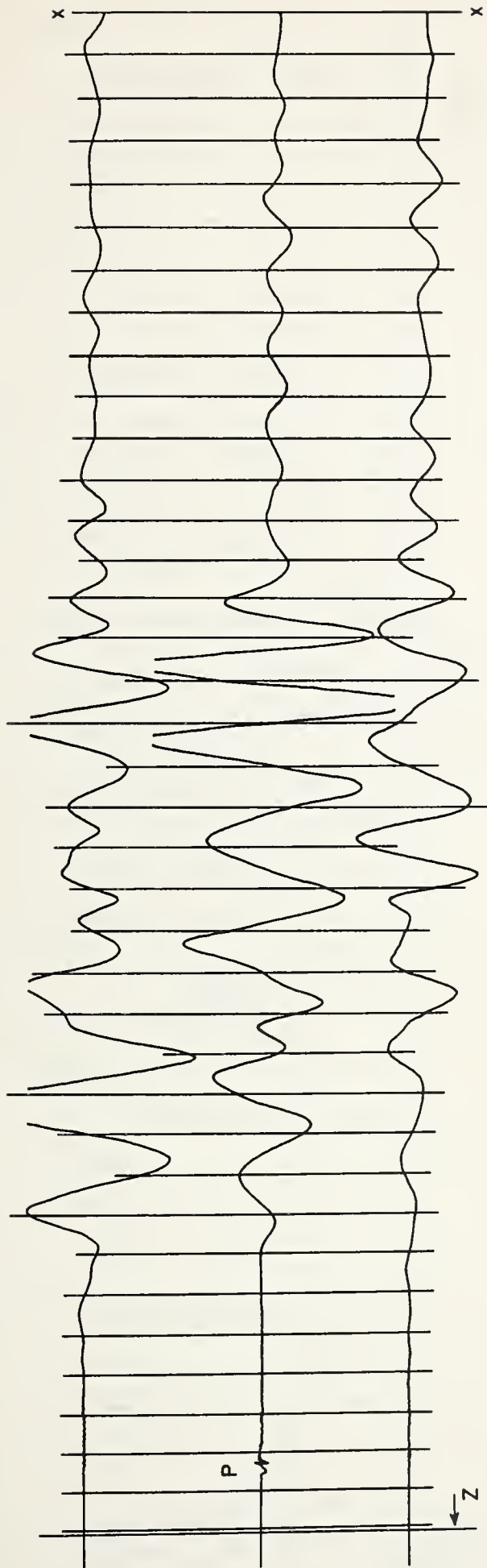
TIMING MARKS = 0.2 SEC.
 Z = ZERO TIME
 HALF SCALE

106 H
 2000 FT.

0 1 2
 RECORD VERTICAL SCALE
 (INCHES)



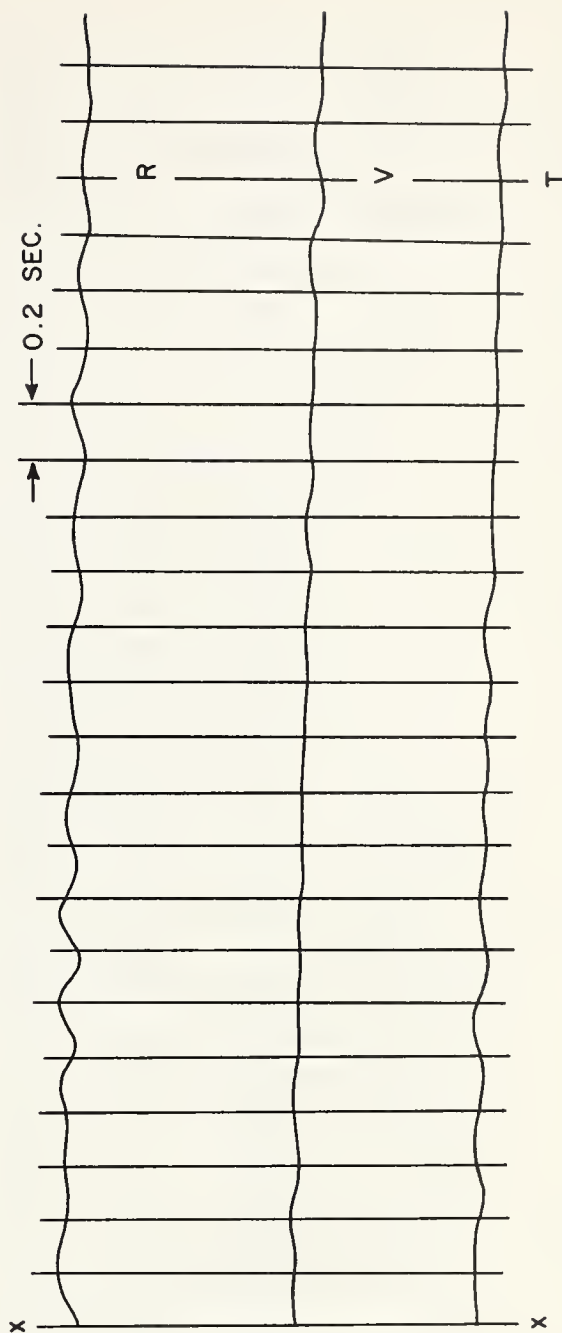
SEISMOGRAMS FROM
 CYLINDRICAL 1000 LB. CHARGE BURIED 50 FT. — SOIL TAMPED
 WATCHING HILL SITE



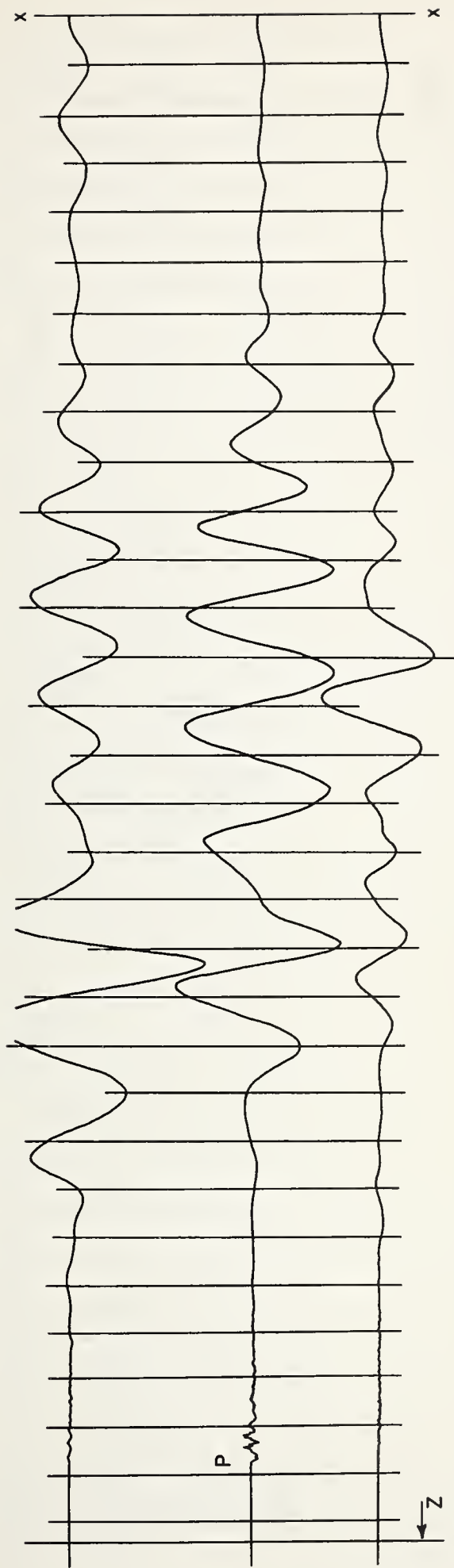
TIMING MARKS = 0.2 SEC.
 Z = ZERO TIME
 HALF SCALE

107 H
 2000 FT.

0 1 2
 RECORD VERTICAL SCALE
 (INCHES)



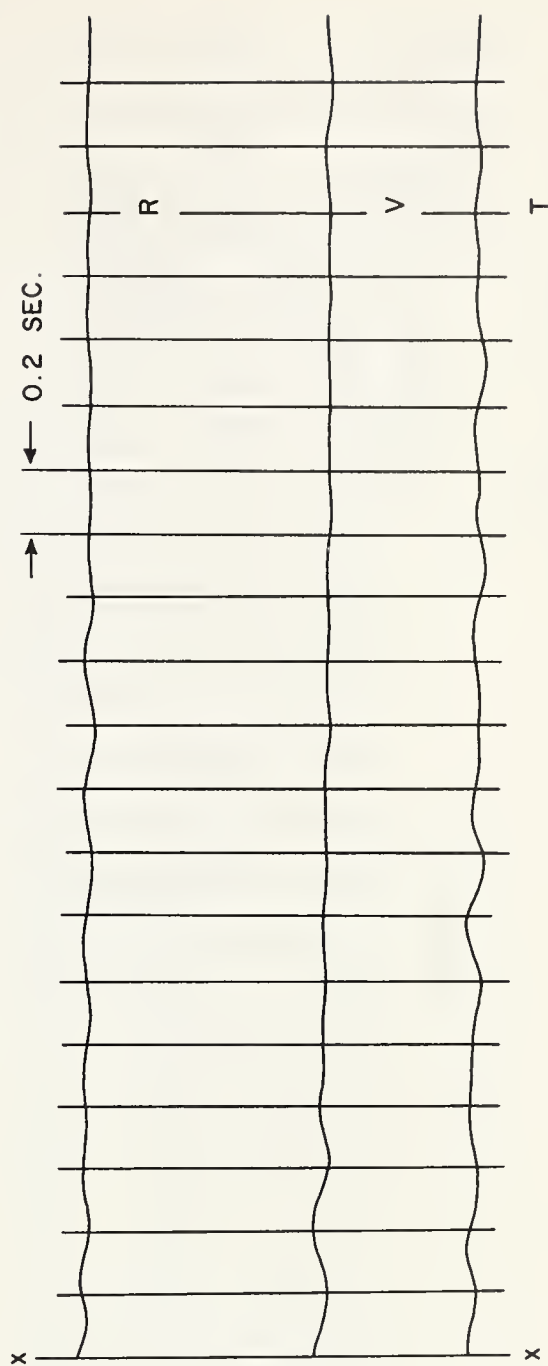
SEISMOGRAMS FROM
 CYLINDRICAL 1000 LB. CHARGE BURIED 50 FT. — SOIL TAMPED
 WATCHING HILL SITE



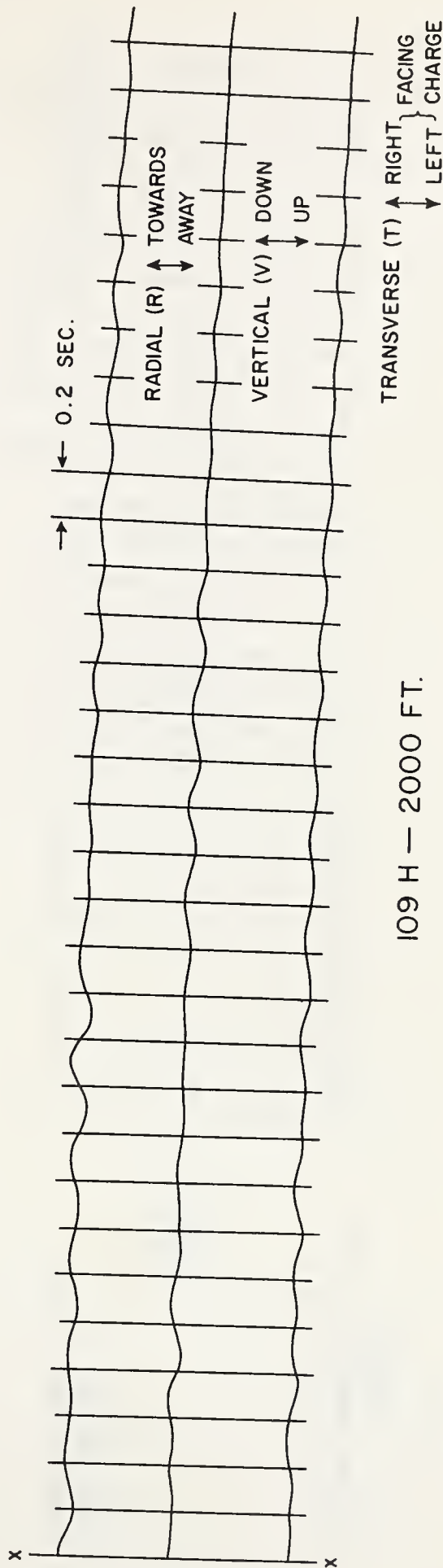
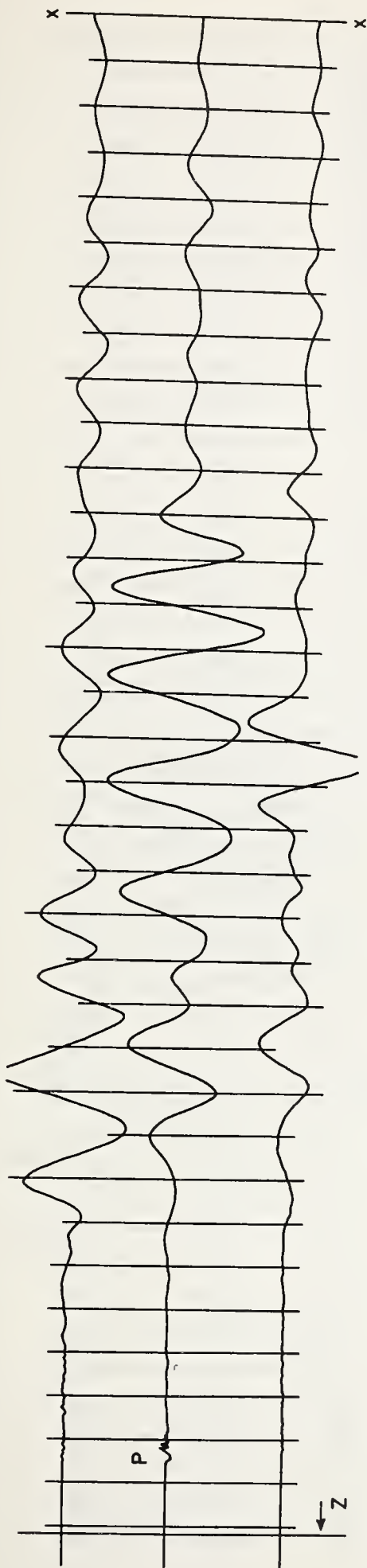
TIMING MARKS = 0.2 SEC.
 Z = ZERO TIME
 HALF SCALE

108 H
 2000 FT.

0 1 2
 RECORD VERTICAL SCALE
 (INCHES)



SEISMOGRAMS FROM
 CYLINDRICAL 1000 LB. CHARGE BURIED 50 FT. — SOIL TAMPED
 WATCHING HILL SITE

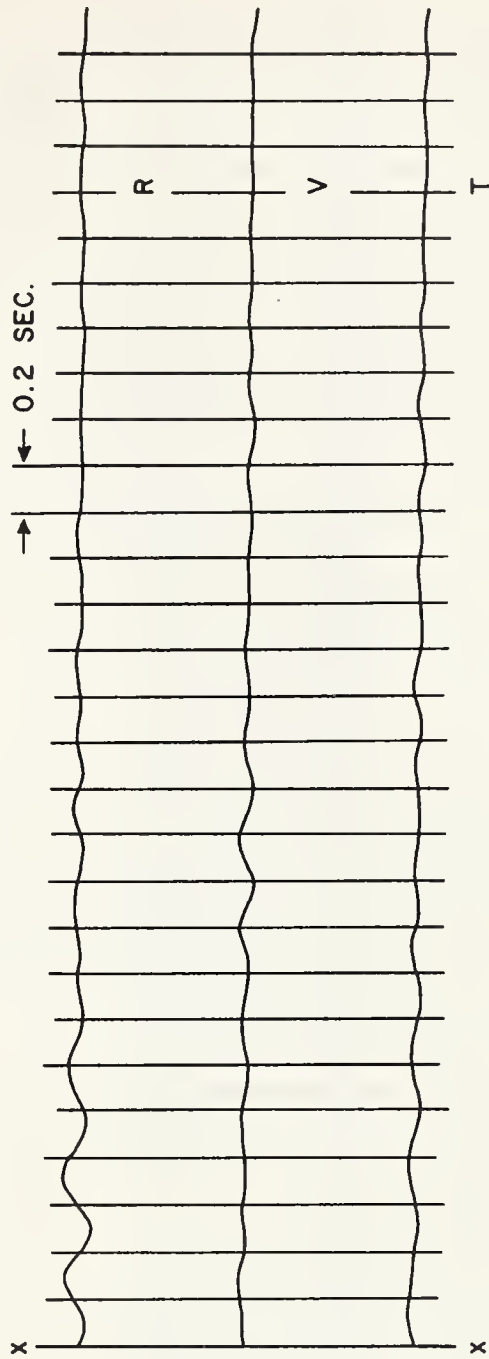
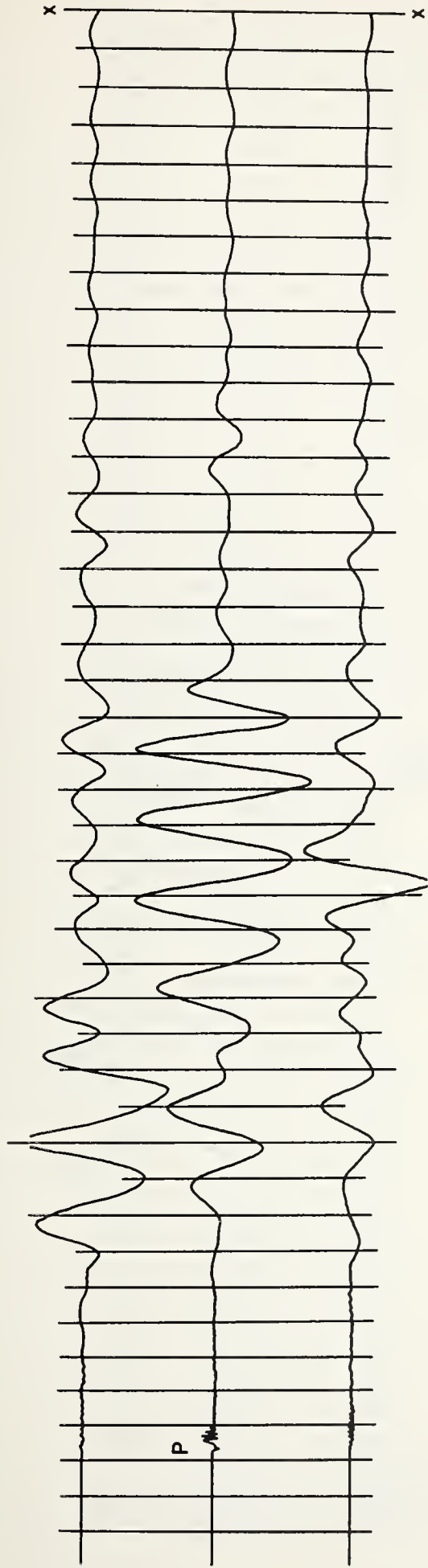


109 H — 2000 FT.

TIMING MARKS = 0.2 SEC.
Z = ZERO TIME
HALF SCALE

0 1 2
RECORD VERTICAL SCALE (INCHES)

SEISMOGRAMS FROM
CYLINDRICAL 1000 LB. CHARGE BURIED 50 FT. — WATER TAMPED
WATCHING HILL SITE

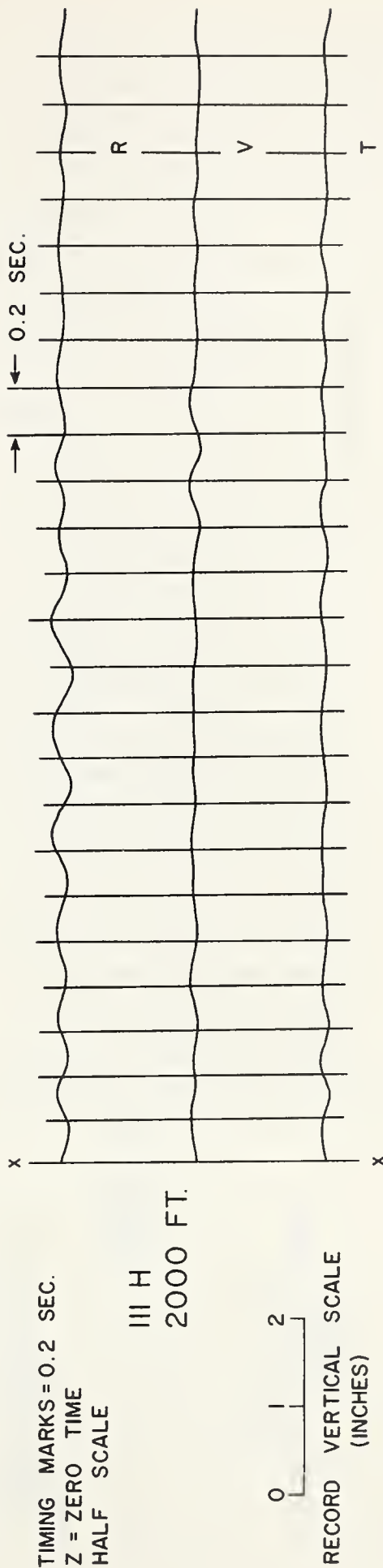
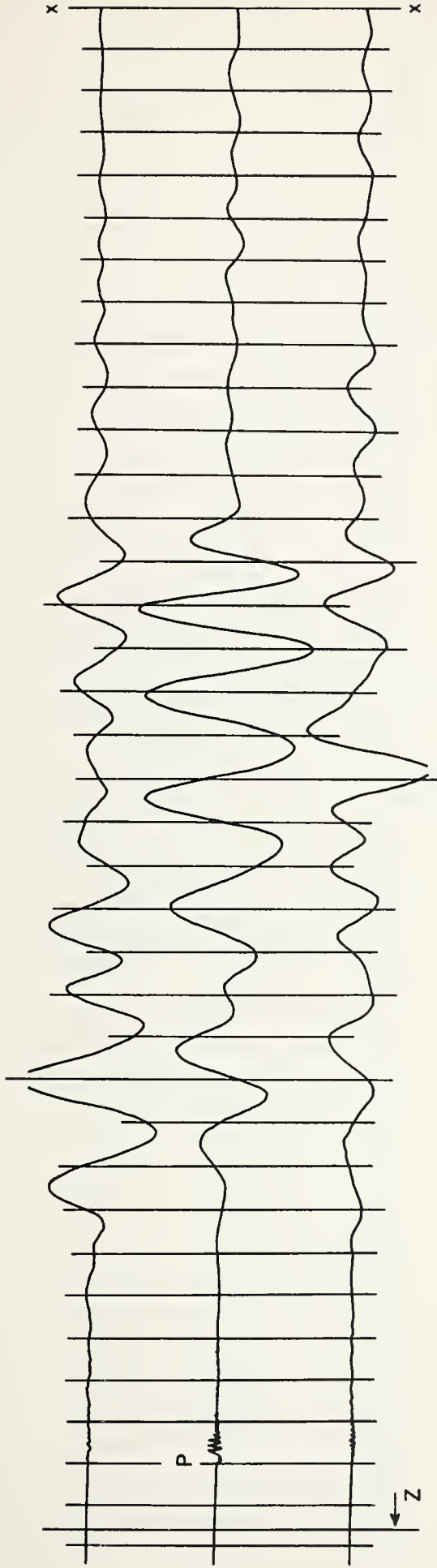


TIMING MARKS = 0.2 SEC.
HALF SCALE

110 H
2000 FT.

0 1 2
RECORD VERTICAL SCALE
(INCHES)

SEISMOGRAMS FROM
CYLINDRICAL 1000 LB. CHARGE BURIED 50 FT. — WATER TAMPED
WATCHING HILL SITE

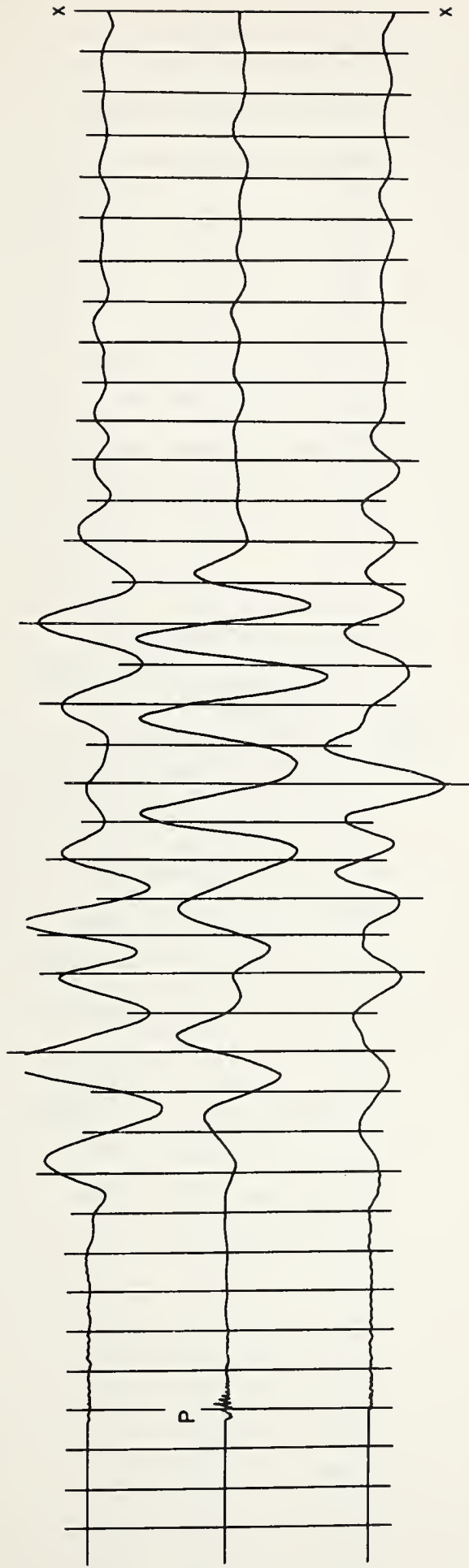


TIMING MARKS = 0.2 SEC.
 Z = ZERO TIME
 HALF SCALE

III H
 2000 FT.

0 1 2
 RECORD VERTICAL SCALE
 (INCHES)

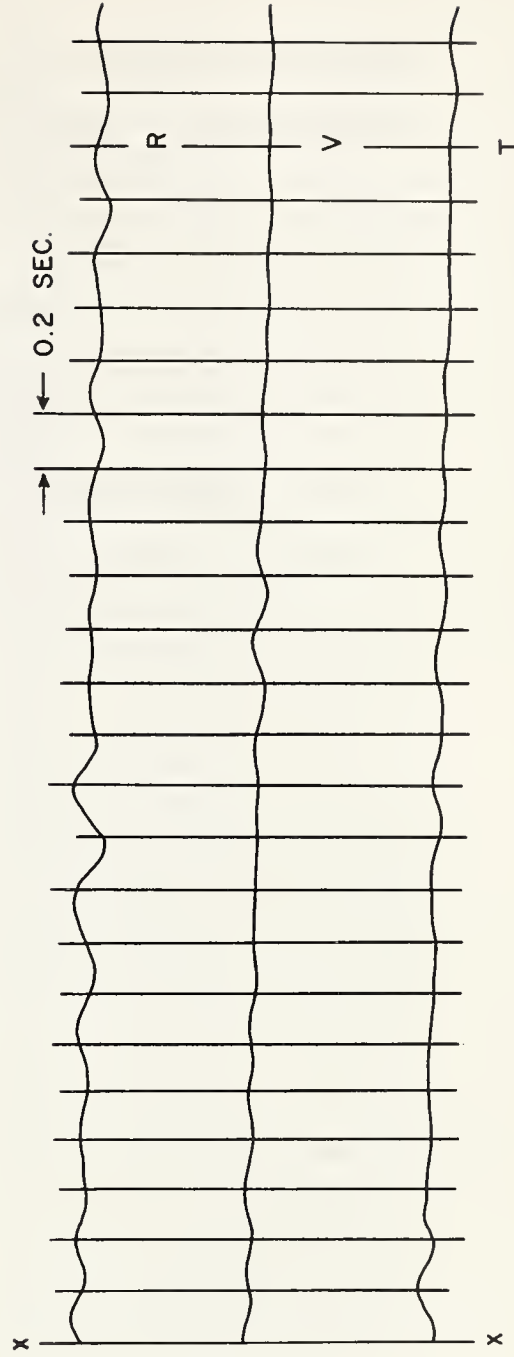
SEISMOGRAMS FROM
 CYLINDRICAL 1000 LB. CHARGE BURIED 50 FT. — WATER TAMPED
 WATCHING HILL SITE



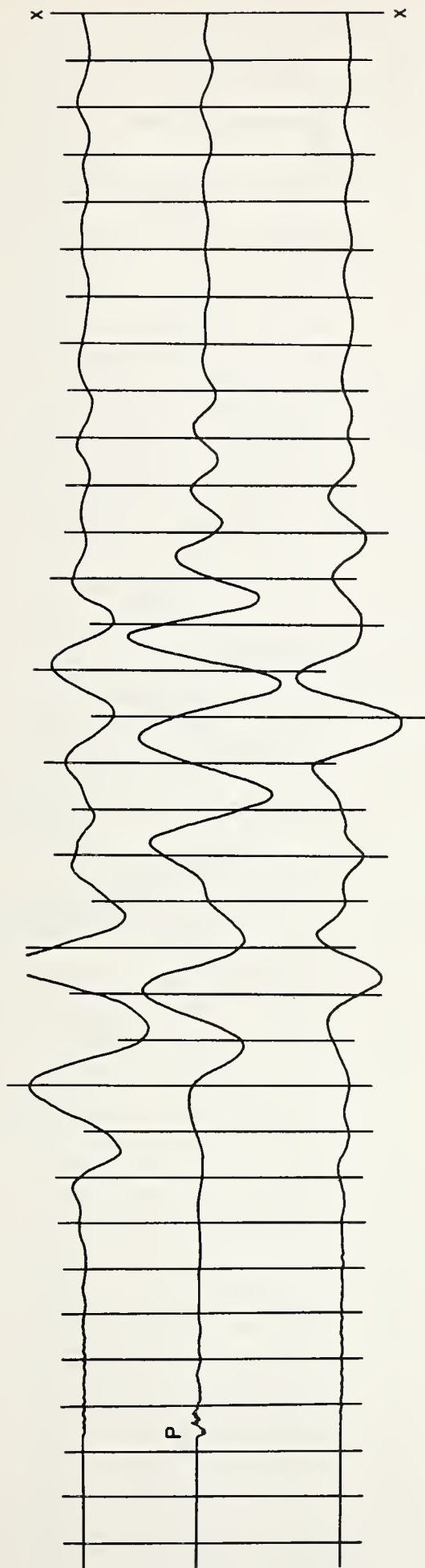
TIMING MARKS = 0.2 SEC.
HALF SCALE

112 H
2000 FT.

0 1 2
RECORD VERTICAL SCALE
(INCHES)



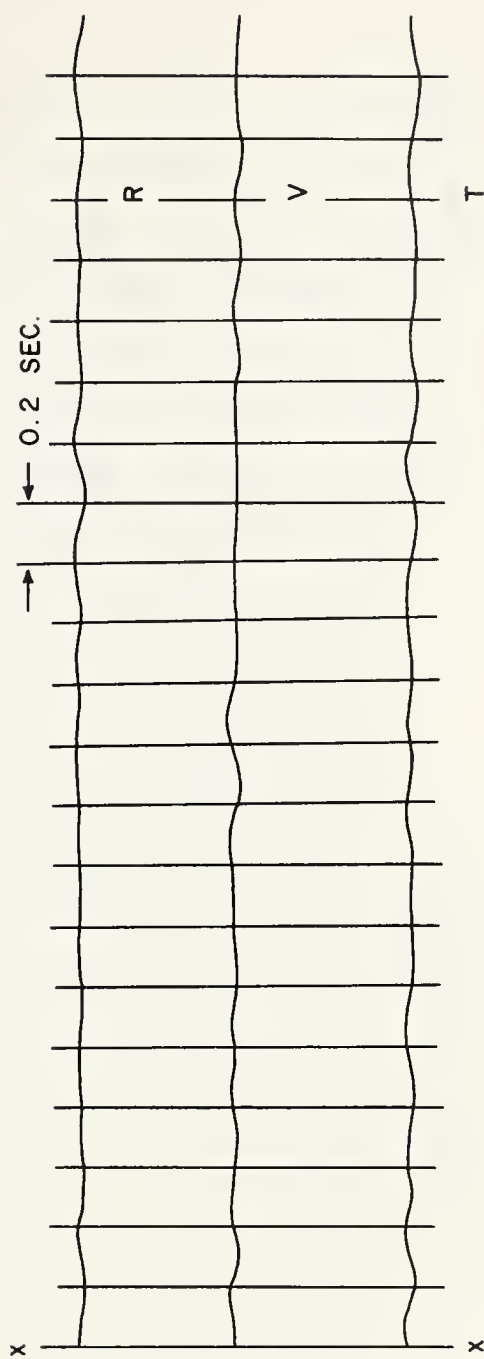
SEISMOGRAMS FROM
CYLINDRICAL 1000 LB. CHARGE BURIED 50 FT. — WATER TAMPED
WATCHING HILL SITE



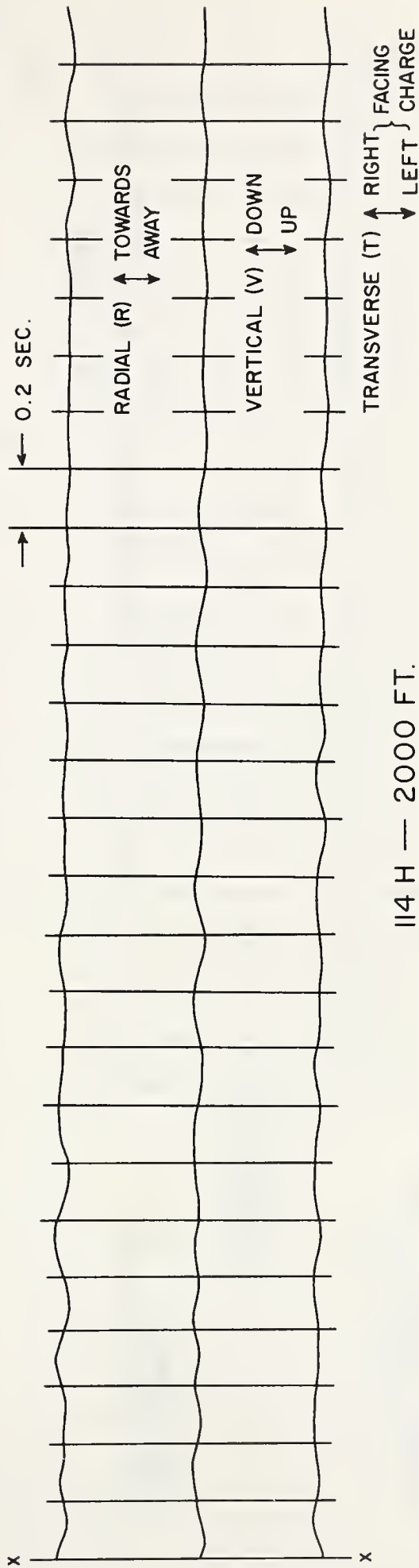
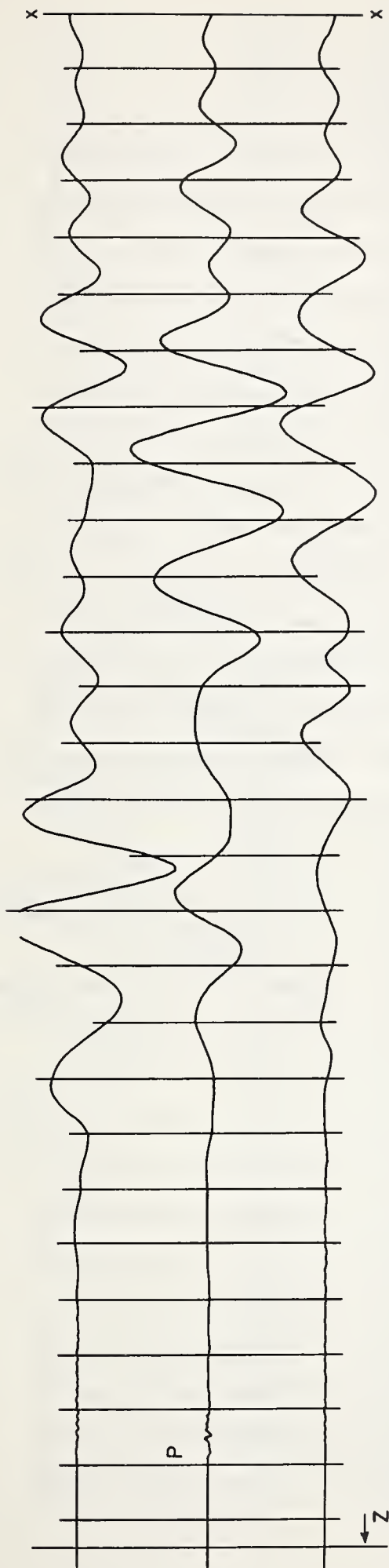
TIMING MARKS = 0.2 SEC.
HALF SCALE

113 H
2000 FT.

0 1 2
RECORD VERTICAL SCALE
(INCHES)



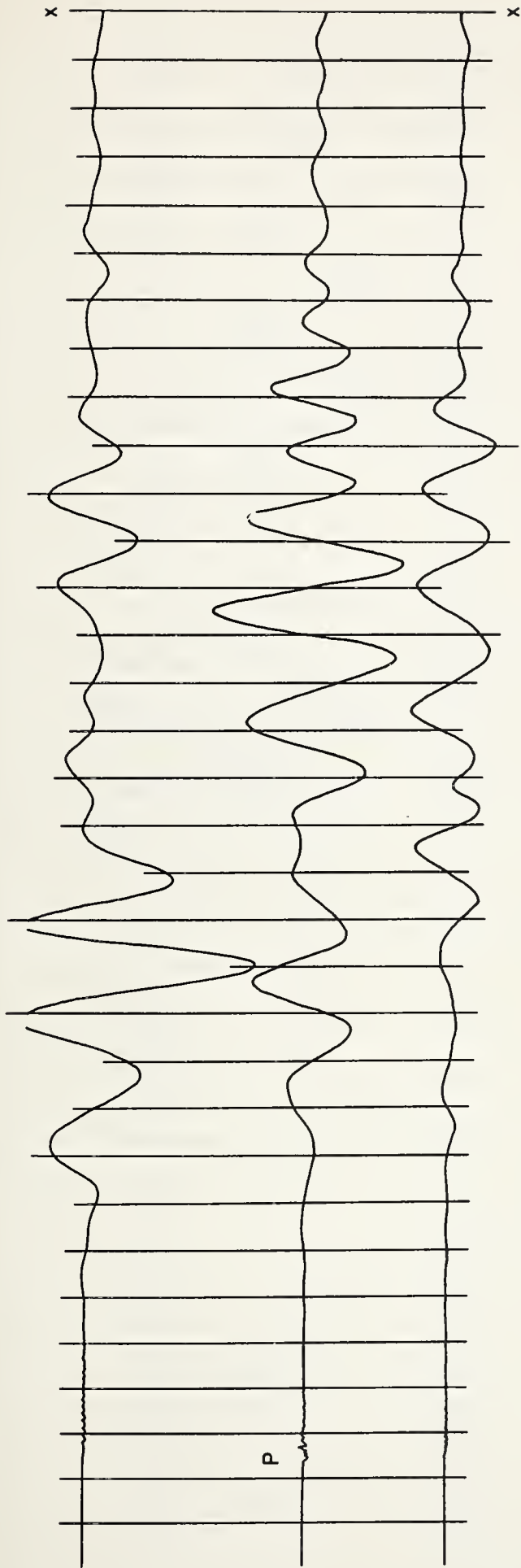
SEISMOGRAMS FROM
CYLINDRICAL 1000 LB. CHARGE BURIED 50 FT. — WATER TAMPED
WATCHING HILL SITE



TIMING MARKS = 0.2 SEC.
 Z = ZERO TIME
 HALF SCALE

0 1 2
 RECORD VERTICAL SCALE (INCHES)

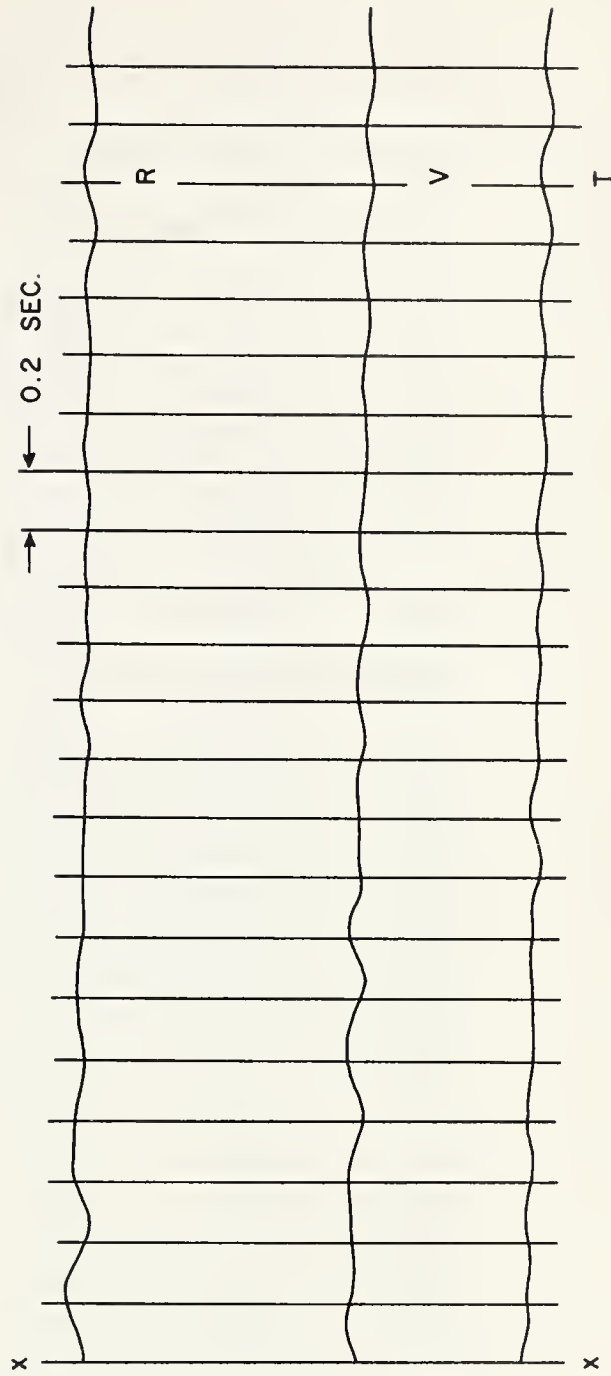
SEISMOGRAMS FROM
 CYLINDRICAL 1000 LB. CHARGE BURIED 50 FT. — WATER TAMPED
 WATCHING HILL SITE



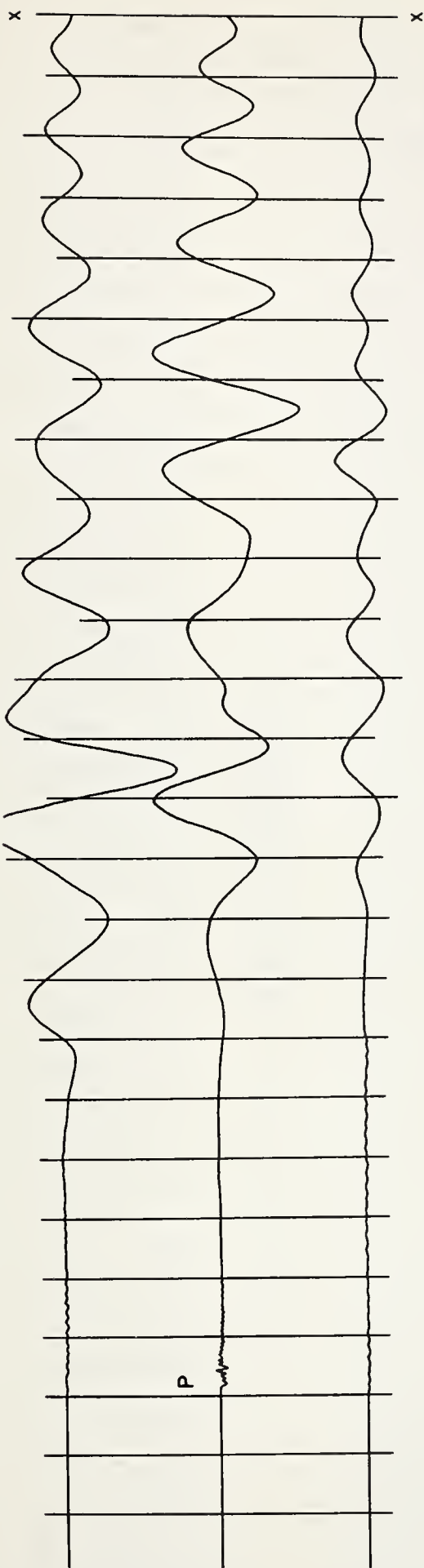
TIMING MARKS = 0.2 SEC.
HALF SCALE

115 H
2000 FT.

0 1 2
RECORD VERTICAL SCALE
(INCHES)



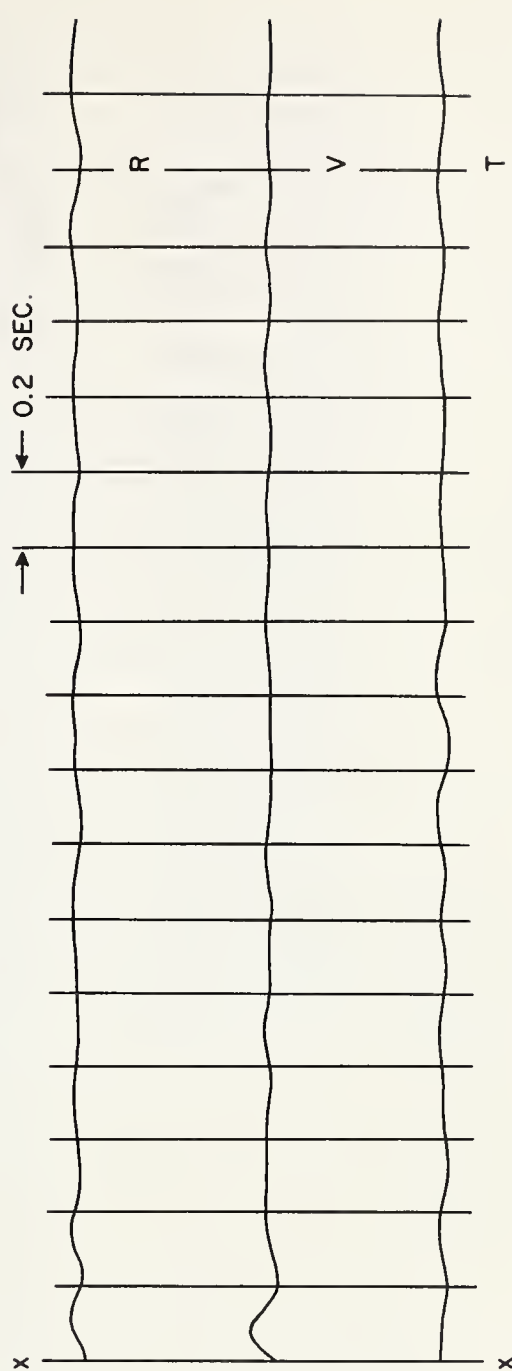
SEISMOGRAMS FROM
CYLINDRICAL 1000 LB. CHARGE BURIED 50 FT. — WATER TAMPED
WATCHING HILL SITE



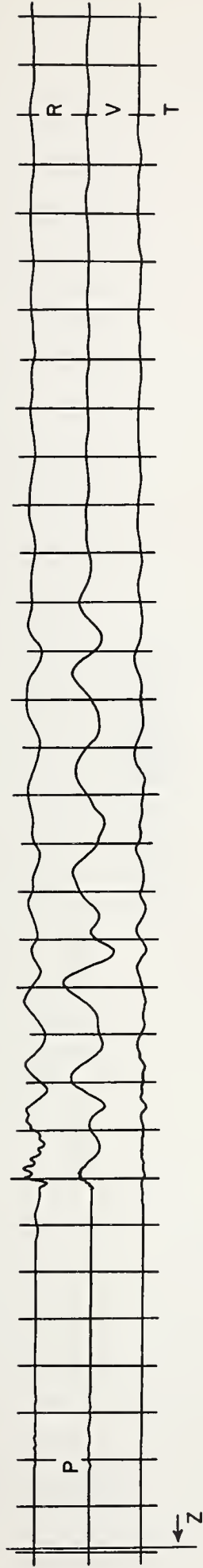
TIMING MARKS = 0.2 SEC.
HALF SCALE

116 H
2000 FT.

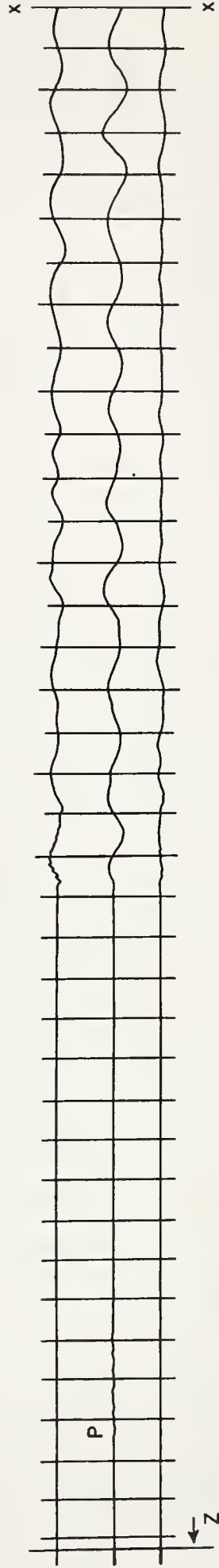
0 1 2
RECORD VERTICAL SCALE
(INCHES)



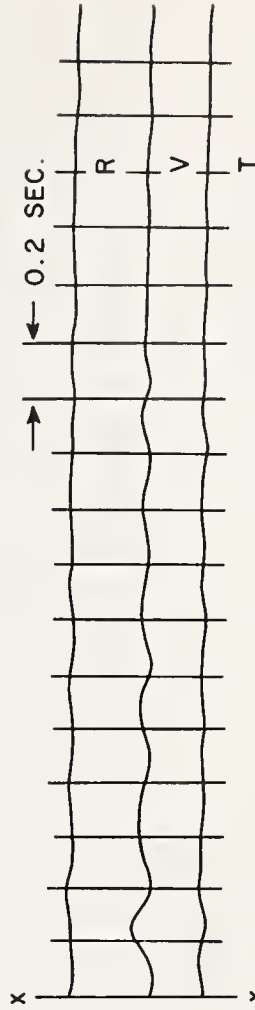
SEISMOGRAMS FROM
CYLINDRICAL 1000 LB. CHARGE BURIED 50 FT. — WATER TAMPED
WATCHING HILL SITE



122 H - 2000 FT.



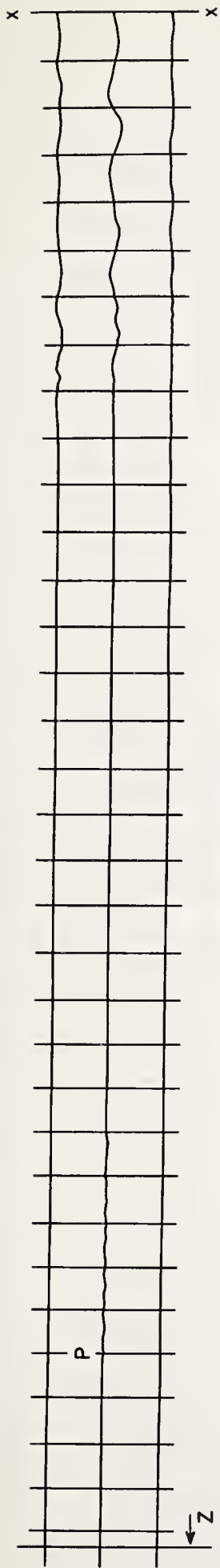
123 H - 4000 FT.



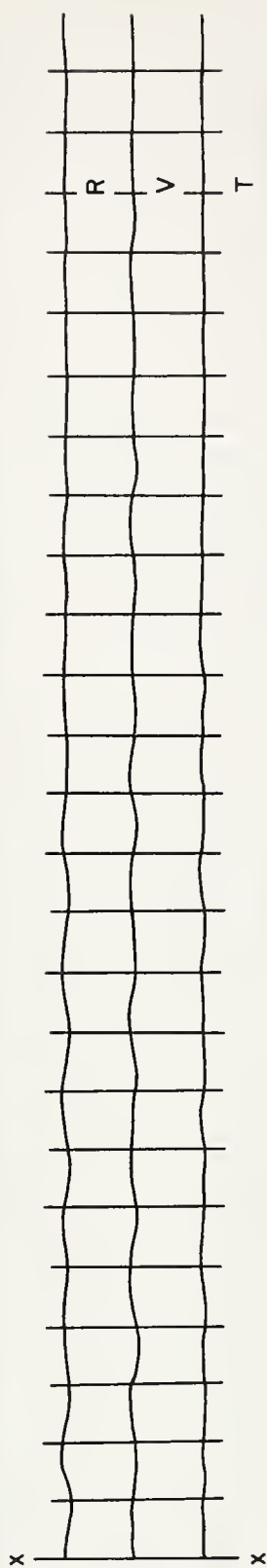
TIMING MARKS = 0.2 SEC.
Z = ZERO TIME
HALF SCALE

0 1 2
RECORD VERTICAL SCALE (INCHES)

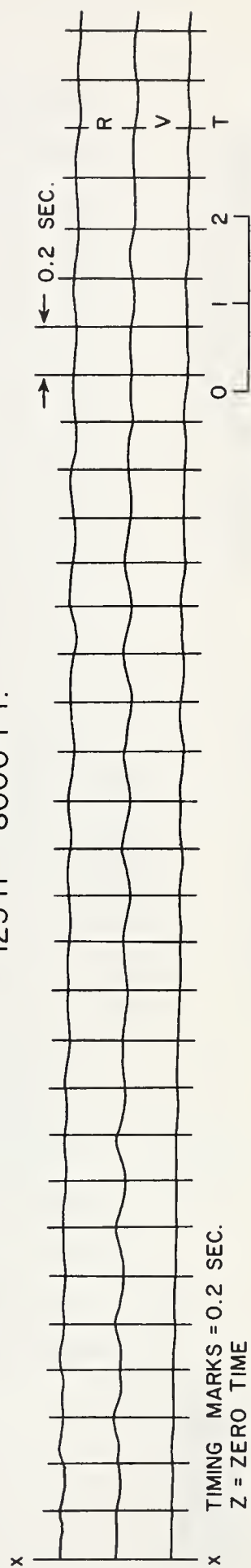
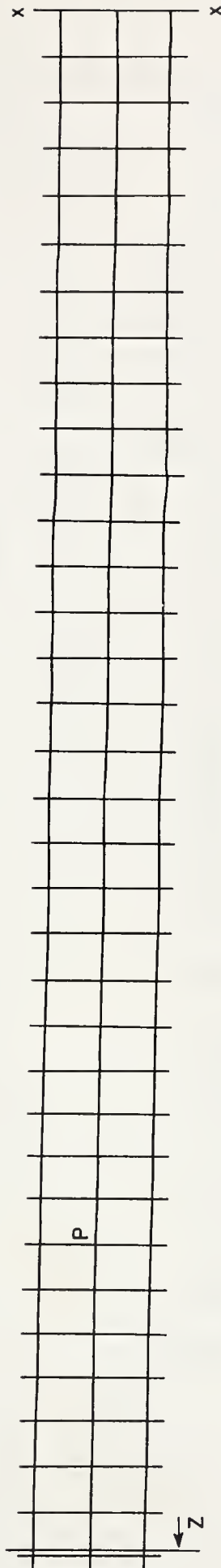
SEISMOGRAMS FROM
SPHERICAL 1000 LB. CHARGE ON SURFACE
WATCHING HILL SITE



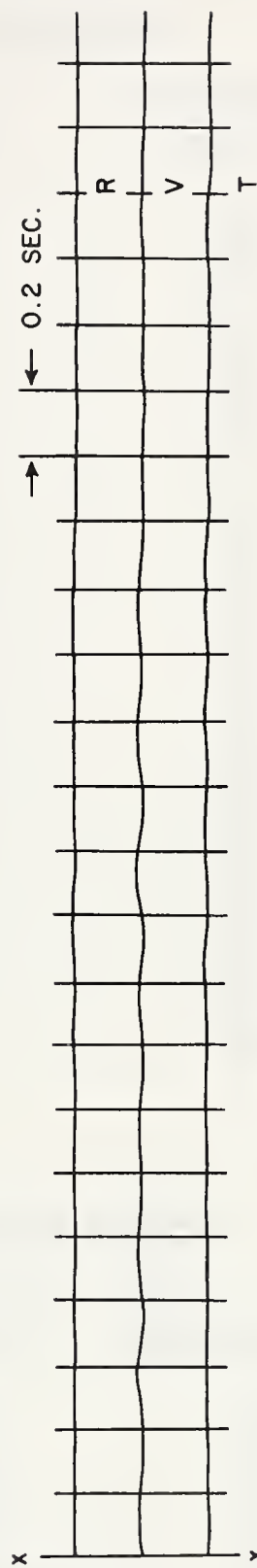
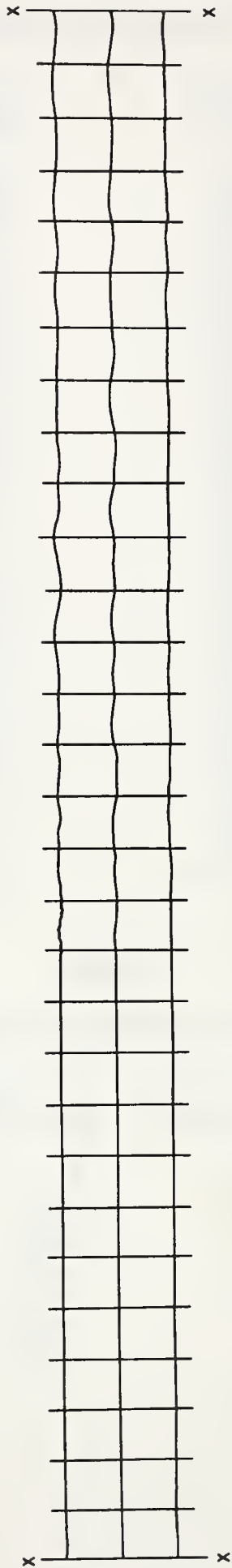
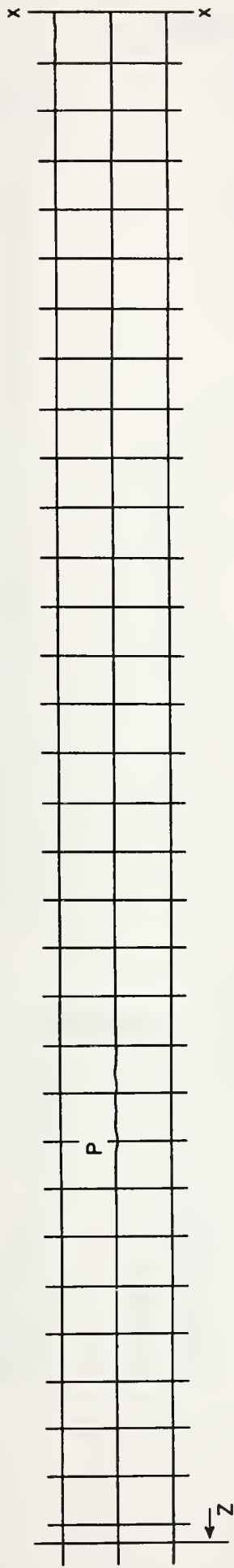
124 H - 6000 FT.



125 H - 8000 FT.



SEISMOGRAMS FROM
SPHERICAL 1000 LB. CHARGE ON SURFACE
WATCHING HILL SITE



126 H - 10,000 FT.

TIMING MARKS = 0.2 SEC.
Z = ZERO TIME
HALF SCALE

0 1 2

RECORD VERTICAL SCALE (INCHES)

SEISMOGRAMS FROM
SPHERICAL 1000 LB. CHARGE ON SURFACE
WATCHING HILL SITE

TABLE 1PREDICTED PRESSURE-DISTANCE DATA FOR 200,000 LB TNTSURFACE BURST AT THE WATCHING HILL SITE

<u>Distance</u> <u>(ft)</u>	<u>Pressure</u> <u>(psi)</u>	<u>Distance</u> <u>(ft)</u>	<u>Pressure</u> <u>(psi)</u>
200	98.549	8500	.254
300	37.302	9000	.239
400	19.784	9500	.226
500	12.524	10000	.214
600	8.819	10500	.203
700	6.661	11000	.193
800	5.283	11500	.184
900	4.342	12000	.176
1000	3.666	13000	.162
1250	2.608	14000	.150
1500	2.007	15000	.140
1750	1.624	16000	.131
2000	1.361	17000	.123
2500	1.024	18000	.116
3000	.820	19000	.109
3500	.682	20000	.104
4000	.584	22500	.092
4500	.511	25000	.082
5000	.454	27500	.075
5500	.408	30000	.068
6000	.370	40000	.051
6500	.339	50000	.041
7000	.313	75000	.027
7500	.290	100000	.020
8000	.271		

TABLE 2HOPKINSON'S LAW SCALING FACTORS FOR VARIOUS CHARGES

<u>Charge</u> <u>(lb)</u>	<u>Scale to</u> <u>1 lb</u>	<u>Scale to</u> <u>10,000 lb</u>	<u>10,000 lb scaled</u> <u>to Charge</u>	<u>100 ft for Charge</u> <u>scaled to 10,000 lb</u>
8	2.00	.0928	10.8	1080
30	3.107	.1442	6.93	693
60	3.936	.1818	5.50	550
500	7.938	.3684	2.71	271
10000	21.54	1.0	1.0	100
40000	34.20	1.587	.6299	63
200000	58.48	2.714	.38	38

TABLE 3

CLASSIFICATION OF SOIL SAMPLES FROM BORING AT GZ FOR 1961 100-TON TEST SHOT

<u>Sample No.</u>	<u>Depth (ft)</u>	<u>Group Symbol</u>	<u>Classification and Remarks</u>	<u>Water Content</u>
1	1	ML	tan clayey silt, soft	7.6
2	5	CL	tan silty clay, soft	11.2
3	7	CL	tan silty clay, med.	13.3
4	10	CL	tan silty clay, med.	14.4
5	12	CL	tan silty clay, med.	14.5
6	15	CH	gray clay, stiff	26.0
7	17	CL	gray clay, med.	23.9
8	20	CL	gray silty clay, med.	21.8
9	22	CL	gray clay, soft	34.4
10	25	CH	gray clay, med.	35.8
11	27	CH	gray clay, med.	33.4
12	30	CH	gray clay, soft	36.6
13	32	CL	gray silty clay, soft	34.1
14	35	CH	gray clay, med.	38.8
15	37	CH	gray clay, soft	37.3
16	40	CH	gray clay, soft	25.1
17	42	CH	gray clay, w/coarse sand (jar broken	
18	45	GC	gray gravel, sand, clay, mixed and soft	15.2
19	48.5	CH	gray clay, w/few small gravel, med.	27.0

Atterburg Limits

<u>Sample</u>	<u>LL</u>	<u>PL</u>	<u>PI</u>
2	36.2	18.0	18.2
4	48.0	20.1	27.9
7	47.6	20.7	26.9
10	51.4	22.1	29.3

TABLE 4

ACQUISITION DATA FOR SEISMOGRAMS

DRB Code	Thesis Code	Charge Wt (lb)	Distance from GZ (ft)	Wind Speed (mph)	Wind Direction (OT)	Temperature (OF)	Seismometer Bearing (OT)	Static Magnification		
								Radial	Vertical	Transverse
LT259										
-14	1D	8	217	15.8	150	68.3		↑	↑	↑
-15	2D	8	228	15.7	150	68.7		↑	↑	↑
-54	3D	8.5	50	4.5	15	73.2		↑	↑	↑
-55	4D	↑	75	5	20	73.5		↑	↑	↑
-56	5D	↑	100	3.5	Variable	69.4	355	48	52	47
-57	6D	↑	125	3	360	71		↑	↑	↑
-58	7D	8.5	150	2.5	290	69.4		↑	↑	↑
-59	8D	↑	200	3.5	360	68.9		↑	↑	↑
-60	9D	↑	250	2	360	69.5		↑	↑	↑
-61	10D	↑	300	6	290	72.1		↑	↑	↑
-46	11D	↑	100	-	-	-		↑	↑	↑
-45	12D	↑	150	5.7	350	75.3		↑	↑	↑
-47	13D	↑	200	5	360	75.9		↑	↑	↑
-48	14D	↑	250	2.5	20	75.3		↑	↑	↑
-49	15D	30	300	3.8	330	76	355	48	52	47
-50	16D	↑	400	7	350	67.9		↑	↑	↑
-51	17D	↑	500	7	50	69.8		↑	↑	↑
-52	18D	↑	600	4.5	25	70.5		↑	↑	↑
-53	19D	↑	700	4.5	20	71		↑	↑	↑

TABLE 4 (Cont'd)

DRB Code	Thesis Code	Charge Wt (lb)	Distance from GZ (ft)	Wind Speed (mph)	Wind Direction (°T)	Temperature (°F)	Seismometer Bearing (°T)	Static Magnification		
								Radial	Vertical	Transverse
LT259		↑					↑	↑	↑	↑
-34	20D		250	8.5	240	66.2		↑	↑	↑
-35	21D		400	8	265	67		↑	↑	↑
-3	22D		419	7.6	100	56.6		↑	↑	↑
-4	23D		450	4	110	59.1		↑	↑	↑
-5	24D	60	480	11.5	140	58.2	355	48	52	47
-6	25D		510	12	145	60.9		↑	↑	↑
-7	26D		541	11	140	61.1		↑	↑	↑
-8	27D		571	16.4	140	63.2		↑	↑	↑
-36	28D		600	2	245	69.4		↑	↑	↑
-37	29D		800	0	-	69		↑	↑	↑
LT273										
-4	30D	521	500	2.1	180	64.2	↑	↑	↑	↑
-3	31D	523	1095	15	210	71.7		↑	↑	↑
-1	32D	551	965	8	280	69.8	355	48	52	47
-2	33D	600	1030	7	270	69		↑	↑	↑
-6	34D	10,000	2000	-	-	-	172	48	52	47
FE522										
-3-1	35D	↑	2500	43	215	42	↑	48	52	47
-1-1	36D		3000	3	355	39.4		48	52	47
-2-1	37D	10,000	3500	11.3	260	41		48	52	47
-1-2	38D		4000	3	355	39.4		49	53	47
-2-2	39D	↓	4500	11.3	260	41	172	49	53	47

TABLE 4 (Cont'd)

DRB Code	Thesis Code	Charge Wt (lb)	Distance from GZ (ft)	Wind Speed (mph)	Wind Direction (°T)	Temperature (°F)	Seismometer Bearing (°T)	Static Magnification		
								Radial	Vertical	Transverse
FE522										
-1-3	40D	↑	5450	3	355	39.5	↑	47	53	48
-3-2	41D	10,000	6000	4.3	215	42	172	49	53	47
-3-3	42D		6500	4.3	215	42	↓	47	53	48
-2-3	43D		7000	11.3	260	41		47	53	48
FE521										
-1-1	44W	10,000	1000	6.6	105	51	197	48	52	47
-1-2	45W	10,000	3000	6.6	105	51	197	49	53	47
-1-3	46W	10,000	5000	6.6	105	51	197	47	53	48
FE536										
-1-1	47W	10,000	2000	1.5	230	32	293	48	52	47
-1-2	48W		2000	1.5	230	32	23	49	53	47
-1-3	49W		2000	1.5	230	32	113	47	53	48
-1-4	50W		2000	1.5	230	32	203	48	48	52
-1-5	51W		3000	1.5	230	32	203	48	51	51
-2-1	52W	10,000	2100	5.5	180	18.7	293	48	52	47
-2-2	53W		2000	5.5	180	18.7	338	49	53	47
-2-3	54W		2000	5.5	180	18.7	68	47	53	48
-2-4	55W		2000	5.5	180	18.7	158	48	48	52
-2-5	56W		2000	5.5	180	18.7	248	48	51	51
-3-2	57W		1974	7.6	265	28.3	293	48	52	47
-3-1	58W		2012	7.6	265	28.3	68	49	53	47

TABLE 4 (Cont'd)

DRB Code	Thesis Code	Charge Wt (lb)	Distance from GZ (ft)	Wind Speed (mph)	Wind Direction (°T)	Temperature (°F)	Seismometer Bearing (°T)	Static Magnification		
								Radial	Vertical	Transverse
FE535										
-1-1	59W	↑	3000	↑	↑	↑	↑	48	52	47
-1-2	60W		4000					49	53	47
-1-3	61W	40,000	5000	6.5	232	80	203	47	53	48
-1-4	62W	↓	7000	↓	↓	↓	↓	48	48	52
-1-5	63W		10000					48	51	51
FE538										
-K6	64W		2000	↑	↑	↑	↑	7.5	7.5	7.5
-S1	65W		4000					48	52	47
-S2	66W		6000					49	53	47
-S3	67W		7000				215.32.12	47	53	48
-S4	68W		10000				↓	48	48	52
-S5	69W	200,000	12000					48	51	51
-K4	70W	±200	15000	4	90			87	146	91
-K1	71W		7000				228.01.20	49	50	49
-K5	72W		12000				228.01.20	91	144	88
-K3	73W		15000				228.01.20	89	146	90
-K2	74W		7000				316.08.15	53	51	49
FE531										
75D		↑	3000				↑	48	49	52
76D			4000					49	53	49
77D		40,000	5000				225	49	53	49
78D		↓	6000				↓	50	52	50
79D			7000					52	50	51

TABLE 4 (Cont'd)

DRB Code	Thesis Code	Charge Wt (lb)	Distance from GZ (ft)	Wind Speed (mph)	Wind Direction (°T)	Temperature (°F)	Seismometer Bearing (°T)	Static Magnification		
								Radial	Vertical	Transverse
NTS 1										
	80N	40,000	3000					48	52	47
	81N	at	4000					49	53	47
	82N	80 ft	5000					47	53	48
NTS 2										
	83N	40,000	3000					48	52	47
	84N	at	4000					49	53	47
	85N	17.1 ft	5000					47	53	48
NTS 3										
	86N	40,000	3000					48	52	47
	87N	at	4000					49	53	47
	88N	34.2 ft	5000					47	53	48
LT285										
-1-1	89D		500					48	52	47
-1-2	90D	296	1000					49	53	47
-1-3	91D	at	2000					47	53	48
-1-4	92D	20 ft	3000					48	48	52
-1-5	93D		5000					48	51	51

TABLE 4 (Cont'd)

DRB Code	Thesis Code	Charge Wt (lb)	Distance from GZ (ft)	Wind Speed (mph)	Wind Direction (°T)	Temperature (°F)	Seismometer Bearing (°T)	Static Magnification	
								Radial	Vertical Transverse
FE549									
-4-1	94J	1000	1000	↑	↑	↑		48	49 52
-4-2	95J	sphere	2000					49	53 49
-4-3	96J	at	3000	3	150	76		49	53 49
-4-4	97J	23.5	4000	↓	↓	↓		50	52 50
-4-5	98J	ft	5000					52	50 51
FE549									
-1-1	99H	1000	-						
-1-2	100H	cylinder	4000					49	53 49
-1-3	101H	at	6000					49	53 49
-1-4	102H	50 ft	8000					50	52 50
-1-5	103H	soil tamped	10000					52	50 51
FE549									
-3-1	104H	1000						48	49 52
-3-2	105H	cylinder						49	53 49
-3-3	106H	at 50 ft	2000					49	53 49
-3-4	107H	soil						50	52 50
-3-5	108H	tamped						52	50 51
FE552									
-7-1	109H	1000						48	49 52
-7-2	110H	cylinder						49	53 49
-7-3	111H	at 50 ft	2000					49	53 49
-7-4	112H	water						50	52 50
-7-5	113H	tamped						52	50 51

No record obtained.

TABLE 4 (Cont'd)

DRB Code	Thesis Code	Charge Wt (lb)	Distance from GZ (ft)	Wind Speed (mph)	Wind Direction (°T)	Temperature (°F)	Seismometer Bearing (°T)	Static Magnification	
								Radial	Vertical Transverse
FE552									
-8-1	114H	1000						48	49 52
-8-2	115H	Cyl 50 ft						49	53 49
-8-3	116H	water tamp.	2000					49	53 49
BTL 5/62									
-1	117D		2000					48	49 52
-2	118D		4000					49	53 49
-3	119D	10,000	5000					49	53 49
-4	120D		6000					50	52 50
-5	121D		7000					52	50 51
FE549									
-2-1	122H		2000					48	49 52
-2-2	123H	1000	4000					49	53 49
-2-3	124H	sphere	6000					49	53 49
-2-4	125H		8000					50	52 50
-2-5	126H		10000					52	50 51
FE556									
-1	127D								
-2	128D								
-3	129D	40,000	4000	↑	↑	↑	178	48	49 52
-4	130D			4	270	79	155.5	49	53 49
-5	131D			↓	↓	↓	133	49	53 49
							110.5	50	52 50
							196	52	50 51

TABLE 5

AIRBLAST TRAVEL-TIME FROM SEISMOGRAMS

Code	Seismogram		Measured Time (sec)	Corrected to Zero Wind and 32°F	Scaled to 10,000 lb	Scaled Distance (ft)
	Wt (lb)	Dist. (ft)				
3D	8.5	50	.025	.0239	.2585	540
4D	"	75	.055	.0526	.5676	810
5D	"	100	.080	.0771	.8329	1080
6D	"	125	.105	.1007	1.0876	1350
7D	"	150	.130	.1251	1.3515	1620
10D	"	300	.255	.2444	2.640	3240
11D	30	100	.08	-	-	693
12D	"	150	.13	.1237	.8575	1039
13D	"	200	.145	.1382	.9578	1386
14D	"	250	.19	.1817	1.2590	1732
15D	"	300	.24	.2290	1.5869	2079
16D	"	400	.355	.3207	2.2222	2772
17D	"	500	.405	.3884	2.6917	3465
18D	"	600	.48	.4601	3.1887	4158
19D	"	700	.57	.5459	3.7836	4851
20D	60	250	.195	.1893	1.0412	1375
21D	"	400	.325	.3140	1.7270	2200
28D	"	600	.51	.4919	2.7057	3300
29D	"	800	.68	.6557	3.6066	4400
34D	10,000	2000	1.58	-	-	2000
35D	"	2500	2.16	2.1249	2.1249	2500
36D	"	3000	2.58	2.5755	2.5755	3000
37D	"	3500	3.065	3.0110	3.0110	3500
38D	"	4000	3.48	3.4473	3.4473	4000
39D	"	4500	4.00	3.9519	3.9519	4500
40D	"	5450	4.785	4.7628	4.7628	5450
41D	"	6000	5.52	5.4415	5.4415	6000
42D	"	6500	6.00	5.9146	5.9146	6500
43D	"	7000	6.38	6.324	6.324	7000
46W	"	5000	4.354	4.2646	4.2646	5000
52W	"	2100	1.755	1.7839	1.7839	2100
53W	"	2000	1.55	1.5805	1.5805	2000
56W	"	2000	1.66	1.6787	1.6787	2000
57W	"	1974	1.655	1.6476	1.6476	1974
59W	40,000	3000	2.43	2.3038	1.4350	1890
60W	"	4000	3.31	3.1329	1.9515	2520
62W	"	7000	5.95	5.6390	3.5125	4409

TABLE 6

DATA RELATING TO P WAVE AND EVENT A
(Vertical Component)

<u>Seismogram No.</u>	<u>Distance (ft)</u>	<u>P Wave Arrival (sec)</u>	<u>Period (sec)</u>	<u>Event "A"</u>
12D	150	.08		
13D	200	.085		
14D	250	.09		
15D	300	.12	.08	
16D	400	.13	.08	
17D	500	.14	.08	
18D	600	.16	.08	
19D	700	.205	.08	
20D	250	.11	.08?	
21D	400	.125	.085	
22D	419		.085	
23D	450		.08	
24D	480		.08	
25D	510		.09	
26D	541		.085	
27D	571		.095	
28D	600	.17	.085	
29D	800	.21	.085	
30D	500		.10	
31D	1095		.085	
32D	965		.08	
33D	1030		.08	
34D	2000	.33	.095	
35D	2500	.42	.10	1.26
36D	3000	.50	.095	1.56
37D	3500	.54	.10	1.58
38D	4000	.57	.105	1.8
39D	4500	.67	.10	1.89
40D	5450	.76	.11	2.2
41D	6000	.84	.105	3.14
42D	6500	.89	.105	3.24
43D	7000	.92	?	3.4
44W	1000		.75	
45W	3000		.10	
46W	5000	.70	.10	
47W	2000		.09	
48W		no wave recorded due to temporary fault.		
49W	2000		.08	
50W				
51W	3000		.09	
52W	2100	.35		
53W	2000	.33	.085	

TABLE 6 (Cont'd)DATA RELATING TO P WAVE AND EVENT A
(Vertical Component)

<u>Seismogram No.</u>	<u>Distance (ft)</u>	<u>P Wave Arrival (sec)</u>	<u>Period (sec)</u>	<u>Event "A"</u>
54W	2000		.04?	
55W	2000		.08	
56W	2000	.33		
57W	1974	.34	.065?	
58W	2012		.09	
59W	3000	.48	.08	
60W	4000	.58		
61W	5000		.04?	
62W	7000	.91	.12	
63W	1000		.15	

TABLE 7

AIRBLAST AND GROUND SHOCK ARRIVAL TIMES AT SHORT RANGES

F.E. 556 (40,000 lb)
1963

Air Blast				Ground Shock		
Switch No.	Dist. Feet	Diaphragm Type Time m.secs.	Piezo-Electric Type Time m.secs.	Ground Switch	Dist. (ft)	Time m.secs.
1	7.52		0.37			
2	10.28	0.47		1	10.06	x
3	11.98	0.58				
4	15.05	0.77		2	15.06	1.11
5	15.78	x				
6	17.97	0.99				
7	20.30	1.19		3	20.08	1.65
8	21.24		1.28			
9	25.18	1.62		4	25.08	x
10	27.23	1.84				
12	30.97	2.25				
13	33.96		2.48			
14	38.11		2.60?			
15	40.94	3.47		5	40.01	x
16	43.74	3.89		6	45.04	4.69
17	46.11	4.28				
18	48.74		4.69			
19	52.55	5.28				
21	57.22	6.07				
22	60.03	6.54				
23	64.38		7.33			
24	68.90	8.17		7	70.00	9.22
25	73.02	8.96		8	75.11	x
26	78.21		9.99			
27	82.01	10.79				
29	90.94	12.69				
30	95.93	13.74				
31	99.94		x	9	100.00	x
32	105.25	15.93		10	105.20	17.80
34	118.03	19.27				
35	123.02	20.78				
37	137.90	25.75				
38	145.88	28.88				
39	150.52	30.75		11	150.00	35.06
40	154.94	32.55		12	155.06	37.14

TABLE 7 (Cont'd)

Air Blast				Ground Shock		
Switch No.	Dist. Feet	Diaphragm Piezo-Electric		Ground Switch	Dist. (ft)	Time m.secs.
		Type Time m.secs.	Type Time m.secs.			
41	157.18	33.48				
42	160.27	34.84				
43	173.04	40.68				
44	185.14	46.61				
45	192.02	50.69				
46	199.91	54.42				
47	209.91	60.00				
48	220.11	65.90				
49	229.84	71.70				
50	240.15	77.78		13	250.00	86.48
51	264.04	92.45		14	255.07	89.90
52	275.23	99.51				
53	282.77	104.36				
54	290.00	109.06				
55	303.24	117.86				
56	389.96	178.91		15	400.00	192.62
57	414.76	201.26		16	405.00	194.96
58	459.80	248.56				
59	523.05	280.01		17	600.00	348.91
60	675.17	401.21		18	605.06	x
61	719.94	437.61				
62	899.71	585.81		19	900.00	594.76
63	974.85	662.64		20	904.00	x
64	1049.96	703.46				
65	1169.81	812.60				
66	1279.59	906.21				
67	1389.70	1000.21		21	1400.00	1011.56
68	1499.81	1092.00		22	1405.52	x
69	1629.81	1230.00				
70	1759.44	1317.26				
71	1869.57	1417.56				
72	2049.41	1568.56				
73	2219.57	1716.56				
74	2399.42	1871.56				
75	2749.23	2267.56				
78	4299.02	3605.56				

BIBLIOGRAPHY

(a) Papers and Reports by the Writer and his Immediate Associates

- | | | |
|--|-------|--|
| Jones, G.H.S. | 1958 | "The Use of Models in the Study of the Blast Effects of Simulated Nuclear Weapons",
Suffield Technical Paper 132. |
| | 1960 | "Introductory Paper with Notes on Five-ton Surface Burst Charges",
Suffield Technical Paper 180. |
| | 1961 | "Geophysical Aspects of the Suffield Explosions",
Canadian Geophysical Bull. <u>V</u> , 14,
pp 127-147.
(also as Suffield Special Publication 14/61). |
| | 1962a | "Some Comments on Cratering",
Suffield Special Publication 22. |
| | 1962b | "Transverse Motion from Repeated Explosions",
Jour. Geophys. Res. <u>V</u> , 67, No. 7
pp 2994-2997. |
| | 1962c | "Experimental Evidence of the Coupling of Rayleigh and Love Events",
Earthquake Notes <u>V</u> , 23 No. 4,
pp 55-70. |
| | 1963 | "On the Identification of Phases in the Surface Waves from Explosions",
Presented at I.U.G.G. meetings,
Berkeley, California. |
| Jones and Krohn, J. | 1960a | "Permanent and Transient Displacements due to Five-Ton Surface Bursts",
Suffield Technical Paper 178. |
| | 1960b | "Ground Displacement Near the Detonation of a 40,000 lb Charge",
Suffield Technical Paper 213. |
| Jones, Krohn, J. and
Dewey, John M. | 1962 | "Ground Displacement from the 200,000 lb Charge, With Notes on Scaling",
Suffield Technical Paper 250. |

- | | | |
|--|------|--|
| Jones, G.H.S., Kisslinger, C.
and Cyganik, S.A. | 1961 | "Seismograms From the Strong
Motion Region Near a 200,000 lb
Detonation",
Suffield Trial Record 435. |
| Jones, G.H.S., Maureau, G.
and Cyganik, S.A. | 1963 | "Airblast Coupling to Prograde
and Retrograde Surface Waves",
Jour. Geophys. Res. <u>V</u> , 68, (Sept). |
| Jones, G.H.S., Reiniger, R.
and Cyganik, S.A. | 1962 | "The Surface Wave Preceding the
Arrival of the Airblast From Multi-
ton Charges",
Suffield Technical Paper 229. |
| Jones, G.H.S., Spackman, N.
and Winfield, F.H. | 1959 | "Cratering by Ground Burst TNT
Charges at SES",
Suffield Technical Paper 158. |
| Jones, G.H.S. and Winfield, F.H. | 1960 | "Close-in Seismic Effects of
Operation Stagecoach",
Suffield Trial Record 431. |

(b) General

- | | | |
|---|------|--|
| Anderson, E.A. and
Henriksen, N. | 1962 | "Nogle Målinger af Jordrystelser
fra Sprængninger",
Danish Defence Research Board
Report CHA 1862. |
| Anderson, J.R. and
Nestler, D.E. | 1962 | "Shock Wave Propagation in Solids",
Literature Survey, Project Frank,
University of Pennsylvania. |
| Anderson, L.D. | 1962 | "Love Wave Dispersion in Hetero-
geneous Anisotropic Media",
Geophysics <u>V</u> , 27, No. 4, p. 445. |
| A.I.D.
(Library of Congress
Air Information Div.) | 1961 | "Preliminary Bibliography of
Soviet Seismology and Seismometry",
A.I.D. Report 61-135. |
| | | |
| Barton, M.V. | 1960 | "Ground Shock Spectrum Measurements
on the 20 Ton HE Tests at SES",
Space Tech. Labs. TR 60PDol 19245. |
| Bartunek P.F. and Igel, E.U. | 1955 | "Preliminary Report on the Problem
of Seismic Sensing",
Colorado Sc. of Mines Res. Found.
Proj. 541216. |
| Bateman, H. | 1938 | "Rayleigh Waves"
Proc. Nat. Acad. of Sci. USA
<u>V</u> 24 pp 315-320. |
| Beare, H.T. | 1962 | "Surface Burst 100 Ton TNT Charge:
Trench Wall Failure",
Suffield Technical Paper 225. |
| Benioff, H., Ewing M.
and Press, F. | 1951 | "Sound Waves in the Atmosphere
Generated by a Small Earthquake",
Proc. Nat. Acad. of Sci. USA <u>V</u> . 37
pp 600-603. |
| Bethe, H.A., Fuchs K.
Hirschfelder, J.O., Magee
J.L. Peierls, R.E. and von
Neumann, J. | 1951 | "Blast Wave",
Los Alamos Sc. Lab. Rep. LA-2000
TID 4500 13th Ed. Suppl. |
| Brillouin, L. | 1960 | "Wave Propagation and Group Velo-
city", Academic Press. |

- | | | |
|---|------|---|
| Century | 1961 | "Report on Survey",
Century Geophysical Corp. of
Canada,
(Report held in Library, SES). |
| Cole, J.D. and Huth, J.H. | 1958 | "Stresses Produced in a Halfplane
by Moving Loads",
Jour. App. Mech. Vol. 25, Trans.
ASME, Vol. 80. |
| Common, R. | 1962 | "The Geomorphology of the Medicine
Hat Area",
Geophys. Bull. No. 18, pp 86-107,
Ottawa. |
| Coon, J.H., Houghton, H.M.
and Nobles, N. | 1945 | "100 Ton Test at Trinity - Report
on Earth Velocity Measurements",
AECD 2841 Los Alamos Sci. Labs. |
| Davies, R.M. | 1953 | "Stress Waves in Solids",
App. Mech. Revs. <u>V</u> 6, No. 1,
pp 1-3. |
| Dewey, John M. | 1961 | "The Measurement of Air Velocity
in a Blast Wave",
Suffield Technical Paper 199. |
| | 1962 | "Air Velocity Measurements in the
Blast Wave From a Surface Burst
100 Ton Hemispherical Charge",
Suffield Technical Paper 251. |
| Dix, C.H. | 1955 | "The Mechanics of Generation of
Long Waves from Explosions",
Geophys. <u>V</u> 20, No. pp 87-103. |
| Dobbie C.B. and Hamilton, S.R. | 1963 | "Electromagnetic Measurements
on Canadian 100 Ton TNT Explosion,
E.G. and G. Report No. B-2572,
ASTIA No. AD RADG-TDR-63-193. |
| Dobrin, M.B., Simon, R.F.
and Lawrence, P.L. | 1951 | "Rayleigh Waves from Small Explosions",
Trans. A.G.U., <u>V</u> 32 No. 6, pp 822-832. |
| Dobrin, Lawrence, P.L.
and Sengbush, R. | 1954 | "Surface and Near Surface Waves in the
Delaware Basin",
Geophysics <u>V</u> 21, No. 4, pp 695-715. |

- Duvall, W.I. 1960 "Design Criteria for Portable Seismographs",
Earthquake Notes V, 31, No. 3.
- Ewing, W.M., Jardetsky, W.S. 1957 "Elastic Waves in Layered Media",
and Press, F. McGraw-Hill, New York.
EJP...abbreviation used for above in text.
- Frantti, G.E. 1963 See page 90.
- Friedlander, F.G. 1946 "The Diffraction of Sound Pulses.
1. The Diffraction by a Semi-
infinite Plate",
P.R.S.A. V 186.
- Friedman, M.P. 1960 "A Simplified Description of
Spherical and Cylindrical Blast
Waves",
NYO-9352 TID 4500, New York
University.
- Groves, T.K. 1960 "A Photo-optical System for
Recording Shock Profiles from
Chemical Explosions",
Suffield Technical Paper 192.
- 1962 "Surface Burst 100 Ton TNT
Charge: Free Field Air Blast
Overpressure",
Suffield Technical Paper 269.
- 1963a "Summary Report on Air Blast
from 60 Ground Burst Charges
in the Range 8 lb to 60 lb TNT.
(in prep.)
- 1963b "Air Blast Triple Point Locus
from TNT Spheres Exploded Over
a Plane Concrete Surface".
(in prep.)
- 1963c "Mach Waves Air Blast Pressure
from TNT Spheres Detonated Over
Concrete". (in prep.)
- Halsey, J.F. and Barton, M.V. 1961 "Ground Shock Spectrum Measure-
ments, 100 Ton HE Test",
Space Tech. Labs. 6120-0039-RV000.

- | | | |
|---|-------|--|
| Harkrider, D.G. and
Anderson, D.L. | 1962 | "Computation of Surface Wave Dispersion for Multi-layer Anisotropic Media",
Bull. Seis. Soc. Amer. <u>V</u> 52
No. 2, p 321. |
| Harvey, R.B. | 1957 | "A Photo-optical Method for the Measurement of Free Airshock Overpressure",
Suffield Technical Paper 122. |
| Haskell, N.A. | 1951 | "A Note on Air-coupled Surface Waves",
Bull. Seis. Soc. Amer. <u>V</u> 41,
No. 4, pp 295-300. |
| Hastrup, O. | 1963a | "Numerical Calculation of the Fourier Integral",
Suffield Technical Note 121. |
| | 1963b | "Surface Waves from 1000 lb TNT Buried at 23.5 Ft",
Suffield Technical Paper 290. |
| Horton, C.W. | 1953 | "On the Propagation of Rayleigh Waves on the Surface of a Visco-elastic Solid",
Geophysics <u>V</u> 18, pp 70-74. |
| Howell, B.F. | 1949 | "Ground Vibrations Near Explosions",
Bull. Seis. Soc. Amer. <u>V</u> 39, p.285. |
| Howell, L.G., Neuenschwander,
E.F. and Pierson, A.L. | 1953 | "Gulf Coast Surface Waves",
Geophysics <u>V</u> 18, pp 41-53. |
| Hubbert, M.K. | 1937 | "Theory of Scale Models as Applied to the Study of Geologic Structures",
Bull. Geol. Soc. Amer. <u>V</u> 48,
pp 1459-1520. |
| Jardetsky, W.S. and Press, F. | 1952 | "Rayleigh Wave Coupling to Atmospheric Compression Waves",
Bull. Seis. Soc. Amer. <u>V</u> 42,
pp 135-144. |
| Johnson, O. | 1962 | "100 Ton Surface Burst Charge: Meteorological Aspects",
Suffield Technical Note 83. |

- | | | |
|--|-------|--|
| Johnson, O, Clink, W.L.
and Gilbert, G.H. | 1962 | "The Prediction of Anomalous Blast Areas for the 100 Ton Suffield Explosion",
Jour. App. Meteorology, <u>V</u> 4,
pp 537-543. |
| Katz, A.Z. and Puchkov, S.V. | 1955 | "Concerning the Effects of Seismic Waves on Structures",
Trudy Geof. Inst. Aka. Nauk SSSR No. 30 (157) pp 226-239. |
| Katz, S. and Woerber, A.F. | 1960a | "Propagation of Plane Waves in Granular Materials" Part 1. |
| | 1960b | Part 2,
Rensselaer Polytech. Institute Reports 1 and 2. |
| Keller, J.B. and Karal, F.C. | 1960 | "Surface Wave Excitation and Propagation",
Jour. Appli. Physics <u>V</u> 31, No. 6,
pp 1039-1046. |
| Kempster, D.J. | 1962 | "Surface Burst 100 Ton Charge: Crater and Ejecta Deposit Measurements",
Suffield Technical Note No. 85. |
| Kisslinger, C. | 1959 | "Observations of the Development of Rayleigh-type Waves in the Vicinity of Small Explosions",
Jour. Geophys. Res., <u>V</u> 64, No. 4,
pp 429-436. |
| | 1960 | "Motion at an Explosive Source as Deduced by Surface Waves", Earthquake Notes V. 31 p. 5 - 17. |
| | 1961a | "Ground Motion from 100 Ton HE Shot at Short Ranges"
Presented at Annual Meeting Eastern Section, Seis. Soc. Amer. |
| | 1961b | Semi-annual Tech. Report No. 1. |
| | 1962 | Semi-annual Tech. Report No. 2
"Seismic Waves Generated by Chemical Explosions",
Contract AF 19(604)-7402, Saint Louis University. |

- Kisslinger, C., Mateker, E.J. 1961 "SH Motion from Explosions in Soil",
and McEvelly, T.V. Jour. Geophys. Res. V 66 pp 3487-3496.
- Kogan, Pasechnik, I.P. and 1959 "The Difference in the Periods of
Sultanov, D.D. Seismic Waves Excited by Underground
Explosions and Earthquakes",
Dok. Akad. Nauk, 1299.
- 1960 "Seismic Effects of Underground
Explosions",
Trans. O. Yu. Schmidt Inst. of
Geophys. No. 15 (182) (authorized
translation).
- Kuo, J.T.F. 1958 "Theoretical and Experimental Study
of Seismic Surface Waves",
Ph.D. Dissertation, Stanford Univ.
- Lamb, H. 1904 "On the Propagation of Tremors Over
the Surface of an Elastic Solid",
Phil. Trans. Roy. Soc. A 203, 1-42.
- 1916a "On Waves Due to a Travelling Dis-
turbance With an Application to
Waves in Superposed Fluids",
Phil. Mag. and Jour. of Sci. V 30,
pp 386-398.
- 1916b "On Wave Patterns Due to a Travelling
Disturbance",
Phil. Mag. and Jour. of Sci. V 30,
pp 539-548.
- 1932 "Hydrodynamics"
(1945) First Amer. Edition, Dover Press.
- Leet, L.D. 1939 "Ground Vibrations Near Dynamite
Blasts",
Bull. Seis. Soc. Amer, V 29,
pp 487-496.
- 1944 "Earth Motion From an Atomic Bomb
Test", Amer. Scientist, V 34, 198-211.
- 1945a "100 Ton Test: Ground Vibrations"
Los Alamos Sci. Lab. ARCD 2840.
- 1945b "Ground Vibrations from Trinity Test",
Los Alamos Sci. Lab. AECD 2844.

- | | | |
|----------------------------------|-------|---|
| Leet, L.D. (cont'd) | 1950 | "Earth Waves",
Harvard Univ. Press (and Wiley and Son). |
| | 1960 | "Vibrations From Blasting Rocks",
Harvard Univ. Press. |
| | 1962 | "The Detection of Underground Ex-
plosions",
Scientific American, <u>V</u> 206, No. 6,
pp 55-59. |
| Mair, J.A. | 1960 | "Feasibility Study of Future Upper
Atmospheric Research by Distant
Airblast Measurements",
Imperial Oil Report to C.S.E.G.,
Calgary. |
| McLean, W.D. and
Caless, T.W. | 1961 | "A Bibliography of Seismology for
the Vela Uniform Programme",
Acoustics and Seis. Lab. Rep.
4410-10-B, The Univ. of Michigan. |
| Mitalas, R. and Harvey, R.B. | 1958 | "Peak Pressures from Distance-Time
Data of an Expanding Spherical Shock",
Suffield Technical Paper 130. |
| Mikowitz, J. | 1960 | "Recent Developments in Elastic Wave
Propagation",
App. Mech. Revs. <u>V</u> 13, No. 12,
pp 865-878. |
| Miles, J.W. | 1960 | "On the Response of an Elastic
Half-Space to a Moving Blast Wave",
ASME <u>V</u> 27, Series E pp 710-716.
(and Space Tech. Lab. GM-TR-0165-00524). |
| Nagamune, T. | 1956 | "M2 Waves in a Medium With Double Sur-
face Layers",
Geophys. Mag. Tokyo <u>V</u> 27, pp 345-352. |
| Nestler | ND | See Anderson and Nestler. |
| Parkin, B.R. | 1958 | "A Review of Similitude Theory in
Ground Shock Problems",
Rand. Res. Memo RM 2173. |
| Pekeris, C.L. | 1955a | "The Seismic Surface Pulse",
Proc. Nat. Acad. Science, USA <u>V</u> 41,
pp 469-480. |

(x)

- Pekeris, C.L. (cont'd) 1955b "The Seismic Buried Pulse",
Ibid pp 629-639.
- 1959 "Propagation of Seismic Pulses
in Layered Liquids and Solids",
Int. Symp. on Stress Propagation
in Materials (Ed. N. David).
- Penney, W.G. and Reines, F. 1945 "100 Ton Test: Permanent Earth
Movements: Earth and Air Shocks",
Los Alamos Sc. Lab. AECD 2842.
- Pennie, A.M., Philips, A.C. and 1960 "The Preparation of Large Spheri-
Holdsworth, J. cal Charges of TNT",
Suffield Technical Paper 190.
- Philips, A.C., Ditto, J. and 1960 "The Building of Hemispheres of
Holdsworth, J. HE from Cast Blocks",
Suffield Technical Paper 194.
- Press, F. 1963 "Statement Before the Joint
Committee on Atomic Energy",
5-7 March, 1963.
- Press, F. and Dobrin, M.B. 1956 "Seismic Studies Over a Surface
Layer",
Geophysics V 21, No. 2 pp 285-298.
- Press, F., Crary, A.P., Oliver, J. 1951 "Air Coupled Flexural Waves in
and Katz, S. Floating Ice",
Trans. A.G.U. V 32, No. 2,
pp 166-172.
- Press F. and Archimbeau, C. 1962 "Release of Tectonic Strain by
Underground Nuclear Explosions",
Jour. Geophys. Res. V 67, No. 1,
pp 337-343.
- Press, F. and Ewing, M. 1951a "Ground Roll Coupling to Atmospheric
Compression Waves",
Geophysics V 16, pp 416-430.
- 1951b "Propagation of Elastic Waves in a
Floating Ice Sheet",
Trans. A.G.U. V 32, No. 5, pp 673-
678.
- 1951c "Theory of Air-coupled Flexural
Waves",
Jour. App. Physics, V 22 pp 892-899.

- | | | |
|---------------------------|-------|---|
| Rayleigh, Lord | 1885 | "On Waves Propagated Along the Plane Surface of an Elastic Solid", Proc. Lond. Math. Soc. <u>V</u> 17 pp 4-11. |
| | 1900 | "Scientific Papers", Cambridge University Press p 447. |
| Richter, C.F. | 1958 | "Elementary Seismology", W.H. Freeman Co., San Francisco. |
| Russel, L. and Landes, R. | 1940 | "Geology of the Southern Prairie Plains", Geological Survey Memoir 221 Canada. |
| Satô, Y. | 1955a | "Analysis of Dispersed Surface Waves by Means of Fourier Transforms, Pt.1", Bull. Earth. Res. Inst., Tokyo <u>V</u> 23, pp 32-48. |
| | 1955b | Pt. 2 Loc. Cit. <u>V</u> 24, pp 9-18. |
| | 1955c | Pt. 3 Loc. Cit. <u>V</u> 24, pp 131-138 (listed on P7 as '1956'). |
| | 1959 | "Analysis of Dispersed Surface Waves", Int. Symp. on Stress Wave Propagation in Materials (Ed. N. David). |
| SES | 1960 | "Preliminary Observations on the Detonation of 20 Tons of TNT", Suffield Experimental Station. |
| | 1962 | "Surface Burst 100 Ton TNT Hemispherical Charge (1961)", Suffield Report No. 205. |
| Sezawa, K. and Kanai, K. | 1935a | "Discontinuity in the Dispersion Curve of Rayleigh Waves", Bull. of the Earth. Res. Inst. Tokyo <u>V</u> 13, p 238. |
| | 1935 | "The M2 Seismic Wave", Bull. Earth. Res. Inst. Tokyo <u>V</u> 13, p 471. |
| | 1939 | "Dispersive Rayleigh Waves of Positive and Negative Orbital Motion and Allied Problems", Bull. Earth. Res. Inst. Tokyo <u>V</u> 18, pp 1-9. |

- | | | |
|--|------|--|
| Sneddon, I.N. | 1951 | "Fourier Transforms",
McGraw-Hill Book Co. |
| Stalker, A.M. | 1961 | "Buried Valleys in Central and
Southern Alberta",
Paper 60-32, report and map 47-
1960, Geological Survey of
Canada. |
| Stoker, J.J. | 1956 | "Water Waves",
Interscience publishers, N.Y. |
| Stoneley, R. | 1924 | "Elastic Waves at the Surface
of Separation of Two Solids",
P.R.S.A. <u>V</u> 106, pp 416-428. |
| Taylor, G.I. | 1940 | "Propagation of Earth Waves from
an Explosion",
Min. of Home Sec. Def. Res. Comm.
Memo RC 70 (UK). |
| Tolstoy, I. and Usdin, E. | 1953 | "Dispersive Properties of Strati-
fied Elastic and Liquid Media:
A Ray Theory",
Geophysics <u>V</u> 18 pp 844-871. |
| Vesso, J.J., Winfield, F.H.
and Sanders, B.R. | 1963 | "Modifications to the Sprengnether
Seismographs",
Suffield Technical Note 42 (in prep). |
| Vesiac | ND | Vela Uniform Periodic Information
Digest, The University of Michigan,
Box 618, Ann Arbor, Mich. |
| Wilson, J.T. and Caless, T.W. | 1963 | "Project Vela Uniform and
Seismology",
Trans. Amer. Geoph. Union <u>V</u> 44,
No. 2, pp 337-339. |
| Williams, M.Y. and Dyer, W.S. | 1930 | "Geology of Southern Alberta and
South-Western Saskatchewan",
Geological Survey Memoir 163
(Canada). |

Winfield, F.H.

1962 "Surface Burst 100 Ton: Field
Installation of Instrumentation
for the Physics and Meteorology
Section",
Suffield Technical Note 87.

APPENDIX A

FORMAL MATHEMATICAL THEORY OF AIR COUPLING

A1 Original Concept of 'Air-coupled Wave'

It would appear that the study of air-coupled waves was introduced by Bateman (1938) who described an oscillation of the surface of a semi-infinite medium due to the effect of a sound wave in the air above the medium. Bateman's approach was essentially as given below, though the notation and one or two of the steps in the derivation are somewhat different. Bateman's original formulation is not too easy to follow, due to his introduction of many abbreviating terms. In addition, Bateman's development included the effect of a surface wind and went on to discuss the focussing effects of wind-shear. Thus he compounds two problems which are normally considered as quite distinct effects in his discussion of the 'air-coupled wave'. Bateman's solution is two-dimensional, but may be converted to the case of axial symmetry. The axially symmetric case, however, is an added complication without throwing much additional light on the problem. We treat a semi-infinite half space in association with a semi-infinite atmosphere, the plane of separation being the plane $z = 0$. Let C be the velocity of sound in the air (treated as a constant velocity) and let ρ_0 and ϕ_0 be the density and a velocity potential in the air. The other medium is characterized by densities, displacement potentials and elastic constants in the usual notation. We wish to investigate the effect on the plane boundary of the lower half space of a small disturbance in the air.

We may write a small irrotational disturbance in the air as satisfying:

$$\frac{\partial^2 \phi_0}{\partial x^2} + \frac{\partial^2 \phi_0}{\partial z^2} = \frac{1}{c^2} \frac{\partial^2 \phi_0}{\partial t^2}$$

(Note - This, of course, removes us immediately from the case of the supersonic blast wave).

We now look for solutions of the type $\phi_0 = f(z)e^{ik(x - vt)}$

$$i^2 k^2 f(z) e^{ik(x - vt)} + \frac{d^2 f(z)}{dz^2} e^{ik(x - vt)} = \frac{1}{c^2} f(z) v^2 c^2 k^2 e^{ik(x - vt)}$$

$$k^2 \left\{ \frac{v^2}{c^2} - 1 \right\} f(z) + \frac{d^2 f(z)}{dz^2} = 0$$

If we put $f = A e^{mz}$ we get

$$m = \pm k \sqrt{1 - \frac{v^2}{c^2}} = \pm ik \sqrt{\frac{v^2}{c^2} - 1}$$

$$f(z) = A_0 e^{ik(v^2/c^2 - 1)^{1/2} z} + B_0 e^{-ik(v^2/c^2 - 1)^{1/2} z}$$

Now put $\frac{v^2}{c^2} - 1 = M^2$ and we get

$$\phi_0 = \left\{ A_0 e^{ikMz} + B_0 e^{-ikMz} \right\} e^{ik(x - vt)} \quad \text{A.1}$$

Similarly we may write for the potentials in the ground:

$$\phi_1 = \left\{ A_1 e^{ikRz} + B_1 e^{-ikRz} \right\} e^{ik(x - vt)}$$

$$\psi_1 = \left\{ A_2 e^{ikS_z} + B_2 e^{-ikS_z} \right\} e^{ik(x - vt)}$$

where $R^2 = \frac{v^2}{a^2} - 1$ and $S^2 = \frac{v^2}{\beta^2} - 1$, and we note

that these potentials are displacement potentials.

Now we are interested in a solution which corresponds to a surface wave, so that the displacement potentials must diminish

indefinitely with distance from the interface. This means, in the usual way, that the one constant must be zero and the exponential term in the other part must have a real and negative exponent.

This gives us immediately:

$$\phi_1 = A_1 e^{ik(R_z + x - vt)} \quad \text{A.2}$$

$$\psi_1 = A_2 e^{ik(S_z + x - vt)} \quad \text{A.3}$$

where R and S are imaginary, that is $v < \alpha, \beta$.

At the plane $z = 0$ we have the boundary condition that the velocities normal to the plane must be the same in both media. As we are using a mixed system of potentials, this leads to the simple relationship

$$\frac{\partial \phi_0}{\partial z} = \frac{\partial}{\partial t} \left\{ \frac{\partial \phi_1}{\partial z} + \frac{\partial \psi_1}{\partial x} \right\}$$

which gives

$$ikM(A_0 - B_0)e^{ik(x - vt)} = -i^2 k^2 R v A_1 e^{ik(x - vt)} - i^2 k^2 v A_2 e^{ik(x - vt)}$$

$$\text{or } iM(A_0 - B_0) = kv(RA_1 + A_2) \quad \text{A.4}$$

We have the further condition that there is no horizontal stress

in the interface, since the upper medium is assumed to be an ideal fluid. (Note - This implies that there is no 'drag force'. In the case of a travelling blast wave there is in any practical case a very marked drag force on the ground, but the writer is not aware of any mathematical treatment in which this condition is included). On this

assumption of no drag force we may write:

$$\rho_z x = \mu \left\{ \frac{2\partial^2 \phi_1}{\partial x \partial z} + \frac{\partial^2 \psi_1}{\partial x^2} - \frac{\partial^2 \psi_1}{\partial z^2} \right\} = 0$$

which leads to:

$$2i^2 k^2 R A_1 + i^2 k^2 A_2 - i^2 k^2 S^2 A_2$$

or, finally,

$$A_2(S^2 - 1) - 2R A_1 = 0 \quad \text{A.5}$$

We now assume, as is relevant in our case, that the motion in the solid medium is induced directly by the forces deriving from the motion of the air. With our mixed system of potentials it is easier to apply this condition in the form of Newton's Law relating the inverse effect, that is, the acceleration in the air is assumed to derive from the normal stress in the ground, thus:

$$\rho_o \frac{\partial \phi_o}{\partial t} = \lambda \left\{ \frac{\partial \phi_1}{\partial x^2} + \frac{\partial^2 \phi_1}{\partial z^2} \right\} + 2\mu \left\{ \frac{\partial^2 \phi_1}{\partial z^2} + \frac{\partial^2 \psi_1}{\partial x \partial z} \right\}$$

This gives us

$$\begin{aligned} -\rho_o i k v (A_o + B_o) e^{ik(x - vt)} &= \lambda \left\{ i^2 k^2 A_1 + i^2 k^2 R^2 A_1 \right\} e^{ik(x - vt)} \\ &+ 2\mu \left\{ i^2 k^2 A_1 + i^2 k^2 S^2 A_2 \right\} e^{ik(x - vt)} \end{aligned}$$

which reduces easily to:

$$\rho_o i v (A_o + B_o) = \lambda k A_1 (1 + R^2) + 2\mu k (R^2 A_1 + S A_2) \quad \text{A.6}$$

Equations 4, 5 and 6 give in effect relationships between the integration constants, of which there are four. Thus we require an additional relationship before proceeding. The relationship introduced by Bateman appears to be the weakest part of his derivation, since he assumes that, without loss of generality, we may assume there is some height H in the atmosphere at which the normal component of velocity vanishes. It is by no means clear that this is acceptable, but one may assume that Bateman considered the disturbance from a finite source likely to decay to small values at distances sufficiently far from the boundary. Alternatively, in the case of wind shear and inversion, which are included in Bateman's analysis, it may be assumed that this height H is that height at which the 'sound ray' has curved so that the tangent to its path is parallel with the surface and the ray is just 'bending down' to a focus.

Be that as it may, if such a condition exists we may write:

$$A_0 = Ke^{ikMH} \quad , \quad B_0 = Ke^{-ikMH}$$

This is equivalent to writing:

$$A_0 + B_0 = 2K \cos kMH$$

$$A_0 - B_0 = 2iK \sin kMH$$

Substituting for these terms we get:

$$-2KM \sin kMH = kv(RA_1 + A_2) \quad A.7$$

$$2\rho_0 ivK \cos kMH = \lambda kA_1(1 + R^2) + 2\mu k(R^2A_1 + \rho A_2) \quad A.8$$

A (vi)

Using equation 5 to substitute for A, and dividing 7 by 8 we get:

$$\begin{aligned} \frac{-M}{\rho_0 i v^2} \tan kMH &= \frac{(S^2 + 1)R}{\lambda(1 + R^2)(S^2 - 1) + 2\mu \{ R^2(S^2 - 1) + 2RS \}} \\ \frac{-M\beta^2}{\rho_0 i v^4} \tan kMH &= \frac{R}{\lambda(1 + R^2)(S^2 - 1) + 2\mu(R^2 S^2 - R^2 + 2RS)} \\ &= \frac{R}{\lambda \left\{ \frac{v^2}{\beta^2} - 2 \right\} \frac{v^2}{\alpha^2} + 2\mu \left\{ \frac{v^4}{\alpha^2 \beta^2} - \frac{v^2}{\alpha^2} - \frac{v^2}{\beta^2} + 1 - \frac{v^2}{\alpha^2} + 1 + 2RS \right\}} \\ &= \frac{R}{\lambda \left\{ \frac{v^4}{\alpha^2 \beta^2} - \frac{2v^2}{\alpha^2} \right\} + 2\mu \left\{ \frac{v^4}{\alpha^2 \beta^2} - \frac{2v^2}{\alpha^2} - \frac{v^2}{\beta^2} + 2 + 2RS \right\}} \\ &= \frac{R}{\gamma^2 \rho_1 \left\{ \frac{v^4}{\alpha^2 \beta^2} - \frac{2v^2}{\alpha^2} \right\} + 2 \rho_1 \beta^2 \left\{ 2RS - \frac{v^2}{\beta^2} + 2 \right\}} \end{aligned}$$

$$\frac{-M\beta^2 \rho_1}{i v^4 \rho_0} \tan kMH = \frac{R\beta^2}{v^4 - 4v^2\beta^2 + 4\beta^4 RS + 4\beta^4}$$

$$\frac{-M\beta^2}{i v^4 \rho_0} \tan kMH = \frac{R}{v^4 - 4v^2\beta^2 + 4\beta^4 RS + 4\beta^4}$$

or finally

$$M\rho_1(v^4 - 4v^2\beta^2 + 4\beta^4 RS + 4\beta^4) \tan kMH = -R i v^4 \rho_0 \quad A.9$$

Since R, S are imaginary, we may change the above to make the terms in the equation real, by writing $iR = R^1$, $iS = S^1$

This gives:

$$M\rho_1(v^4 - 4v^2\beta^2 - 4\beta^4 R^1 S^1 + 4\beta^4) \tan kMH = R^1 v^4 \rho_0$$

Now note that the term

$$V_R^4 - 4V_R^2\beta^2 - 4\beta^4 R^1 S^1 + 4\beta^4 = 0 \text{ is the Rayleigh Wave condition.}$$

If we have the condition that in our equation $v < c$, and both quantities are less than the value v_R which satisfies the Rayleigh condition, then both sides of the equation are positive. In particular cases therefore, we may find a value of v corresponding to a given H , or alternatively, if we know the value of v we can determine H uniquely.

It will be seen that Bateman's solution, when written in the above form, is essentially a derivation for a Stonely Wave (see Stoneley, 1924) in the case of a semi-infinite fluid ocean over a semi-infinite elastic half space. Further, Bateman's 'coupled wave' is a case of free vibrations of the system, not the case of impulsive forcing. Bateman points out that solutions will only be possible for certain ranges of the elastic constants, and for rather specialized atmospheres. On the other hand, it is pointed out by EJP (page 112) that these 'Generalised Rayleigh Waves', 'Stoneley Waves' or Bateman's 'Coupled Waves' are always possible at the interface of a fluid and solid medium, and their velocity is smaller than that of regular surface waves. This agrees with the Bateman derivation.

It should be noted that there is a fundamental difference between Bateman's coupled waves and the Press-Ewing waves discussed below. The Bateman wave, or Stonely wave, may exist in a semi-infinite medium, that is in a medium which is not normally considered to be dispersive to Rayleigh waves. On the other hand, in the normal derivation of the Stonely wave the two media are strictly 'semi-infinite' so that only one velocity is possible. In the Bateman case a variation in the velocity can occur, depending upon the variation in the effective height H . Presumably for certain types of inversion and wind shear

conditions it would be possible to produce a form of 'dispersion' with distance from the point of origin.

A2 The Press-Ewing Air-Coupled Wave

The type of coupled wave produced by a constant velocity pressure step travelling over the boundary of a dispersive half space is usually called the 'Press-Ewing' air-coupled wave, since the detailed analysis for this case was given by Press and Ewing (1951). However, several other papers bearing on similar problems appeared in a very brief span of time, and some of the properties of the wave were discussed in papers prior to the main source. Reference should be made, for example, to Press, Crary, Oliver and Katz (1951), which deals with a similar form of coupling in the case of a floating ice sheet, and to Haskell (1951) who deals with the case where the ground surface is constrained to move sinusoidally. The essential part of these discussions is available in detail in EJP. The essential difference between this treatment and that of Bateman is the requirement of a dispersive medium. A general discussion would be prohibitively lengthy for this appendix, and attention is therefore restricted to the simplest system, and further restricted only to those aspects which are essential to a superficial understanding of the process. As mentioned previously, we require as a minimum a homogeneous atmosphere overlying a half space which can maintain dispersive waves. For simplicity, we take the case where the dispersion is introduced by an elastic layer welded to the surface of an otherwise uniform half space. Our intention is to show that a 'coupling term' enters into the frequency equation, so that at some frequency a form of 'resonant' increase in amplitude will

occur. We shall use the notation of EJP, which is now more or less standard. The simplest case would be to consider a plane wave propagating in the air, but it is more realistic to include the effect of a point source in the preliminary derivation. Let this point source be at height h above the plane $z = 0$ and let $\rho_j, \alpha_j, \beta_j$ ($j = 0, 1, 2$) be the densities and wave velocities in the three media as and when applicable. Let the elastic layer welded to the half space be of thickness H . In order to write the distribution of potentials in a convenient form, it is convenient to divide the atmosphere into two zones separated by the plane $z = -h$ (Note: the z axis is taken positive in the solid medium, negative in the fluid). Then the upper zone will have a potential depending only upon the source (or alternatively we may say dependent only upon the 'interface' $z = -h$), while other zones will have potentials which are the sums of two terms relating to the two boundary planes, except for the lowest zone, the half space, which will again have single term potentials. Further, in the fluid there will be a single potential only corresponding to compressional waves, while in the solid there will, in general, be both 'compressional' and 'shear' potentials. As we are assuming perfectly elastic, homogeneous media, there will not be, in general, any coupling between the two modes - we may treat the shear waves and the compressional waves as independently travelling waves, though, of course, the displacement at any point will be a summation of the two modes.

If now we denote by ϕ_i and ψ_i the compressional and shear displacement potentials we may write six equations corresponding to the four 'distributions' of potentials of compressive type and two shear type, as below:

$$\phi_0' = Ae^{v_0 z} J_0(kv)$$

$$\phi_0'' = \{Be^{v_0 z} + Ce^{-v_0 z}\} J_0(kv)$$

$$\phi_1 = \{De^{v_1 z} + Ee^{-v_1 z}\} J_0(kv) \quad (1 - 6)$$

$$\phi_2 = Fe^{-v_2 z} J_0(kv)$$

$$\psi_1 = \{Me^{v_1 z} + Ne^{-v_1 z}\} J_0(kv)$$

$$\psi_2 = Pe^{-v_2 z} J_0(kv)$$

In order to evaluate the nine coefficients we require nine boundary conditions. These we obtain from the continuity of stress and displacement at the welded interface $z = H$ (four equations), the continuity of vertical displacement and stress at the plane $z = 0$ (two equations), the vanishing of horizontal stress at $z = 0$ (one equation) and an expression of the fact that at the plane $z = -h$ there is a discontinuity in the vertical displacement (one equation) and continuity in pressure (one equation). The condition that displacements vanish at infinite distance from the plane $z = 0$ is included in the equations. We get:

$$\rho_0 w^2 (B + C) + (2\mu_1 k^2 - \rho_1 w^2) (D + E) + 2\mu_1 v_1^! k^2 (M - N) = 0$$

$$2v_1 (D - E) + (v_1^!^2 + k^2) (M + N) = 0$$

$$(2\mu_1 k^2 - \rho_1 w^2) (De^{v_1 H} + Ee^{-v_1 H}) - (2\mu_2 k^2 - \rho_2 w^2) Fe^{-v_2 H} + 2\mu_1 v_1^! k^2 (Me^{v_1^! H} - Ne^{-v_1^! H}) \\ + 2\mu_2 v_2^! k^2 Pe^{-v_2^! H} = 0 \quad (7 - 15)$$

$$2\mu_1 v_1 (De^{v_1 H} - Ee^{-v_1 H}) + 2\mu_2 v_2 Fe^{-v_2 H} + \mu_1 (v_1^!^2 + k^2) (Me^{v_1^! H} + Ne^{-v_1^! H}) \\ - \mu_2 (v_2^!^2 + k^2) Pe^{-v_2^! H} = 0$$

$$v_0 (B - C) - v_1 (D - E) - k^2 (M + N) = 0$$

$$v_1 (De^{v_1 H} - Ee^{-v_1 H}) + v_2 Fe^{-v_2 H} + k^2 (Me^{v_1^! H} + Ne^{-v_1^! H} - k^2 Pe^{-v_2^! H}) = 0$$

$$De^{v_1 H} + Ee^{-v_1 H} - Fe^{-v_2 H} + v_1^! (Me^{v_1^! H} - Ne^{-v_1^! H}) + v_2^! Pe^{-v_2^! H} = 0$$

$$Ae^{v_0 h} - Be^{v_0 h} - Ce^{-v_0 h} = 0$$

$$v_0 Ae^{v_0 H} + v_0 (Ce^{-v_0 h}) = 2Z$$

In the last equation, Z represents the strength of the source, but we need not define it further at the present time. The last two equations enable us to eliminate B and C in terms of A and Z . In theory we can, following the method of Lamb, solve explicitly for the potentials (and hence the displacements) for any particular case, including that of the pulse type point source, provided we generalize the Z term in terms of Fourier-Bessel integrals. Practically this is difficult, and for our present purpose we restrict ourselves to the frequency equation. For this we need only consider the vanishing of the determinant on the LHS of the foregoing set of equations. Effectively, we eliminate the wave amplitude function. We could proceed with the determinant as it stands, but it has been reduced (Jardetzky and Press, 1952) to the form:

A (xii)

1	$\frac{2\mu_1 k^2 - \rho_1 w^2}{\rho_0 w^2 \cosh v_1 H}$	0	0	$\frac{2\mu_1 v_1^2 k^2}{\rho_0 w^2 \sinh v_1 H}$	0	0	
0	0	$\frac{2v_1}{\sinh v_1 H}$	$\frac{2k^2 \beta_1^2 - w^2}{B_1^2 \cosh v_1 H}$	0	0	0	
0	$\rho_1 w^2$	$-\rho_1 w^2$	0	0	$\rho_2 w^2 + 2(\mu_1 - \mu_2)k^2$	$2(\mu_2 - \mu_1)v_2^2 k^2$	
0	0	0	$-\rho_1 w^2$	$-\rho_1 w^2$	$2(\mu_2 - \mu_1)v_2$	$\rho_2 w^2 + 2(\mu_1 - \mu_2)k^2$	= 0
0	$\frac{-2\mu_1 k^2 - \rho_1 w^2}{\rho_0 w^2 \cosh v_1 H}$	0	$\frac{-w^2}{2v_1 \beta_1^2 \cosh v_1 H}$	$\frac{-w^2}{\rho_0 w^2 \sinh v_1 H}$	0	0	
0	$v_1 \tanh v_1 H$	$v_1 \coth v_1 H$	k^2	k^2	v_2	$-k^2$	
0	1	1	$v_1^2 \tanh v_1 H$	$v_1^2 \coth v_1 H$	-1	v_2^2	

After purely algebraic (but considerable) manipulation, the determinant may be expanded into a single frequency equation. Details are given in EJP, and to avoid tedium in presentation, we merely state that the final form may be written:

$$L_0 + L_1 \sinh(n_1 kH) \sinh(n_3 kH) + L_2 \sinh(n_1 kH) \cosh(n_3 kH) + L_3 \cosh(n_1 kH) \sinh(n_3 kH) + L_4 \cosh(n_1 kH) \cosh(n_3 kH) = 0$$

This deceptively simple equation is complicated by the fact that each of the L and n terms is far from simple. We confine ourselves to discussing the L terms, which include the effect of the air. The effect does not enter into L_0 but L_1 in expanded form is:

$$\begin{aligned}
L_1 = & \left\{ 2 - v^2 \right\}^2 \left[\frac{\frac{\rho_2}{\rho_1} v^2 - v^2 - 2\left(\frac{\mu_2}{\mu_1} - 1\right)^2 \sqrt{1 - \frac{v^2 \beta_1^2}{\alpha_2^2}} \sqrt{1 - \frac{v^2 \beta_1^2}{\beta_2^2}} \left\{ v^2 + 2\left(\frac{\mu_2}{\mu_1} - 1\right) \right\}^2}{\sqrt{1 - \frac{v^2 \beta_1^2}{\alpha_0^2}} \sqrt{1 - v^2}} \right] \\
& - 4 \sqrt{1 - \frac{v^2 \beta_1^2}{\alpha_1^2}} \sqrt{1 - v^2} \left[\sqrt{1 - \frac{v^2 \beta_1^2}{\alpha_2^2}} \sqrt{1 - \frac{v^2 \beta_1^2}{\beta_2^2}} 4\left(\frac{\mu_2}{\mu_1}\right)^2 - \left\{ \frac{\rho_2}{\rho_1} v^2 - 2\left(\frac{\mu_2}{\mu_1} - 1\right) \right\}^2 \right] \\
& - \frac{\rho_0 \rho_2}{\rho_1^2} \frac{\sqrt{1 - \frac{v^2 \beta_1^2}{\alpha_1^2}} \sqrt{1 - \frac{v^2 \beta_1^2}{\beta_2^2}}}{\sqrt{1 - \frac{v^2 \beta_1^2}{\alpha_0^2}} \sqrt{1 - v^2}} v^8
\end{aligned}$$

where $v = c/\beta_1$

We note that the last term in this formidable expression involves ρ_0 and α_0 , and thus represents the effect of the air. The air coupling is involved through

$$\frac{\rho_0}{\rho_1 \sqrt{1 - \frac{v^2 \beta_1^2}{\alpha_0^2}}} = \frac{\rho_0}{\rho_1 \sqrt{1 - \frac{c^2}{\alpha_0^2}}}$$

A similar expansion of the other L terms results in each case in a term of the above form. We see that, provided the phase velocity "c" in the ground is different from the velocity of 'sound' in the air, then the coupling term will be very small, due to the small value of the ratio ρ_0/ρ_1 . If, on the other hand, the velocity of the pulse in the air approaches the phase velocity c in the ground, for some frequency, then the air-coupling term may

become very large, and possibly dominant. In such a case we would expect to see this particular frequency excited strongly so that in a displacement record at the surface, the small amplitude dispersed train of surface waves would be interrupted by a large amplitude constant frequency train. This train is the 'Press Ewing' coupled wave. This theory is verified in the case of points reasonably remote from small air-burst explosive charges. Obviously, in the case of the explosions considered in this dissertation, the main departure from the theory is that we do not have a constant value for the velocity α_0 , and so the first two equations in 1-6 are not strictly valid. We require to replace them by a pair of equations similar in form to the pulse used by Miles. Analagous to the above, however, we should expect that in a given region (short compared to the rate of decay of velocity) we should obtain a coupling effect to the relevant frequency. We should expect, however, that the particular frequency selected may (a) change with distance from a given charge and (b) change with charge size, since the rate of decay decreases with increase in charge size. The experimental data given in this dissertation verify that this does, indeed, occur. In addition, at points very remote from the charge the effective 'dispersion' in the coupled wave train should have reduced the period of the train to that predicted by the above theory for the constant velocity pulse. Thus in the case of normal dispersion we would expect to have a relatively high frequency train at points remote from the charge, and a relatively long period train close to the charge.

APPENDIX B

SEISMIC SURVEY OF THE TWO MAIN SITES

The information given in this Appendix is based upon the report submitted by the Century Geophysical Corporation of Canada upon a contract completed in 1961. Mr J. L. Robinson, a vice-president of the Corporation, took an active part in the planning and interpretation, and the field operation was directed by Mr D. R. McDonald. The Corporation showed great interest and collaborated closely with the present writer, undertaking both field and interpretive work beyond that called for in the contract. The detailed report is summarized in this appendix to give only immediately relevant information.

B1 Operational Details

A series of seismic measurements was conducted by the Corporation, party No. 10, on two sites at Suffield Experimental Station, on the week-end of 7th June, 1961. The objectives were (a) to obtain bedrock profiles beneath the sites, (b) to identify ground-waves generated by buried charges and (c) to measure the velocities in the various ground waves.

The ground locations, elevations and bearings of the two seismic lines were provided by SES surveyors. Shot points and geophone locations and elevations were then obtained by alidade plane table and chain survey. A Mayhew 1000 Special Drilling Rig, owned by the Corporation, was used for drilling the shot holes. Drilling conditions were fair. Very little gravel was encountered on the Watching Hill site. However, near surface sand and gravel required 50-ft of casing to be set in VH3 and 60-ft of casing in VH4 on the Drowning Ford site.

Recording instruments used included Century Model 510B amplifiers, Century Model 301BZ 6.5 cps geophones and a Century 24 trace

B (ii)

mirror-type oscillograph and camera. The above instruments were also connected to a Fortune Model SR3 A.M. tape recorder. The filter setting used for shooting was NF-100, so that the effective low filter would be the 6.5 cps geophones. The AVC setting was on the fast position for all shooting. Pre-suppression was used where needed. Input gains varied to keep trace interference to a minimum.

The shooting was carried in groups as follows:

- | | | |
|-------|------|--|
| Group | IA | Refraction Profile S.P.'s 1-5 Watching Hill |
| | IB | Refraction Profile S.P.'s 38-37 5-A Watching Hill |
| | IC | Air shooting 6000 ft spread from S.P. 38 Watching Hill |
| | IIA | 5-ft geophone spacing shooting from S.P.1 Watching Hill |
| | IIB | 5-ft geophone spacing shooting from S.P.4 Watching Hill |
| | IIIA | Surface 3-component phone survey 25-ft spacing, S.P.'s 11-27 Watching Hill |
| | IIIB | 50-ft spacing surface phones from S.P.1 Watching Hill |
| | IIIC | Sub-surface pressure phone survey in VH 1 and VH 2, S.P.'s 11-27 Watching Hill |
| | IVA | Refraction Profile S.P.'s 6-10 Drowning Ford |
| | IVB | Short spreading air shooting from S.P.6 Drowning Ford |
| | VA | Surface 3-component phone survey S.P.'s 28-36 Drowning Ford |
| | VB | Sub-surface pressure phone survey VH 3 and VH 4 S.P.'s 28-36 Drowning Ford |

B (iii)

Two geophones were connected in parallel for each station for all refraction profiling. Ranks of amplifiers were parallel whenever possible, to provide high and low sensitivity traces. Deep holes containing pressure phones were kept filled with water during that phase of the programme. Good ground-to-geophone coupling was achieved in the 3-component phase by first softening the ground with water. Explosive used was CIL Hi-Velocity Gelatin 60%.

B2 Interpretation Report, Watching Hill Site

Fig. B1 (this appendix) shows the location of the velocity and refraction survey on Watching Hill and Drowning Ford. The refraction survey was shot for bedrock control. The velocity survey was shot to measure the velocity and direction of the seismic waves, both surface and sub-surface. Fig. B2 shows the design of the refraction and velocity profiles. Reading from the top we have first the refraction lines with phones spread 250 ft apart to obtain bedrock control. Secondly, a group of stations spaced 5 ft apart at S.P.'s 1 and 4 to obtain dispersion data. Third, a design to analyse wave types. Three-component phones were set out near S.P. 11 to respond to shots at S.P.'s 11-27. Finally, the velocity profile was obtained by lowering the two cables containing pressure phones in VH1 and VH2, to respond to energy from S.P.'s 11-27. This determined the velocity and direction of waves propagating below the surface.

Fig. B3 shows the refraction profile, together with the lithology actually logged by the driller. Water was found at 55 ft in a thin gravel seam, although the soft grey clay above and below it appeared relatively dry. This suggests a false water table, since the stream level

of the South Saskatchewan is at least 250 ft below the Watching Hill surface*.

Fig. B4 shows the refraction time-distance plot obtained from the horizontal measurements. Here the velocity distribution is roughly 5500 fps, 7500 fps and 8500 fps. The base of the 5500 fps material is considered to be the bedrock. Fig. B5 gives the data obtained from the vertical velocity survey.

In any given velocity bed there seems to be little evidence of anisotropy when wave front directions change.

(Additional data and interpretation are available in the full report. This appendix merely abstracts the essential items. No detailed interpretation is yet available for the Drowning Ford site, but no unexpected features have been noted in the layering system).

* See comments in Section 2.20. This water-bearing gravel has frequently been broached by high explosive trials. In these cases the craters filled briefly with water, the water subsiding to leave dry craters. The bed seems to tap local surface water, the available volume being small.

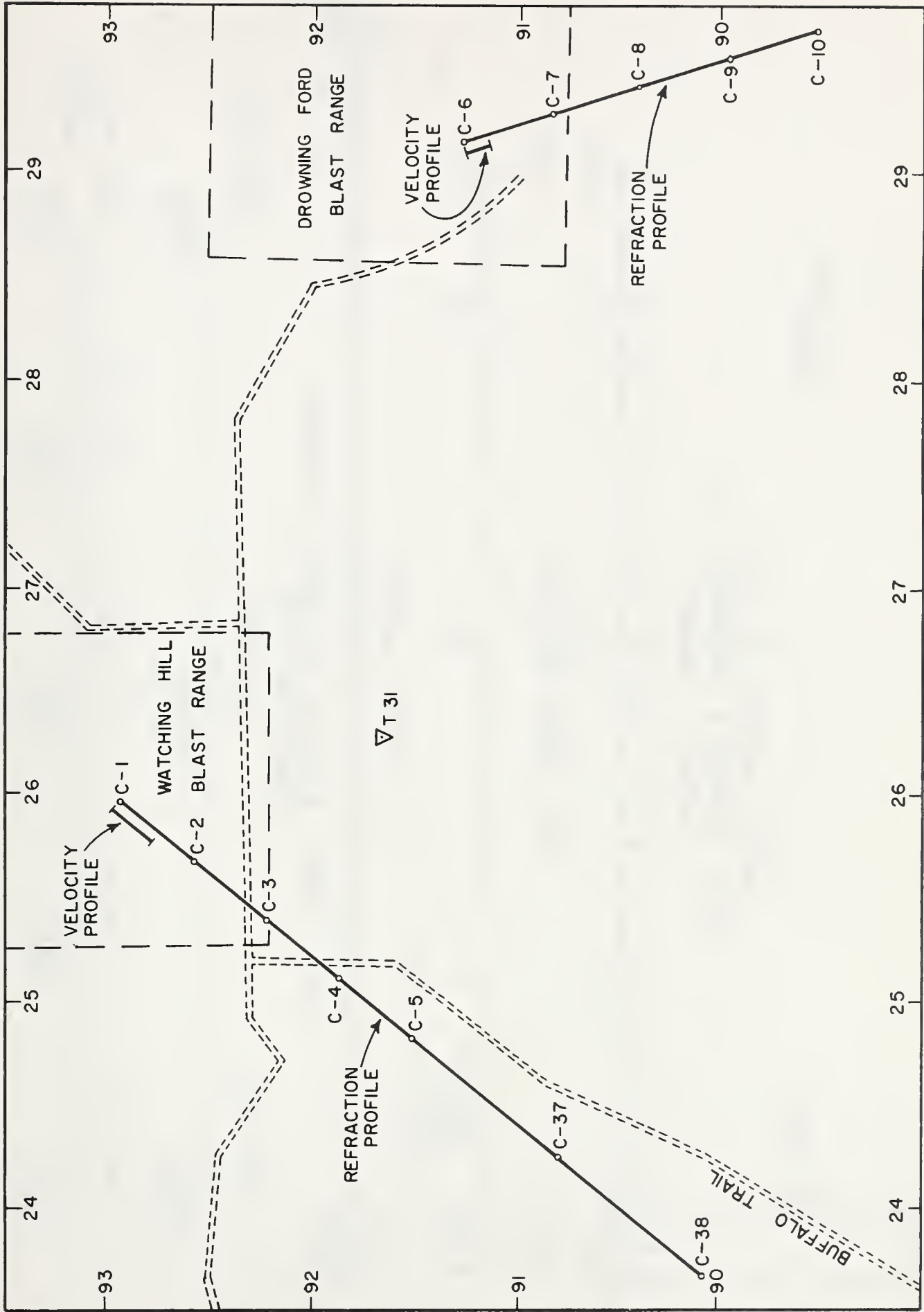


FIG. B1
LOCATION OF VELOCITY AND REFRACTION SURVEY

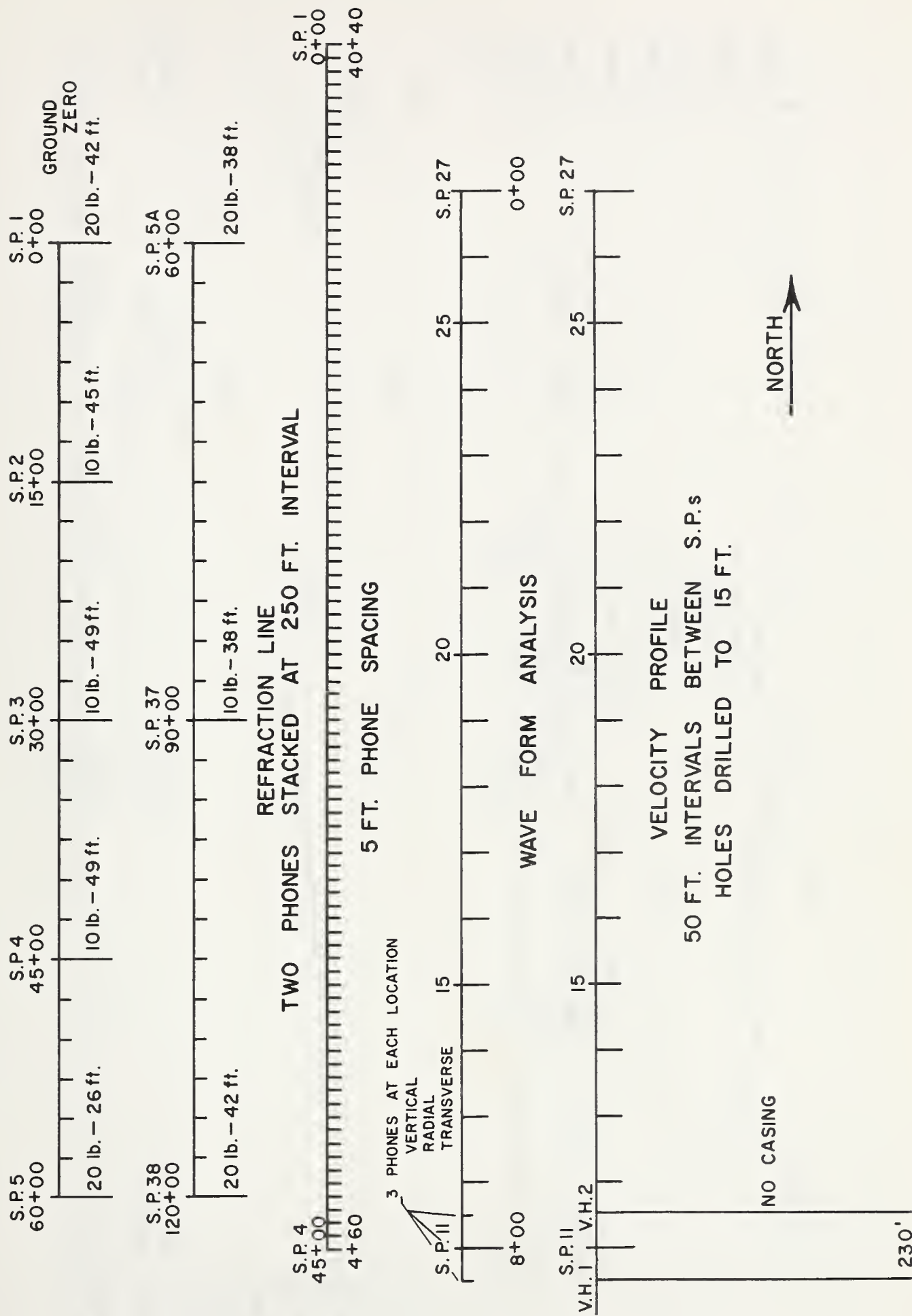


FIG. B2

REFRACTION AND VELOCITY PROFILES

WATCHING HILL SITE

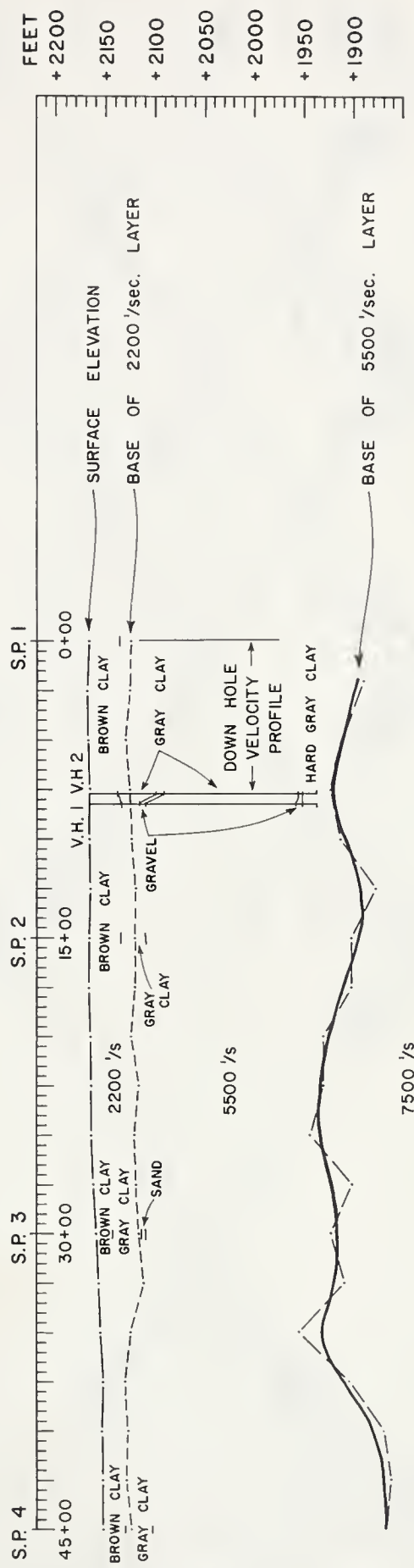


FIG. B3
 SEISMIC SECTION — WATCHING HILL SITE

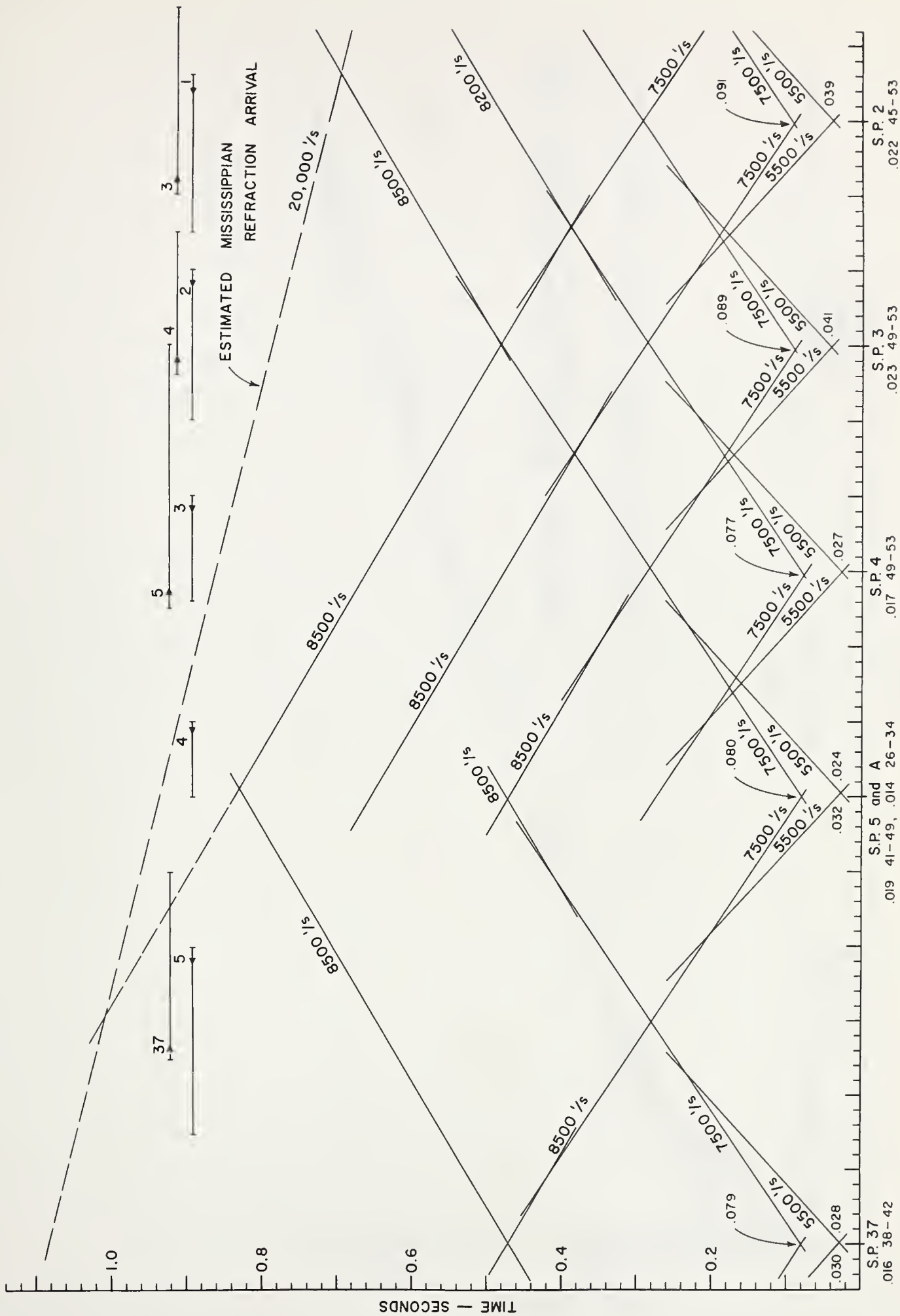
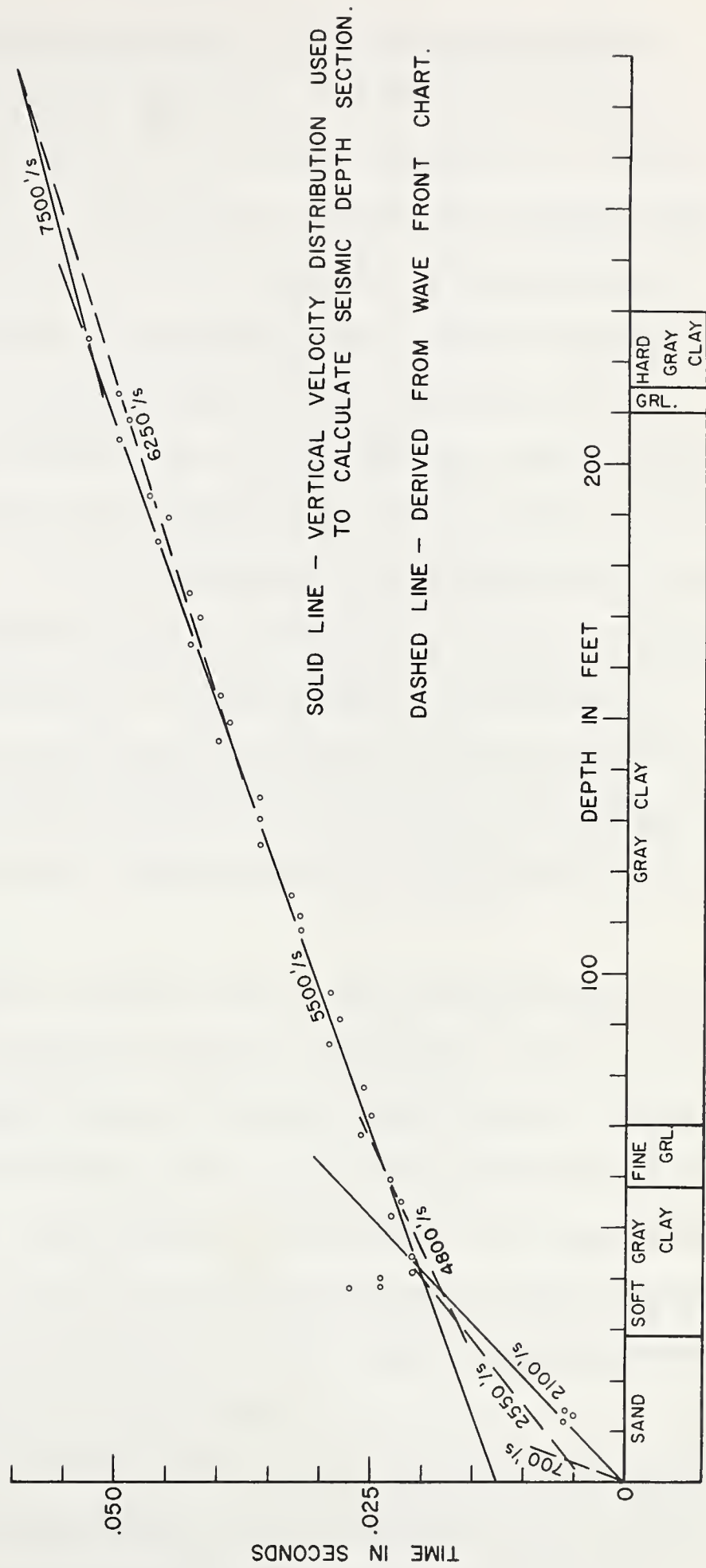


FIG. B4

TIME — DISTANCE PLOT
WATCHING HILL SITE



SOLID LINE - VERTICAL VELOCITY DISTRIBUTION USED TO CALCULATE SEISMIC DEPTH SECTION.

DASHED LINE - DERIVED FROM WAVE FRONT CHART.

FIG. B5

VERTICAL VELOCITY SURVEY - WATCHING HILL SITE
S.P. II - V.H. I

APPENDIX C

THEORETICAL RAYLEIGH WAVE DISPERSION CURVES FOR VARIOUS MODELS

This appendix gives the details of some of the dispersion curves computed for the writer on the Toronto IBM 7090 by Dr Fraser, the DRB representative at the Computation Centre. The programme used was provided to the writer by Dr D. L. Anderson, Seismology Labs., Pasadena. It was noted that the programme will not handle input data in which the starting or ending points of the computation are fixed outside the asymptotic limits, and, if such starting or ending points are included considerable machine malfunction occurs, leading to reams of nonsensical output. No such difficulty occurs provided the asymptotic velocities are not approached closer than one phase velocity decrement (100 fps in the present case). The group velocity calculations are slightly suspect since in all cases the values computed for 2000 fps and 1000 fps are apparently in gross error, departing radically from the generally smooth curve. The reason for this malfunction has not been traced.

Fig. C1 gives a pictorial plot of eight physical models, in which the velocity and density parameters approximate to those of the test sites. The layering system of the first model (listed as Model 6) is based directly upon the survey data, and is the preferred model of the Saint Louis group. Model 8 modifies this model at the high velocity end only, and model 9 and model 10 similarly retain the upper layering constant but modify the high-velocity system. Model 11 introduces two thin low-velocity layers near the surface.

The outputs for these models are given as photo-copies of the computer output, and models 6 and 11 are also plotted in Fig. C2a. The points marked 'K' give the approximate limits of the computation for

this model by Kisslinger, using the Lamont programme. It will be seen that Model 11 departs radically from Model 6 in the high frequency region, a maximum shift in period of 0.1 sec at 1000 fps. In the low frequency region Model 11 shifts to somewhat higher velocities than those of Model 6. It should be noted that Models 8, 9 and 10, which retain the upper layering of Model 6, conform quite closely to Model 6 up to the point where Models 6 and 11 cross, and then conform to Model 11. Thus, the general shift towards lower frequencies in the range from 2 cps to 10 cps between Model 6 and Model 11, is purely the result of the introduction of two thin low velocity layers at the surface. This zone is equivalent to the silty-clay zone above the water bearing gravel, and is liable to large changes in water content, depending upon the precipitation history of the area. Thus the probability of shifts in the dispersion curves of the order shown in the figure is quite large. In addition, these surface layers are precisely those most likely to be modified by the minor relief in the plains areas.

The remaining three models (Models 12, 15 and 16) indicate the variation which may be expected when we change from a 'best selection' to an arbitrary layering system. Model 12 uses approximately the same parameters as Model 8, but fixes the layer interval at 50 ft. Models 15 and 16 are identical with Model 12, except that the layering is cut short at the third and second layer respectively, the half space become the third or fourth level of Model 12. The computer outputs are included, and the curves plotted in Fig.C2b. It will be seen that the curves in C2b are similar in pattern to the curves in C2a, and generally speaking the phase velocity curves fall between those of Models 6 and 11.

Thus, the selection of a 'best model' on the basis of limited ranges in the experimental data is not satisfactory. If only a narrow range of frequencies is available, particularly if this range is at the high frequency end, almost any model which is physically not too far removed from the correct one will satisfy the data. Selection of the correct model requires a wide range of frequencies.

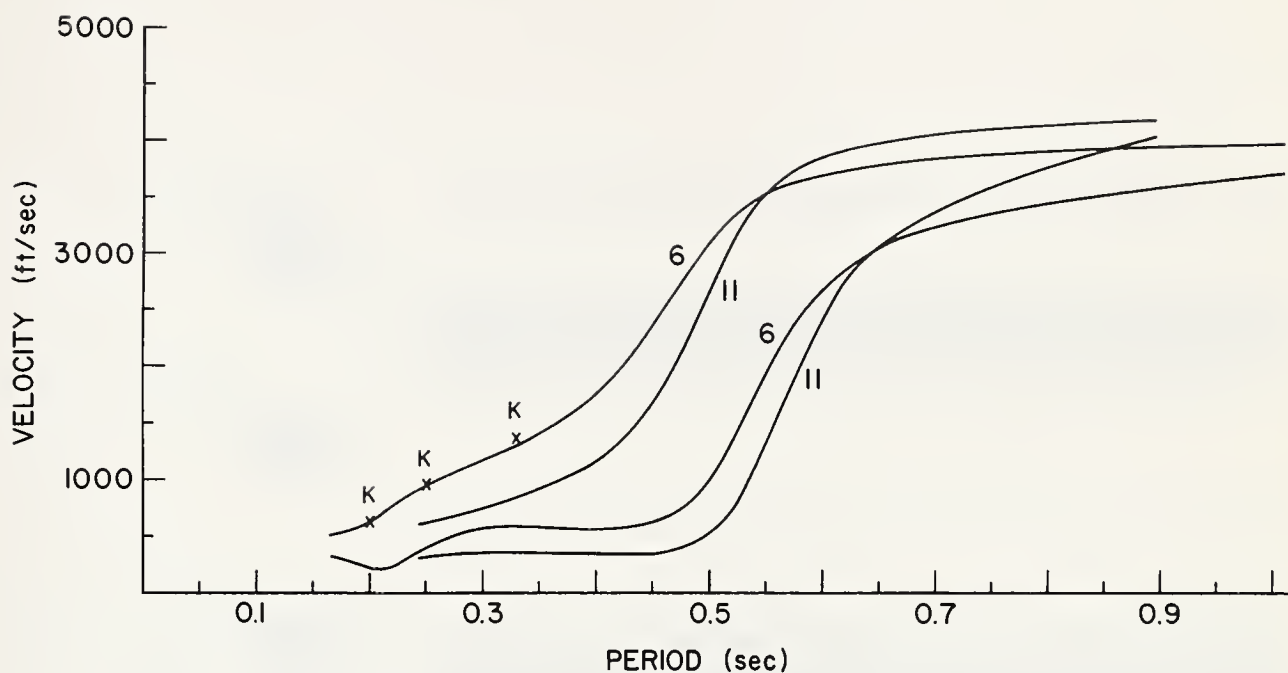
It will be noted that in all the models the possibility of Press-Ewing-type air-coupling exists. A 'group period' of between 0.5 and 0.6 sec., pre-existing in the ground, will be interrupted by, or have superimposed upon it, a constant frequency train of about 0.3 sec. period.

Attention is drawn to the Group Velocity plateau between 0.3 sec. and 0.6 sec. in these models.

MODEL 6	MODEL 8	MODEL 9	MODEL 10	MODEL 11	MODEL 12	MODEL 15	MODEL 16		
45-2200-460-1.8	45-2200-460-1.8	45-2200-460-1.8	45-2200-460-1.8	10-1000-210-1.6	50-2200-460-1.8	50-2200-460-1.8	50-2200-460-1.8		
				10-2000-300-1.7					
				25-2200-460-1.8					
35-5500-1000-2.0	35-5500-1000-2.0	35-5500-1000-2.0	35-5500-1000-2.0	35-5500-1000-2.0	50-5500-1000-2.0	50-5500-1000-2.0	50-5500-1000-2.0		
131-5500-2000-2.3	131-5500-2000-2.3	131-5500-2000-2.3	131-5500-2000-2.3	131-5500-2000-2.3	50-5500-2000-2.3	50-5500-2000-2.3	1/2 Space 5500-2000-2.3		
					50-7900-4600-2.35	1/2 Space 7900-4600-2.35			
					50-8100-4700-2.4				
1/2 Space 7900-4600-2.5	100-7900-4600-2.35	100-7900-4600-2.35	150-7900-4600-2.5	100-7900-4600-2.35	50-8400-4800-2.5	1/2 Space 8500-4900-2.6	1/2 Space 5500-2000-2.3		
	100-8100-4700-2.4	1/2 Space 8100-4700-2.4		100-8100-4700-2.4					
	1/2 Space 8500-4900-2.5		1/2 Space 8500-4900-2.6	1/2 Space 8500-4900-2.5					

* Thickness in feet, P wave and S wave velocities in fps, relative density.

FIG. C1
CHART FOR LAYERING MODELS



(a) THEORETICAL DISPERSION CURVES
MODELS 6 AND 11

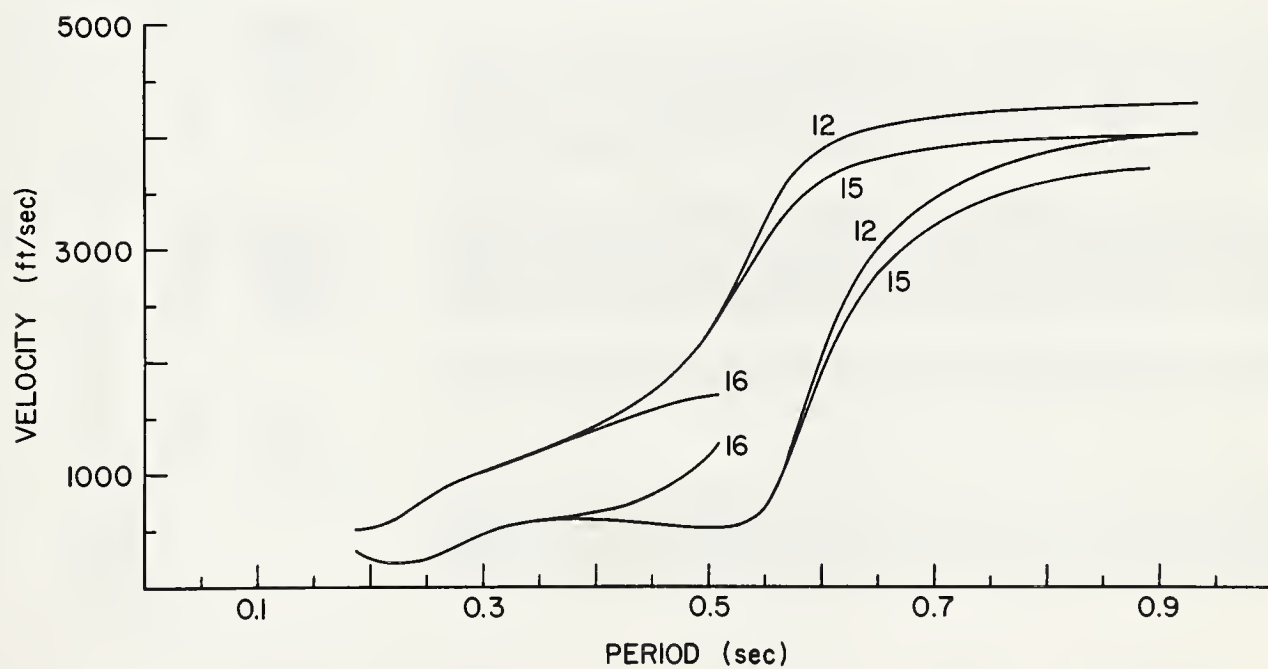


FIG. C2
(b) THEORETICAL DISPERSION CURVES
MODELS 12, 15 AND 16

ANISOTROPIC RAYLEIGH WAVE DISPERSION
MODEL 68

N# 4 DELT# 0.0000010 FK# 0.00100 FKDH 0.00050
NW# -0 DKS# 1.0 CPERT# 1.0010C

D	ALPHA	BETA	RHO	PHI	NADA
45.00	2200.0000	460.0000	1.8000	1.0000	1.0000
35.00	5500.0000	1000.0000	2.0000	1.0000	1.0000
131.00	5500.0000	2000.0000	2.3000	1.0000	1.0000
-0.	7900.0000	4600.0000	2.5000	1.0000	1.0000

KD1	T	C	U	W*	N	SUM DI	V
0.06748	1.047	4000.0000	3758.1095	-0.16090E 01	4	211.00	0.
0.09302	0.779	3900.0000	3495.1392	-0.28425E 01	4	211.00	0.
0.11287	0.659	3800.0000	3137.3507	-0.58336E 01	4	211.00	0.
0.12745	0.600	3700.0000	2693.1353	-0.16343E 02	4	211.00	0.
0.13871	0.566	3600.0000	2240.8112	0.16212E 03	4	211.00	0.
0.14820	0.545	3500.0000	1849.7925	0.19680E 02	4	211.00	0.
0.15686	0.530	3400.0000	1542.6323	0.12158E 02	4	211.00	0.
0.16521	0.519	3300.0000	1311.5094	0.94273E 01	4	211.00	0.
0.17356	0.509	3200.0000	1139.5954	0.79875E 01	4	211.00	0.
0.18213	0.501	3100.0000	1011.3136	0.70769E 01	4	211.00	0.
0.19106	0.493	3000.0000	914.0550	0.64333E 01	4	211.00	0.
0.20051	0.486	2900.0000	839.3490	0.59422E 01	4	211.00	0.
0.21058	0.480	2800.0000	780.8539	0.55457E 01	4	211.00	0.
0.22143	0.473	2700.0000	734.2384	0.52113E 01	4	211.00	0.
0.23319	0.466	2600.0000	696.5266	0.49221E 01	4	211.00	0.
0.24602	0.460	2500.0000	665.7566	0.46571E 01	4	211.00	0.
0.26011	0.453	2400.0000	640.5209	0.44157E 01	4	211.00	0.
0.27571	0.446	2300.0000	619.6189	0.41886E 01	4	211.00	0.
0.29308	0.439	2200.0000	602.7731	0.39712E 01	4	211.00	0.
0.31258	0.431	2100.0000	589.2660	0.37592E 01	4	211.00	0.
0.33232	0.425	2000.0000	2350.4832	0.34456E 01	4	211.00	0.
0.35998	0.413	1900.0000	571.8652	0.33381E 01	4	211.00	0.
0.38928	0.404	1800.0000	568.0744	0.31225E 01	4	211.00	0.
0.42371	0.393	1700.0000	567.3794	0.28989E 01	4	211.00	0.
0.46484	0.380	1600.0000	569.7036	0.26638E 01	4	211.00	0.
0.51502	0.366	1500.0000	574.4381	0.24128E 01	4	211.00	0.
0.57773	0.350	1400.0000	580.0260	0.21412E 01	4	211.00	0.
0.65833	0.330	1300.0000	582.5611	0.18436E 01	4	211.00	0.
0.76465	0.308	1200.0000	574.1275	0.15157E 01	4	211.00	0.
0.90622	0.284	1100.0000	539.3827	0.11583E 01	4	211.00	0.
1.07570	0.263	1000.0000	1097.8721	0.77410E 00	4	211.00	0.
1.30835	0.240	900.0000	347.2103	0.43910E-00	4	211.00	0.
1.56632	0.226	800.0000	247.4517	0.14568E-00	4	211.00	0.
1.89194	0.213	700.0000	201.8721	-0.89179E-01	4	211.00	0.
2.37299	0.199	600.0000	219.2096	-0.28089E-00	4	211.00	0.
3.38639	0.167	500.0000	308.8331	-0.44860E-00	4	211.00	0.
3.38640	0.167	500.0000	309.4011	-0.44860E-00	3	80.00	0.

ROOT NOT BRACKETED AFTER 20 TRIES

ANISOTROPIC RAYLEIGH WAVE DISPERSION
MODEL 10

N# 5 DELT# 0.0000010 FK# 0.00100 FKD# 0.00050
NW# -0 DKS# 1.0 CPRT# 1.00100

D
45.00
35.00
131.00
150.00
-0.

ALPHA
2200.0000
5500.0000
5500.0000
7900.0000
8500.0000

RETA
460.0000
1000.0000
2000.0000
4600.0000
4900.0000

RHO
1.8000
2.0000
2.3000
2.5000
2.6000

PHI
1.0000
1.0000
1.0000
1.0000
1.0000

NADA
1.0000
1.0000
1.0000
1.0000
1.0000

KD1	T	C	U	W _r	N	SUM D1	V
0.02811	2.286	4400.0000	4293.1297	-0.93774E 00	5	361.00	0.
0.05384	1.221	4300.0000	4084.2089	-0.13848E 01	5	361.00	0.
0.07726	0.871	4200.0000	3843.4973	-0.22573E 01	5	361.00	0.
0.09650	0.715	4100.0000	3529.5620	-0.41201E 01	5	361.00	0.
0.11109	0.636	4000.0000	3122.1884	-0.87604E 01	5	361.00	0.
0.12219	0.593	3900.0000	2665.3615	-0.29150E 02	5	361.00	0.
0.13121	0.567	3800.0000	2231.6104	0.55129E 02	5	361.00	0.
0.13912	0.549	3700.0000	1865.8600	0.13481E 02	5	361.00	0.
0.14650	0.536	3600.0000	1577.2950	0.12440E 02	5	361.00	0.
0.15369	0.526	3500.0000	1356.3741	0.98741E 01	5	361.00	0.
0.16090	0.517	3400.0000	1188.6838	0.84613E 01	5	361.00	0.
0.16829	0.509	3300.0000	1060.6574	0.75412E 01	5	361.00	0.
0.17598	0.502	3200.0000	961.7488	0.68803E 01	5	361.00	0.
0.18406	0.496	3100.0000	884.3553	0.63668E 01	5	361.00	0.
0.19264	0.489	3000.0000	822.6397	0.59602E 01	5	361.00	0.
0.20181	0.483	2900.0000	772.9098	0.56133E 01	5	361.00	0.
0.21167	0.477	2800.0000	732.1365	0.53114E 01	5	361.00	0.
0.22234	0.471	2700.0000	698.2248	0.50418E 01	5	361.00	0.
0.23396	0.465	2600.0000	669.8421	0.47955E 01	5	361.00	0.
0.24667	0.458	2500.0000	645.8354	0.45661E 01	5	361.00	0.
0.26066	0.452	2400.0000	625.5685	0.43489E 01	5	361.00	0.
0.27617	0.445	2300.0000	608.5123	0.41399E 01	5	361.00	0.
0.29346	0.438	2200.0000	594.3099	0.39360E 01	5	361.00	0.
0.31290	0.430	2100.0000	582.9632	0.37342E 01	5	361.00	0.
0.33265	0.425	2000.0000	568.1138	0.34278E 01	5	361.00	0.
0.36019	0.413	1900.0000	568.6941	0.33265E 01	5	361.00	0.
0.38944	0.403	1800.0000	565.8668	0.31150E 01	5	361.00	0.
0.42383	0.392	1700.0000	565.7405	0.28944E 01	5	361.00	0.
0.46493	0.380	1600.0000	568.7548	0.26612E 01	5	361.00	0.
0.51507	0.366	1500.0000	573.8198	0.24115E 01	5	361.00	0.
0.57776	0.350	1400.0000	579.7888	0.21406E 01	5	361.00	0.
0.65835	0.330	1300.0000	582.3490	0.19435E 01	5	361.00	0.
0.76465	0.308	1200.0000	574.1291	0.15157E 01	5	361.00	0.
0.90623	0.284	1100.0000	539.3130	0.11583E 01	5	361.00	0.
1.07570	0.263	1000.0000	1097.8687	0.77410E 00	5	361.00	0.
1.30835	0.240	900.0000	347.2048	0.43910E-00	5	361.00	0.
1.56632	0.226	800.0000	247.4568	0.14568E-00	5	361.00	0.
1.89194	0.213	700.0000	201.8682	-0.89238E-01	5	361.00	0.
2.37300	0.199	600.0000	219.3460	-0.28089E-00	5	361.00	0.
2.37299	0.199	600.0000	219.1563	-0.28089E-00	4	211.00	0.
3.38638	0.167	500.0000	308.6609	-0.44861E-00	4	211.00	0.
3.38640	0.167	500.0000	309.4003	-0.44860E-00	3	80.00	0.

ROOT NOT BRACKETED AFTER 20 TRIES

ANISOTROPIC RAYLEIGH WAVE DISPERSION
MODEL 11

N#	8 DELT#	0.000010 FK#	0.00100 FKD#	0.00050					
NW#	-0 DKS#	1.0 CPERT#	1.00100						
	10.00	1000.0000	210.0000	1.6000				PHI	NADA
	10.00	2000.0000	300.0000	1.7000				1.0000	1.0000
	25.00	2200.0000	460.0000	1.8000				1.0000	1.0000
	35.00	5500.0000	1000.0000	2.0000				1.0000	1.0000
	131.00	5500.0000	2000.0000	2.3000				1.0000	1.0000
	100.00	7900.0000	4600.0000	2.3500				1.0000	1.0000
	100.00	8100.0000	4700.0000	2.4000				1.0000	1.0000
	-0.	8500.0000	4900.0000	2.5000				1.0000	1.0000

KD1	T	C	U	W*	N	SUM DI	V
0.00603	2.367	4400.0000	4293.6074	-0.94039E 00	8	411.00	0.
0.01160	1.259	4300.0000	4085.8926	-0.14124E 01	8	411.00	0.
0.01670	0.896	4200.0000	3846.1877	-0.23703E 01	8	411.00	0.
0.02088	0.734	4100.0000	3529.1102	-0.44468E 01	8	411.00	0.
0.02401	0.654	4000.0000	3108.0527	-0.96035E 01	8	411.00	0.
0.02635	0.611	3900.0000	2627.4664	-0.30202E 02	8	411.00	0.
0.02823	0.586	3800.0000	2167.5370	0.94968E 02	8	411.00	0.
0.02985	0.569	3700.0000	1779.1006	0.25147E 02	8	411.00	0.
0.03136	0.557	3600.0000	1472.9140	0.16450E 02	8	411.00	0.
0.03282	0.547	3500.0000	1238.6565	0.13058E 02	8	411.00	0.
0.03427	0.539	3400.0000	1060.6201	0.11213E 02	8	411.00	0.
0.03576	0.532	3300.0000	924.4407	0.10032E 02	8	411.00	0.
0.03729	0.526	3200.0000	818.7489	0.91955E 01	8	411.00	0.
0.03890	0.521	3100.0000	735.4843	0.85591E 01	8	411.00	0.
0.04059	0.516	3000.0000	668.6690	0.80489E 01	8	411.00	0.
0.04239	0.511	2900.0000	613.9968	0.76230E 01	8	411.00	0.
0.04431	0.506	2800.0000	568.7462	0.72556E 01	8	411.00	0.
0.04637	0.502	2700.0000	530.5057	0.69301E 01	8	411.00	0.
0.04860	0.497	2600.0000	497.8354	0.66352E 01	8	411.00	0.
0.05101	0.493	2500.0000	469.4906	0.63590E 01	8	411.00	0.
0.05364	0.488	2400.0000	444.7121	0.61072E 01	8	411.00	0.
0.05651	0.483	2300.0000	422.9549	0.58637E 01	8	411.00	0.
0.05968	0.479	2200.0000	403.7582	0.56286E 01	8	411.00	0.
0.06318	0.474	2100.0000	386.8714	0.53990E 01	8	411.00	0.
0.06670	0.471	2000.0000	369.8813	0.50242E 01	8	411.00	0.
0.07147	0.463	1900.0000	359.8813	0.49460E 01	8	411.00	0.
0.07642	0.457	1800.0000	349.4891	0.47181E 01	8	411.00	0.
0.08206	0.450	1700.0000	341.6039	0.44864E 01	8	411.00	0.
0.08858	0.443	1600.0000	335.9601	0.42490E 01	8	411.00	0.
0.09619	0.435	1500.0000	332.9612	0.40037E 01	8	411.00	0.
0.10521	0.427	1400.0000	332.1495	0.37487E 01	8	411.00	0.
0.11611	0.416	1300.0000	334.4814	0.34819E 01	8	411.00	0.
0.12957	0.404	1200.0000	339.0239	0.32017E 01	8	411.00	0.
0.14670	0.389	1100.0000	345.1274	0.29064E 01	8	411.00	0.
0.17355	0.362	1000.0000	961.9659	0.28396E 01	8	411.00	0.
0.20029	0.349	900.0000	355.2979	0.22670E 01	8	411.00	0.
0.24533	0.320	800.0000	352.8005	0.19192E 01	8	411.00	0.
0.31495	0.285	700.0000	339.5551	0.15375E 01	8	411.00	0.
0.42911	0.244	600.0000	304.7724	0.10667E 01	8	411.00	0.
0.80121	0.112	700.0000	189.6126	0.79120E 01	6	211.00	0.
1.00415	0.104	600.0000	221.2353	0.48135E 01	6	211.00	0.
1.00416	0.104	600.0000	222.2915	0.48135E 01	5	80.00	0.
1.42285	0.088	500.0000	292.1393	0.24418E 01	5	80.00	0.
0.89577	0.175	400.0000	167.5771	-0.64294E-01	5	80.00	0.

ROOT NOT BRACKETED AFTER 20 TRIES

ANISOTROPIC RAYLEIGH WAVE DISPERSION
MODEL 12

N# 7 DELT# 0.0000010 FK# 0.00100 FKD# 0.00050
NW# -0 DKS# 1.0 CPERT# 1.00100

D	ALPHA	BETA	RHO	PHI	NADA
50.00	2200.0000	460.0000	1.8000	1.0000	1.0000
50.00	5500.0000	1000.0000	2.0000	1.0000	1.0000
50.00	5500.0000	2000.0000	2.3000	1.0000	1.0000
50.00	7900.0000	4600.0000	2.3500	1.0000	1.0000
50.00	8100.0000	4700.0000	2.4000	1.0000	1.0000
50.00	8400.0000	4800.0000	2.5000	1.0000	1.0000
-0.	8500.0000	4900.0000	2.6000	1.0000	1.0000

KD1	T	C	U	W*	N	SUM DI	V
0.04345	1.643	4400.0000	4288.8811	-0.10355E 01	7	300.00	0.
0.07837	0.932	4300.0000	4039.3994	-0.18721E 01	7	300.00	0.
0.10232	0.731	4200.0000	3652.7823	-0.28348E 01	7	300.00	0.
0.11696	0.655	4100.0000	3101.4192	-0.84901E 01	7	300.00	0.
0.12679	0.619	4000.0000	2507.1373	-0.24577E 02	7	300.00	0.
0.13443	0.599	3900.0000	1990.5803	0.16887E 03	7	300.00	0.
0.14109	0.586	3800.0000	1591.2634	0.26796E 02	7	300.00	0.
0.14732	0.576	3700.0000	1298.1133	0.16561E 02	7	300.00	0.
0.15342	0.569	3600.0000	1086.2621	0.12734E 02	7	300.00	0.
0.15957	0.562	3500.0000	933.1192	0.10681E 02	7	300.00	0.
0.16590	0.557	3400.0000	821.4981	0.93682E 01	7	300.00	0.
0.17248	0.552	3300.0000	739.4961	0.84321E 01	7	300.00	0.
0.17940	0.547	3200.0000	678.6479	0.77137E 01	7	300.00	0.
0.18675	0.543	3100.0000	633.4870	0.71322E 01	7	300.00	0.
0.19459	0.538	3000.0000	599.8254	0.66420E 01	7	300.00	0.
0.20301	0.534	2900.0000	575.0132	0.62156E 01	7	300.00	0.
0.21211	0.529	2800.0000	557.1624	0.58351E 01	7	300.00	0.
0.22199	0.524	2700.0000	544.7894	0.54888E 01	7	300.00	0.
0.23278	0.519	2600.0000	536.7652	0.51683E 01	7	300.00	0.
0.24463	0.514	2500.0000	532.5846	0.48632E 01	7	300.00	0.
0.25774	0.508	2400.0000	531.2072	0.45822E 01	7	300.00	0.
0.27234	0.502	2300.0000	532.5590	0.43086E 01	7	300.00	0.
0.28871	0.495	2200.0000	536.1751	0.40442E 01	7	300.00	0.
0.30723	0.487	2100.0000	541.7072	0.37866E 01	7	300.00	0.
0.32768	0.479	2000.0000	4590.5683	0.35255E 01	7	300.00	0.
0.35280	0.469	1900.0000	557.1023	0.32840E 01	7	300.00	0.
0.38134	0.458	1800.0000	566.3623	0.30356E 01	7	300.00	0.
0.41518	0.445	1700.0000	576.0083	0.27865E 01	7	300.00	0.
0.45598	0.431	1600.0000	585.1647	0.25346E 01	7	300.00	0.
0.50615	0.414	1500.0000	592.8854	0.22771E 01	7	300.00	0.
0.56918	0.394	1400.0000	597.1586	0.20103E 01	7	300.00	0.
0.65027	0.372	1300.0000	594.8201	0.17289E 01	7	300.00	0.
0.75677	0.346	1200.0000	579.4471	0.14261E 01	7	300.00	0.
0.89744	0.318	1100.0000	539.0402	0.10959E 01	7	300.00	0.
1.05502	0.298	1000.0000	1051.5041	0.71003E 00	7	300.00	0.
1.29385	0.270	900.0000	345.9187	0.40972E-00	7	300.00	0.
1.54951	0.253	800.0000	251.2037	0.12616E-00	7	300.00	0.
1.87571	0.239	700.0000	209.2611	-0.99496E-01	7	300.00	0.
2.36120	0.222	600.0000	225.0666	-0.28410E-00	7	300.00	0.
3.38255	0.186	500.0000	310.8863	-0.44884E-00	7	300.00	0.
3.38254	0.186	500.0000	310.4794	-0.44884E-00	6	250.00	0.
3.38253	0.186	500.0000	310.3836	-0.44884E-00	5	200.00	0.

ROOT NOT BRACKETED AFTER 20 TRIES

ANISOTROPIC RAYLEIGH WAVE DISPERSION
MODEL 15

N# 4 DELT# 0.0000010 FK# 0.00100 FKD# 0.00050
NW# -0 DKS# 1.0 CPERT# 1.00100

D	ALPHA	HEIA	RHO	PHI	NADA
50.00	2200.0000	460.0000	1.8000	1.0000	1.0000
50.00	5500.0000	1000.0000	2.0000	1.0000	1.0000
50.00	5500.0000	2000.0000	2.3000	1.0000	1.0000
-0.	7900.0000	4600.0000	2.3500	1.0000	1.0000

KD1	T	C	U	W*	N	SUM DI	V
0.08857	0.887	4000.0000	3704.1411	-0.20186E 01	4	150.00	0.
0.11255	0.716	3900.0000	3306.7010	-0.41020E 01	4	150.00	0.
0.12775	0.647	3800.0000	2773.0042	-0.91793E 01	4	150.00	0.
0.13841	0.613	3700.0000	2226.3942	-0.30543E 02	4	150.00	0.
0.14700	0.594	3600.0000	1767.3180	0.70991E 02	4	150.00	0.
0.15467	0.580	3500.0000	1420.1146	0.21453E 02	4	150.00	0.
0.16199	0.570	3400.0000	1168.9236	0.14087E 02	4	150.00	0.
0.16927	0.562	3300.0000	989.2502	0.11022E 02	4	150.00	0.
0.17670	0.556	3200.0000	860.5254	0.93256E 01	4	150.00	0.
0.18443	0.549	3100.0000	767.7650	0.82076E 01	4	150.00	0.
0.19257	0.544	3000.0000	700.2370	0.73930E 01	4	150.00	0.
0.20123	0.538	2900.0000	651.0818	0.67660E 01	4	150.00	0.
0.21052	0.533	2800.0000	615.3110	0.62421E 01	4	150.00	0.
0.22057	0.528	2700.0000	589.6915	0.57875E 01	4	150.00	0.
0.23150	0.522	2600.0000	571.6701	0.53944E 01	4	150.00	0.
0.24348	0.516	2500.0000	559.7113	0.50398E 01	4	150.00	0.
0.25670	0.510	2400.0000	552.5551	0.47137E 01	4	150.00	0.
0.27139	0.503	2300.0000	549.2876	0.44090E 01	4	150.00	0.
0.28785	0.496	2200.0000	549.3118	0.41205E 01	4	150.00	0.
0.30645	0.488	2100.0000	552.0985	0.38440E 01	4	150.00	0.
0.32692	0.480	2000.0000	4096.8756	0.35696E 01	4	150.00	0.
0.35218	0.469	1900.0000	563.4411	0.33152E 01	4	150.00	0.
0.38079	0.458	1800.0000	571.2446	0.30573E 01	4	150.00	0.
0.41471	0.446	1700.0000	579.7072	0.28017E 01	4	150.00	0.
0.45560	0.431	1600.0000	587.9609	0.25446E 01	4	150.00	0.
0.50585	0.414	1500.0000	594.8149	0.22833E 01	4	150.00	0.
0.56896	0.394	1400.0000	598.4085	0.20138E 01	4	150.00	0.
0.65013	0.372	1300.0000	595.6174	0.17306E 01	4	150.00	0.
0.75670	0.346	1200.0000	579.8164	0.14268E 01	4	150.00	0.
0.89742	0.318	1100.0000	539.1582	0.10961E 01	4	150.00	0.
1.05504	0.298	1000.0000	1051.5585	0.71051E 00	4	150.00	0.
1.29385	0.270	900.0000	345.9127	0.40972E 00	4	150.00	0.
1.54951	0.253	800.0000	251.2066	0.12634E 00	4	150.00	0.
1.87570	0.239	700.0000	209.2612	-0.99068E 01	4	150.00	0.
2.36120	0.222	600.0000	225.0898	-0.28410E 00	4	150.00	0.
3.38253	0.186	500.0000	310.1560	-0.44884E 00	4	150.00	0.

ROOT NOT BRACKETED AFTER 20 TRIES

ANISOTROPIC RAYLEIGH WAVE DISPERSION
MODEL 16

N# 3 DELT# 0.0000010 FK# 0.00100 FK0# 0.00050
NW# -0 DKS# 1.0 CPERT# 1.00100

D	ALPHA	BETA	RHO	PHI	NADA
50.00	2200.0000	460.0000	1.8000	1.0000	1.0000
50.00	5500.0000	1000.0000	2.0000	1.0000	1.0000
-0.	5500.0000	2000.0000	2.3000	1.0000	1.0000

KD1	I	C	U	W#	N	SUM DI	V
0.36227	0.510	1700.0000	1273.6206	0.17519E 02	3	100.00	0.
0.42963	0.457	1600.0000	879.8789	0.40911E 01	3	100.00	0.
0.48996	0.427	1500.0000	722.3500	0.28826E 01	3	100.00	0.
0.55869	0.402	1400.0000	660.1893	0.22975E 01	3	100.00	0.
0.64376	0.375	1300.0000	627.4248	0.18677E 01	3	100.00	0.
0.75339	0.347	1200.0000	596.0139	0.14857E 01	3	100.00	0.
0.89636	0.319	1100.0000	545.5875	0.11129E 01	3	100.00	0.
1.05579	0.298	1000.0000	1054.0739	0.71540E 00	3	100.00	0.
1.29339	0.270	900.0000	345.2151	0.40556E-00	3	100.00	0.
1.54890	0.254	800.0000	251.5977	0.12496E-00	3	100.00	0.
1.87535	0.239	700.0000	209.7734	-0.99831E-01	3	100.00	0.
2.36111	0.222	600.0000	225.1869	-0.28411E-00	3	100.00	0.
3.38253	0.186	500.0000	310.5063	-0.44884E-00	3	100.00	0.

ROOT NOT BRACKETED AFTER 20 TRIES

APPENDIX D

EDITED EXTRACTS FROM SEMI-ANNUAL REPORTS ON CONTRACT AF 19(604)-7402

D1 The contents of this appendix are entirely abstracted from the above semi-annual reports submitted by Prof. Carl Kisslinger, Saint Louis University, on the contract 'Seismic Waves Generated by Chemical Explosions' No. AF 19(604)-7402 Project Code No. 8100 - Task 2 (Vela-Uniform). The present writer takes no credit and accepts no responsibility for the contents, which are due to Kisslinger, Mateker, and McEvilly -- except for the fact that the records discussed were obtained at the SES test site under the writer's supervision. It is felt that there is some merit in including these verbatim transcriptions herein in order to make the dissertation as comprehensive as possible.

D2 Semi-Annual Report No. 2

The report starts with a detailed description of the participation at SES. Then follows a general description of the results, which continues:

"The amplitude of the first arrival at 2000 ft on the vertical is about 300 microns, with a pulse duration of 0.037 second. This was determined to be a head wave from the top of the hard clay with a velocity of 5600 fps. The relatively small radial component agrees with the interpretation that this is primarily refracted energy coming from below. The maximum peak-to-peak motion is about 4 mm, with a period of 0.5 second, corresponding to an acceleration of about 0.03 g. The maximum motion, as at all distances, occurs after the arrival of the airblast.....

Transverse motion, of particular interest to the (Saint Louis) investigators is small, with a maximum amplitude in the body waves of 80 microns, or about 0.27 of the maximum P wave. The maximum peak to peak SH amplitude is 754 microns, 20% of the maximum vertical motion. At 4000 ft the compressional waves arriving by various paths are well separated. The first arrival, which can be correlated over the rest of the profile to 15,000 ft, gives a velocity of 8600 fps. The event, which was the first arrival at 2000 ft, is a prominent event following the onset by 0.13 sec.

..... the first motion at 10,000 ft is noteworthy. The period is 0.18 sec., and the peak to peak amplitude of 27 microns is greater than the extension of the attenuation curve for the first 7000 ft would predict. At 12,000 ft and 15,000 ft the period becomes 0.3 sec. The apparent surface velocity is very high, about 50,000 fps. If we accept a value of 20,000 fps in the Mississippian, a dip of about 15 degrees is required to reconcile the values. Since the profile could not be reversed there is no confirmation of this interpretation.

(At 4000 ft and 6000 ft the transverse motion)..... has separated into three distinct events, all of which can be correlated, though with difficulty, because of the small amplitude, to 12,000 ft. The ratio of the maximum SH to maximum Vertical P is .26 at 4000 ft and .23 at 12,000 ft. The velocities of 3840 and 5060 fps correspond with 5600 and 8600 fps for the P waves in the same refractor. This clear cut development of refracted SH waves from the explosive source is of considerable interest.

D (iii)

If the 8500 fps arrival is a shear wave, the corresponding P wave would have a velocity of about 14,000 fps. No such arrival could be identified on the verticals. Since the velocity and time intercept of this event are in close agreement with the 8500 fps event on the verticals, and its amplitude is small compared to the other SH arrivals, it is likely that this is actually a component of a P wave returning from a dipping refractor, so that it has a small component not in the vertical plane through the profile.....

The surface wave motion preceding the airblast is very similar on lines A and B. The motion on Line C is slightly larger. The apparent time delay in the arrivals at this station may be explained by the fact that the air blast travel times have not been corrected for the slight wind blowing in the direction of the C line*. The motion over the first two seconds is in phase on all three, but the event arriving at 5 sec. is reversed in phase on the C line record as compared to the other two. This indicates that the two long period events have different origins, one of which has a node between the B and C lines..... The presence of refracted SH waves, about one-fourth as large as the corresponding P waves is of interest as it adds evidence that SH motion must be expected as a normal result of an explosion in or on the earth.

Small Scale Tests at SES

As part of the effort to complete work on explosion generated SH waves, it was desired to extend the observations into

* See discussion in para 3.60. The above is incorrect.

new media.....the experiments were designed to be of the same type as those carried out previously for clay sandstone and limestone. However, the availability of ten seismographs made possible more complete observations than in any of the earlier work. The layout was completed by the Saint Louis team...but...the work was carried out by the SES staff.....

The analysis of the results (at Saint Louis) has been directed to the buried charges. The surface and air-bursts yielded records that are markedly different, and open a new area of enquiry. The transverse motion was derived from the seismograms...and the presence of clear-cut nodes with polarity reversal on either side is evident. The presence of high frequency small amplitude motion near the nodes is also interesting...The results confirm the previous conclusion of unsymmetrical radiation of SH motion.

Another interesting result from the same set of records concerns the P wave radiation. The pattern shows a bulge corresponding to an SH node.....according to Knoppoff and Gilbert's model of crack propagation there should be a lobe of P energy in the direction of propagation....The amplitude of the long period motion for the shallow shot was found to be less than from the deeper shot...which contradicts the Florissant results....and is obviously connected with the generating mechanism....the surface wave portion of the longitudinal and vertical traces for the 10 lb shot at 18.5 ft, recorded from 60-800 ft have been examined. Rayleigh type motion is well developed with an early prograde event showing little dispersion, and a prominent packet of Rayleigh waves. The period of the train is fairly constant at about 0.20 sec...and the maximum amplitude moves through the packet with

a group velocity of about 310 fps. The observed phase velocities range from 600 to 800 fps.....

D3 Semi-Annual Report No. 3

... Results obtained at SES, and by other investigations, indicate that the amount of energy in the seismic waves changes radically as a shot depth is varied from just below to just above...

The spectra of the entire radial motion at about 15 metres from shots in sandy clay (SES).... were calculated. In the sandy clay at SES the spectra peaked at 4 cps, the predominant Rayleigh wave frequency, with secondary peaks at 6-7 cps and 9 cps corresponding to the prograde Rayleigh waves and possibly body waves respectively.

... Fourier spectra of the horizontal transverse motion (Love wave) have been calculated for the profiles at SES. Charges of 10 lb at a depth of 18 ft and 7.5 ft, and a 500 lb shot at the surface have been compared. For the shot at 18 ft the energy in the wave train is contained in the 2-11 cps band with prominent peaks at 3.5 and 5 cps.

For the shot at 7.5 ft, the general energy distribution is similar to the deeper source with the exception that the peaks at 3.5 and 5 cps no longer stand out above the overall energy background. Record amplitudes for this shot are visibly smaller than for 18 ft depth.

Spectra from the 500 lb shot are very similar in shape to those of the 18 ft shot with the significant features occurring at frequencies 1 cps lower for the surface shot.

The transverse components of the three sets of azimuthal records (2 lb at 10.5 ft, 2 lb at 5 ft and 4 lb at 5 ft recorded at 100 ft) were digitized and the corresponding radiation patterns for the first large amplitude motion were plotted. The position of the nodes was found to be about the same for the three sets of data.

Spectral analysis of surface wave portions of the records... have been completed. At SES dispersed Rayleigh waves and Love waves exist, as well as a Rayleigh-type prograde wave. Ultimately, these data will be used to contribute the necessary parameters for Fourier re-synthesis of the source motion.

Attenuation coefficients based upon the relationship

$$A_r = A_0 r^{-1/2} e^{-\alpha r}$$

were determined for individual Fourier components. At SES α varies from 0.004/meter to 0.006/meter in the range 3.5 to 5 cps.

One of the most significant features of the SES data that as yet is unexplained completely is the absence of the normal 4 cps Rayleigh wave associated with the low velocity surface layer from the 100 ton shot. This event, usually contributing the biggest motion on the vertical and radial records for a buried charge, could not be found in the 100 ton records. The characteristic of the Rayleigh wave are known from an analysis of two buried 10 lb charges and a 500 lb surface charge. The event presents an almost identical appearance for these three sets of records, so it is not the fact that the 100 ton charge was surface-burst that accounts for the absence.

An inspection of the SES records from earlier trials indicates that the Rayleigh wave appears for small shots, but not large ones, of 5 tons or greater. There is Rayleigh-type motion following the airblast arrival, but it is much too early to be the same event as that recorded from the smaller shots.

The Rayleigh wave observed in the small scale shots has a very narrow spectrum, a few cps wide, sharply peaked at 4 cps, with a group velocity at this frequency of about 460 fps. One possible explanation of the absence of the wave is that the larger shots, including the 100 ton, do not generate appreciable energy at this frequency. This point is worthy of further study. The Rayleigh waves that are observed for the larger shots are probably associated with deeper interfaces with higher velocities. In the case of the 100 ton shot, the entire thickness of the low velocity layer was involved in the source region, so that the input impulse was applied directly to the top of the hard clay. This would account for the generation of the higher speed waves not seen in smaller sources".

APPENDIX E

A MODIFIED SATO PROGRAMME FOR DETERMINING PHASE VELOCITIES (Hastrup Programme)

At some stage in the analysis of seismograms it becomes necessary to investigate the spectra and the dispersion curves for the various pulses. The most elegant way of doing this is, without doubt, some modification of the method of Sato (1955), but the precise form in which the method is applied will depend upon the type of record and the particular computing facilities available. In this appendix, methods of determining the spectra and the dispersion curves which are peculiarly suited to the Suffield records are described. The formulation is due to O. Hastrup, of the Danish Defence Research Board, and was prepared during his tenure of a DRB Fellowship at SES during the summer of 1963. Examples of the computations using these programmes are given earlier in this dissertation, and will also appear in greater detail for specific cases elsewhere (Hastrup, 1963a, b).

Numerical Calculation of Fourier Integrals

The Fourier Integral is defined by

$$F(\omega) = \frac{1}{\sqrt{2\pi}} \int_{-\infty}^{\infty} f(t) e^{-i\omega t} dt^* \quad \text{E.1}$$

where $f(t)$ is the transient function,

$F(\omega)$ is generally a complex function of the frequency ω and can be written either as

$$F(\omega) = \text{Re} [F(\omega)] + i \text{Im} [F(\omega)] \quad \text{E.2}$$

$$\text{or as} \quad F(\omega) = |F(\omega)| e^{i\theta(\omega)} \quad \text{E.3}$$

$$\text{where } |F(\omega)| = \sqrt{\text{Re}^2[F(\omega)] + \text{Im}^2[F(\omega)]} \quad \text{and}$$

* The factor $\frac{1}{\sqrt{2\pi}}$ is introduced to make the Fourier integral and the inverse transformation $f(t) = \frac{1}{\sqrt{2\pi}} \int_{-\infty}^{\infty} F(\omega) e^{i\omega t} d\omega$ of the same form.

E (ii)

$$\theta(\omega) = \arctan \frac{\text{Im}[F(\omega)]}{\text{Re}[F(\omega)]} \quad \text{E.4}$$

If $f(t)$ is a complicated function, or is only known graphically, it is necessary to evaluate E.1 numerically. The present method is based upon linear interpolation of the function.

Consider the signal between $t_{n-1} = (n-1)\Delta t$ and $t_n = n\Delta t$; then $f(t)$ in this region may be approximated by

$$f(t) \approx g(t) = f_{n-1} + \delta_n \left(\frac{t}{\Delta t} - n + 1 \right) \quad \text{E.5}$$

where $\delta_n = f_n - f_{n-1}$.

The Fourier Integral for this small trapezoid is then given by

$$\Delta F_n(\omega) = \frac{1}{\sqrt{2\pi}} \int_{t_{n-1}}^{t_n} \left\{ f_{n-1} + \delta_n \left(\frac{t}{\Delta t} - n + 1 \right) \right\} e^{-i\omega t} dt \quad \text{E.6}$$

This may be re-written as

$$\begin{aligned} \text{Re}[\Delta F_n(\omega)] &= \frac{1}{\sqrt{2\pi}} \frac{\Delta t}{\psi} \left[\sin \psi (f_n \cos(2n-1)\psi - \frac{\delta_n}{2\psi} \sin(2n-1)\psi) + \right. \\ &\quad \left. \frac{\delta_n}{2} \sin 2(n-1)\psi \right] \\ \text{Im}[\Delta F_n(\omega)] &= \frac{1}{\sqrt{2\pi}} \frac{\Delta t}{\psi} \left[-\sin \psi \left\{ f_n \sin(2n-1)\psi + \frac{\delta_n}{2\psi} \cos(2n-1)\psi \right\} + \right. \\ &\quad \left. \frac{\delta_n}{2} \cos 2(n-1)\psi \right] \end{aligned}$$

where we have introduced the angle $\psi = \frac{\omega \Delta t}{2}$.

To get $f(\omega)$ we have to sum (6) over all the intervals to get

$$F(\omega) = \sum_{n=1}^N \text{Re}[\Delta F_n(\omega)] + i \sum_{n=1}^N \text{Im}[\Delta F_n(\omega)] \quad \text{E.7}$$

E (iii)

The input tape for this calculation on the SES Stantec Zebra computer is given below in Zebra Simple Code.

```

+  $\frac{\omega_0}{2\pi}$           ( $\omega_0$  Initial frequency)
+  $\frac{\Delta\omega}{2\pi}$         ( $\Delta\omega$  Frequency increment)
+  $\frac{\omega_m}{2\pi}$         ( $\omega_m$  Maximum frequency)
Y
Blank tape
+ Identification Number
+  $\Delta t$ 
+ h (bias level)
Y
Blank tape
+  $f_0$ 
+  $f_1$ 
+ .
+ .
+  $f_N$ 
Y

```

} First record ordinates

Route Selection by Key		
YLY00	Key	+ Ident. No.
+ $\frac{\omega_0}{2\pi}$	U1 < 0	+ Δt
+ $\frac{\Delta\omega}{2\pi}$	U1 < 1	+ h
+ $\frac{\omega_m}{2\pi}$	U2 < 0	Y
Blank	U2 < 1	Blank
+ Ident. No.	U4 < 0	+ f_0
+ Δt	U4 < 1	+ f_1
+ h		+ .
Y		. . .
Blank		+ f_N
+ f_0		Y
+ f_1		Blank
. . .		YYLY00 (STOP)
+ f_N		
Y		
Blank		
YYLY00 (STOP)		

Programme may be re-entered at punch by dialling Q14. U4 then selects output.

No purpose would be served by listing the actual computer programme. The output from this calculation may then be used as the input into the dispersion programme.

APPENDIX F

SPECTRAL ANALYSIS OF POST AIR BLAST PHASE OF TWO SEISMOGRAMS

In this appendix is given an example of the method of detailed reduction which must be applied to all the individual phases in the seismograms before complete interpretation is possible. The example is chosen as illustrating both the power and the weakness of the method.

It was decided to attempt an analysis, post airblast phase, of three seismograms from the Watching Hill 40,000 lb charge, F.E. 535, seismograms 60W, 61W and 62W being selected as apparently consistent records showing air-coupling. The analysis was undertaken without reference to previous analyses of these records or associated records, in order to illustrate the complete approach. The analysis therefore proceeded in the following stages.

Stage 1. Digitization

The records were digitized onto punched tape including the following data: identification number, charge size, epicentral distance, bias from base line to the transverse trace, vertical trace, and radial trace, at the zero position; number of counts at 0.02 second intervals from zero to the start of digitization (in this case, the arrival of the airblast); digital data in sets of three, giving transverse, radial and vertical in that order, to a point well beyond the phases of interest; total number of counts.

Stage 2. Verification

The punched paper tape from stage 1 was used as the input to a plotting programme on the Stantec Zebra computer. Errors in digitization could thus be detected by direct comparison between the

original trace and the plotted trace, or by machine failure in the event of gross error. The computer plotted traces for the vertical components of the three seismograms are given as Fig. F.1.

Stage 3. Particle Trajectories

From the corrected digital data, particle trajectories were plotted for the immediate post airblast region. These trajectories are given as Figs. F2, F3 and F4. It was immediately apparent that the trajectories were not completely consistent with each other. The trajectory for seismogram 62W is grossly different in appearance from the other two, and can not be correlated with them. On the other hand, the orbits from 60W and 61W showed a basically similar pattern, although there are differences even in the direction of rotation of regions of the orbits. The assumption was made that comparison was possible from the moment of arrival of the airblast to a distinct transition in the orbits. These starting and ending points were selected, and are indicated in the figures.

Stage 4. Smoothing of Traces

It is essential that the analysis be performed upon phases which start and end at zero amplitude. The vertical component digital data for the selected region were therefore abstracted from the punched tape, and a fresh tape made in which the first and last few values were corrected or 'smoothed' so that the first and last reading in the smoothed data became equal to the bias level for the vertical trace.

Stage 5. Spectral Analysis

The smoothed data from stage 4 were then used as input data into the Hastrup spectral analysis programme of Appendix E. The output

data for the two seismograms are tabulated as Fig. F.5. These data were not used directly, but used as an input to stage 6.

Stage 6. Dispersion and Spectrum Programme

The output tapes from stage 6 were used as the input data for the Hastrup programme of a Satô-type analysis (see Hastrup, 1963b). This programme computes firstly the spectral amplitude for the two seismograms at selected frequencies (in this case, at intervals of 0.25 cps from 1 cps to 6 cps). Finally, it computes the family of dispersion curves, provided the spectral distribution is consistent between the two seismograms. The output for the first part of this analysis is given in Fig. F.6, and plotted in Fig. F.7. It will be seen that the spectra are similar in pattern, with a large amplitude peak in the vicinity of 2 cps, and a smaller amplitude peak in the vicinity of 3.5 cps, followed by several minor peaks of small significance. Visual inspection of these seismograms immediately suggests that a Satô-type dispersion analysis, which assumes that the spectral distribution remains constant between stations, will not give a consistent picture in this case. The actual computation verifies this since the families of velocity data for each frequency of the computed values are negative in most cases, which is physically meaningless.

Stage 7. Interpretation

Interpretation of a single analysis of the above type is, obviously, a dangerous proceeding. Nevertheless, certain deductions may be made. In the first place, it is noted that the mean peak frequencies for the two spectra are 2 cps and 3.5 cps for the two

dominant peaks, most of the energy being in the 2 cps region. Comparison with the theoretical dispersion curve of Model 6, Appendix C, shows that these two frequencies correspond exactly with the sonic velocities in the group and phase dispersion curves respectively, which is what one would expect if the post airblast region is composed of a Press-Ewing air-coupled wave superimposed upon a pre-existing surface wave. Despite this precise agreement, attention is drawn to the fact that the pre-existing wave is a prograde wave, not a retrograde Rayleigh wave.

If we interpret the seismograms in this way, that is as an air-coupled wave superimposed upon a pre-existing wave, the appearance of the trajectories, and the impossibility of applying Sato's method to compute the phase dispersion curve may be explained readily. The precise appearance of the orbit will depend upon the individual orbits of the two components, and changes in the relative phase of these two components may modify the composite orbit to such an extent that changes of the order shown in Figs. F2 and F3 may occur.

An analysis of the above type is a comparatively slow process. Digitization of the records takes approximately six hours for a pair of seismograms. Verification of the digitization requires approximately 30 minutes of computer time followed by about two hours of teleprinter time. Plotting of the particle trajectories, after correction of the data amounts to roughly an hour per trajectory. The spectral analysis programme takes approximately three hours for records of the length used in the present case. The final stage, computing the spectral amplitude and the phase velocities takes about 30 minutes of computer time. The time schedule given assumes, of course, that we are dealing with clearly

F (v)

separated phases which may be correlated. Where it becomes necessary to use subjective judgment in selecting the data to be analysed, the time involved may be increased by a large factor.



60 W



61 W



62 W

FIG. F. I
COMPUTER VERIFICATION OF DIGITIZATION — VERTICAL COMPONENT

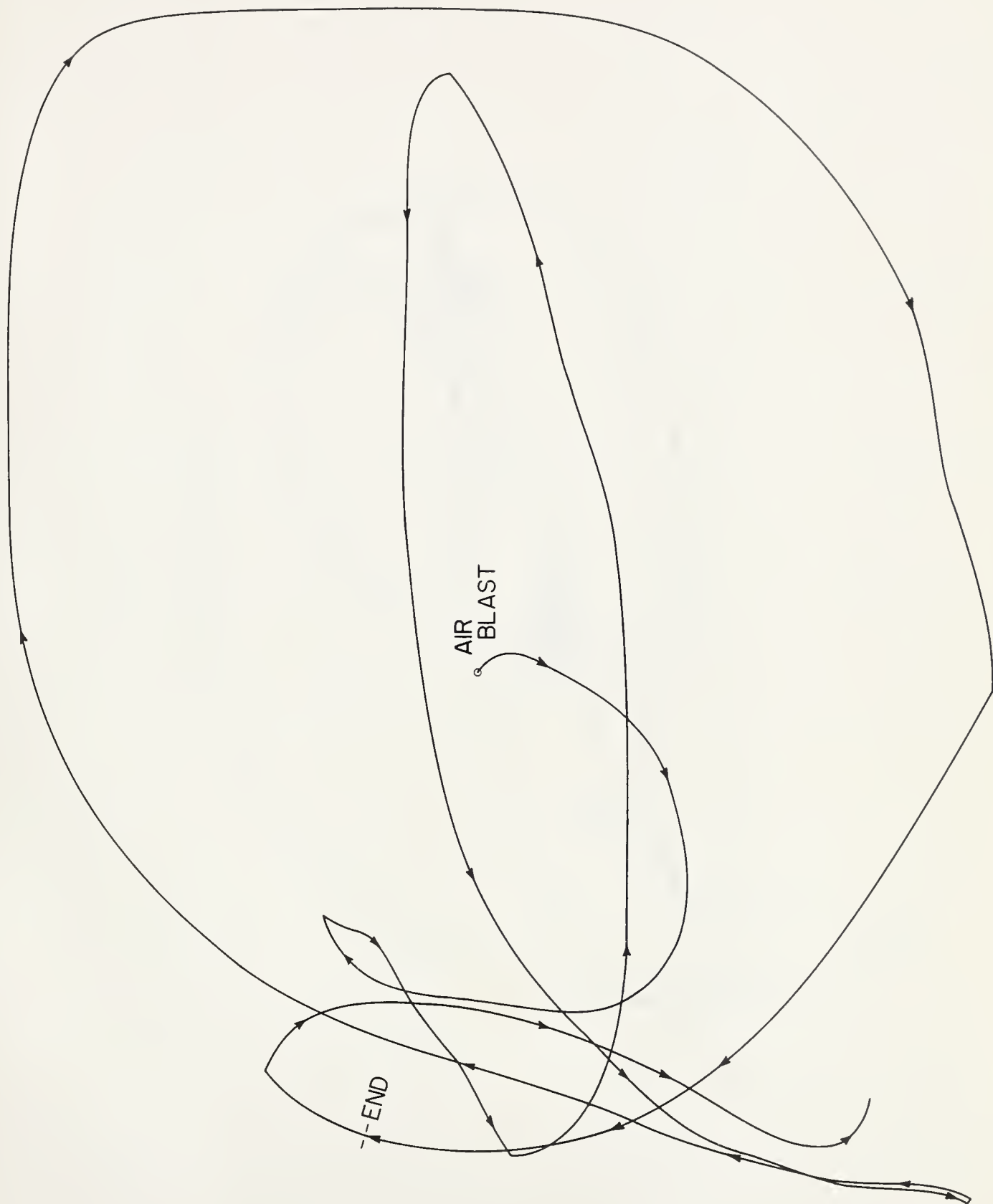


FIG. F.2
POST AIRBLAST ORBIT — 60 W

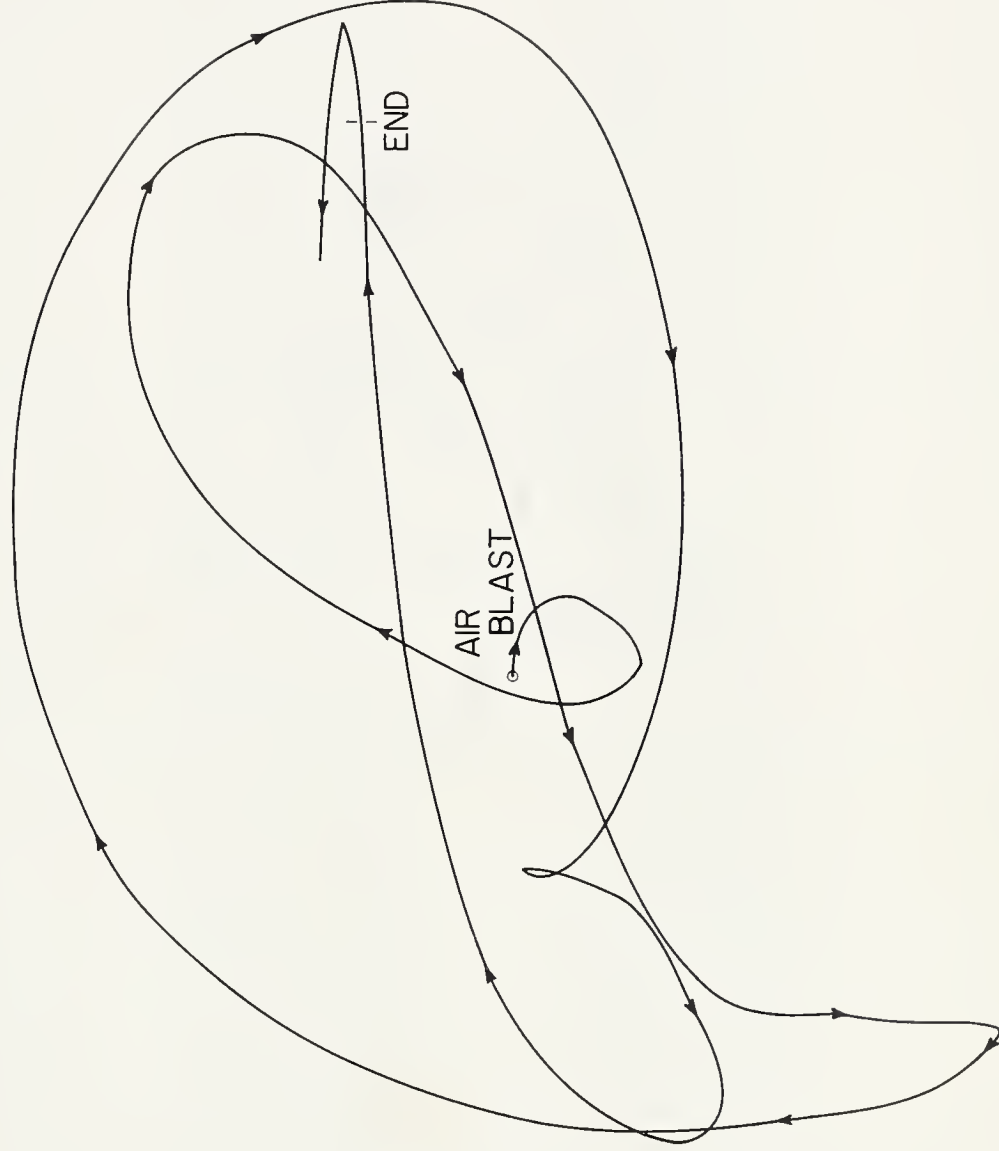


FIG. F.3
POST AIRBLAST ORBIT — 61 W



FIG. F. 4
POST AIRBLAST ORBIT — 62 W

T	RECORD	NUMBER OF FREQUENCIES	TRAVEL TIME	DISTANCE
	+0.600000000 + 2	+0.210000000 + 2	+0.334000000 + 1	+0.400000000 + 4
	<u>ANGULAR FREQUENCY</u>	<u>FREQUENCY CPS</u>	<u>REAL PART</u>	<u>IMAGINARY PART</u>
	+0.628318530 + 1	+1.000000000 + 0	-0.111980497 + 2	+0.212992636 + 2
	+0.785398163 + 1	+0.125000000 + 1	+0.364943949 + 2	+0.336831966 + 2
	+0.942477794 + 1	+0.150000000 + 1	+0.407695419 + 2	-0.431778140 + 2
	+0.109955743 + 2	+0.175000000 + 1	-0.642616815 + 2	-0.255177842 + 2
	+0.125663706 + 2	+0.200000000 + 1	-0.171778816 + 2	+0.109274870 + 3
	+0.141371669 + 2	+0.225000000 + 1	+0.143919460 + 3	+0.392652289 + 2
	+0.157079632 + 2	+0.250000000 + 1	+0.653531312 + 2	-0.130713925 + 3
	+0.172787595 + 2	+0.274999999 + 1	-0.864065750 + 2	-0.515563474 + 2
	+0.188495559 + 2	+0.299999999 + 1	-0.329348742 + 1	+0.619080966 + 2
	+0.204203522 + 2	+0.324999999 + 1	+0.700658625 + 2	-0.292614352 + 2
	+0.219911485 + 2	+0.349999999 + 1	-0.223402680 + 2	-0.726944982 + 2
	+0.235619448 + 2	+0.374999999 + 1	-0.440285867 + 2	+0.600213594 + 1
	+0.251327411 + 2	+0.399999999 + 1	+0.107742141 + 2	+0.794781424 + 1
	+0.267035375 + 2	+0.424999999 + 1	-0.395627615 + 1	-0.238077516 + 2
	+0.282743338 + 2	+0.449999999 + 1	-0.186687164 + 2	-0.158362856 + 1
	+0.298451301 + 2	+0.474999999 + 1	+0.516252486 + 0	-0.399059385 - 1
	+0.314159264 + 2	+0.499999999 + 1	-0.884915091 + 1	-0.112995775 + 2
	+0.329867227 + 2	+0.524999998 + 1	-0.130053843 + 2	+0.419438448 + 1
	+0.345575191 + 2	+0.549999998 + 1	+0.170163987 + 1	+0.304274347 + 1
	+0.361283154 + 2	+0.574999998 + 1	-0.398101381 + 1	-0.613955907 + 1
	+0.376991117 + 2	+0.599999998 + 1	-0.698330204 + 1	+0.254067066 + 1

5	RECORD	NUMBER OF FREQUENCIES	TRAVEL TIME	DISTANCE
	+0.610000000 + 2	+0.210000000 + 2	+0.419000000 + 1	+0.500000000 + 4
	<u>ANGULAR FREQUENCY</u>	<u>FREQUENCY CPS</u>	<u>REAL PART</u>	<u>IMAGINARY PART</u>
	+0.628318530 + 1	+1.000000000 + 0	-0.221907582 + 2	-0.157205634 + 2
	+0.785398163 + 1	+0.125000000 + 1	-0.526961270 + 2	+0.301728989 + 2
	+0.942477794 + 1	+0.150000000 + 1	-0.281084782 + 1	+0.866831842 + 2
	+0.109955743 + 2	+0.175000000 + 1	+0.756165760 + 2	+0.598974400 + 2
	+0.125663706 + 2	+0.200000000 + 1	+0.896448558 + 2	-0.151078140 + 2
	+0.141371669 + 2	+0.225000000 + 1	+0.476370756 + 2	-0.626569146 + 2
	+0.157079632 + 2	+0.250000000 + 1	-0.785023590 + 1	-0.649769951 + 2
	+0.172787595 + 2	+0.274999999 + 1	-0.424213873 + 2	-0.234677952 + 2
	+0.188495559 + 2	+0.299999999 + 1	-0.192941829 + 2	+0.230872893 + 2
	+0.204203522 + 2	+0.324999999 + 1	+0.272549268 + 2	+0.111628526 + 2
	+0.219911485 + 2	+0.349999999 + 1	+0.213632857 + 2	-0.327617601 + 2
	+0.235619448 + 2	+0.374999999 + 1	-0.173280359 + 2	-0.333470417 + 2
	+0.251327411 + 2	+0.399999999 + 1	-0.233882522 + 2	-0.623010972 + 1
	+0.267035375 + 2	+0.424999999 + 1	-0.116226083 + 2	-0.135170123 + 1
	+0.282743338 + 2	+0.449999999 + 1	-0.147101838 + 2	-0.206622987 + 1
	+0.298451301 + 2	+0.474999999 + 1	-0.128761288 + 2	+0.875203596 + 1
	+0.314159264 + 2	+0.499999999 + 1	-0.614090883 + 0	+0.902852080 + 1
	+0.329867227 + 2	+0.524999998 + 1	+0.390643663 + 0	+0.631426012 + 0
	+0.345575191 + 2	+0.549999998 + 1	-0.375325928 + 1	+0.170069994 + 1
	+0.361283154 + 2	+0.574999998 + 1	-0.527602498 + 0	+0.375697936 + 1
	+0.376991117 + 2	+0.599999998 + 1	+0.530579267 + 0	+0.279648300 + 0

FIG. F. 5

FOURIER INTEGRAL COMPUTATION 60W AND 61W

ANGULAR FREQUENCY			FREQUENCY			S P E C T R A L			A M P L I T U D E		
			CPS			60W			61W		
+0.628318530	+	1	+1.000000000	+	0	+0.240635605	+	2	+0.271949602	+	2
+0.785398163	+	1	+0.125000000	+	1	+0.496628492	+	2	+0.607230239	+	2
+0.942477794	+	1	+0.150000000	+	1	+0.593841660	+	2	+0.867287455	+	2
+0.109955743	+	2	+0.175000000	+	1	+0.691427582	+	2	+0.964653818	+	2
+0.125663706	+	2	+0.200000000	+	1	+0.110616802	+	3	+0.909089996	+	2
+0.141371669	+	2	+0.225000000	+	1	+0.149179654	+	3	+0.787094652	+	2
+0.157079632	+	2	+0.250000000	+	1	+0.146140898	+	3	+0.654494927	+	2
+0.172787595	+	2	+0.274999999	+	1	+0.100618851	+	3	+0.484800115	+	2
+0.188495559	+	2	+0.299999999	+	1	+0.619956409	+	2	+0.300880112	+	2
+0.204203522	+	2	+0.324999999	+	1	+0.759306044	+	2	+0.294523397	+	2
+0.219911485	+	2	+0.349999999	+	1	+0.760498366	+	2	+0.391116722	+	2
+0.235619448	+	2	+0.374999999	+	1	+0.444358198	+	2	+0.375803941	+	2
+0.251327411	+	2	+0.399999999	+	1	+0.133884816	+	2	+0.242038139	+	2
+0.267035375	+	2	+0.424999999	+	1	+0.241342321	+	2	+0.117009452	+	2
+0.282743338	+	2	+0.449999999	+	1	+0.187357640	+	2	+0.148545889	+	2
+0.298451301	+	2	+0.474999999	+	1	+0.517792539	+	0	+0.155689700	+	2
+0.314159264	+	2	+0.499999999	+	1	+0.143522794	+	2	+0.904938095	+	1
+0.329867227	+	2	+0.524999998	+	1	+0.136650240	+	2	+0.742496653	+	0
+0.345575191	+	2	+0.549999998	+	1	+0.348623953	+	1	+0.412059892	+	1
+0.361283154	+	2	+0.574999998	+	1	+0.731728478	+	1	+0.379384479	+	1
+0.376991117	+	2	+0.599999998	+	1	+0.743111800	+	1	+0.599764562	+	0

FIG. F. 6

SPECTRAL AMPLITUDES SEISMOGRAMS 60W AND 61W

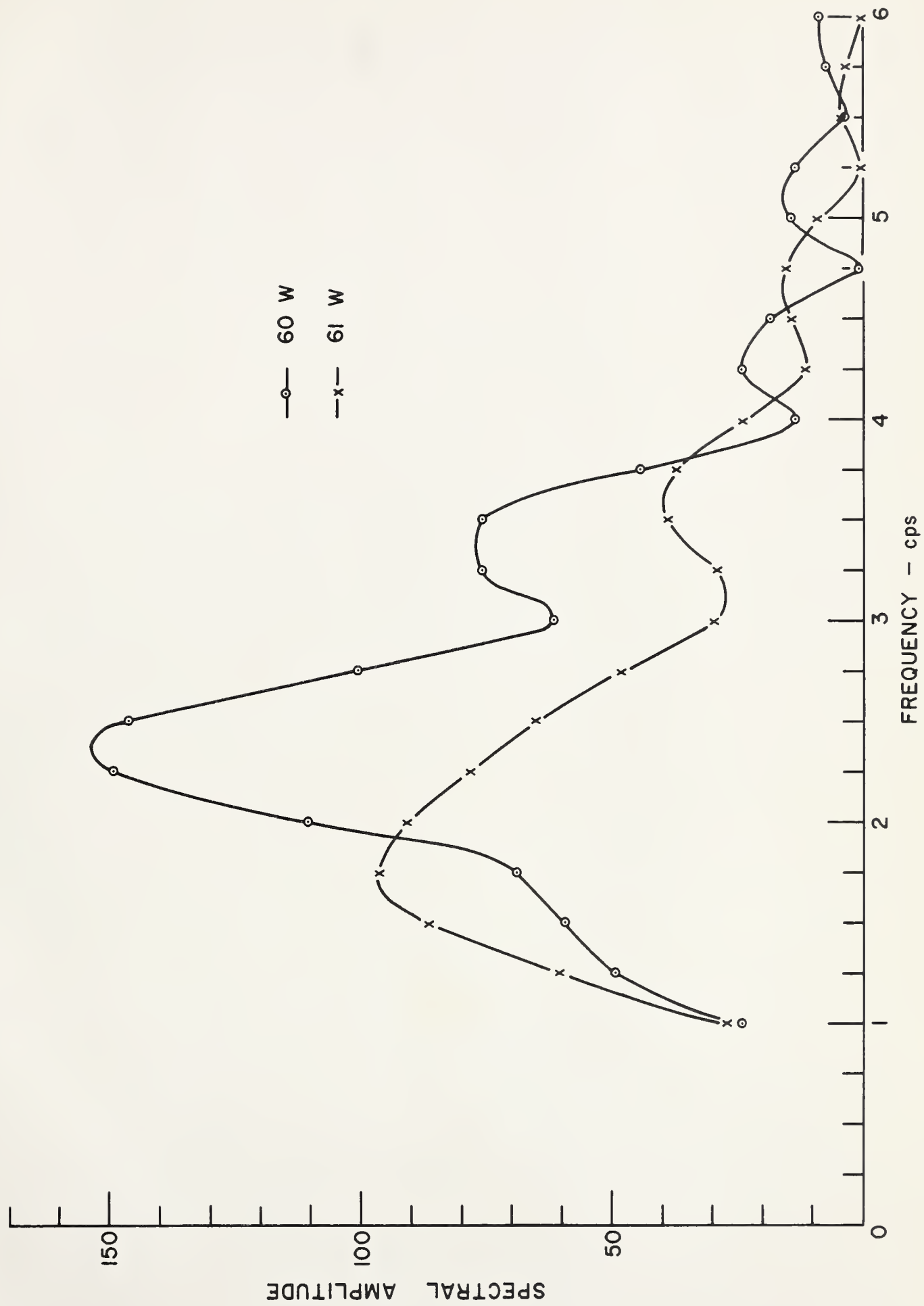


FIG. F.7
SPECTRA 60 W AND 61 W

B29814